Analysis of Pathways Affected by the Viral Oncogenes in Human Papillomavirus 16-Induced Neoplastic Progression

Christina Verena Untersperger

November 2013

Division of Virology
MRC National Institute for Medical Research
The Ridgeway
Mill Hill, London
NW7 1AA

Division of Infection and Immunity
University College London

This thesis is submitted to University College London for the degree of Doctor of Philosophy

Statement of declaration

I, Christina Untersperger, confirm that the work presented in this thesis is my own. Where information has been derived from other sources, I confirm that this has been indicated in the thesis.

Acknowledgments

I would like to acknowledge my supervisor John Doorbar for giving me the opportunity to work in the lab and allowing me to tackle this project.

I would like to thank everyone in the Doorbar lab, both past and present members, for your general support and for answering many questions over the past four years. In particular I want to thank:

Clare, for your endless supply of information on anything to do with HPVs and the ins and outs of lab work. Your patience when answering many, sometimes awkward, questions has been much appreciated. Your proofreading services have also been extremely useful on several occasions. Without your guidance and insight, I am not sure that this thesis could have been written.

Deb, for being an amazing technician without whom the lab would not function. Our conversations have managed to brighten many of my otherwise mundane, tissue-cultured filled days. Also, your input in this project has been very helpful.

Pauline, for all your help and advice around the lab and also general moral support. But more importantly, all our coffee and lunch breaks with hilarious stories.

Qian, for letting me use many of your reagents and being incredibly patient when explaining experiments to me. And also, for feeding my cells on several occasions.

Ed, Saran, Jo, Lietta, Cinzia, Emilio and Gareth - my whole experience was definitely improved by you guys. You made the lab a fun place to work. Ed, thanks for your help in seeding some of my big experiments.

Kate Bishop and Jonathan Stoye - my thesis committee - for your useful comments during our TC meetings. Your suggestions have helped maintain focus in the project.

My parents for your encouragement and helping me stay positive; Alex, for your amusing anecdotes about life; Mo, for your constant supply of funny photos and videos, Toni, for being an amazing sister and sending me daily motivational emails and of course Sunny, for being, by far, the best dog in the world!

Fraser, for being an incredible boyfriend and putting up with my lab work-related rants on a daily basis. And for managing to feign interest in the intricacies of HPV and E6 and helping me stay motivated.

Abstract

While many studies have looked at the role of the high-risk E6 and E7 proteins in the development of cancer, few have looked at their role in the progression from productive infection to LSIL and HSIL+, which can occur soon after infection in the absence of integration.

I analyze isogenic NIKS lines containing HPV16 episomes, which have previously been shown to have LSIL- or HSIL-like phenotypes in raft culture. In monolayer culture, the HSIL-like cells proliferate more than the LSIL-like cells, and I have found that this appears to be due to the activity of the E6 protein. In contrast, the E7 protein is only able to drive proliferation when the cells are cultured without serum. At confluence, the HSIL-like cells divide to form increasingly small cells in a monolayer, whilst the LSIL-like cells tend to stratify, like the parental line. This indicates that the LSIL- and HSIL-like cells respond differently to cell density. Furthermore I see a similar fast-growing phenotype with an E6 mutant that is unable to bind p53, suggesting that the effect on proliferation is independent of p53 degradation. Increasing or decreasing the levels of E6 leads to LSIL-like cells now having a more HSIL-like growth phenotype or vice versa, respectively. Analysis of contact inhibition signaling pathways shows that the levels of active Notch are significantly higher in the LSIL-like cells. Additionally, I have observed what may be a novel truncated form of active Notch.

My results suggest that in productive infections any elevation in cell proliferation in the basal cells may be dependent on E6, while E7-stimulated cell cycle entry may be limited to the suprabasal cells. Aberrant expression of E6 level can then further promote proliferation by overcoming cellular contact inhibition pathways and this contributes to the progression from low- to high-grade lesions.

Table of Contents

List of Figures

List of Tables

List of Abbreviations

APC	adenomatous polyposis coli
APS	ammonium persulphate
BPV	bovine papillomavirus
BSA	bovine serum albumin
c-Myc	myelocytomatosis viral oncogene homolog (avian)
C8:O	N 1,2-dioctanoyl-sn-glycerol
CDK	cyclin dependent kinase
cDNA	complementary DNA
CIN	cervical intraepithelial lesion
cm	centimeter
CMV	cytomegalovirus
CRPV	cottontail rabbit papillomavirus
Ct	cycle threshold
DAPI	4'-6' diamidino-2-phenylindol
dH_2O	distilled water
DMEM	Dulbecco's Modified Eagle's Medium
DMSO	dimethyl sulphoxide
DNA	deoxyribonucleic acid
dNTP	deoxyribonucleotide triphosphate
DTT	dithiothreitol
E2BS	E2 binding site
E6ΔPDZ	16E6 protein with a deleted PDZ-binding motif
E6AP	E6-associated protein
E6SAT	E6 protein that is unable to degrade p53
EBV	Epstein-Barr virus
EDTA	ethylenediaminetetraacetic acid
EGF	epidermal growth factor
EV	epidermodysplasia verucciformis
FBS	fetal bovine serum

g	gram
x g	times gravity
GAPDH	glyceraldehyde 3-phosphate dehydrogenase
GRE	glucocorticoid responsive elements
Gy	gray unit
hDlg	human homolog of *Drosophila* disc large
HRP	horseradish peroxidase
hScrib	human homolog of *Drosophila* scribble
HSIL	high-grade squamous intraepithelial lesion
HTLV-1	Human T-lymphotropic virus Type 1
IFN	interferon
IgG	immunoglobulin G
kb	kilobase
kDa	kilo Dalton
L	liter
LB	lysogeny broth
LCR	long control region
LSIL	low-grade squamous intraepithelial lesion
MAPK	mitogen-activated protein kinase
MCM	minichromosome maintenance protein
µg	microgram
µl	microliter
µm	micrometer
µM	micromolar
M	molar
mg	milligram
ml	milliliter
mm	millimeter
mM	millimolar
mRNA	messenger RNA
NICD	notch intracellular domain
NIKS	normal immortalized human keratinocytes
ng	nanogram
NGS	normal goat serum

nm	nanometer
nM	nanomolar
NLS	nuclear localization signal
NP40	nonyl phenoxylpolyethoxylethanol 40
ORF	open reading frame
PAGE	polyacrylamide gel electrophoresis
PBS	phosphate buffered saline
PCNA	proliferating cell nuclear antigen
PCR	polymerase chain reaction
PDZ	structural domain named after PSD95, Dlg1 and ZO-1
pen/strep	penicillin/streptomycin solution
poly(A)	polyadenylation
PV	papillomavirus
PVDF	polyvinylidene fluoride
qPCR	quantitative PCR
RAM	RBPJ associated protein
RBPJ	Recombining binding protein suppressor of hairless
RNA	ribonucleic acid
ROPV	rabbit oral papillomavirus
rpm	revolutions per minute
RRP	recurrent respiratory papillomatosis
RT-qPCR	real-time qPCR
SDS	sodium dodecyl sulphate
SV40	Simian virus 40
TAE	tris-acetate EDTA
TBS	tris-buffered saline
v/v	volume/volume
VIN	vulval intraepithelial lesion
VLP	virus-like particle
w/v	weight/volume

Chapter 1: Introduction

1.1 Introduction to papillomaviruses

Papillomaviruses (PVs) are small, non-enveloped viruses, consisting of a circular double-stranded DNA genome within an icosahedral capsid of approximately 55 nm in diameter (Howley, 1996). They infect many mammals, including ungulates and cetaceans, birds (de Villiers et al., 2004, Bernard et al., 2010) and some reptiles (Herbst et al., 2009). PVs are very host-tropic with interspecies transmissions being rare, suggesting that these viruses have been co-evolving with their specific hosts through time (Bernard et al., 2006). PVs infect mucosal and cutaneous epithelial tissues, through abrasions or microwounds (Roberts et al., 2007), and the viral life cycle is tightly linked to the differentiation program of host cells and utilizes the entire epithelium (Favre et al., 1997). The production of new virions is restricted to the most apical layers of the tissue (reviewed in (Doorbar et al., 2012)) where cells are most differentiated. Infection by PVs can cause a whole spectrum of diseases in their hosts, ranging from asymptomatic infections to skin warts, including *Verruca vulgaris* (common wart), *Verruca plantaris* (plantar wart) and *Verruca plana* (flat wart), C*ondyloma acuminata* (genital wart) and cancers (reviewed in (Mammas et al., 2009)). The vast majority of infections in humans are sub-clinical and for this reason it has been estimated that the rate of incidence is much higher than the reporting rate (http://virus.stanford.edu/papova/HPV.html).

1.2 Classification of papillomaviruses

Papillomaviruses are a member of the *Papillomaviridae* family, which consists of about 200 different types of viruses (Bernard et al., 2010). When PVs were first discovered they were classified into the family of *Papoviridae*, with polyomaviruses, due to their structural similarities and small, double-stranded DNA genome. However, it was found that PVs are quite different in terms of the organization of their genomes and also transcriptional regulation, leading to the categorization into their own taxonomic family.

The organization of PVs into their respective genera is based on the homology of the L1 open reading frame (ORF). L1 is the major capsid protein of the virus and is the most conserved of all PV ORFs. All virus types within one genus generally share more than

60 % nucleotide sequence identity within the L1 gene, while types within the same species have 71-89 % identity to each other (de Villiers et al., 2004).

1.3 Human papillomaviruses (HPVs)

Over 160 different types of HPVs have been described in 5 out of 24 PV genera (Alpha, Beta, Gamma, Mu and Nu). HPVs can infect a variety of epithelial tissues of the cervix, vulva, anus, penis and the oral cavity, larynx, esophagus, tonsils and tracheobronchial tree (reviewed in (zur Hausen, 2009, Graham, 2010)). HPVs are additionally sub-divided into two broad categories; low-risk viruses are associated with predominantly benign disease while high-risk types can cause cancer (Laimins, 1993, Favre et al., 1997, Walboomers et al., 1999).

The genus that is most medically significant is Alpha as it comprises the high-risk HPV types that are implicated in, among other things, genital cancers (zur Hausen, 2009), such as HPV16 and 18. Additionally, this genus also encompasses some low-risk types, for instance HPV6 and 11, which cause genital warts (Longworth and Laimins, 2004) and HPV2 and 4, which are associated with common warts. Beta HPVs, for example HPV5 and 8, infect cutaneous epithelia and are generally associated with mild skin lesions. HPVs of the Gamma, Mu and Nu genera, including HPV65, 1 and 41, respectively, also infect mainly cutaneous sites and cause benign lesions such as verrucas (Pfister, 1992).

1.4 HPVs and disease

Studies have shown that there is a correlation between the severity of disease caused by different types of HPV and the degree to which they can immortalize cells in culture. Many low-risk types such as HPV6 and 11 are unable to immortalize primary epithelial cells while several high-risk types, such as HPV16, 18 and 31 can (Schlegel et al., 1988) (Pecoraro et al., 1989) (Woodworth et al., 1989).

1.4.1 Low-risk HPVs

As mentioned, low risk-HPVs are generally not linked to cancer but can cause a range of different warts and benign symptoms. However, in individuals that have autoimmune disorders, are immunosuppressed or suffer from the inherited disease epidermodysplasia verruciformis (EV) (Harwood and Proby, 2002, Pfister, 2003), low-risk

papillomaviruses can cause more severe disease or cancer. In the case of EV patients, HPVs of type 5 and 8 from the beta genus can cause non-melanoma skin cancer. Some low-risk HPVs of the alpha genus, predominantly HPV6 and 11 (Gissmann et al., 1982, Mounts et al., 1982), are also implicated in the development of recurrent respiratory papillomatosis (RRP) (Major et al., 2005). This rare condition, found mainly in children, is brought about by HPV infection in the larynx. Without treatment it can be potentially fatal as papillomas can spread to the lungs and obstruct airways (Derkay, 1995, Hsueh, 2009).

1.4.2 High-risk HPVs

Twelve HPV types (16, 18, 31, 33, 35, 39, 45, 51, 52, 56, 58 and 59) are categorized in the high-risk category. Additionally, there are other types that are classed as high-risk due to sequence similarities with the cancer-causing types (Schiffman et al., 2005) although for many there is no clinical data as of yet to prove that they promote malignancy. One such type for which some data exist is cutaneous HPV8, which has been linked to carcinogenesis in immunosuppressed patients (O'Shaughnessy et al., 2007a) and also shown to increase the rate of tumorigenesis in transgenic mice (Schaper et al., 2005).

The cancer type most often associated with these high-risk HPVs is that of the cervix, with over 99 % of all cervical cancer cases being brought about by the virus (zur Hausen, 2002). There are about 530000 new cervical cancer cases worldwide every year with about 275000 deaths (WHO/ICO Information Centre on Human Papilloma Virus (HPV) and Cervical Cancer; http://www.who.int/hpvcentre/en/), making it the second most common cancer associated with women worldwide. HPV16 and 18 alone are involved in bringing about over 70 % of these (Schiffman et al., 2007), with the other high-risk HPV types accounting for the rest (Bosch et al., 1995, Walboomers et al., 1999).

HPV is predominantly transmitted sexually, though it can also be spread through casual physical contact and perinatal vertical transmission (Mammas et al., 2009). When transmitted sexually, infection generally occurs soon after sexual activity is initiated, with the highest prevalence associated with women below the age of 25. However it has been shown that while HPV prevalence decreases with age, there seems to be a second

peak after the age of 55 (Herrero et al., 2000), which may be caused by the reactivation of latent viral infections. The vast majority of infections are cleared rapidly, with one study showing that 70 % of women in their late teens and early 20s showed no signs of HPV DNA within 12 months after the first detection (Ho et al., 1998) and 80 % of women after 18 months. Most cervical cancer cases occur in women that are in their late 40s or early 50s (reviewed in (Baseman and Koutsky, 2005)), and it is thought that they arise from persistent viral infection for years or even decades. Although the mechanism is not yet clearly understood, high-risk HPVs associated with cancer have evolved the ability to persist at some sites of infection, with the development of disease requiring the prolonged aberrant expression of the viral oncogenes E6 and E7 (Schiffman and Kjaer, 2003).

The majority of cervical cancers occur in the transformation zone of the cervix (Arends et al., 1998, Herfs et al., 2013). This is where the ectocervical squamous epithelium and the endocervical columnar cells meet to form the squamo-columnar junction (Burghardt and Ostor, 1983) and is an area of metaplastic change. It is thought that the reason why this zone is highly susceptible to HPV infection is because the basal layer of the epithelium is more easily accessible to the virus and also because immunosurveillance may be perturbed compared to other areas of the cervix (Giannini et al., 2002).

1.4.3 Cervical screening

The lag-phase between infection with HPV and progression to cancer allows for screening of the cervix for HPV-associated lesions. George Papanicolaou first described the cervical smear, or Papanicolaou (Pap) smear test, in 1941 and it involves swabbing the surface of the cervix to remove cells that can be assessed for signs of neoplasia. Many developed countries have population-wide screening programs where women are tested on a regular basis for the presence of HPV and dysplasia. These programs are highly effective which means that over 80 % of all cervical cancer cases arise in the developing world (Jones, 1999), where such programs are not commonly in place. However, the Pap smear test is not 100 % efficient, predominantly because its overall format has not changed in the last 70 years and evaluation of cervical cells still relies on DNA testing and also subjective cytopathological analysis. New screening methods are being developed at the moment with some approaches using multiparameter testing that makes use of a whole panel of

biomarkers associated with neoplastic progression (Baldwin et al., 2003, Middleton et al., 2003, Doorbar, 2007).

1.4.4 Prophylactic vaccines against HPVs

In recent years, two prophylactic vaccines have been developed, based on work using virus-like particles (VLPs) expressing only the main structural L1 protein of HPV (Zhou et al., 1991, Kirnbauer et al., 1992) that stimulated high levels of neutralizing antibodies (Brown et al., 2001, Evans et al., 2001, Harro et al., 2001) and T-cell responses (Emeny et al., 2002) upon injection in human volunteers. Cervarix (GlaxoSmithKline Biologicals) is a bivalent vaccine and protects against HPV16 and 18, associated with 70 % of cervical cancers (Schiffman et al., 2007), while Gardasil (Merck & Co. Inc.) is quadrivalent and protects additionally against HPV6 and 11, which are the two types associated with 90 % of genital warts (Schiffman et al., 2007). While these vaccines have 98 and 100 % efficacy in clinical trials, respectively (Garland et al., 2007, Paavonen et al., 2009), they do not protect against any other high-risk HPV types associated with cancer. Moreover, the lag in the onset of cervical cancer after HPV infection means that it is likely that the reduction in mortality rates will not be significant for 30-50 years (reviewed in (Stanley, 2012)). Furthermore, a recent study in Scotland has shown that public knowledge of HPV and its precise link to cervical cancer, which is essential for good coverage of the UK vaccination program, is low in educated young males and females (McCusker et al., 2013). Hence, further public health campaigns may be necessary to promote the vaccine in the general population. Additionally, due to the high cost of both vaccines, and also the fact that both involve multiple vaccinations, the coverage across developing countries will likely be very low (Agosti and Goldie, 2007).

1.5 Morphological classification of HPV-associated lesions

The development of cervical cancer is preceded by a number of well-defined neoplastic stages. There are two grading systems; one was developed in 1960 and is based on histological analysis of a lesion and uses the cervical intraepithelial neoplasia (CIN) nomenclature. The second one, the Bethesda system, was devised in 1988 (Solomon, 1989) and refers to the risk of the lesion progressing to cancer.

According to the first system, a CIN1 is the mildest form of a lesion, with only one third of the epithelium considered dysplastic, a CIN2 is more severe with up to two-thirds of the epithelium showing signs of dysplasia while in a CIN3 the epithelium is fully dysplastic (Richart, 1973, Woodman et al., 2007). In the newer Bethesda system a low-grade squamous intraepithelial lesion (LSIL) is equivalent to a CIN1 while a high-grade squamous intraepithelial lesion (HSIL) comprises both CIN2 and 3.

In normal cervical tissue, cells within the basal layer are small and uniformly sized and can undergo normal stratification and differentiation within the suprabasal layers. In low-grade lesions (LSILs), cells in the lower third are generally disorganized and lack polarity. Additionally, in the basal layer nuclei are variable in terms of their shape and size, and the presence of koilocytes is common in the upper parts of the epithelium. This is associated with a delay in the onset of the normal differentiation program of cells. In high-grade lesions (HSILs), nuclear abnormalities are more widespread and many more cells have lost polarity. Moreover, differentiation is even further delayed. Within the HSIL classification, a CIN2 lesion will show overall less abnormality than a CIN3. Generally in a CIN3 lesion, cells have completely lost their potential to differentiate.

1.6 HPV16 genome

HPV16 contains an 8 kb double-stranded DNA genome encoding eight ORFs (Fig 1.1). The genome is divided into three major regions separated by two polyadenylation, or poly(A), sites; the early, late and long control regions (LCR) (Zheng and Baker, 2006). The early promoter (P_E), also called p97, lies within the LCR and controls expression of the E1, E2, E4, E5, E6 and E7 genes. The L1 and L2 structural proteins are expressed from the late, differentiation-dependent promoter (P_L), or p670, which lies within the E7 ORF (Smotkin and Wettstein, 1986, Hummel et al., 1992, Grassmann et al., 1996). This promoter can also be used to express E1, E2, E4 and E5 in certain stages of differentiation due to its precise location within the genome (Wang et al., 2009, Johansson and Schwartz, 2013). The LCR of the viral genome lies immediately upstream of the E6 ORF and, in addition to the p97 promoter, also contains several *cis*-acting regulatory elements that are involved in viral genome replication and transcription. The binding sites for several cellular transcription factors have been identified, including Sp1, AP-1, Oct-1 and YY1 (Gloss and Bernard, 1990, Chong et al., 1991, Morris et al., 1993, Lace et al., 2009) which can up- and down-regulate

transcription. There are also glucocorticoid responsive elements (GREs) that, upon binding glucocorticoid, can bring about an increase in replication (Piccini et al., 1997).

The LCR also contains four viral E2 protein binding sites (E2BS1-4) (Androphy et al., 1987). E2 can have both positive and negative regulatory effects on viral transcription (Spalholz et al., 1985, Phelps and Howley, 1987, Bernard et al., 1989, Romanczuk et al., 1990, Bouvard et al., 1994) and it has been suggested that these differential effects may be determined by the physical state of the viral genome within the cells (Bechtold et al., 2003, Schmidt et al., 2005) and also the exact levels of the E2 protein (Steger and Corbach, 1997). Additionally, the E2BS3 is located next to viral origin of replication, which is also found in the LCR (Chiang et al., 1992). When E2 binds to this site it can then recruit E1, a viral DNA helicase, to induce viral replication (Desaintes and Demeret, 1996).

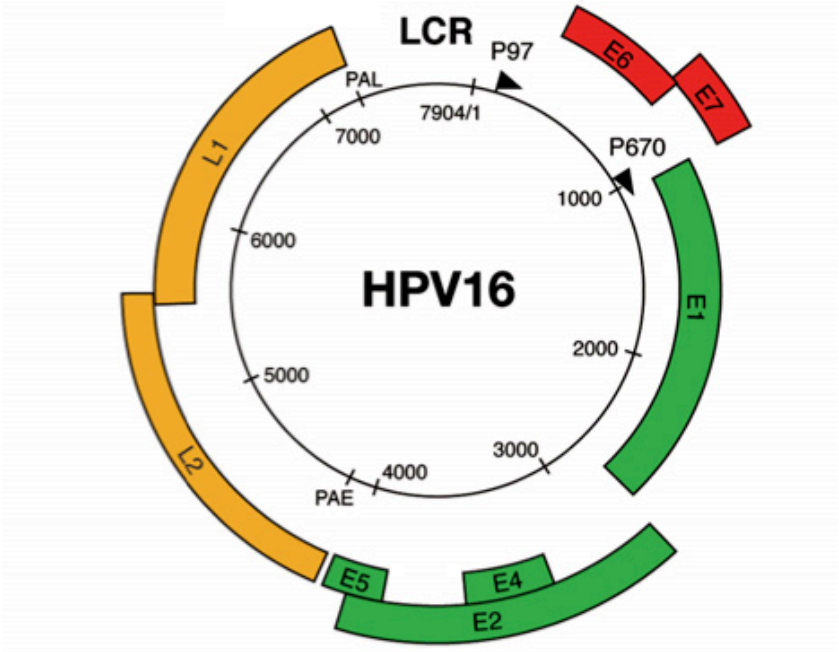

Figure 1.1: The HPV16 genome

The HPV16 genome is a circular, double-stranded DNA genome approximately 8 kb in size and consists of eight ORFs. These encode for six non-structural early proteins, E1, E2, E4, E5, E6 and E7, and two structural late proteins, L1 and L2. The early proteins are expressed from the early promoter, p97, and a subset of these (E1, E2, E4 and E5) along with the two late genes are expressed from the late promoter, p670. There are also two polyadenylation sites, PAE and PAL. The LCR, long control region, is located upstream of the first early ORF and contains not only the viral origin of replication but also *cis*-acting regulatory elements, such as binding sites for cellular transcription factors and the viral E2 protein, that are involved in regulating viral transcription and replication. (This figure has been modified from (Doorbar, 2006)).

1.7 HPV16 transcription

The study of HPV16 transcripts has been done mostly in W12 cells (Doorbar et al., 1990, Milligan et al., 2007), which are keratinocytes isolated from a LSIL cervical lesion containing HPV16 episomes (Stanley et al., 1989). Due to the episomal nature of the viral genomes, these cells are much more suited to studying viral transcripts than cervical cancer cell lines such as CaSki and SiHa, which contain only integrated genomes and do not support the viral life cycle.

All HPV16 genes are transcribed as polycistronic messages from either p97 or p670. The p97 early promoter is regulated by cellular transcription factors binding to their respective sites and also by E2 (Zheng and Baker, 2006). It has been suggested that transcription from the early promoter is quite constant throughout the viral life cycle while the p670 late promoter controls transcription within a certain window of time and relies on cellular differentiation to be activated (Grassmann et al., 1996, Spink and Laimins, 2005). The activation of the late promoter in addition to the early one leads to high levels of E2 transcripts. This causes an inhibition of p97 (McBride, 2008, Thierry, 2009) leading to abrogation of E6 and E7 expression, which allows cells to commit to their terminal differentiation program and thereby enables the virus to finish the late stages of its life cycle (Johansson and Schwartz, 2013).

In addition to these two well-characterized HPV16 promoters, evidence suggests that other promoters exist throughout the genome. One study reported the location of a promoter upstream of p97, within the E6 ORF at nucleotide 542, that controls transcription of a monocistronic E7 message (Glahder et al., 2003). While this specific E7 mRNA is not plentiful, translation initiation from this message is very abundant. Another group (Hansen et al., 2010) has found an additional promoter within the E6 ORF, even further upstream at nucleotide 441. These authors reported that both of these lesser-known promoters (at nucleotides 542 and 441) are involved in regulating gene expression in differentiaing cells. A different study has suggested that another HPV16 promoter can be found at the start of the E1 ORF, however more evidence for this is needed (Milligan et al., 2007). This same group and two others (Doorbar et al., 1990, Ozbun and Meyers, 1997) have also found a promoter at the start of the E4 ORF. It has been suggested that L1 is the first mRNA transcribed from this promoter. This may allow efficient accumulation of the L1 capsid protein and hence packaging of the new

virions (Graham, 2010). A further promoter at the start of the E5 ORF, involved in transcribing L2 mRNA (Milligan et al., 2007), may complement the function of the promoter described above.

The viral polycistronic messages are heavily regulated by constitutive and alternative splicing which give rise to various different mRNA products (Zheng and Baker, 2006). One example of this is the E6/E7 polycistronic or bicistronic transcripts. E6 from high-risk HPVs, such as HPV16, contains an intron and several alternative splice sites to generate various E6 products. In addition to full-length E6 there are at least two truncated species, E6*I and II, that share the N-terminal sequence until the splice junction, lack the intron and have distinct C-terminal truncations (Schneider-Gadicke and Schwarz, 1986, Smotkin et al., 1989). It has been suggested that E6* mRNAs are more abundant than full-length E6 in cervical carcinoma cells (Smotkin et al., 1989, Cornelissen et al., 1990) as this favors the expression of E7 (Zheng et al., 2004, Tang et al., 2006). The mechanism regulating E6 splicing to bring about the alternate transcripts has not been well characterized. A recent study has shown that the presence of epidermal growth factor (EGF) promotes full-length E6 while its absence brings about higher levels of E6* and E7 (Rosenberger et al., 2010). This suggests a mechanism that regulates splicing in differentiating cells, as EGF, also shown by Rosenberger *et al.*, is generally only present at very low levels in areas of the epithelium where differentiation occurs. The E6*I species can be translated into a truncated protein (Schneider-Gadicke et al., 1988) although its exact role and function remains to be elucidated.

1.8 HPV16 viral life cycle

Due to their clinical importance, a big proportion of work on HPV has been carried out using the high-risk types. As mentioned earlier, the virus utilizes the full epithelium to complete its life cycle (Fig 1.2). This means that not only the precise levels but also the exact patterns of viral gene expression are tightly regulated. They are very different in the basal layer, where HPVs first infect and cells are actively cycling, as compared to the upper layers where cells are differentiating. The life cycle is divided into early and late events; early events include mainly viral infection and the establishment of episomes within the host cell nucleus while late events include genome amplification, expression of the structural capsid proteins, assembly of new virions and their subsequent release from the cell.

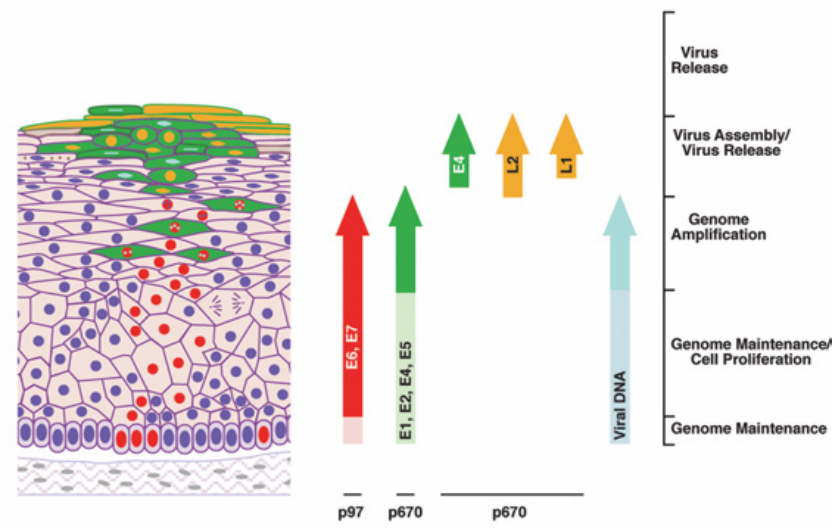

Figure 1.2: The HPV life cycle

HPVs infect the basal layer of the epithelium through microwounds. In basal cells the virus is established within the nucleus in an episomal form at a low copy number. The p97 early promoter brings about expression of E1, E2, E6 and E7, which are required for early life cycle events. As cells are pushed out of the basal layer they remain in cycle, where they normally do not cycle, due to the activities of the E6 and E7 oncoproteins. As cells are pushed further up the epithelium they exit the cell cycle and begin to differentiate which leads to activation of the p670 late promoter. At this point expression of E1, E2, E4 and E5 is augmented to enable viral genome amplification. Once this is completed, L1 and L2 are expressed and package the viral DNA to make new infectious virions that are released from cells when the surface of the epithelium is reached. (This figure has been modified from (Doorbar, 2006)).

1.8.1 Infection of the basal layer of the epithelium

HPVs must gain entry into basal cells of the epithelium. The cervical transformation zone is the place must commonly associated with HPV16-dependent neoplasia as this area is where ectocervical squamous epithelium and the endocervical columnar cells meet (Burghardt and Ostor, 1983). It seems that this area is highly prone to infection due to the basal layer of the epithelium being easily accessible to the virus and also because immunosurveillance may be low (Giannini et al., 2002).

Within a normal epithelium, cells in the basal layer are the only cells that are mitotically active. It is generally accepted that there are two types of cells within the basal and adjacent suprabasal layers; epidermal stem cells and transit amplifying cells. Stem cells in the basal layer divide and exit their compartment to enter the first suprabasal layer, giving rise to transit amplifying cells (Watt, 2001, Fuchs et al., 2004). These stem cell daughter cells can then undergo a finite number of cell divisions before exiting the cell cycle and committing to the cellular terminal differentiation program (Kolly et al., 2005). It is thought that the virus must gain entry into a stem cell so that the infection can persist (Schmitt et al., 1996, Egawa, 2003) but conclusive proof as to whether this is true does not exist.

The proposed mechanism of HPV infection implicates the two capsid proteins, L1 and L2, in the process (Schiller et al., 2010). L1 binds to heparan sulfate proteoglycans located on the basement membrane that become accessible to the virus via microwounds in the tissue (Joyce et al., 1999). This leads to the cleavage of L2 by enzymes such as furin (Richards et al., 2006), which in turn allows L1 to bind to receptors, such as alpha-6 integrin (Evander et al., 1997), on the surface of keratinocytes. Subsequently the virus is internalized by endocytosis, which may involve both clathrin- and cavelolae-mediated pathways depending on the specific HPV type (Bousarghin et al., 2003).

1.8.2 Early events

1.8.2.1 Establishment and maintenance of HPV episomes

After infection, the virus is uncoated and the viral genomes are established as episomes within the nucleus of the cell. The virus must first undergo a transient replication phase

to increase its own copy number before replicating along with cellular DNA and dividing equally into two daughter cells with every cell division (Kadaja et al., 2009). It is thought that the virus is maintained at a fairly constant copy number, of between 10-200 copies (De Geest et al., 1993), in basal cells.

1.8.2.2 Early proteins

The two viral replications proteins, E1 and E2, are expressed from the early p97 promoter to enable viral DNA replication. E2 can bind to the viral origin of replication and recruit the E1 helicase (Masterson et al., 1998), which in turn promotes binding of cellular replication proteins (Kadaja et al., 2009). It has been suggested that HPV must infect cells that can undergo mitosis (Pyeon et al., 2009) and that phosphorylation of cyclin E/CDK2 (cyclin dependent kinase 2) and cyclin A/CDK2 complexes are important for nuclear localization of E1 (Deng et al., 2004). Another role of E2 is to anchor viral genomes to mitotic chromosomes during cell division, to promote their equal segregation amongst daughter cells and localization to the nucleus (You et al., 2004, Feeney and Parish, 2009).

Due to the lack of sensitive detection methods it is not entirely clear which other viral proteins are expressed in basal cells. However, several studies in monolayer cell culture have shown that E6 and E7 (Thomas et al., 1999), or even just E7 (Flores et al., 2000, Laurson et al., 2010) or just E6 (Nicolaides et al., 2011), are important for the persistence of viral episomes. Therefore it seems likely that the viral oncoproteins are expressed from the early p97 promoter in the basal layer.

1.8.2.3 Cell proliferation

As mentioned above, in an uninfected epithelium only basal cells are mitotically active and when they are pushed out of the basal layer, they exit the cell cycle and commit to terminal differentiation. However, this is detrimental to the virus, as it relies on the host replication machinery to copy its own genome. Therefore, in an infected epithelium, the virus can bring about a delay in the onset of differentiation and push cells to cycle, even in suprabasal layers. This involves the expression of the viral E6 and E7 proteins, which can push cells into S phase (Dollard et al., 1992, Cheng et al., 1995). The most well characterized function of the E7 protein to enable DNA replication, is its ability to bind to and degrade the Rb protein (Dyson et al., 1989, Boyer et al., 1996), which causes

release of E2F and in turn promotes G1/S phase transition (Zerfass et al., 1995, Black and Azizkhan-Clifford, 1999). E6 can bind to and bring about degradation of the p53 protein to inhibit apoptosis (Scheffner et al., 1990, Werness et al., 1990). Additionally high-risk E6 can also bind to and promote degradation of PDZ proteins to bring about epidermal hyperproliferation (Nguyen et al., 2003, Lee and Laimins, 2004).

1.8.3 Late events

While the combined activities of E6 and E7 push suprabasal cells into S phase, these cells must eventually stop dividing and begin their terminal differentiation program. This is necessary for activation of the late differentiation-dependent p670 promoter, and subsequent expression of the late proteins (Grassmann et al., 1996).

1.8.3.1 Genome amplification

As cells migrate closer to surface of the epithelium, the virus must amplify its own genome, up to several 1000-fold (Bedell et al., 1991), in preparation for packaging new virions. The expression of E1, E2 (Klumpp and Laimins, 1999), E4 and E5 (Hummel et al., 1992) from the p670 promoter is necessary to allow genome amplification to take place. Additionally, it has been suggested that in this stage of the life cycle, the virus switches to rolling circle replication that requires only a single initiation event, and that this mechanism contributes to the high levels of viral DNA observed (Flores and Lambert, 1997).

In the upper layers it is known that E4 is expressed abundantly. It is first detected in the apical most cell layers of the epithelium that express E7 and are in S phase, and hence this is where the switch from early to late gene expression is proposed to occur (Peh et al., 2002, Middleton et al., 2003, Peh and Doorbar, 2005). Additionally, this is also where the first amplified viral genomes may arise (Doorbar et al., 1997). E4 has been shown to arrest cells in G2 phase, preventing mitotic entry (Davy et al., 2002, Davy et al., 2005). This is hypothesized to keep the cells in a pseudo-S phase state that enables amplification of the viral genomes. E7 is thought to aid in this process by inducing expression of the host cell replication machinery that is essential for amplifying genomes (Flores et al., 2000). The precise role of E5 is not entirely clear. It seems that E5 can promote an environment that is conducive to viral DNA replication, as well as increase transcription from the late promoter (Fehrmann et al., 2003).

1.8.3.2 Virus assembly and release

The last stage of the viral life cycle involves packaging new infectious virions that can then be shed and go on to infect other cells. L1 and L2 capsid proteins are expressed, typically in cells that also express E4 (Peh et al., 2002), and localize to the nucleus (Doorbar and Gallimore, 1987, Day et al., 1998) where encapsidation of the new amplified viral genomes occurs. The encapsidation process may be enhanced by E2 (Day et al., 1998, Zhao et al., 2000). As HPV is a non-lytic virus, new progeny virions are only released when cells at the very surface of the epithelium are shed (Bryan and Brown, 2001). However, the E4 protein may contribute to viral release as it can disrupt the keratin network of cells and make the whole epithelium more fragile (Doorbar et al., 1991, Wang et al., 2009, McIntosh et al., 2010). To do this, E4 can bring about the phosphorylation and subsequent ubiquitylation of keratin in cells, in much the same way that is observed in response to a stress stimulus (McIntosh et al., 2010).

1.8.4 Abortive infections

As mentioned previously, HPVs can cause both high- and low-grade disease. Generally a low-grade squamous intraepithelial lesion (LSIL) constitutes a productive HPV infection, where new infectious virions are produced (reviewed in (Doorbar et al., 2012)). In sites where a productive infection is inefficiently supported, such as in the cervical transformation zone, the virus can cause an abortive infection, which is associated with a high-grade squamous intraepithelial lesion (HSIL) (reviewed in (Doorbar, 2006)). In these types of lesions, progeny virions are not produced and if left untreated they can progress to cancer. An example of site-specific PV malignancy is the cottontail rabbit papillomavirus (CRPV), which can cause productive infections in its natural cottontail rabbit host but is associated with tumor outgrowth and cancer development in domestic rabbits (Hu et al., 2007).

Within the HSIL classification a CIN3 describes a lesion that is more severely deregulated in terms of viral gene expression patterns than a CIN2 (reviewed in (Doorbar et al., 2012)). As a lesion becomes more high-grade, the differentiation program of cells is further delayed and this is associated with less, or even no, expression of the late proteins such as E4, L1 and L2 (Middleton et al., 2003). Moreover, there are high levels of the viral E6 and E7 oncoproteins. This allows cells in

the upper layers of the epithelium (which would be differentiating in a productive infection) to stay in cycle and retain their pseudo-S phase state. Aberrant expression of E6 and E7 predisposes cells to the accumulation of genetic changes, which further contribute to neoplastic progression (reviewed in (Doorbar et al., 2012)). High-grade disease is also associated with the integration into host chromosomes of the viral genomes, which is promoted by viral deregulation but at the same time promotes further deregulation. In vulval intraepithelial lesions (VINs) it seems that integration of HPV16 genomes is generally associated with high levels of E7 and also AKT1 (Ekeowa-Anderson et al., 2012). Integrated genomes usually do not express any E1 and E2 and hence at least some of the negative regulation of the early p97 promoter that is normally brought about by E2, is lost, which leads to aberrant E6 and E7 expression (Steger and Corbach, 1997). Integration has also been shown to correlate with an increase in E6 and E7 mRNA stability and higher E6 and/or E7 protein levels (Jeon and Lambert, 1995, Dong et al., 1994, Alazawi et al., 2002).

1.9 Immune response and clearance of HPV infection

One of the main reasons why, in some situations, an HPV infection can persist for so many years without being cleared by the immune system is because the virus is non-lytic and therefore does not cause inflammation at the site of infection. Moreover, due to the fact that PVs infect the epithelium, neither the site of infection nor that of viral release are close to blood vessels or the lympathic system (Stanley, 2009). Furthermore, both E6 and E7 have been shown to interfere interferon (INF) signaling (Barnard and McMillan, 1999, Park et al., 2000, Ronco et al., 1998) and hence repress IFN-inducible genes (Chang and Laimins, 2000, Nees et al., 2001).

Moreover both E6 and E7 can bring about a reduction in the levels of E-cadherin (Matthews et al., 2003, Laurson et al., 2010) which correlates with a decrease in antigen-presenting Langerhans cells (Hubert et al., 2005), leading to a reduction of the anti-viral immune response. Interestingly, several other tumor viruses including Hepatitis B (Liu et al., 2006) and C (Iso et al., 2005) and Epstein-Barr viruses (Fahraeus et al., 1992) also share this ability to suppress E-cadherin.

Although the virus seems to be have evolved a number of mechanisms to avoid the immune system it remains to be said (as mentioned earlier) that most infections are

cleared rapidly, with up to 80 % of women in their late teens and early 20s showing no signs of HPV DNA after 18 months of initial detection (Ho et al., 1998). Additionally, the fact that many low-risk viruses can cause malignant disease in immunocompromised or immunosuppressed patients or people that have EV, shows that the immune system does play a pivotal role in the clearance of infection. Moreover in response to lesions of different grades (Coleman and Stanley, 1994) and even just the presence of the viral proteins E2 and E6 (Welters et al., 2003), T-cell responses have been observed.

1.10 Papillomavirus models

Studying the full HPV life cycle has proved challenging due to its dependence on the full stratified, differentiating epithelium. This means that although vast amounts of work have been done in monolayer cell cultures, from these it has not always been easy to infer the function of the viral proteins in the late stages of the life cycle in the upper layers. This means that most monolayer cultures can only be used to study the virus in its basal cell environment. A lot of this work has been done in keratinocytes, including primary foreskin keratinocytes (Thomas and Banks, 1999), immortalized foreskin keratinocytes (NIKS) (Flores et al., 1999) and the W12 line. To study the late stages of the life cycle a lot of clinical samples are used but these are not easy to come to and they are generally removed from patients with high-grade disease, so studying the productive viral life cycle is difficult.

Another challenge of studying HPV is the fact that it very host-tropic and does not have the same effect in other species as humans. The first PV to be identified in animals was the cottontail rabbit PV (CRPV) (Shope and Hurst, 1933), which means that these rabbits have been used to study the virus for many years. CRPV can cause cutaneous lesions that sometimes have the capacity to progress to malignancy. Although mice have been used extensively to study PVs, including HPVs, it was only recently that the first murine papillomavirus was discovered (Ingle et al., 2011). The fact that the genetic backgrounds in mice can be controlled so precisely and that they have very well characterized immune systems, for which an extensive range of reagents are available, means, that now that murine PVs have been described, this laboratory model will prove even more useful in the coming years.

1.10.1 The organotypic raft culture model system

Over the past decade the organotypic raft culture system has further facilitated the study of the full life cycle of PVs (Lambert et al., 2005, Wilson and Laimins, 2005). Raft cultures are a three-dimensional cell culture system in which keratinocytes can form a fully stratified and differentiated epithelium. To achieve this, keratinocytes are seeded on a dermal equivalent support structure made of mainly collagen and fibroblasts, thus mimicking a real dermis. Upon seeding on the dermal equivalent, cells are first allowed to grow to confluence to form a confluent basal layer and then exposed to the air and fed with high calcium medium to promote differentiation and stratification. After the rafts are harvested they can by sectioned and stained, like clinical biopsies, allowing for the visualization of viral and cellular gene expression patterns. Although other methods to induce differentiation in keratinocytes do exist, including the use of high-calcium medium (Hennings et al., 1980) or methylcellulose (Ruesch et al., 1998), only rafts enable the production of a stratified epithelium, and they have proven to be a very useful tool. Additionally, raft cultures have also been used for producing virions for infectivity studies (McLaughlin-Drubin et al., 2004).

1.11 The E7 protein

E7 is one of the viral oncoproteins and for HPV16, it is approximately 11 kDa in size. It can bind to several cellular proteins and its main functions are brought about by these interactions. E7 has been shown to immortalize keratinocytes in culture (Halbert et al., 1991) and can cause hyperplasia in mouse epithelium (Herber et al., 1996).

As described in more detail above, only cells within the basal layer of the epithelium are mitotically active. However, to complete its life cycle the virus needs to extend the S phase compartment to allow replication of its genome. The major role of E7 is to keep cells in cycle and delay the onset of terminal differentiation to allow the virus to replicate (McLaughlin-Drubin and Munger, 2009). A summary of the oncogenic activities of the E7 protein is shown in Figure 1.3.

Figure 1.3: Oncogenic activities of the HPV E7 protein

The major mechanisms used by E7 (white boxes) to bring about cellular characteristics commonly associated with human tumors (black boxes) as described by Hanahan and Weinberg in 2000.

1.11.1 Association with Rb and effects on cell cycle regulators

The most well established role of high-risk E7 is its ability to bind to primarily Rb but also p107 and p130, which together comprise the pocket protein family (Cobrinik, 2005), and target them for proteasomal degradation (Dyson et al., 1989, Munger et al., 1989, Davies et al., 1993, Boyer et al., 1996, Jones and Munger, 1996). The main role of phosphorylated Rb is to bind to the transcription factor E2F (Chellappan et al., 1991) and thereby prevent it from carrying out its cell cycle progression promoting role (reviewed in (Donjerkovic and Scott, 2000)). E7 targets preferentially these phosphorylated forms of Rb (Boyer et al., 1996), bringing about the release of E2F. This allows E2F to activate its downstream targets that include cyclin A and E, minichromosome maintenance proteins (MCMs) and the proliferating cell nuclear antigen (PCNA) (Cheng et al., 1995, Leone et al., 1998, Chien et al., 2000).

E7 from low-risk viruses can also bind to Rb, though with a much lower efficiency than high-risk E7. This might explain why low-risk E7 cannot bring about the transformation of cells (Gage et al., 1990, Heck et al., 1992), yet can still extend the S phase compartment and cause hyperproliferation in the suprabasal layers of the epithelium. It has also been shown that while high-risk E7 can bring about degradation of all three members of the pocket protein family, low-risk E7 can only destabilize p130 (Zhang et al., 2006). Both p107 and p130 share the role of Rb to modulate E2F levels. Rb degradation by E7 is more abundant in undifferentiated cells, such as those found in the basal layer, than p130 degradation which has been observed predominantly in differentiating suprabasal cells (Collins et al., 2005). Hence, inefficient Rb degradation in favor of p130 destabilization may also contribute to the lack of transformation potential of low-risk E7.

The ability of HPV E7 to interact with Rb seems to be a function that is shared with other tumor viruses as both SV40 large T antigen (DeCaprio et al., 1988) and also the adenovirus E1A protein (Whyte et al., 1988) have been attributed this role.

Furthermore, E7 from both high- and low-risk HPVs have been show to increase the activity of CDK complexes. This has been observed for both the cyclin E/CDK2 complex, involved in G1/S transition, and also the cyclin A/CDK2 complex, which plays a role in pushing cells from G2 phase into mitosis (Arroyo et al., 1993,

Tommasino et al., 1993, He et al., 2003, Nguyen and Munger, 2008). Moreover, E7 can repress the function of the CDK inhibitors p21 and p27, thereby further promoting cell cycle progression (Zerfass-Thome et al., 1996, Funk et al., 1997).

1.11.2 Association with other cellular binding partners

Another role of E7 is its ability to bind to histone deacetylase 1 (HDAC1) (Brehm et al., 1999). HDACs normally repress transcription, as they allow histones to wrap DNA tightly, thus hindering access of transcription co-activators to DNA (de Ruijter et al., 2003). The interaction of E7 with HDAC1 brings about further transcriptional activation by E2F (Longworth et al., 2005). Additionally, E7 can also bind and augment the activity of members of the AP-1 family of transcription factors, such as c-Jun and c-Fos (Antinore et al., 1996). The AP-1 family can regulate several important cellular processes that include proliferation and differentiation (Hess et al., 2004).

1.12 The E6 protein

E6 is one of the viral oncoproteins and is just over 150 amino acids long (Foster et al., 1994) and approximately 18 kDa in size for HPV16. Like E7, E6 can bind to many different cellular proteins and additionally bind directly to DNA (Ristriani et al., 2000). Both low- and high-risk E6 can bind to the cellular E3 ubiquitin ligase, E6-associated protein (E6AP). It is through this interaction that E6 can bring about many of its functions, including the degradation of p53 and some PDZ proteins. However, it seems that the relationship between E6 and E6AP is very complex as their binding has been shown to lead to the degradation of E6AP via the proteasome (Kao et al., 2000). At the same time E6AP can stabilize the E6 protein itself to protect it from degradation (Tomaic et al., 2009). Hence it appears that the association of E6 and E6AP is controlled by several factors, including their precise levels and localization within the cell and signal transduction pathways that are active at different stages in the viral life cycle and throughout neoplastic progression.

E6 can interfere with a number of important cellular pathways to modulate apoptosis, proliferation and immune evasion. The presence of this oncoprotein alone has been shown to induce hyperplasia and also to transform epithelial cells in transgenic mice (Song et al., 1999, Nguyen et al., 2003). The oncogenic activities of the E6 protein and cellular interaction partners are summarized in Figure 1.4 and 1.5, respectively.

Figure 1.4: Oncogenic activities of the HPV E6 protein

The major processes targeted by E6 (white boxes) to bring about cellular characteristics commonly associated with human tumors (black boxes) as described by Hanahan and Weinberg in 2000.

Figure 1.5: A summary of cellular proteins affected by high-risk E6

Proteins marked with an asterisk are affected by E6 at a transcriptional level while all others are directly bound by E6. These include the E3 ubiquitin ligase E6AP, transcriptional regulators, mediators of apoptosis, immune recognition, chromosomal stability, epithelial organization and differentiation and those involved in cell-cell adhesion, polarity and proliferation.

1.12.1 Association with p53

The most well characterized activity of E6 is its ability to bind to and degrade p53 (Scheffner et al., 1990, Werness et al., 1990), mediated by E6AP (Huibregtse et al., 1991, Scheffner et al., 1993). The transcription factor p53 is a key tumor suppressor in cells and in response to stress it can initiate DNA repair, bring about growth arrest of cells and initiate apoptosis if DNA damage is irreparable (Gottlieb and Oren, 1996). When E6 is not present, E6AP does not bind to p53 (Huibregtse et al., 1991). Due to the important role of p53 in signal transduction, its mutation in cancers is widespread, with more than 50 % of all cancers being shown to have them (Vogelstein et al., 2000). As E6 can efficiently degrade p53, cervical cancers are usually not associated with mutations in this protein. Additionally, other tumor viruses such as the Simian viruses 40 (SV40), a type of polyomavirus, and adenoviruses have proteins that share the ability of E6 to bind to p53 (Lane and Crawford, 1979, Sarnow et al., 1982).

In normal cells, when p53 does not have to fulfill its role, its levels are regulated by the cellular E3 ubiquitin ligase Mdm2 (Haupt et al., 1997). At times when p53 needs to be stabilized, for example in instances of DNA damage or abnormal cell cycle activity, Mdm2 is phosphorylated resulting in the loss of its ability to bind to p53. As mentioned earlier, E7 can drive keratinocytes to cycle actively at times when they should not be. Thus, in cells expressing only E7 this results in the up-regulation of p53 levels (Demers et al., 1994, Laurson et al., 2010). However, during normal HPV infection E6 can circumvent this and bring about degradation of p53 thus allowing cells to stay in cycle and the virus to replicate its genomes.

Both high- and low-risk E6 proteins can bind to p53, however only the high-risk variety can bring about its degradation (Foster et al., 1994). This difference is brought about by the ability of high-risk E6 to associate with the main DNA-binding region of p53 (Li and Coffino, 1996), which is a requirement of E6-mediated p53 degradation. In contrast, low-risk E6 is associated with binding to the C-terminal region of p53. Additionally, in low-risk HPV E6-expressing cells, p53 is sequestered to the cytoplasm (Sun et al., 2008), where it cannot carry out its normal function. This shows that irrespective of its ability to degrade p53, low-risk E6 can still impact on the function of this protein.

1.12.2 Inhibition of apoptosis

While degradation of p53 by E6 can bring about inhibition of apoptosis, E6 can interfere directly with the extrinsic and intrinsic apoptosis pathways independently of p53. E6 can bring about the degradation of the Fas-associated death domain (FADD) and procaspase 8 (Filippova et al., 2004, Garnett et al., 2006), which are involved in the extrinsic pathway, in response to viral infection. Additionally, E6 can target Bak for proteasomal degradation (Thomas and Banks, 1998, Jackson et al., 2000), which is part of the intrinsic apoptosis pathway that is activated in response to cellular stress and DNA damage.

1.12.3 Degradation of PDZ proteins by E6 and disruption of cell-cell adhesion and polarity

The stratified epithelium consists of several cell layers, each with highly regulated gene expression patterns. In order for each cell to fulfill its appropriate role, it needs to be sent correct signals from neighboring cells and also from the extracellular matrix (ECM). For this reason both cell-cell adhesion and apico-basal polarity of cells need to be very tightly regulated (Bilder, 2004). In uninfected epithelium only basal cells are mitotically active. This is due to their attachment to the basement membrane and receiving appropriate proliferation signals. When HPV is present cells are driven to cycle in suprabasal layers by E7 (as outlined above) but also by E6, in part by its ability to disrupt cell adhesion and polarity.

PDZ-domain proteins are a large group of proteins that all have one or more PDZ domains involved in the interaction with other proteins. PDZ proteins derive their name from the first letter of the three proteins in which the domain was first discovered: post synaptic density protein (PSD95), *Drosophila* disc large tumor suppressor (Dlg1), and Zonula occludens-1 protein (ZO-1) (Kennedy, 1995). The high-risk E6 protein can bind to and bring about the degradation of certain cellular PDZ proteins due to a PDZ-binding motif located on its extreme carboxy terminus. The degradation mediated by E6 can occur in both E6AP-dependent (Nakagawa and Huibregtse, 2000) and -independent (Pim et al., 2000, Storrs and Silverstein, 2007) manners. E6 from low-risk viruses do not have a PDZ motif and are unable to bind to PDZ proteins (Kiyono et al., 1997). The PDZ proteins that have been studied most with respect to their interaction with E6 are hScrib, hDlg and MAGI-1, -2 and -3, and these are all involved in epithelial polarity

and scaffolding (Kiyono et al., 1997, Gardiol et al., 1999, Lee et al., 1997, Nakagawa and Huibregtse, 2000, Thomas et al., 2002).

The hScrib and hDlg genes are the human homologues of the *Drosophila melanogaster scribble* and *disc large* genes, respectively (Lue et al., 1994, Dow et al., 2003). The resulting gene products are involved in several important functions in the cell, including signal transduction, cell polarity and proliferation, and they have been classified as tumor suppressors (Woods and Bryant, 1989, Bilder et al., 2000, Dow et al., 2003). They can localize to adherens junctions, in an E-cadherin-dependent manner (Navarro et al., 2005), as part of the Scribble polarity complex and as such have been attributed a role in the formation of these cell-cell junctions (Bilder et al., 2000, Firestein and Rongo, 2001). Moreover, non-membrane-associated forms of these proteins have been described (McLaughlin et al., 2002, Garcia-Mata et al., 2007) and in the case of hDlg its precise localization to the nucleus or cytoplasm seems to be regulated by phosphorylation (Mantovani et al., 2001). Interestingly, highly phosphorylated forms of the protein seem to be most susceptible to degradation by E6 (Massimi et al., 2006, Narayan et al., 2009). Additionally, both hDlg and hScrib can bind to the adenomatous polyposis coli (APC) protein (Matsumine et al., 1996, Takizawa et al., 2006), via the PDZ-binding motif of the latter. APC forms part of the destruction complex of the canonical Wnt pathway that actively degrades β-catenin in the absence of Wnt ligands, to prevent activation of β-catenin transcriptional targets (Logan and Nusse, 2004). Binding of both hDlg and hScrib to APC has been shown to be involved in this cell cycle inhibitory function (Ishidate et al., 2000, Nagasaka et al., 2006). Hence, degradation of these two PDZ proteins by E6 may lead to malignancy by several different mechanisms. (A recent study has been shown that E6 can also augment Wnt signaling in an E6AP and PDZ-motif independent manner (Lichtig et al., 2009).)

The various MAGI PDZ-domain proteins are primarily involved in regulation of cell proliferation and differentiation due to their role in the formation of tight junctions (Balda and Matter, 2003). Additionally, MAGI can also stabilize the tumor suppressor Phosphatase and tensin homolog (PTEN) (Wu et al., 2000b) and thus facilitate its role of inhibiting growth-promoting signaling (Stambolic et al., 1998). Based on these roles of the MAGI proteins it seems feasible that their disruption by E6 can promote neoplastic progression.

Studies looking at the PDZ motif of E6 have shown that different types of HPV bind to PDZ proteins with varying affinity. In the case of HPV16 and 18, this is brought about by a slight amino acid variation within their PDZ motifs (Thomas et al., 2005). While MAGI is targeted equally well by both types, it seems that 18E6 binds predominantly to hDlg with only minor effects on hScrib, while 16E6 can bring about degradation of mainly hScrib (Pim et al., 2000, Thomas et al., 2001).

While the interaction of E6 with PDZ proteins has been studied predominantly in terms of progression to malignancy, a role of PDZ proteins in the productive viral life cycle, although not well characterized, has also been suggested. It seems that PDZ proteins are involved in the persistence of viral episomes (Lee and Laimins, 2004), and that this may rely on the ability of E6 to bind hScrib and other PDZ-domain proteins (Nicolaides et al., 2011).

Cellular PDZ proteins have been shown to interact with proteins from other viruses, including the Tax protein of Human T-lymphotropic virus Type 1 (HTLV-1) and the Adenovirus 9 E4ORF1 protein (Lee et al., 1997, Glaunsinger et al., 2000). These two proteins and also the influenza virus protein NS1, also have a PDZ motif (Obenauer et al., 2006).

1.12.4 Induction of telomerase activity

One mechanism by which E6 can bring about immortalization of cells (Band et al., 1991), is through activation of telomerase. Telomerase is a ribonucleoprotein that adds specific DNA sequence repeats to telomeres at the end of chromosomes to avoid loss of important coding DNA with each replication event (reviewed in (Wai, 2004)). In normal somatic cells, unlike stem cells, telomerase is expressed at very low levels and this contributes to the finite life-span of a cell (Hayflick, 1965). Telomerase is made up of two components, the catalytic subunit (hTERT) and the RNA template (TERC). E6 can bring about an increase in hTERT transcription (Veldman et al., 2001) and also interact directly with the enzyme and with telomeres (Liu et al., 2009). Targeting of telomerase has been shown to occur independently of p53 (Klingelhutz et al., 1996) and through both E6AP-dependent (Liu et al., 2005) and -independent (Sekaric et al., 2008) mechanisms.

1.12.5 Association with other cellular binding partners

The functions of E6 described so far are the most well studied and characterized ones. In addition to the proteins already mentioned, E6 can interact with a variety of other cellular proteins and these associations correlate with neoplastic progression. One such target is E6-targeted protein 1 (E6TP1), a GTPase-activating protein. High-risk E6 can bring about its degradation (Gao et al., 1999) in an E6AP-dependent manner (Gao et al., 2002). Furthermore, E6 from both low- and high-risk HPVs have been shown to bind to (Kukimoto et al., 1998) and, in the case of HPV18 E6, degrade MCM7 (Kuhne and Banks, 1998). One of the functions of MCM7 is to allow DNA to replicate only once per cycle (Chong et al., 1996), hence its interaction with E6 contributes to genomic instability. The association of E6 with several proteins involved in DNA repair such as XRCC1 (Iftner et al., 2002) and O(6)-methylguanine DNA methyl-transferase (MGMT) (Srivenugopal and Ali-Osman, 2002) further contributes to genomic instability. Additionally, E6 can bring about the degradation of TIP60 (Jha et al., 2010), a histone acetyltransferase involved in regulation of transcription and the DNA damage response (Gorrini et al., 2007), one of its main targets being p53. TIP60 can repress the viral p97 early promoter (Jha et al., 2010) and its degradation, mediated by E6, may counteract this.

1.13 E6 and E7 interaction with adherens junction proteins

E6 and E7 together have transforming potential through their interactions with adherens junction proteins. Adherens junctions are important adhesive junctions found at specific cell-cell contact sites in the epithelium and allow adjacent cells to bind to each other and form connections (reviewed in (Balda and Matter, 2003)). They play essential roles in cell adhesion, recognition and motility, epithelial polarity, contact inhibition and differentiation. The main component of the junction is the cell adhesion receptor E-cadherin and it associates with β-catenin, and also indirectly with α-catenin through β-catenin. Increasing grades of HPV-dependent neoplasia have been linked to a reduction of E-cadherin expression (Vessey et al., 1995). Both E6 and E7 have been shown to not only associate directly with the E-cadherin receptor (Wilding et al., 1996, Caberg et al., 2008) but also reduce its levels (Matthews et al., 2003, Yuan et al., 2009, Laurson et al., 2010). This leads to loss of adherens junctions-mediated cell-cell adhesion and polarity.

Another role of E-cadherin is to sequester β-catenin out of the nucleus to the cell membrane (reviewed in (Balda and Matter, 2003)). β-catenin is a transcription factor that is the key downstream effector of the Wnt pathway (reviewed in (Huelsken and Behrens, 2002)). It forms a complex with LEF/TCF transcription factors to transactivate proteins such as cyclin D and c-Myc, which promote cell cycle progression. Hence loss of E-cadherin, through E6 and E7, can lead to hyperproliferation of cells.

Moreover, hDlg and hScrib, discussed in more detail earlier, are recruited to adherens junctions in an E-cadherin-dependent manner (Navarro et al., 2005), as part of the Scribble polarity complex. The PDZ proteins can stabilize the linkage between E-cadherin and the catenins (Qin et al., 2005) and also seem to have a role in the formation of the junction (Bilder et al., 2000, Firestein and Rongo, 2001). E6 can bind to and degrade both hDlg and hScrib thereby destabilizing adherens junctions.

1.14 Cellular contact inhibition

Contact inhibition of proliferation refers to the inherent ability of cells to stop growing in a density-dependent manner. The concept first came about 50 years ago to explain why cells in monolayer culture stop growing upon reaching confluence. As the term "contact inhibition" suggests, growth arrest is brought about by contact between cells. It involves the association of cell surface receptors on adjacent cells and subsequent repression of growth promoting pathways that are affected by the receptors (reviewed in (McClatchey and Yap, 2012)). One such cell receptor is E-cadherin, which is an essential component of adherens junctions, discussed in more detail above. It has been shown that in cancer cell lines, the ability of cells to grow past confluence is mediated by an absence of E-cadherin (St Croix et al., 1998). Moreover, expressing E-cadherin in E-cadherin deficient skin cancer cells reduces tumor formation upon implantation into mice (Navarro et al., 1991).

The Hippo signal transduction system is a major pathway involved in regulating growth and also apoptosis. Its key effector of proliferation is Yes-associated protein (YAP) 1, which, in its unphosphorylated form, is a transcriptional co-activator of growth-promoting genes such as c-Myc (Zhao et al., 2011). The Hippo pathway has been implicated in contact inhibition due the observation that YAP1 is phosphorylated and

relocates to the cytoplasm, and is thus unable to fulfill its role, when monolayer cultures reach confluence (Kim et al., 2011, Schlegelmilch et al., 2011). This nuclear exclusion of YAP1 is dependent on the presence of α-catenin (Schlegelmilch et al., 2011, Silvis et al., 2011), which is another component of adherens junctions.
Another key regulatory pathway of growth, and hence in contact inhibition, is the Notch signal transduction pathway which will be discussed in more detail in the next section.

Generally, transformed keratinocytes, such as those expressing the HPV oncoproteins E6 and E7, can present with a pattern of proliferation where cells have the tendency to grow past the point of confluence. Additionally, it has been shown that both proteins can repress E-cadherin (Matthews et al., 2003, Yuan et al., 2009, Laurson et al., 2010). Hence, it is highly likely that in these cells normal contact inhibition pathways are attenuated.

1.15 Notch signal transduction pathway

The Notch signaling pathway (Figure 1.6) is a highly conserved signal transduction system that is present in most multi-cellular organisms (Artavanis-Tsakonas et al., 1999) and is involved in regulating cellular proliferation and differentiation. The Notch gene was originally discovered in *Drosophila melanogaster,* when it was observed that those individuals with a mutant Notch allele had "notches" at the margin of their wings (Morgan, 1917). The Notch family consists of four single spanning cell-surface receptors (Notch1-4) and five Notch ligands of the delta and jagged family: Delta-like-1, -3 and -4 and Jagged-1 and -2 (reviewed in (Dotto, 2008, Watt et al., 2008, Borggrefe and Liefke, 2012)). A simplified schematic of the Notch receptor is shown in Figure 1.7. When an appropriate ligand binds to its receptor, activation of Notch is brought about by two sequential cleavages. The first one is mediated by ADAM metalloproteinase and occurs extracellularly. NICD subsequently gets cleaved intracellularly by the gamma secretase complex, consisting of, among other proteins, presenillin (PS), anterior pharynx-defective 1 (APH-1) and nicastrin. The released NICD can then translocate to the nucleus where it associates with DNA-bound RBPJ (Recombining binding protein suppressor of hairless). The interaction with RBPJ is brought about by the RAM domain (RBPJ Associated Molecule) and ankyrin repeat region, or ANK domain, of NICD (Johnson and Barrick, 2012). In the absence of Notch, RBPJ is a repressor complex (Dou et al., 1994) and can inhibit transcription of

its target genes through the recruitment of the histone deacetylase HDAC1 (Kao et al., 1998). However when NICD is bound, other proteins such as MAML1 (Mastermind-like protein 1) (Petcherski and Kimble, 2000, Wu et al., 2000a)and p300 (E1A binding protein p300) (Oswald et al., 2001) are recruited to the, now, activator complex and this enables transcriptional regulation of Notch targets including, amongst many others, HES1 (Iso et al., 2003), p21, p27 and AP-1 (reviewed in (Borggrefe and Liefke, 2012)).

In mammals, Notch signaling is regulated on another level by three Fringe N-acetylglucosamine-transferases, called lunatic, manic or radical fringe. These enzymes can bring about a so-called "fringe" effect whereby Notch signaling through the Delta-like ligands is promoted while Jagged ligands can not bring about Notch activation (Yang et al., 2005, Thomas and van Meyel, 2007).

Figure 1.6: Simplified schematic of the Notch pathway

Upon binding of an active ligand, the Notch receptor is cleaved extracellularly by ADAM metalloproteinase (S2 cleavage) and then intracellularly by the gamma secretase complex (S3 cleavage). The released NICD can then translocate to the nucleus where it associates with DNA-bound CSL (CBF1, Su(H), Lag-1), also known as RBPJ (Recombining binding protein suppressor of hairless). When NICD is bound, other proteins such as MAML1 (Mastermind-like protein 1) are recruited and this enables transcriptional regulation of Notch target genes including, amongst many others, members of the HES1 family and p21.

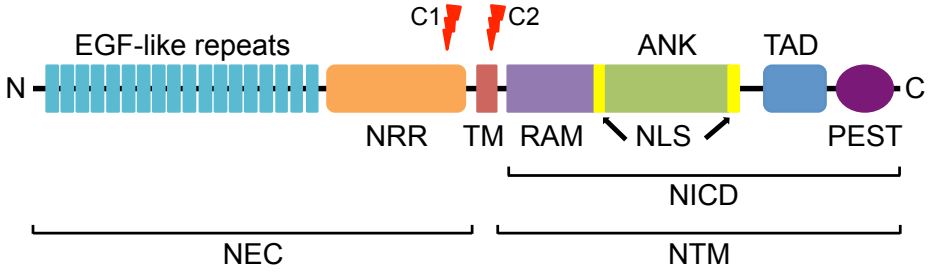

Figure 1.7: Simplified schematic of the Notch receptor

The Notch receptor is comprised of two main portions; the Notch ExtraCellular (NEC) subunit and Notch TransMembrane (NTM) subunit, located within the cell. Notch ligands on adjacent cells bind to the EGF-like repeats which leads to the activation of Notch by two sequential cleavages (C1 and C2, respectively). C1 is mediated by ADAM metalloproteinase and brings about a membrane-tethered form of Notch IntraCellular Domain (NICD). NICD subsequently gets cleaved (C2) in the transmembrane-spanning segment (TM) by the gamma secretase complex. NICD is then free to translocate to the nucleus, using two nuclear localization signals (NLS), where it associates with Recombining binding protein suppressor of hairless (RBPJ). The interaction with RBPJ is brought about by the RBPJ Associated Molecule (RAM) domain and ankyrin repeat region (ANK) of NICD. Notch regulatory region (NRR), which is composed of three Lin12/Notch repeats and the heterodimerization domain (HD), is involved in regulating the activation of the receptor. The transactivation domain (TAD) and proline, glutamate, serine, and threonine (PEST) domain are required for transcriptional activation and degradation of Notch, respectively.

1.15.1 Role of Notch in stem cell maintenance and cell fate determination

Stem cells are characterized by their inherent ability to differentiate into multiple lineages and undergo self-renewal (Weissman, 2000), allowing them to produce differentiated daughter cells without depleting the stem cell pool. It is important to understand the pathways that control stem cell function, not only because they are instrumental during development but also because their deregulation has been implicated in carcinogenesis (Reya et al., 2001). Signal transduction pathways, such as Notch (Austin and Kimble, 1987, Henrique et al., 1997, Varnum-Finney et al., 2000), Hedgehog (Wechsler-Reya and Scott, 1999) and Wnt (Korinek et al., 1998) are considered to be the core stem cell signaling pathways and are involved in regulating the capacity of stem cells to self-renew. For Notch specifically this was originally shown in hematopoietic stem cells (Karanu et al., 2000, Varnum-Finney et al., 2000).

These signal transduction pathways, including Notch, have been found to be defective in a variety of tumors, allowing cancer cells to undergo self-renewing cell divisions similar to those of stem cells (Ellisen et al., 1991, Chan et al., 1999, Gailani and Bale, 1999). In the majority of cancers this is associated with aberrant, uncontrolled Notch activation, resulting in high Notch levels. However, in some cases even a lack of Notch can have oncogenic effects, including in the epidermis and head and neck squamous cell carcinomas (Nicolas et al., 2003, Restivo et al., 2011).

Notch signaling occurs between adjacent cells and hence the fate of any given cell in response to Notch is dependent on its neighbors and precise physiological context (reviewed in (Hori et al., 2013)). This means that the consequence of any given level of Notch being present in a cell is strictly context dependent, with it promoting proliferation in one tissue and differentiation in another. One hallmark of Notch-regulated cell fate is lateral specification (Greenwald, 1998). This refers to the ability of a cell that has adopted a specific lineage, for example to differentiate into a neuroblast in a developing embryo, to inhibit its cellular neighbors from adopting the same cell fate. High levels of expression of the Notch ligand Delta1 from an epidermal stem cell have been shown to induce neighboring cells to become transit amplifying cells, with a limited number of cell divisions (Lowell et al., 2000). This example of lateral specification has a differentiation-promoting effect. This means that Notch signaling

allows one cell to distinguish itself from a group of developmentally identical cells and also to segregate two populations of cells (Bray, 2006).

1.15.2 Role of Notch in the epithelium

In the epidermis, Notch is implicated mainly in cell cycle withdrawal and keratinocyte differentiation (reviewed in (Watt et al., 2008, Dotto, 2008)), though some of its targets are involved in actively promoting cell growth. Calcium is one of main regulators of differentiation (reviewed in (Bikle et al., 2012)). The calcium gradient within the stratified epithelium is involved in the sequential differentiation of keratinocytes. Hence, it has been suggested that the calcium receptors of cells are the main initiators of differentiation in response to extracellular calcium in suprabasal layers. Notch activation has also been shown to be a requirement of epithelial cells to commit to their cellular differentiation program. This is brought about by the ability of NICD to activate p21 and p27 (Rangarajan et al., 2001b), which are potent suppressors of c-Myc (Horiguchi-Yamada et al., 2002), and can bring about cell cycle arrest, in a p63-dependent manner (Wu et al., 2012). However, a recent study has shown that cell density rather than high calcium levels in keratinocyte cell medium are determinants of Notch activation (Kolly et al., 2005). Once initiated, calcium is necessary to bring terminal differentiation to completion but it does not control the beginning of the process. This study suggests that Notch is activated in response to cell-cell contact and can bring about growth arrest and contact inhibition. It seems plausible that Notch receptor activation generally requires cell-cell contact because its ligands (Delta-like1, -3, -4 and Jagged-1, -2) are cell surface anchored molecules (Mumm and Kopan, 2000, Baron, 2003).

1.15.3 Notch in cervical carcinogenesis

Notch1 expression was originally shown to correlate with the progression from low-grade disease to invasive carcinoma (Zagouras et al., 1995, Daniel et al., 1997). Thereafter it was postulated that Notch activation cooperates with HPV-dependent malignant transformation of cells to induce cell survival, as Notch1 was found to be elevated in cervical carcinoma (Rangarajan et al., 2001b, Nair et al., 2003). Additionally, the down-regulation of Notch1 was shown to lead to a reduction of anchorage independent growth of cervical cancer cells (Weijzen et al., 2002).

However, it has also been suggested that high levels of Notch in cervical carcinoma, could be reflective of more highly differentiated parts of the tumor (that have abundant Notch) (Dotto, 2008) rather than represent the overall levels of Notch in the whole tumor. Furthermore, it has been shown that primary keratinocytes containing HPV, express lower levels of Notch than uninfected cells (Yugawa et al., 2007) and that the growth potential of these cells is suppressed when Notch activity is high (Lowell et al., 2000, Lefort et al., 2007). Additionally, Notch1 was shown to suppress viral protein expression through its ability to activate of AP-1 (Talora et al., 2002), which has a role in the transcriptional regulation of HPV due to the presence of AP-1 binding sites within the LCR of the viral genome (Thierry et al., 1992, Soto et al., 1999).

The studies outlined above represent the tip of the iceberg in terms of the vast amount of work that has been done to characterize the involvement of Notch in neoplasia and cervical cancer. However, they are representative of the current divide in the HPV field concerning the function of Notch and whether this signal transduction pathway promotes or represses neoplastic progression. Based on this, it is conceivable that the effect of Notch in cells infected with HPV may depend on not only the exact type of virus and levels of viral proteins but also the precise location of the cell within the epithelium and the activity of other signaling pathways.

1.15.4 Notch and E6

Several groups have shown that E6 from low-risk HPV8 and also bovine papillomaviruses (BPVs) can suppress Notch activation through a mechanism that inhibits the formation of the RBPJ/NICD/MAML1 complex (Brimer et al., 2012, Tan et al., 2012, Meyers et al., 2013). Furthermore, a study using HPV16 E6 and E7 has suggested that their repression leads to a significant activation of the Notch pathway in oropharyngeal cancer cell lines (Rampias et al., 2008). Additionally, further work using both HPV16- and -18 positive cervical cancer cell lines has demonstrated that Notch1 expression is reduced by a mechanism involving inactivation of p53 by E6 (Yugawa et al., 2007).

In contrast it has also been postulated that both HPV16 oncoproteins can cooperate with Notch1 to promote malignant transformation of HaCaT keratinocytes (Rangarajan et al., 2001a). Moreover, both HPV16 E6 and E7 independently can up-regulate Notch1

expression, with inhibition of Notch1 resulting in the loss of the tumorigenic phenotype of cells (Weijzen et al., 2003). Another study has shown that HPV16 E6 can activate the Notch ligand Jagged-1 and bring about the activation of both Notch1 and 2 (Veeraraghavalu et al., 2005).

This shows that even when it comes to the effects of just one viral protein on Notch signaling, in this case E6, there is disagreement in the field. While the exact mechanism by which E6 affects Notch has yet to be determined, it seems that depending on the precise expression levels and cellular environment (Henken et al., 2012), Notch, as deregulated by E6, can have both growth inhibitory and promoting effects.

1.16 Gamma secretase complex

Gamma secretase is a membrane complex with unusual aspartyl protease activity, consisting of various subunits, that is involved in cleaving single-pass type I transmembrane proteins (reviewed in (Strooper and Annaert, 2001)). It is has been highly conserved throughout evolution and is found in essentially all animal species. Its substrates include proteins such as Notch, amyloid precursor protein (APP), E-cadherin, N-cadherin, Nectin-1 and the ErbB4 receptor tyrosine kinase. Interestingly, target specificity and proteolytic activity of the gamma secretase complex is not critically dependent on a specific sequence that is recognized but on the size of the extracellular domain of its targets, with smaller domains resulting in more efficient cleavage (Struhl and Adachi, 2000). The gamma secretase complex was first described through its role in the production of amyloid beta (Aβ), which is brought about through cleavage of Amyloid precursor protein (APP) (Selkoe, 2001). In patients with Alzheimer's disease, Aβ is processed abnormally and this is associated with amyloid plaques in the brain (Hardy and Allsop, 1991).

Though not yet fully characterized, the gamma secretase complex consists of four essential proteins; presenilin (PS), presenilin enhancer-2 (PEN-2), nicastrin (Nct) and anterior pharynx-defective-1 (APH-1) (reviewed in (Kaether et al., 2006)). Additionally, the complex may also comprise a fifth non-essential protein, CD147, which is a negative regulator of its activity (Zhou et al., 2005, Zhou et al., 2006). Presenilin is encoded by two genes giving rise to two homologues, presenilin-1 and -2 (PS-1 and -2) (Levy-Lahad et al., 1995, Sherrington et al., 1995). Moreover, in mammalian cells two

homologues of APH-1 have been found, APH-1α and APH-1β, with APH-1α having two additional splice variants that differ in their C-termini (Francis et al., 2002). It has been shown that PS-1 and -2 and APH-1α and APH-1β can all assemble into different gamma secretase complexes (Steiner et al., 2002, Shirotani et al., 2004). This suggests that the exact components of the complex and thus its precise activity are likely to reflect the tissue-specific expression of the various subunits (Kaether et al., 2006).

In addition to a role in proteolytic activity, APH-1 promotes the assembly of all the components into the gamma secretase complex (Lee et al., 2004). Once it is fully formed the complex is activated through autocatalytic processing of PS-1, which is the main proteolytic component. This involves its cleavage into an N- and a C-terminal fragment that are both retained within the complex (Thinakaran et al., 1996, Capell et al., 1998). The main role of Nct is to stabilize the whole complex (Zhang et al., 2005) while additionally PEN-2 is also involved in complex stabilization after the two fragments of PS-1 have been formed (Prokop et al., 2004).

1.16.1 Inhibition of gamma secretase

Much of the characterization of the gamma secretase complex and also identification of its core components has been done using protein inhibitors (reviewed in (Wolfe, 2001)). By doing this it was discovered that the absence of even just one of the four essential subunits brings with it loss of function of the whole complex (Pardossi-Piquard et al., 2009). As PS-1 is the active site of the complex, a lot of work has focused on the study of this protein and it has been shown that PS-1 knock-out mice are embryonically lethal (Herreman et al., 1999). PS-1 on its own was first described to be involved in Alzheimer's disease (Levy-Lahad et al., 1995, Rogaev et al., 1995, Sherrington et al., 1995) and then gradually over several years it was discovered that, to bring about cleavage of APP, it associates with other proteins to form the gamma secretase complex (reviewed in (Smolarkiewicz et al., 2013)). Alzheimer's is a widespread type of dementia and the most common neurological disorder in the developed world. It has been predicted that by 2050, 1 in 85 people on a global scale will be affected by the disease (Brookmeyer et al., 2007). Due to it being so widespread a lot of work has been done on developing drugs and inhibitors against the gamma secretase complex to prevent the formation of amyloid plaques. This means that they are readily available for research purposes. Many of them do not distinguish between APP and other gamma

secretase substrates, such as Notch, and therefore they can be used for studying signaling pathways that are not necessarily involved in Alzheimer's disease.

1.17 The PI3K/AKT pathway

The serine/threonine kinase AKT (Jones et al., 1991, Bellacosa et al., 1991, Coffer and Woodgett, 1991), also known as Protein Kinase B (PKB), is a downstream mediator of the phosphatidylinositol 3-kinase (PI3K) pathway (Figure 1.8) (reviewed in (Brazil and Hemmings, 2001, Hemmings and Restuccia, 2012)) and as such an important cellular regulator of the fine balance between cell survival and apoptosis. As the PI3K/AKT pathway is activated by members of the insulin-like growth factor (IGF) protein family, AKT is also considered to be a key regulator of growth factor responsiveness. When receptor tyrosine kinases (RTKs) are activated by appropriate growth factors, such as IGF, this leads to activation of PI3K, bound directly to RTK via its regulatory subunit or indirectly through insulin receptor substrate (IRS) proteins. Upon activation PI3K is catalytically converted to PIP3. AKT binds to PIP3, leading to subsequent partial activation of AKT by 3-phosphoinositide-dependent protein kinase 1 (PDK1). This allows AKT to activate mTORC1. Two of the main substrates of mTORC1 include the eukaryotic translation initiation factor 4E binding protein 1 (4EBP1), and ribosomal protein S6 kinase 1 (S6K1). These can, when activated, bring about protein synthesis and cellular proliferation. Inhibitors of the PI3K pathway include protein phosphatase 2 (PP2A) (Andjelkovic et al., 1996), phosphatase and tensin homolog (PTEN) (Stambolic et al., 1998), and the PH-domain leucine-rich-repeat-containing protein phosphatases (PHLPP1/2) (Brognard et al., 2007).

The AKT pathway is involved in the normal cellular differentiation program of keratinocytes (Janes et al., 2004, Calautti et al., 2005, Thrash et al., 2006, O'Shaughnessy et al., 2007b) and mice deficient in both AKT1 and 2 isoforms have been found to die neonatally (Peng et al., 2003). In cancers of many cell types, including keratinocytes (Segrelles et al., 2002, Mao et al., 2004), the PI3K pathway has been shown to be attenuated, leading to dysregulation of apoptosis and proliferation. In instances where the pathway is too active, the functional inactivation of PTEN is often involved. PTEN is one of the most commonly inactivated tumor suppressors associated with human cancers (Chen et al., 2005).

1.17.1 HPV and AKT

Increased AKT activity has been linked to anogenital HPV infection (Pim et al., 2005, Menges et al., 2006). Current literature suggests that AKT can be deregulated by E7. A recent study with vulval intraepithelial lesions (VINs) has suggested that in the presence of HPV, AKT levels correlate with E7 expression (Ekeowa-Anderson et al., 2012). When the virus first infects and is maintained episomally, with low E7 levels due to heavy regulation by E2, patient tissue sections are negative for AKT expression. However, after integration, when E2 regulation is lost, E7 levels are much higher and AKT can be readily detected. Furthermore, when E7 is expressed in human foreskin keratinocytes (HFKs) this leads not only to enhanced cell proliferation and inhibition of differentiation but also increased AKT activity in raft culture (Menges et al., 2006). This seems to be dependent on the ability of E7 to bring about the degradation of Rb. Additional it has been suggested that HFKs expressing HPV16 E7 have to ability to promote the cytoplasmic retention of the cyclin-dependent kinase inhibitor p27 via the PI3K/AKT pathway. This not only removes normal cellular restrictions on cell cycle progression but also allows cells to migrate more rapidly (Charette and McCance, 2007).

Although generally high levels of the AKT1 isoform are associated with malignancy, especially in head and neck squamous cell carcinoma (SCC) (Amornphimoltham et al., 2005, Lim et al., 2005, Moral and Paramio, 2008) it has been shown that upon infection with a cutaneous HPV, specifically HPV8, AKT1 is downregulated while high AKT2 levels are correlated with tumor progression (O'Shaughnessy et al., 2007a).

All in all, current literature suggests that AKT may be an important prognostic marker for disease and also a good target for therapeutic intervention in treating cervical and also other HPV-associated malignancies.

Figure 1.8: Simplified schematic of the PI3K/AKT pathway

When a tyrosine kinase receptor is activated by an appropriate growth factor, such as insulin-like growth factor (IGF), this leads to activation of PI3K. Upon activation PI3K is able to bind to and bring about the partial activation of AKT. This allows AKT to activate mTORC1. Two of the main substrates of mTORC1 include the eukaryotic translation initiation factor 4E binding protein 1 (4EBP1), and ribosomal protein S6 kinase 1 (S6K1). These can, when activated, bring about protein synthesis and cellular proliferation.

1.18 Rationale and aims of this study

The overall aim of this study was to increase the understanding of neoplastic progression resulting from HPV infection by characterizing viral gene expression and the effects of the E6 and E7 viral oncoproteins.

This was addressed primarily using HPV16-expressing, episomal NIKS cell lines that had previously been shown to give rise to LSIL- and HSIL-like rafting phenotypes and also corresponding growth patterns in monolayer culture (Isaacson Wechsler et al., 2012). Once this unique model of viral deregulation was fully established I used it to understand how HPV16 can cause different grades of neoplasia and how pathology is regulated by gene expression patterns.

HPV research has been carried out for several decades and a lot is known about the virus, its mechanism of infection and how it causes diseases. Nevertheless, to date it is often difficult to say with 100 % certainty whether a lesion, detected during a routine cervical smear test, has to be treated or not. It is generally accepted that, if detected, a LSIL is monitored while an advanced HSIL is removed. However, the stage in between (equating to a CIN2) seems to be a grey area and there have been recent debates as to whether treating this type of lesion is good or bad (Mosicki et al., 2012). On the one hand, treatment is essential to prevent the lesion from progressing to an advanced HSIL or even cervical carcinoma. On the other hand, it is important not to treat unnecessarily as treatment can be invasive and may bring with it the risk of premature births. Hence, the age of the affected woman is an important consideration in this decision. In younger individuals, of childbearing age, the tendency is to monitor as oppose to treat while in older women, no longer wishing to or able to have children, treatment is more common. In light of this, it is important to further describe the molecular differences between low- and high-grade lesions (as shown in this report) so that physicians can say with more certainty whether treatment is required.

My overall hypothesis was that differences in the expression levels and precise expression patterns of E6 and/or E7, and the resulting differential deregulation of certain molecular pathways, are involved in giving rise to the LSIL- and HSIL-like phenotypes. To test this, I decided to break the hypothesis down into three smaller more easily testable ones to be addressed one after the other.

1) **Hypothesis:** Differences in E6 and/or E7 are involved in regulating the LSIL- and HSIL-like phenotypes.

Aims/Objectives:

a) Test the reproducibility of the previously published LSIL- and HSIL-like rafting and growth patterns.

b) Determine whether the LSIL- and HSIL-like phenotypes arise as a consequence of the way experiments are routinely carried out.

c) Find out whether E6 and/or E7 mRNA and/or protein levels differ between the LSIL- and HSIL-like cell lines.

d) Investigate whether the role of E6 and/or E7 is dependent on where in the stratified epithelium the proteins are expressed.

2) **Hypothesis:** Modulating E6 and/or E7 levels will lead to a corresponding effect on the proliferation of cells and alter the LSIL- and HSIL-like phenotypes.

Aims /Objectives:

a) Test various previously published siRNA sequences or shRNA vectors to achieve the best possible knock-down of E6 and/or E7 in highly transfectable cells.

b) Use the sequences/vectors identified and tested in a) to achieve knock-down of E6 and/or E7 in NIKS HPV16-expressing clonal cells.

c) Determine whether knock-down of E6 and/or E7 has an effect on the LSIL- and HSIL-like growth patterns.

d) Use a plasmid(s) to overexpress E6 and/or E7 in the clonal HPV16-expressing NIKS cell lines.

e) Find out whether the overexpression of E6 and/or E7 has an effect on the proliferation of the LSIL- and HSIL-like cell lines.

3) **Hypothesis:** E6 can deregulate a pathway(s) involved in cell proliferation and/or contact inhibition to bring about the LSIL- and HSIL-like phenotypes.

Aims/Objectives:

a) Determine whether E6 can interfere with contact inhibition by binding to and degrading PDZ proteins.

b) Investigate whether E6 can attenuate normal growth pathways through its ability to degrade the p53 protein.

c) Test whether the deregulation of the Notch and/or Hippo pathway(s) by E6 gives rise to the LSIL- and HSIL-like growth patterns.

d) Challenge the findings in c) by using siRNA and/or shRNA or chemical agonists and/or antagonists specific to the pathway(s) identified.

e) Find out whether the pathway(s) involved in deregulating proliferation of the HPV16-expressing NIKS cell lines are also involved in giving rise to LSIL- and HSIL-like rafting phenotypes.

Chapter 2: Materials and Methods

2.1 Suppliers of reagents

Unless otherwise stated, all chemicals were purchased from Sigma-Aldrich (UK), BDH Laboratory Supplies (UK), Fisher Scientific (UK) or VWR International Ltd. (UK).

2.1.1 Commonly used buffers and reagents

Commonly used buffers and reagents were made according to Table 2.1. All buffers listed were prepared by the NIMR media facility.

Table 2.1: Buffers and reagents

Name	Components
Penicillin/Streptomycin (for cell culture)	0.6 % (v/v) penicillin, 1 % (v/v) streptomycin
Trypsin-versene (for cell culture)	0.8 % NaCl, 0.02 % KCl, 0.12 % Na_2HPO_4, 0.02 % KH_2PO_4, 0.01 % EDTA, 0.13 % trypsin, 0.001 % phenol
1X Phosphate buffered saline (PBS)	1 % NaCl, 0.025 % KCl, 0.14 % Na_2HPO, 0.025 % KH_2PO_4
1X Tris-buffered saline (TBS)	2.42 g Tris base, 8 g NaCl; pH 7.6 (for 1L)
Lysogeny broth (LB)	1 % Bacto-Tryptone, 0.5 % Bacto-yeast extract, 1 % NaCl
LB agar	LB medium plus 2 % Bacto agar
50X Tris acetate EDTA (TAE)	242 g Tris base, 57.1 ml glacial acetic acid, 18.6 g EDTA (for 1L)
SDS electrophoresis buffer	25 mM Tris base, 200 mM glycine, 0.1 % sodium dodecyl sulfate (SDS); pH 8.3
Transfer buffer	25 mM Tris-HCl, 200 mM glycine, 20 % (v/v) methanol; pH 8.3

2.2 Basic monolayer cell culture methods

2.2.1 Cell lines

2.2.1.1 J2-3T3 mouse fibroblasts

J2-3T3 is an immortalized fibroblast cell line that was originally isolated from Swiss albino mouse embryos (Todaro and Green, 1963). J2-3T3 cells were γ-irradiated and used as a bed of feeder cells for culturing NIKS.

2.2.1.2 SiHa cells

SiHa are an HPV16-positive squamous cell carcinoma (SCC) cell line isolated from the cervix of a 55 year old patient (Friedl et al., 1970). The viral DNA in these cells is fully integrated with at least 11 chromosomal sites of HPV16 integration having been described (Mincheva et al., 1987).

2.2.1.3 EF-1F human foreskin fibroblasts

EF-1F cells were originally isolated from human foreskin epithelium. The cell line was used for preparing dermal equivalents as part of the rafting process.

2.2.1.4 Normal Immortalized Human Keratinocytes (NIKS)

NIKS are a spontaneously immortalized HPV-negative human foreskin keratinocyte cell line. These cells arose originally from their parental BC-1-Ep cell line, isolated from neonatal foreskin, through serial passaging (Allen-Hoffmann et al., 2000). All HPV16 and the vast majority of other experiments used NIKS cells.

2.2.1.5 NIKS HPV16-positive cells

HPV16 clonal cell lines were established from two independent transfection events by Kenneth Raj; NIMR, London, UK and Qian Wang; NIMR, London, UK. This process involved cotransfecting NIKS with recircularized replication competent HPV16 wild type (WI2) genomes and a pcDNA6 vector containing a blasticidin resistance gene. Clonal cell lines were recovered after selection with 6 μg/ml of blasticidin. After individual colonies became visible, cells were first cultured in single wells of 60 mm 6-well plates (Thermo Scientific; 140675) and subsequently expanded to make cell stock.

2.2.2 Media and supplements

The various media used for culturing the cell lines as well as for freezing of cells for long-term storage are described in Table 2.2. The supplements used in the FI medium for NIKS were prepared either as 100 or 1000X stock, filter sterilized using a 0.2 µM filter unit (Sartorius; 16534) and frozen at -20 °C in 5 ml aliquots.

Table 2.2 Cell culture and freeze media

Cell type	Medium type	Medium components
NIKS, HPV16 clones and other NIKS-derived cell populations	FI medium	500 ml F Medium (3 part F12-Hams + 1 part high glucose DMEM) (PAA; T15-355), 5 % (v/v) FBS (Biosera; S1900-500), 24 µg/ml adenine (Sigma-Aldrich; A2786), 8.4 ng/ml cholera toxin (Sigma-Aldrich; C8052), 0.4 µg/ml hydrocortisone (Calbiochem; CAS 50-23-7), 5 µg/ml insulin (Sigma-Aldrich; I4011) and 1 % (v/v) pen/strep
NIKS, HPV16 clones and other NIKS-derived cell populations	FC medium	FI medium with Epidermal Growth Factor (EGF) added prior to use at a concentration of 10 ng/ml (R&D Systems; 236-EG)
NIKS, HPV16 clones and other NIKS-derived cell populations	NIKS freezing medium	90 % (v/v) FBS, 10 % (v/v) DMSO (Sigma-Aldrich; D2650)
NIKS, HPV16 clones and other NIKS-derived cell populations	Keratinocyte plating medium	500 ml FI Medium with 0.5 % (v/v) FBS and 610 µl $CaCl_2$ (Ca^{2+} final concentration of 1.88 mM)
NIKS, HPV16 clones and other NIKS-derived cell populations	Cornification medium 1	500 ml FI medium with 5 % (v/v) FBS and 610 µl $CaCl_2$ (Ca^{2+} final concentration of 1.88 mM). N 1,2-dioctanoyl-sn-glycerol (C8:0) (Calbiochem; 317505) was added fresh to a final concentration of 10 µM

J2-3T3, SiHa	DMEM complete	500 ml high glucose DMEM (Sigma-Aldrich; D6429), 10 % (v/v) FBS and 1 % (v/v) pen/strep
EF-1F	F12 medium	500 ml F12-Ham's (Gibco; 21765-029), 10 % (v/v) FBS and 1 % (v/v) pen/strep
J2-3T3, EF-1F, SiHa	J2-3T3 / EF-1F / SiHa freezing medium	95 % (v/v) FBS, 5 % (v/v) DMSO

2.2.3 Maintenance of monolayer cells

All cells were cultured in 5 % CO_2 at 37 °C.

2.2.3.1 J2 3T3 and SiHa

J2-3T3 fibroblasts and SiHa cells were cultured in 10 ml of DMEM complete medium in T75 flasks (Fisher Scientific; TKV-123-013L). Cells were split between 1:10 and 1:40 as needed. To harvest, cells were washed with 7 ml of PBS and then incubated with 2 ml of trypsin-versene for 2 minutes at 37 °C. Thereafter, 8 ml of fresh medium was added, cells were resuspended into a single cell suspension and a small aliquot transferred to a new flask for further culturing. Cells were given fresh medium every 3-4 days. For long-term storage, a confluent flask of low passage cells was harvested, spun down at 1500 rpm using a MSE Mistral 1000 centrifuge for 5 minutes, resuspended in 2 ml of J2-3T3/SiHa freezing medium, transferred to 2 cryovials (Thermo Scientific; 5000-1012) and frozen down at -80 °C or in liquid nitrogen. J2 3T3 cells above passage 25 were not used for experimental purposes.

2.2.3.2 EF-1F

EF-1F fibroblasts were cultured in 10 ml of F12 medium in T75 flasks and split 1:3 or 1:5, as needed. To harvest, cells were washed with 7 ml of PBS and then incubated with 2 ml of trypsin-versene for 5-10 minutes at 37 °C. Thereafter, 8 ml of fresh DMEM complete medium was added, cells were resuspended into a single cell suspension and a small aliquot transferred to a new flask for further culturing. Cells were given fresh medium every 2-3 days. For long-term storage, a confluent flask of cells was harvested, spun down at 1500 rpm for 5 minutes, resuspended in 1 ml of EF-1F freezing medium, transferred to a cryovial and frozen down at -80 °C or in liquid nitrogen.

2.2.3.3 Routine passaging of NIKS, NIKS HPV16 clones and other NIKS-derived cell populations

NIKS, and variations thereof, were cultured on a layer of γ-irradiated J2-3T3 cells (feeders). J2-3T3 were irradiated at a dosage of 60 Gy using a Caesium source. For routine passaging approximately $1.4x10^6$ feeders were seeded in a T75 flask in 10 ml of FI medium and left to attach for 2 hours prior to plating NIKS cells. NIKS were cultured to a maximum of 80 % confluence and split approximately once a week between 1:5 and 1:30, depending on the growth rate of the cells. Generally, only cells below passage 15 were used for experimental purposes. To harvest, NIKS were washed with 7 ml of PBS and then incubated with 2 ml of trypsin-versene for 2 minutes at 37 °C, in order to remove the feeder layer. After tapping the flask several times to completely lift off the feeders, trypsin was aspirated. Keratinocytes were incubated in 2 ml of fresh trypsin-versene at 37 °C for about 15 minutes. When all cells had detached from the flask, 8 ml of FI medium was added, cells were resuspended into a single cell suspension and transferred to a flask of γ-irradiated feeders for further culturing. Cells were provided with fresh FI or FC medium every second day. For long-term storage, a flask of low passage cells was harvested, spun down at 1500 rpm for 5 minutes. Approximately $2\text{-}3x10^6$ cells were resuspended in 1 ml of NIKS freezing medium, transferred to a cryovial and frozen down at -80 °C or in liquid nitrogen.

2.2.4 Counting of NIKS, NIKS HPV16 clones and other NIKS-derived cell populations

For all experiments involving NIKS, cells were counted using a Z1 Coulter® particle counter (Beckman Coulter; UK). After cell harvest, as described above, 0.5 ml of the cell suspension was resuspended in 9.5 ml of isoton III diluent (Beckman Coulter; 8546733) in a coulter counter cuvette (VWR International Ltd.; 720-0812). The coulter counter program used was optimized specifically for NIKS (Erin Isaacson; NIMR, London, UK), which are between 11 and 20 μm in size. To account for cells that are slightly larger, the counter parameters were set to count all cells above 11 μm.

2.2.5 Transfection of NIKS and NIKS HPV16-positive cells

For transfections, NIKS and varieties thereof, were harvested and plated on 60 mm 6-well plates at a density of $5x10^5$ cells per well on a layer of $1x10^5$ feeders and left to grow overnight in FC medium. Transfections were carried out using the Effectene®

Transfection Reagent Kit (Qiagen; 301425) following the manufacturer's instructions. Cells were transfected with up to a total of 1 µg of circular or linearized DNA, which was purified from bacterial cultures. Six hours after transfection cells were given fresh FC medium.

2.2.6 Treatment with DAPT

N-[N-(3,5-Difluorophenacetyl)-L-alanyl]-S-phenylglycine t-butyl ester), or DAPT (Thermo Fisher; D5942), is a gamma secretase inhibitor. DAPT was made up in either DMSO or ethanol and stored at -20 °C in 2 mM aliquots. To use the inhibitor NIKS and NIKS varieties were seeded in a short growth assay format (as described in Section 2.4)**.** From day 1 onwards cells were treated with 10 µM of DAPT or DMSO/ethanol as a control (either DMSO or ethanol was used depending on the experiment) that was replaced every 24 hours. Cells are normally only given fresh FC medium (with EGF) every second day of a growth assay (on days 2, 4, and 6). To enable the change of medium every day, to replace the DAPT and DMSO/ethanol, additional wells with completely untreated cells for each cell type were seeded. The medium given to these cells one day (2, 4, or 6) was used to feed the cells that were part of the growth assay on the next day (3 or 5). Since nothing but fresh DAPT or DMSO/ethanol was added to this "conditioned" FC medium prior to feeding cells, the growth factors and other supplements were presumably equally depleted in the medium in these wells as in the one of treated cells. This system ensured that the growth conditions throughout the experiment were consistent.

2.2.7 Treatment with R04929097

R04929097 (BioVision Inc.; 2011-1) is a gamma secretase inhibitor. R04929097 was made up in DMSO and stored at -20 °C in 8 mM aliquots. To use the inhibitor NIKS and NIKS varieties were seeded in a short growth assay format (as described in Section 2.4) following the same set-up as for DAPT in Section 2.2.7. Cells were treated with 8 nM of the drug or DMSO as a control.

2.3 Growth assays of NIKS, NIKS HPV16 clones and other NIKS-derived cell populations

To assess the proliferation patterns of NIKS, and varieties thereof, $1x10^5$ keratinocytes were seeded on top of a layer of $1x10^5$ γ-irradiated J2-3T3 fibroblasts per well of a

6-well plate. Duplicate wells were set-up for each cell type and time-point. The day of seeding was denoted as day 0. Cells were left to grow overnight in 2 ml of FI medium. On the following day (day 1) cells were counted to determine the seeding efficiency. For most experiments cells were grown for a total of 9 days and counted at days 1, 3, 5, 7 and 9. On day 1 and every other day thereafter (days 3, 5, and 7) cells were fed with 2 ml of FC medium. For harvesting, cells were washed with 2 ml of PBS and then incubated for 2 minutes with trypsin-versene at 37 °C to dislodge the feeders. After tapping the plate several times to completely lift off the fibroblasts, trypsin was aspirated. To remove the keratinocytes, 1 ml of fresh trypsin-versene was added to each well and cells were incubated at 37 °C for about 15 minutes. When all cells had detached from the bottom of the wells, 4 ml of FI medium was added, cells resuspended into a single cell suspension and 0.5 ml of the mix used for counting. The cell numbers at seeding were optimized in such a way that at day 3 the wells are sub-confluent (individual NIKS colonies are not contacting), at day 5 the wells are confluent (individuals colonies are contacting) and from day 7 onwards the wells are post-confluent (individual colonies have merged completely). Cells left over from counting at each time-point were pelleted and frozen at -80 °C for protein and/or transcript analysis.

2.4 Short growth assays of NIKS, NIKS HPV16 clones and other NIKS-derived cell populations

This growth assay format was developed to assess the proliferation patterns of NIKS, and varieties thereof, during a shorter time frame to allow for the treatment of cells with certain drugs. $6x10^5$ keratinocytes were seeded on top of a layer of $1x10^5$ feeders per well of a 6-well plate in FI medium. Duplicate wells were set-up for each cell type and time-point. The day of seeding was denoted as day 0. On the following day (day 1) cells were given fresh FI medium and counted as described in Section 2.3 to assess the seeding efficiency of cells. On days 2, 4 and 6 cells were counted and all remaining cells fed with 2 ml of FC medium. The cell numbers at seeding were optimized in such a way that at day 2 the wells were confluent (equivalent to day 5 of a full-length time-course) and at days 4 and 6 the wells were post-confluent (equivalent of days 7 and 9 of a regular growth-assay). Cells left over from counting at each time-point were pelleted and frozen at -80 °C for protein and/or transcript analysis.

2.5 siRNA treatment

All siRNA sequences that were custom designed are listed in Table 2.3. Additionally, the regions of the E6 and E7 ORFs that they target are shown in Figure 2.1. The siRNAs were ordered from Thermo Scientific (UK) as a dried pellet and had 3' dTdT overhangs. siRNAs were made up to a concentration of 20 μM using 5X siRNA buffer (Thermo Scientific; B-002000-UB-100) and stored in 100 μl aliquots (to avoid repeat freeze-thawing) at -20 °C. siNT (non-target) and siGAPDH were commercially available from Thermo Scientific.

Table 2.3: List of siRNAs and sequences		
Name and target *(Target specificity)*	**Sequence**	**Reference(s)**
siE6 *(E6 only)*	GAGGUAUAUGACUUUGCUU	(Jiang and Milner, 2002, Allison et al., 2009)
siE7-1 *(E7 only)*	AGGAGGAUGAAAUAGAUGG	(Jiang and Milner, 2002, Allison et al., 2009)
siE7-2 *(E7 only)*	CAGAGCCCAUUACAAUAUU	(Allison et al., 2009)
siE6/E7-1 *(both E6 and E7)*	GACCGGUCGAUGUAUGUC	(Gu et al., 2009)
siE6/E7-2 *(both E6 and E7)*	GCAACAGUUACUGCGACGU	(Putral et al., 2005, Gu et al., 2008)
siE6/E7-3 *(both E6 and E7)*	GAGCUGCAAACAACUAUA	(Ben Khalifa et al., 2011)
siE6/E7-4 *(both E6 and E7)*	UUAAAUGACAGCUCAGAGG	(Accardi et al., 2011)

HPV16 E6 ORF

ATGCACCAAAAGAGAACTGCAATGTTTCAGGACCCACAGGAGCGACCCAGAAAGTTACCACAGTTATGCA

E6/E7-3 E6/E7-2

CAGAGCTGCAAACAACTATACATGATATAATATTAGAATGTGTGTACTGCAAGCAACAGTTACTGCGACGT

SD E6-1

GAGGTATATGACTTTGCTTTTCGGGATTTATGTATAGTATATAGAGATGGGAATCCATATGCTGTATGTG

ATAAATGTTTAAAGTTTTATTCTAAAATTAGTGAGTATAGACATTATTGTTATAGTGTGTATGGAACAA

SA

CATTAGAACAGCAATACAACAAACCGTTGTGTGATTTGTTAATTAGGTGTATTAACTGTCAAAAGCCACT

GTGTCCTGAAGAAAAGCAAAGACATCTGGACAAAAAGCAAAGATTCCATAATATAAGGGGTCGGTGGACC

E6/E7-1 SA

GGTCGATGTATGTCTTGTTGCAGATCATCAAGAACACGTAGAGAAACCCAGCTGTAA

HPV16 E7 ORF

ATGCATGGAGATACACCTACATTGCATGAATATATGTTAGATTTGCAACCAGAGACAACTGATCTCTACT

E6/E7-4 E7-1

GTTATGAGCAATTAAATGACAGCTCAGAGGAGGAGGATGAAATAGATGGTCCAGCTGGACAAGCAGAACC

E7-2

GGACAGAGCCCATTACAATATTGTAACCTTTTGTTGCAAGTGTGACTCTACGCTTCGGTTGTGCGTACAA

AGCACACACGTAGACATTCGTACTTTGGAAGACCTGTTAATGGGCACACTAGGAATTGTGTGCCCCATCT

GTTCTCAGAAACCATAA

Figure 2.1 Sequences of the HPV16 E6 and E7 ORFs showing the regions targeted by the E6, E7 and E6/E7 siRNAs

The DNA sequence of the E6 ORF (region 83-559) and E7 ORF (region 562 to 858) of HPV16 are shown. The regions targeted by E6-1, E7-1, E7-2, E7/E7-1, E6/E7-2, E6/E7-3 and E6/E7-4 siRNAs are shown in colored highlights. Additionally, the splice donor (SD) and slice acceptor (SA) sites of E6 are indicated in red and blue writing, respectively. Please note that the sequences targeted by E6/E7-1, -2 and -3 are located within the E6 ORF while that targeted by E6/E7-4 is located within the E7 ORF.

2.5.1 siRNA transfection

2.5.1.1 SiHa For SiHa, $2x10^5$ cells were seeded into each well of a 6-well plate and left to grow overnight in medium without FBS and pen/strep. Cells were transfected with 20 nM of each siRNA with Lipofectamine® RNAiMAX (Life Technologies; 13778), following the manufacturer's instructions and given fresh DMEM complete 6 hours later. Cells were harvested 48 and/or 72 hours post-transfection to determine the efficiency of the knock-down either by assessing protein and/or mRNA levels.

2.5.1.2 NIKS and NIKS HPV16-positive cells

For NIKS, $3x10^5$ cells were seeded on top of $1x10^6$ feeders per well and left to grow overnight in medium without FBS and pen/strep. Cells were transfected with 100 nM of each siRNA with Lipofectamine® RNAiMAX according to the manufacturer's instructions and given fresh FC medium 6 hours later. Cells were harvested 48 and/or 72 hours post-transfection to determine the efficiency of the knock-down either by assessing protein and/or mRNA levels.

2.5.2 Electroporation

NIKS and NIKS HPV16 clonal cell lines were harvested, washed twice with PBS, counted and divided into aliquots of $1.5x10^6$ cells in individual microcentrifuge tubes. Cells were electroporated with 100 nM of siRNA using the 4D Nucleofector® X Unit from Lonza (UK) and the Amaxa™ SE Cell Line 4D-Nucleofector™ X Kit L (Lonza; V4XC-1024), according to the manufacturer's instructions. The specific program used for NIKS cells was previously optimized by Cinzia Borgogna and Emilio Pagliarulo (both NIMR, London, UK). Subsequently cells were seeded into 6-well plates on top of $1x10^5$ feeder cells in FC medium and given fresh FC medium the next day. The cells were cultured in a short growth assay format, as described above, to assess proliferation patterns of cells, with the day post-electroporation equating to day 1. Due to the short term effects of siRNA, cells were counted at days 1, 2, 3 and 4 only which equates to 24, 48, 72 and 96 hours post-treatment with siRNA.

2.6 Infection of NIKS and NIKS HPV16-positive cells

2.6.1 Retroviral expression system

A retroviral expression system using Phoenix cells was used to make NIKS cell populations stably expressing wild type or mutant E6, E7 or E6/E7.

2.6.1.1 Culture of Phoenix cells

Phoenix cells are a 293T-based cell line which is capable of producing the gag-pol and envelope proteins of amphotropic viruses. The cells were kindly provided by Dr Garry Nolan (Stanford University, Stanford, USA). The cells were cultured in the same way as J2-3T3 cells (see Section 2.2.3.1). On the day prior to transfection, cells were seeded in 10 cm plates (NUNC; 150350) at a density of $6.5x10^6$ cells per plates in 10 ml of DMEM complete.

2.6.1.2 Transfection of Phoenix cells and harvest of retroviruses

Cells were transfected using polyethyleneimine (PEI). The medium in each plate was replaced with 5 ml of high glucose DMEM without supplemented FBS and pen/strep (plain DMEM). Two mixes were prepared (volumes indicated are for one plate): A) 655 µl of plain DMEM and 45 µl PEI (1mg/ml) and B) 15 µg plasmid DNA (LXSN vectors) made up to 700 µl with plain DMEM. Mixtures A and B were combined, vortexed and incubated at room temperature for about 20 minutes. At the very end of the incubation period media was aspirated off the plates. The A + B mixture was diluted with 3.6 ml of plain DMEM and the full volume was added to the cells in each plate. After 6 hours the cells were given 10 ml of fresh DMEM complete medium. The medium was replaced again on the following day with a further 10 ml of DMEM complete. Two days post-transfection the medium in each plate, which contained the retroviruses, was collected and spun down at 240 x g for 4 minutes. The supernatant was collected and 1ml aliquots were used to either directly infect NIKS or HPV16 clones or stored at -80 °C.

2.6.1.3 Retroviral infection of NIKS and NIKS HPV16-positive cells

On the day prior to transfection $5x10^5$ NIKS were plated per well of 6-well plates along with $1x10^5$ feeder cells and allowed to recover in FC medium overnight. On the following day, 1ml of the virus medium was mixed with 3ml of plain F12-Ham's along

with all the supplements (except FBS and EGF) at the required concentrations for making FC medium (volumes indicated are for 1 well). Additionally, polybrene (Santa Cruz; sc-134220) was added to the mix for a final concentration of 10 µg/ml. The medium in the wells was aspirated and replaced with the virus mixture and then the cells were incubated at 37 °C for 6 hours. Subsequently, the medium was aspirated and replaced with fresh FC. On the next day, NIKS cells were passed to T75 flasks on top of $1.4x10^6$ antibiotic-resistant feeders. Cells were left to recover in FC medium overnight and then treated with geneticin (Life Technologies; 10131) at a concentration of 300 µg/ml. Cells were selected for approximately 4-5 days with the medium (and geneticin) being replaced every second day.

2.6.2 Ready-made shE6 lentiviral particles

Two different approaches were used to obtain shE6 lentiviruses.

2.6.2.1 Commercially available ready-made particles

Commercially available shE6 lentiviral particles (Santa Cruz; sc-156008-V) along with shcopGFP (Santa Cruz; sc-108084) and shScrambled (Santa Cruz; sc-108080) control lentiviral particles were ordered. The shE6 sequence is based on the previously published UGUGUACUGCAAGCAACAGTT siE6 sequence (Niu et al., 2006) targeting both E6 and E7. For all three sets, 200 µl of viral stock was supplied containing a total of $1x10^6$ infectious units of virus. On the day prior to transfection, $1.4x10^5$ NIKS were plated per well of a 24-well plate (Thermo Scientific; 142475) along with $2x10^4$ feeder cells and allowed to recover in 1 ml of FC medium overnight. On the following day, the medium in the wells was replaced with 1 ml FC medium without supplemented FBS or pen/strep with added polybrene at a final concentration of 10 µg/ml. Cells were infected at multiplicities of infection (MOIs) of 1, 2 and 3 using 32, 64 and 96 µl, respectively, of the virus solution for the all 3 types. Cells were incubated at 37 °C for 6 hours before replacing the medium with 1 ml of fresh FC. On the next day, cells were passed to T75 flasks on top of $1.4x10^6$ antibiotic-resistant feeders. Cells were left to recover in FC medium overnight and then treated with puromycin (Santa Cruz; sc-108071) at a concentration of 1 µg/ml. Cells were selected for approximately 10 days with the medium (and puromycin) being replaced every second day. At day 7 or 8 of the selection process cells were passed to new T75 flasks

(on top of $1.4x10^6$ antibiotic-resistant feeders). Without this step, uninfected cells in the control plate seem to be able to recover from the puromycin treatment.

2.6.2.2 Custom-designed ready-made particles

shE6 and shE6/E7 lentiviral particles were designed based on published siRNA sequences and supplied by Sigma-Aldrich Mission®. Both sequences were previously tested in the siRNA format (siE6 and siE6/E7-1, respectively), as outlined in Section 2.5. The sequences of the shRNAs are listed in Table 2.4. The lentiviral vector used is pLKO.1_puro and the loop sequence is TCAAGAG.

Table 2.4: Custom-designed shE6 and shE6/E7 sequences

Name and target *(Target specificity)*	**Sequence of sense strand**	**Reference(s)**
shE6 *(E6 only)*	GAGGTATATGACTTTGCTT	(Jiang and Milner, 2002, Allison et al., 2009)
shE6/E7 *(both E6 and E7)*	GACCGGTCGATGTATGTC	(Gu et al., 2009)

In addition to the sequences targeting E6 or E6/E7, shNT (non-target) control lentiviral particles were used (Sigma-Aldrich; SHC002V). For infecting and subsequently selecting cells the same protocol as described in Section 2.6.2.1 was used, the one difference being that all cells were infected at an MOI of 4.

2.6.3 shRNA lentiviruses targeting cellular mRNA

The RNAi Consortium (TRC) lentiviral shRNA pLKO.1 vectors targeting APH-1α and PS-1, which both comprise part of the gamma secretase complex, Notch1 and GFP (as a control) were ordered from Thermo Scientific (UK). To produce virus in 293TT cells, p8.91 and pczVSV-G were co-transfected alongside the shRNA plasmids. p8.91 is a gag-pol vector while pczVSV-G is an envelope plasmid. More details regarding all vectors are provided in Table 2.5 in Section 2.9.1.

2.6.3.1 Culture of 293TT cells

293TT cells are human embryonic kidney cells derived from the HEK 293 adenovirus-transformed cell line (Graham et al., 1977). 293TT cells were generated by introducing SV40 DNA to express a small t antigen and a second SV40 expression cassette with large T antigen into HEK 293 cells (Buck et al., 2005). The cells were cultured in the same way as J2-3T3 cells (see Section 2.2.3.1) and used for the production of lentiviruses. On the day prior to transfection, cells were seeded in 10 cm plates at a density of $4x10^6$ cells per plate in 10 ml of DMEM complete.

2.6.3.2 Transfection of 293TT cells and harvest of lentiviruses

Cells were transfected using polyethyleneimine (PEI). The medium in each plate was replaced with 5 ml of high glucose plain DMEM. For one plate of cells, 650 µl of plain DMEM was mixed with a total of 7.5 µg of DNA. The mixture was vortexed and spun down briefly before adding 45 µl PEI (1mg/ml) and vortexing again. The mixture was incubated at room temperature for 10 minutes and then added drop by drop to the medium in the plate. After 6 hours the cells were given 10 ml of fresh DMEM complete medium. The medium was replaced again on the following day with a further 10 ml of DMEM complete. Two days post-transfection the medium in each plate, which contained the lentiviruses, was collected and spun down at 240 x g for 4 minutes. The supernatant was collected and 1 ml aliquots were used to either directly infect NIKS HPV16 clonal cell lines or stored at -80 °C.

As described above 293TT cells were transfected with a total of 7.5 µg of DNA. 2.5 µg of each of the two packaging vectors, p8.91 and pczVSV-G, was used. Since not just one but a whole set of shRNA vectors was acquired for APH-1α, PS-1 and Notch1, a varying amount of DNA from each individual vector was used, depending on the total number available per target. To knock-down Notch1, 0.5 µg of each of the five vectors was used. To target the gamma secretase complex, 0.4 µg of each vector was used (five specific for PS-1 and 2 specific for APH-1α), giving a total of 2.8 µg.

2.6.3.3 Lentiviral infection of NIKS and NIKS HPV16-positive cells

Cells were infected using the same method described for retroviral infection in Section 2.6.1.3.

2.7 Organotypic Raft Cultures of NIKS and NIKS HPV16-positive cells

2.7.1 Media and reagents for raft cultures

The various media used throughout the rafting process are F12 medium, keratinocyte plating medium and cornification medium 1. Media components and supplements required are listed in Table 2.2.

2.7.2 Preparation of dermal equivalents

Dermal equivalents were made by resuspending 20 ml of collagen (approximately 3.5 mg/ml) (BD Biosciences; 354236) on ice with 2.5 ml 10X F12 medium (Gibco; 21765-029), 460 µl 1M NaOH, 250 µl 100X pen/strep and 2.5 ml filtered FBS. 1 ml of this premix was plated into individual 24 mm transwell inserts (Costar; 3450) that had previously been placed in deep 6-well plates (BD Biosciences; 355467). The plate was left in the hood for 5 minutes at room temperature to allow the collagen mixture to gel. 600 µl of a $10x10^6$ cells/ml suspension of EF-IF cells were added to the remaining collagen premix and 2.6 ml of this mixture was layered into each transwell insert. The plate placed in the incubator to allow the dermal equivalents to solidify at 37 °C. After 30 minutes 19 ml of EF-1F medium was added to each deep well. The plates were left in the incubator for 3-5 days to allow the dermal equivalents to take on their appropriate shape.

2.7.3 Seeding and differentiation of keratinocytes

NIKS or HPV16 clonal cell lines were harvested, counted and resuspended in FI medium at a concentration of $3.75x10^6$ cells/ml. The medium in each deep well was aspirated carefully, using a sterile P20 or P200 pipette tip to cover the end of the glass Pasteur to gently remove excess medium from the top of the dermal equivalent itself. 200 µl of keratinocyte cell suspensions was seeded drop-wise into the center of each dermal equivalent. The plates were placed in the incubator at 37 °C for 2 hours to allow cells to attach. Then 19 ml of keratinocyte plating medium was slowly added to each deep well. Two days later the medium was replaced with a further 19 ml. On the fourth day post-seeding all medium was removed, including excess medium within the insert surrounding the raft, and three sterile cotton pads (2.5 cm x 2.5 cm) (Schleicher & Schuell Bioscience Inc.; 740-E) were placed in the bottom of each deep well to lift transwell inserts. The raft cultures were fed from underneath by gently adding 12 ml of

cornification medium to the deep well, taking great care to keep the raft itself dry. On day 2 post-lifting and every other day thereafter until the point of harvest the medium in the deep well was replaced with 9 ml of fresh medium. Raft cultures were left to differentiate for a varying number of days post-lifting, ranging from 8 to 12.

2.7.4 Harvesting and fixation of raft cultures

Prior to harvest the fixation solution was prepared. To do this 2 g of Bacto Agar (BD Biosciences; 214010) was added to 90 ml of sterile dH_2O and boiled in the microwave on a low-medium setting for approximately 3 minutes until homogeneous. The solution was left to cool and stored at 4 °C. On the day of harvest the 2 % Bacto Agar solution was reheated and 10 ml of 10 % formalin added in the fume hood for a final concentration of 1 % formalin. The fixation solution was then kept in a 50 °C water bath during the harvesting process. To fix each raft, 2-3 ml of the fixation solution was applied to a glass plate in a circular motion, to create a round layer roughly double the size of each raft culture, and left to solidify in the cell culture hood for 1-2 minutes. The medium was removed from each deep well and the transwell insert was lifted out using clean forceps. The raft culture (including any remaining dermal equivalent) was pealed of the membrane of the insert using forceps and placed on the solidified layer of fixation solution. To fix the raft, 2-3 ml of fixation solution was slowly applied on top and left to solidify for 1-2 minutes. Each glass plate was wrapped in cling film and placed at 4 °C overnight. On the following day, excess solidified fixation solution around the perimeter of the raft culture was removed with a sterile blade (Swann Morton Ltd.; 0502). The circular raft (now sandwiched between two layers of fixation solution) was cut into two halves with sterile scissors and placed side by side in a tissue-tek cassette (Simport; M510-10). The cassettes were kept in a 4 % formalin/PBS solution at 4 °C overnight. On the next day, the cassettes were transferred to 70 % ethanol and kept at 4 °C until the time of sectioning.

2.7.5 Sectioning of raft cultures

Rafts were paraffin embedded in wax and sectioned by an NIMR histologist. They were sectioned transversely onto Superfrost plus slides (Thermo Scientific; 8037/1) at a thickness of 10 μm.

2.8 Immunocytology and Immunohistochemistry

2.8.1 Immunohistochemistry of raft culture sections

Prior to beginning the immunostaining process the sections were placed at 42 °C overnight to soften the wax.

2.8.1.1 De-paraffinization and epitope exposure of raft sections

In order to immunostain raft cultures, the paraffin embedded sections underwent a dewaxing and rehydration process followed by epitope exposure. To dewax sections, slides were submerged in xylene, first in one container for 10 minutes and then in a second container with fresh xylene for 5 minutes. The sections were rehydrated using ethanol; first a quick rinse was done in 100 % ethanol to remove excess xylene, then twice for 2.5 minutes each in 100 % ethanol followed by 2 minutes each in 80 %, 50 % and 30 % ethanols and finally in PBS for 5 minutes. To unmask target antigens, the next step was a microwave-based epitope exposure. Slides were transferred into a plastic beaker with 500 ml of 0.01 M citric acid (Sigma Aldrich; 251275) buffer at pH 6 (prepared fresh during the dewaxing and rehydration steps). The container was covered with paper towels with several small punched-out holes. The sections were left to equilibrate in the buffer for 10 minutes prior to two rounds of boiling. Slides were boiled for 7 minutes at a high setting (90 % power), allowed to stand for 2 minutes at room temperature, followed by 5 more minutes of boiling at a high setting (90 % power). The sections were allowed to cool for at least 15 minutes at room temperature prior to blocking and application of antibodies.

2.8.1.2 Applying primary and secondary antibodies to raft sections

Directly following the epitope exposure step, the sections were equilibrated in PBS for 5 minutes. Then slides were gently dried and the area immediately surrounding the sections marked with a hydrophobic pen. The slides were transferred to a humidity chamber and blocked in 3 % BSA (PAA; K41-001) for at least 30 minutes at room temperature. After blocking, the primary MCM7 antibody (Neomarkers; MS-862-P1) was made up in 1 % BSA at a 1:100 dilution, applied to the sections (100 µl each) and left overnight at room temperature. If E4 staining was also required the antibody (prepared in house, B11 clone) was added at a dilution of 1:100 alongside MCM7. The following day the slides were washed in 0.1 % PBS/Tween (Sigma-Aldrich; P1379)

three times for 5 minutes each at room temperature. The biotinylated anti-mouse secondary antibody (Vector Labs; BA9200) for MCM7 was made up in 1 % BSA at a 1:100 dilution, applied to each section (100 µl each) and incubated at room temperature for 30 minutes. Then slides were washed in 0.1 % PBS/Tween 3 times for 20 minutes each.

2.8.1.3 Primary antibody signal amplification

The first step in the signal amplification process for MCM7 involved the avidin-biotin-peroxidase complex (ABC) method following the washes after the secondary antibody incubation. The complexes were made up using the Vectastain ABC Elite kit (Vector Laboratories; PK-7200) at a dilution of 1:400 in 50 mM Tris HCl pH 7.6. The complexes were applied to sections (100 µl each) and allowed to incubate for 30 minutes at room temperature. Thereafter the slides were washed in 0.1 % PBS/Tween three times for 5 minutes each. To complete the amplification process, the TSA™ Cyanine 3 Tyramide Reagent Pack (Perkin Elmer; SAT704A001EA) was used. Fluorochrome (diluted at 1:50) labeled Tyramide (rhodamine) was applied to sections (100 µl each) for 8 minutes at room temperature. Then slides were washed in 0.1 % PBS/Tween three times for 15 minutes each. DAPI (Sigma-Aldrich; D9542) was applied to each section (100 µl each) as a nuclear counterstain at a dilution of 1:800 for up to 1 hour at room temperature. Subsequently, the sections were washed in 0.1 % PBS/Tween three times for 15 minutes each.

2.8.1.4 Mounting raft culture slides for microscopy

Slides were rinsed once in dH_2O and dried. Then 10-20 µl of citifluor reagent (Citifluor Ltd; AF1) was dropped on each section and a coverslip (Menzel-Gläser; BB024060A1) was laid on top. Great care was taken to ensure no air bubbles were trapped underneath the coverslip. Slides were kept in a folder at 4 °C.

2.8.2 Immunoctyology of NIKS, NIKS HPV16 clones and other NIKS-derived cell populations

To harvest monolayer keratinocytes for immunocytology, square coverslips (VWR International Ltd.; 631-0127) were sterilized using 70 % ethanol and placed in 6-well plates. Irradiated fibroblasts and keratinocytes were seeded on top as described in Section 2.3.

2.8.2.1 Fixation of coverslips

Depending on the antibodies to be used for immunostaining, cells on coverslips were fixed with either methanol or paraformaldehyde. To do this, growth medium was aspirated from the wells and cells washed once in PBS. Subsequently, coverslips in each well were submerged in 2 ml of ice-cold 100 % methanol for 10 minutes or 2 ml of 4 % paraformaldehyde/PBS at room temperature for 5 minutes. After the incubation period, cells were washed twice with PBS and stored in 0.01 % sodium azide in PBS at 4 °C.

2.8.2.2 Immunocytology and mounting monolayer coverslips

The PBS/azide solution in each well with the coverslips was aspirated. The cells were blocked in 5 % normal goat serum (NGS) (Cell Signaling Technology; 5425) in PBS for 1 hour at room temperature. After blocking, the phospho-histone 3 antibody (Cell Signaling Technology; 9733) was made up in 5 % NGS in PBS at a 1:200 dilution, applied to the coverslips and left for 1 hour at room temperature. Thereafter, 5 quick rinses of the coverslips (within the wells) were done using PBS. Next, Alexa Fluor® 488 Goat Anti-Rabbit IgG (Life Technologies; A11008) was applied as a secondary antibody in 5 % NGS in PBS at a 1:75 dilution and left for 1 hour at room temperature. DAPI was added as a nuclear counterstain alongside the secondary antibody at a 1:1000 dilution. Subsequently, the coverslips (within the wells) were rinsed 5 times using PBS. Coverslips were rinsed once in dH_2O, lifted out of the wells carefully and dried gently. Then 10-20 µl of citifluor reagent was dropped onto a Superfrost plus slide and the coverslip inverted on top, taking great care to ensure no air bubbles were trapped underneath. Slides were kept in a folder at 4 °C.

2.8.3 Microscopy and imaging software

All fluorescently stained cells were viewed on a Zeiss A1 microscope equipped with fluorescent filters. Fluorescent images were captured using a Zeiss AxioCam MRm camera and images viewed using Axiovision software.

2.9 DNA techniques

2.9.1 DNA constructs used

Table 2.5: List of vectors used in this study

Name of plasmid	Use	Reference and/or source
LXSN, LXSN_E6, LXSN_E7 and LXSN_E6/E7	Retroviral vectors used for the stable expression of HPV16 E6 and E7 proteins	Kindly provided by Denise Galloway (Fred Hutchinson Cancer Research Center, Seattle, USA) (Halbert et al., 1991)
LXSN_E6SAT and LXSN_E6ΔPDZ	Retroviral vectors used for the stable expression of HPV16 E6SAT and E6ΔPDZ	Made by site-directed mutagenesis by Lietta Nicolaides (NIMR, London, UK)
pMV11 and pMV11_E6	Used for overexpressing E6	Kindly provided by John Doorbar (Doorbar et al., 2000)
pcDNA3.1 and pcDNA3.1_E6SD	Used for overexpressing E6	Life Technologies; V790-20 (Elston, 1996)
pBABE_puro	Used for overexpressing E6	Kindly provided by Qian Wang (NIMR, London, UK) (Addgene; 1764)
pczVSV-G	Envelope plasmid for producing viral particles	Kindly provided by Kate Bishop (NIMR, London, UK) (Bock et al., 2000)
p8.91	Plasmid for producing viral particles, includes Gag and Pol	Kindly provided by Kate Bishop (NIMR, London, UK) (Naldini et al., 1996)
pLKO.1_shGFP	Used for the production of control lentiviruses to knock-down GFP	TRC Lentiviral shRNA (Thermo Scientific; UK)

pLKO.1_shNotch1	Used for the production of lentiviruses to knock-down Notch1	TRC Lentiviral shRNA (Thermo Scientific; UK) TRCN0000003358, TRCN0000003359, TRCN0000003360, TRCN0000003361 and TRCN0000003362
pLKO.1_shPS1	Used for the production of lentiviruses to knock-down gamma secretase	TRC Lentiviral shRNA (Thermo Scientific; UK) TRCN0000061738, TRCN0000061739, TRCN0000061740, TRCN0000061741 and TRCN0000061742,
pLKO.1_shAPH1α	Used for the production of lentiviruses to knock-down gamma secretase	TRC Lentiviral shRNA (Thermo Scientific; UK) TRCN0000113336 and TRCN0000113339

2.9.2 Transformation of *E.coli* with DNA

Plasmid DNA was mixed with 50 µl of competent XL10-Gold® Ultracompetent cells (Stratagene; 200314) and incubated on ice for 30 minutes. The mix was heat-pulsed in a water bath at 42 °C for 30 seconds and then cooled on ice for 2 minutes. Subsequently, 800 µl of SOC medium (Life Technologies; 15544-034) was added and cells were incubated at 37 °C for 45 minutes at constant shaking (220 rpm). Cells were plated on LB agar plates containing either ampicillin (Sigma Aldrich; A5454) at 100 µg/ml (for VSV-G, p8.91, pMV11, pMV11_E6, pcDNA3.1, pcDNA3.1_E6SD, pBABE_puro, LXSN, LXSN_E6, LXSN_E6SAT, LXSN_E6ΔPDZ, LXSN_E6/E7) or carbenicillin at 100 µg/ml (for pLKO.1_shGFP, pLKO.1_shNotch1, pLKO.1_shPS1 and pLKO.1_shAPH1α).

2.9.3 Plasmid purification

To extract plasmid DNA from bacteria, three commercial kits were used depending on the amount and purity of plasmid required. The QIAprep® Spin Miniprep Kit (Qiagen; 27106) was used from small-scale preps, from 2-5 ml overnight bacterial cultures. The QIAGEN® Plasmid Midi Kit (QIAGEN; 12143) and the QIAGEN® Plasmid Maxi Kit (QIAGEN; 12162) were used for larger-scale preps, from 100 ml up to 500 ml cultures, respectively. The purification was done according to the manufacturer's instructions.

2.9.4 Quantification of plasmid DNA

Plasmid DNA was quantified using a Nanodrop ND-1000 Spectrophotometer.

2.9.5 Restriction enzyme plasmid digestion

To allow for the transfection of cells with linearized DNA (as outlined in Section 2.2.5), pMV11, pcDNA3.1 and pBABE_puro vectors were digested using restriction enzymes. BglII (New England Biolabs; R0144) is a single cutter for pcDNA3.1 while BamH1 (New England Biolabs; R0136) cuts both pMV11 and pBABE_puro in just one place. A total of 20 µg of plasmid DNA was used in the reaction for each of the vectors and digested with 20 units of the appropriate enzyme. For both restriction enzymes, an additional tube was prepared where dH_2O was used instead of the enzyme. This was used to ensure that both enzymes were working correctly.

2.9.6 Agarose gel electrophoresis

To assess the presence and quality of plasmid DNA or for subsequent gel extraction, DNA was separated on a 1 % (w/v) agarose (company) gel in TAE containing 0.5 µg/ml Ethidium Bromide (Bio-rad; 161-0433) at 120 V for up to 45 minutes.

2.9.7 Gel extraction

To do gel extractions, the relevant bands were visualized in the agarose gel using Ultraviolet light and excised using a sterile blade. The QIAquick Gel Extraction Kit (QIAGEN; 28704) was used according to the manufacturer's instructions.

2.10 Quantitative PCR (qPCR)

Quantitative real-time (RT) polymerase chain reaction (PCR) was carried out using cDNA as a template. Forward and reverse primers were used to assess the levels of

HPV16 E6, HES1 and p21 transcripts in NIKS and HPV16 clonal cell lines. β-actin, GAPDH or ELF1 primers were used as endogenous controls.

2.10.1 Extraction of total RNA

For extraction of RNA, cells were harvested, washed with PBS and then placed on ice. Total RNA extraction was carried out using the RNeasy® Mini Kit (Qiagen; 74104) and QIAshredder™ kit (QIAGEN; 79654) according to the manufacturer's protocol. RNA was stored at -80 °C. If RNA extraction was not carried out immediately after harvest of cells, pellets were resuspended in RNAprotect® Cell Reagent (QIAGEN; 76526) following the manufacturer's instructions and stored at -80 °C indefinitely.

2.10.2 DNase digestion and reverse transcription

Prior to making cDNA, genomic DNA was removed from 2 µg of total RNA using the DNA-*free*™ kit (Ambion; AM1906) according to the manufacturer's protocol. The reverse transcription was done using the SuperScript™ III First-Strand Synthesis Kit (Life Technologies; 18080-051). A volume of 16 µl (approximately 0.5 µg) of clean RNA was added to a tube along with 2 µl oligo$(dT)_{20}$ primers and 2 µl dNTPs. The mixture was incubated at 65 °C for 5 minutes and then placed on ice for at least 1 minute. Subsequently 4 µl of 10X RT Buffer, 8 µl of $MgCl_2$, 4 µl of DTT, 2 µl RNase OUT™ and 2 µl SuperScript™ III reverse transcriptase was added to each tube before incubating at 50 °C for 1 hour. To stop the reaction, tubes were placed at 85 °C for 5 minutes. Thereafter, cDNA was stored at -80 °C or used for qPCR. For each RNA sample an additional tube was prepared where 2 µl of nuclease-free H_2O (Life Technologies; AM9935) was used instead of the enzyme. This was used to control for the absence of genomic DNA. cDNA was generally diluted 50-100-fold with nuclease-free H_2O prior to doing qPCR.

2.10.3 qPCR primer design and primer sequences

E6, β-actin and GAPDH primers were designed using Primer Select software and ordered from Eurogentec (UK). HES1, p21 and ELF1 primers are commercially available through Origene (USA) (HK209713, HK201880, HK202783, respectively) along with appropriate template standards for making standard curves. A list of the primers and their sequences is shown in Table 2.6.

Table 2.6: Primers used for qPCR	
E6 primers*	**Forward:** TGTTTCAGGACCCACAGGAGC **Reverse:** CGCAGTAACTGTTGCTTGCAG
β-actin primers	**Forward:** TGGGCATGGGTCAGAAGGAT **Reverse:** CGGCCAGAGGCGTACAGGGA
GAPDH primers	**Forward:** CCTCCCGCTTCGCTCTCT **Reverse:** CTGGCGACGCAAAAGAAGA
HES1 primers	**Forward:** GGAAATGACAGTGAAGCACCTCC **Reverse:** GAAGCGGGTCACCTCGTTCATG
p21 primers	**Forward:** AGGTGGACCTGGAGACTCTCAG **Reverse:** TCCTCTTGGAGAAGATCAGCCG
ELF1 primers	**Forward:** CTAAAGCAGTGTCCAGGTTGTGG **Reverse:** CGCTGACCTTCCACTTTTGCCA

**The forward and reverse E6 primers amplify a 114bp fragment within the first exon of the HPV16 E6 ORF. Hence, all species of E6 (including the full length protein, E6*I and E6*II) are detected.*

2.10.4 qPCR reagent cocktails

Power SYBR® Green PCR Master Mix (Applied Biosystems; 4367659) was used to amplify and detect cDNA in 96-well PCR plates (Thermo Scientific; TUL-962-011N) using an ABI 7500 Real-Time PCR System. A fresh master mix of reagents was prepared for each primer set (see Table 2.7 below) immediately prior to loading the plate. The final volume in each well was 25 µl.

Table 2.7: qPCR master mix			
Custom-designed primers		**Origene primers**	
Reagent	**µl per reaction (per well)**	**Reagent**	**µl per reaction (per well)**
Forward (F) primer	1.75	Primers (F + R)	1
Reverse (R) Primer	1.75		
Sybr Green	12.5	Sybr Green	12.5
dH_20	6	dH_20	8.5

2.10.5 qPCR plating scheme and cycle parameters

Samples were run in triplicate wells (for each primer set). To set up the reaction, 22 µl of the master mix was pipetted into each well, using a Multipette® Xstream from Eppendorf for added accuracy, followed by 3 µl of cDNA pipetted separately. Table 2.8a outlines the qPCR cycle parameters. They include a dissociation curve at the end of the amplification steps. This was included because SYBR Green can bind to unspecific double stranded DNA, such as primer-dimers, which can interfere with results. The dissociation curve shows whether a single or multiple PCR products have been amplified. Table 2.8b outlines the parameters for the dissociation program.

Table 2.8a: PCR cycle parameters			
Step	**Number of cycles**	**Time per cycle**	**Temperature**
1	1	2 minutes	50 °C
2	1	15 minutes	95 °C
3	40	15 seconds	95 °C
4	1	1 minute	60 °C
Table 2.8b: Dissociation parameters			
Step	**Number of cycles**	**Time per cycle**	**Temperature**
1	1	15 seconds	95 °C
2	1	20 seconds	60 °C
3	1	95 seconds	95 °C

2.10.6 Standard curves for primers

A standard curve was generated for each primer pair used in order to establish its efficiency and sensitivity. To make the standard curve, a DNA plasmid containing the sequence that is amplified by the primers was chosen as a template. For the three pairs of Origene primers (p21, HES1 and ELF1) the template standard was ordered along with primers. Six serial 10-fold dilutions of the template were prepared which corresponded to a known number of copies of the template, from 1 to $1x10^6$, and served as a template for the qPCR reaction. To generate the standard equation, the logarithms

of the values of the known copy numbers in each dilution (either 1, 10, 100, 1000, 10000 or 1000000) were plotted on a graph along the x-axis against the Ct (cycle threshold) value given by the qPCR machine for each dilution along the y-axis, and an equation was obtained in the form of y = mx + c. The slope (m) refers to the efficiency of the primer pairs, where a slope of -3.33 shows a perfect linear relationship between DNA copy number and Ct value and corresponds to an increase of 3.33 Cts for every 10-fold dilution of sample. The y-value in this equation is the Ct value that the qPCR measures, which refers to the number of cycles needed to amplify one copy of DNA.

Table 2.9: Standard curves for primers used for qPCR	
E6 primers	y = -3.328x + 38.26
β-actin primers	y = 3-.308x + 35.757
GAPDH primers	y = -3.416x + 39.632
HES1 primers	y = -3.333 + 42.076
p21 primers	y = -3.338x + 34.526
ELF1 primers	y = -3.306x + 40.524

2.10.7 Calculations for copy number determination

The standard curves for the primer sets were used to calculate the copy numbers of the transcripts of interest in each sample. Each triplicate set of Ct values per sample and primer set was averaged. To account for pipetting error the software calculated the standard deviation for each set, with those above 0.5 indicating excessive variation. If so, the whole qPCR reaction was repeated for that sample. Acceptable Ct averages were used to calculate copy number. To do so, the standard curve equation was solved for x. The number of copies is the inverse log of x ie. 10^x. Once transcript numbers had been established for all primer pairs, the values for E6, p21 and HES1 were divided by the values of either GAPDH, β-actin or ELF1 to normalize the results. The final number obtained is the average amount of transcript per cell relative to the endogenous control.

2.11 Protein Analysis

2.11.1 Cell lysis for western blot analysis

Cells were harvested, washed and then lysed, or frozen at -80 °C and lysed at a later point after being allowed to thaw to room temperature. Prior to lysis, 1-2 µl of Benzonase® Nuclease (Sigma-Aldrich; E1014) in 4-8 µl of PBS was added to each tube and the pellet was resuspended. Then 100-500 µl (depending on pellet size) of either lysis buffer was added. Both the 1 % NP-40 and 6 % SDS RIPA buffers were used with 1X Complete Protease Inhibitor Cocktail (EDTA-free) solution (Roche; 04 693 159 001).

2.11.1.1 1 % NP-40 buffer

The 1 % NP-40 buffer was used to assess the soluble protein fraction of cells and is based on a previously published protein extraction buffer (Nakahara et al., 2005). It consists of 50 mM Tris pH 7.4, 150 ml NaCl, 1 mM EDTA and 1 % NP-40. After adding the buffer to cells and resuspending the pellet, the lysate was placed on ice for 30 minutes. Subsequently, the samples were spun down at 14000 rpm using a Heraeus Fresco 17 centrifuge (Thermo Electron Corporation) for 15 minutes at 4 °C and the supernatant collected and stored at -80 °C.

2.11.1.2 6 % SDS RIPA buffer

The 6 % SDS RIPA buffer was used to prepare whole cell extracts. It is made up of 150 mM NaCl, 1 % Triton X, 0.5 % Sodium deoxycholate, 6 % sodium dodecyl sulfate (SDS), 50 mM Tris pH 8 and 0.005 mM EDTA pH 8. After adding the buffer to the cells and resuspending the pellet, the lysate was boiled at 95 °C for 10 minutes and then spun down at 17000 rpm using a Heraeus Fresco 17 centrifuge (Thermo Electron Corporation) for 5 minutes. Thereafter, the supernatant was transferred to a new boil-proof microcentrifuge tube (Corning; MCT-150-C) and stored at -80 °C.

2.11.2 Protein quantification

Protein quantification was carried out using the D_C Protein Assay Kit (Bio-Rad; 500-0111) according to manufacturer's instructions. BSA standards, prepared in 0.5 mg/ml increments ranging from 0 to up to 10 mg/ml, were used to make a standard curve.

2.11.3 SDS PAGE

2.11.3.1 Preparation of gels and gel electrophoresis

Appleton Woods OmniPAGE Mini gel electrophoresis equipment was used for gels prepared in-house. Different percentage gels were prepared depending on the size of the proteins to be analyzed. Table 2.10 shows the compositions of the stack and 6, 10 or 15 % Tris-glycine polyacrylamide resolving gels. The resolving gel was prepared first (8 ml per gel) and allowed to set for approximately 30 minutes. The stacking gel was then made and poured over the resolving gel (2 ml per gel). The combs, generally with 10 wells, were put in place and the gel was left to polymerize for 30 minutes.

Table 2.10: Composition of 6, 10 and 15 % Tris-glycine SDS-polyacrylamide resolving gels and 5 % stacking gel

Resolving gel (for 10 ml)			
Reagent	**6 %**	**10 %**	**15 %**
dH_20	5.3 ml	4 ml	2.3 ml
30 % acrylamide mix	2 ml	3.3 ml	5 ml
1.5 M Tris (pH 8.8)	2.5 ml	2.5 ml	2.5 ml
10 % SDS	0.1 ml	0.1 ml	0.1 ml
10 % ammonium persulphate	0.1 ml	0.1 ml	0.1 ml
TEMED	8 µl	4 µl	4 µl
Stacking gel (2 ml)			
dH_20	1.4 ml		
30 % acrylamide mix	0.33 ml		
1 M Tris (pH 6.8)	0.25 ml		
10 % SDS	20 µl		
10 % ammonium persulphate	20 µl		
TEMED	2 µl		

For many experiments XCell *SureLock*® Mini-Cell electrophoresis equipment from Life Technologies was used for running ready-made NuPAGE 4-12 % Bis-Tris mini gels (Life Technologies; NP0335B0X), according to the manufacturer's instructions. Between 10 and 30 µg of protein (depending on the protein to be assessed) was loaded into each well. 1 L of SDS electrophoresis buffer (see Table 2.1) was used in each

Appleton Woods tank containing up to 2 gels. Gels were run at 80 V for about 30 minutes and then 150 V for 60-90 minutes.

2.11.3.2 Membrane transfer for western blot

All 15 % gels and some of the ready-made NuPAGE gels (if the protein to be assessed was small) were transferred onto 0.2 µm Immuno-Blot PVDF membranes (Bio-Rad; 162-0176). All other gels were transferred onto 0.45 µm PVDF membranes (Millipore; IPVH00010). Before use, membranes were submerged in methanol, rinsed in dH_2O and then left to soak in transfer buffer for 10-15 minutes. All transfers were done using 500 ml of transfer buffer per Bio-Rad Mini Trans-Blot® Cell tank (containing up to 2 gels) at 4 °C for 90 minutes at 150 V or overnight at 50 V, depending on the antibody to be used.

2.11.3.3 Blocking, antibody incubations and washing

Following transfer, the membranes were blocked in 5 % milk (Oxoid; LP0031) in 0.1 % TBS/Tween for 1 hour at room temperature or overnight at 4 °C. Subsequently, the membranes were incubated with primary antibody for 1-2 hours at room temperature or overnight at 4 °C. Generally, the membranes were cut into several smaller strips before applying antibody to allow incubation with several different antibodies at once. The antibodies were diluted in 5 ml of 5 % milk in 0.1 % TBS/Tween. Table 2.11a lists all the primary antibodies used for protein analysis and their respective dilutions. Following the incubation with the primary antibody, all membrane pieces were washed in 0.1 % TBS/Tween at room temperature for 1-2 hours with a change in wash buffer every 10-15 minutes. The membranes were then incubated with secondary antibody, listed in Table 2.11b, in 5 ml of 5 % milk in 0.1 % TBS/ Tween for 1 hour at room temperature. This was followed by a second round of washing with 0.1 % TBS/Tween at room temperature, lasting up to 4 hours with a change in wash buffer every 20-30 minutes. Table 2.12 lists further E6 antibodies that were tested in an attempt to reduce the level of background in the western blots.

2.11.3.4 Signal detection

All proteins were detected using 3 different kits, partly depending on the level of sensitivity needed. The Amersham™ ECL western Blotting Detection kit (GE Healthcare; RPN2106) was used for highly abundant proteins while the Amersham™

ECL Advance kit (GE Healthcare; RPN2135) was used to detect low level proteins. Halfway through the project the Amersham kits went out of production and the Immobilon western Chemiluminescent HRP Kit (Millipore; WBKLS0500) was used instead.

Table 2.11a: Primary antibodies used for western blotting		
Antibody name	**Dilution (incubation time)**	**Company; catalogue #**
E6 (2E-3F8)	1:1000 (overnight at 4 °C)	Euromedex; 2E-3F8
E7 (NM2) E7 (716-325) (used together)	1:500 each (overnight at 4 °C)	Santa Cruz; sc-65711 and sc-51951
p53 (DO-1)	1:1000 (overnight at 4 °C)	Santa Cruz; sc-126
NICD (VAL1744)	1:1000 (overnight at 4 °C)	Cell Signaling Technology; 2421
p21 (EA10)	1:100 (overnight at 4 °C)	Abcam; ab16767
Rb	1:2000 (overnight at 4 °C)	BD Pharmingen; 554136
Cyclin A (6E6)	1:500 (overnight at 4 °C)	Leica Biosystems; CYCLINA
GAPDH	1:5000 (1-2 hours at room temperature)	Millipore; MAB374
HSP70 (W-27)	1:2500 (1-2 hours at room temperature)	Santa Cruz; sc-24
Table 2.11b: Secondary antibodies used for western blotting		
Antibody name	**Dilution (incubation time)**	**Company; catalogue #**
Anti-mouse IgG-HRP (from sheep)	1:10000 (1-2 hours at room temperature)	GE Healthcare; NA931V
Anti-rabbit IgG-HRP (from donkey)	1:10000 (1-2 hours at room temperature)	GE Healthcare; NA934V

Table 2.12: Additional E6 primary antibodies tested	
Antibody name	**Company; catalogue #**
E6 (1E-6F4)	Euromedex; 1E-6F4
HPV16 E6 / HPV18 E6 (C1P5)	Santa Cruz; sc-460
E6 (N-17)	Santa Cruz; sc-1584
E6	Arbor Vita Corporation; AVC#1007
HPV16 E6 / HPV18 E6 (C1P5)	Abcam; ab70

Chapter 3: Establishing the Role of E6 and E7 in Controlling the Proliferation of Cells Containing Episomal HPV16 Genomes

3.1 Introduction

Previous work from my laboratory suggested that NIKS cells transfected with HPV16 genomes can immediately present with rafting phenotypes that resemble LSILs or HSILs (Isaacson Wechsler et al., 2012). The cell lines also gave rise to corresponding proliferation patterns in monolayer cell culture with the HSIL-like cell lines reaching higher cell densities. These data further showed that the growth phenotypes may be caused, at least in part, by higher levels of the soluble protein fractions of both the viral E6 and E7 proteins.

This novel cell line model has given me the opportunity to further characterize neoplastic progression caused by HPV infection and to investigate the underlying mechanism that causes an LSIL to advance to an HSIL. The fact that the cell lines have distinct growth characteristics even in monolayer has allowed me to work predominantly with this cell culture system; an environment that is much easier to manipulate than raft cultures and *in vivo* models. Hence, this chapter has aimed to address the role of E6 and E7 in giving rise to the LSIL- and HSIL- like growth phenotypes of these cells.

When it comes to HPV-induced neoplastic progression, both E6 and E7 proteins are considered to be the main players (von Knebel Doeberitz et al., 1988, von Knebel Doeberitz et al., 1994). While the precise order and expression levels of all viral gene products is disrupted in high-grade neoplasias, only E6 and E7 (and to some extent E5 (DiMaio and Mattoon, 2001, Barbaresi et al., 2010)) have transforming, tumor-promoting capabilities when expressed at aberrant levels, due to, amongst other things, their well characterized effects on p53 (Werness et al., 1990) and Rb (Dyson et al., 1989), respectively. Generally a low-grade lesion is associated with much lower levels of both proteins than a high-grade lesion, with high levels making cells much more vulnerable to the accumulation of genetic changes that can lead to cancer. It has been suggested that high-grade neoplasia is correlated with integration of the viral genome into host chromosomes (Klaes et al., 1999) and that both E6 and E7 are expressed more

stably once integrated (Jeon and Lambert, 1995), due to increased stability of transcripts and *cis*-regulatory effects on regulation of transcription of integrants (von Knebel Doeberitz et al., 1991). Nevertheless, other data have shown that 89 % of all cervical lesions, 71 % of HSILs and 49 % of HPV-related carcinomas present exclusively with viral episomes (Hafner et al., 2008), with E6 and E7 only being expressed from these extrachromosomal genomes. This means that the aberrant expression of these proteins, that is associated with high-grade neoplasias, can occur from intact viral episomes.

Several groups have assessed the effects of E6 and E7 expression on neoplastic progression in transgenic mouse models (Arbeit et al., 1996, Brake and Lambert, 2005, Buitrago-Perez et al., 2012). However, these studies have not looked at endogenous E6 and E7 expression in the context of the full viral genome.

To explore the underlying mechanism, presumably involving E6 and E7, that gives rise to the LSIL- and HSIL-like proliferation patterns, most of my experiments were carried out in monolayer cultures. Although I have observed the growth phenotypes for several different clonal HPV16 cell lines, from two independent transfection and selection events (Isaacson Wechsler et al., 2012), for simplicities sake I used only two cell lines (one LSIL- and one HSIL-like) for the majority of my experiments. The two clones that were chosen, 1K and 2K, have, in the past, been shown to have the most different growth patterns out of all cell lines tested.

The growth assay experiment was first optimized and carried out by Erin Isaacson Wechsler (NIMR). Proliferation of cells was quantified by counting them at specifically timed increments. The number of cells seeded and the time-points analyzed during the growth assays were such that the cells were sub-confluent at day 3, confluent at approximately day 5 and post-confluent from day 7 onwards. The term “confluent” means that the culture dish is completely covered in cells and looks full, with most NIKS colonies having merged with each other, so that all cells are surrounded by other cells. The divergence of the cell lines, to give rise to the two growth phenotypes, was very much dependent on the point of confluence, with the exact seeding efficiency of cells, which varied slightly from one experiment to another, dictating at which point exactly cells reached confluence. Generally, the cell lines began to diverge from day 3 onwards half of the time, when cells seeded well, and only from day 5 onwards for the

other half, when cells did not seed with as high of an efficiency and looked slightly sick for the first day or two. While the faster growing HSIL-like cells continued proliferating even once confluence had been reached, the slower LSIL-like cells tended to plateau off and not grow very much between days 5 and 7. Hence, the two growth phenotypes could easily be distinguished by day 7.

The dependence of the growth phenotypes on the confluence of cells makes this monolayer model very relevant in terms of studying the virus in the context of its normal environment. Since HPV infects the epithelium, the virus is generally not in a sub-confluent setting, as all cells within the epithelium are packed together tightly and surrounded by other cells, the exception to this being a wound. As a result, we consider a confluent monolayer to represent a reasonable model of the basal layer in raft culture and also real stratified epithelium because the cells are probably of a fairly equally density. Hence, the growth potential of cells and the levels of viral proteins observed at confluence should be similar to that of basal cells. Therefore the effects of the virus and the differences between the LSIL- and HSIL-like clonal cell lines observed during the growth assays, may reflect the real pathways and mechanisms that the virus is deregulating during neoplasia.

3.2 Results

3.2.1 The two phenotypes, that NIKS clonal cell lines containing HPV16 episomes show, are consistently reproducible in monolayer culture

Previous work in the laboratory has shown that in monolayer growth assays, HPV16-transfected, episomal NIKS clonal cell lines spontaneously present with two growth phenotypes (Isaacson Wechsler et al., 2012). One type of clone grows more quickly than the other type, from the point of confluence. The main focus of this project was to determine how this growth difference arises, and in what way and to what extent the two types of clones differ. However, before embarking on this, it was important to ensure that the growth phenotypes could be consistently reproduced. Therefore I repeated the growth assays following the same protocol as had previously been used.

Two clonal HPV16 cell lines, 1K and 2K, were cultured in a 9-day growth assay. Cells were counted at days 1, 3, 5, 7 and 9 post-seeding to assess the differential proliferation patterns (Fig. 3.1A). A bar chart showing fold-increase relative to the previous time-point is shown in Figure 3.1B. The growth rate of 1K and 2K is very similar between day 1 and day 3, when cells are sub-confluent. For NIKS, it is much lower at this point. This may be due to these cells taking longer to adhere to the bottom of the well post-seeding which causes a delay in their growth. Between days 3 and 5 and days 5 and 7, when cells first reach confluence and then continue proliferating into post-confluence, respectively, the distinct slow and fast growth phenotypes start to emerge. The rate of proliferation of LSIL-like 2K cells is lower than that of both NIKS and the HSIL-like 1K clone. It seems that NIKS have the capacity to grow quickly at this point because the wells are less full than those of both 1K and 2K, due to the later onset of growth. From day 7 to 9, 1K and 2K grow at a very comparable pace while NIKS have slowed down. However, since the number of cells for 1K was already much higher at day 7 than for 2K, this results in the overall difference in cell number at day 9 to be even more pronounced than at day 7. Overall, between days 1 and 9, NIKS have increased their cell numbers 22-fold, while 1K and 2K have done so 39- and 24-fold, respectively. This means that 1K have grown to a density that is 2.2-fold higher than that of NIKS while 2K have reached a 1.4-fold higher cell density.

The data in Figure 3.1 are an average of 19 individual experiments that were accumulated throughout the course of this project. Unpaired t-tests were used to compare 1K and 2K cell numbers at each time-point. There is no significant difference at day 1 and 3 with p values of 0.94 and 0.84, respectively. At days 5, 7 and 9 the overall cell numbers are significantly different with p values of 0.02 at day 5 and less than 0.00001 at both days 7 and 9.

The growth curve illustrates that the proliferation phenotypes of my cells are not identical to what was previously described (Isaacson Wechsler et al., 2012). One difference is that my HPV16 clones have the capacity to grow to a much higher cell density than before. Furthermore, the growth of my slow growing LSIL-like clone does not stop after reaching confluence at day 5. Instead, cells continue growing well into post-confluence. Therefore it seems that the overall divergence of the LSIL- and HSIL-like cells is less than before. Nevertheless, the most important feature of the growth phenotypes, that they only diverge from the point of confluence, is readily reproducible.

A.

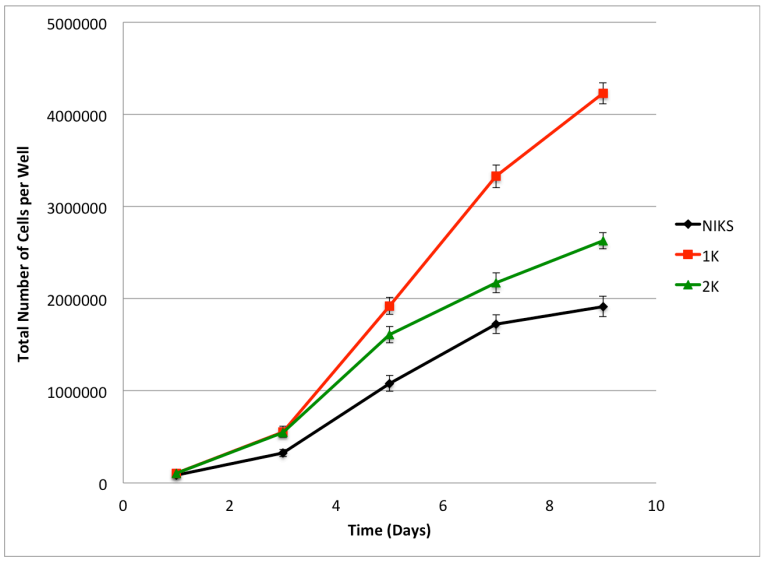

B.

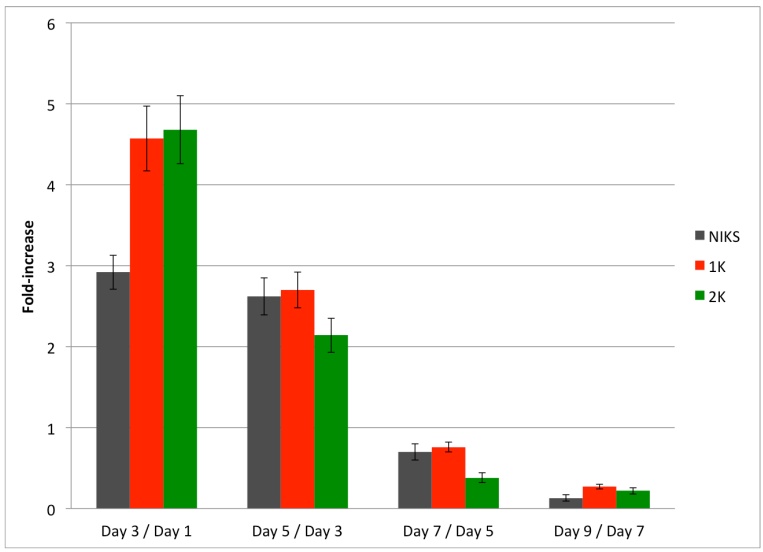

Figure 3.1: The two phenotypes, that NIKS clonal cell lines containing HPV16 episomes show, are consistently reproducible in monolayer culture

NIKS, 1K and 2K cell lines were counted in duplicate at days 1, 3, 5, 7 and 9 post-seeding and compared in terms of their growth phenotypes. The cells become confluent at approximately day 5. The 1K clone (red) consistently grows to a higher cell density than the 2K clone (green). **A)** The mean number of cells per 6-well plate well was plotted against the time in days. The error bars represent +/- the standard error of 19 individual experiments. Unpaired t-tests were used to compare 1K and 2K cell numbers at each time-point. The p values are 0.94, 0.84 and 0.02 at days 1, 3 and 5, respectively, and less than 0.00001 at both days 7 and 9. **B)** Fold-increase relative to the previous time-point was calculated and plotted in a bar chart. The error bars represent +/- the standard error of 19 individual experiments.

3.2.2 The difference in cell densities between NIKS and HPV16-containing clonal cells can be observed by microscopy

The majority of experiments in this project were carried out in monolayer culture, where cell density plays an important role in determining the growth phenotype of the cells. To visualize what the cells look like in the wells at the different time points, NIKS, 1K and 2K were cultured in a growth assay format and photographs of the cells were taken using brightfield microscopy at days 1, 3, 5, 7 and 9 post-seeding.

The images (Fig. 3.2) confirm that at days 1 and 3 the 6-well plate wells are sub-confluent with individual cell colonies visible, more so at day 1 than at day 3. There are plenty of feeder cells that fill up the empty space between colonies. At day 5, for the HPV16 clones, the colonies have merged to give rise to one confluent monolayer, with feeder cells having been pushed out of the way and very few remaining. NIKS are lagging behind with some individual colonies still distinguishable. At days 7 and 9, all the wells are packed tightly with cells. Both the LSIL- and HSIL-like cells have become much smaller in size to accommodate increasing numbers. NIKS too have decreased in size but much less so than the clones. For NIKS, at day 7 some colonies are still discernible, however, most have merged. For the clones, next to no feeders remain adhered to the bottom of the well while for NIKS, even at day 9, the post-confluent monolayer seems to be interspersed with them.

Overall, the images of the cells are helpful in visualizing the various degrees of confluency; the differences between a sub-confluent, confluent and post-confluent well can be readily observed for each cell line. NIKS grow considerably slower than the clones and therefore take longer to reach confluence.

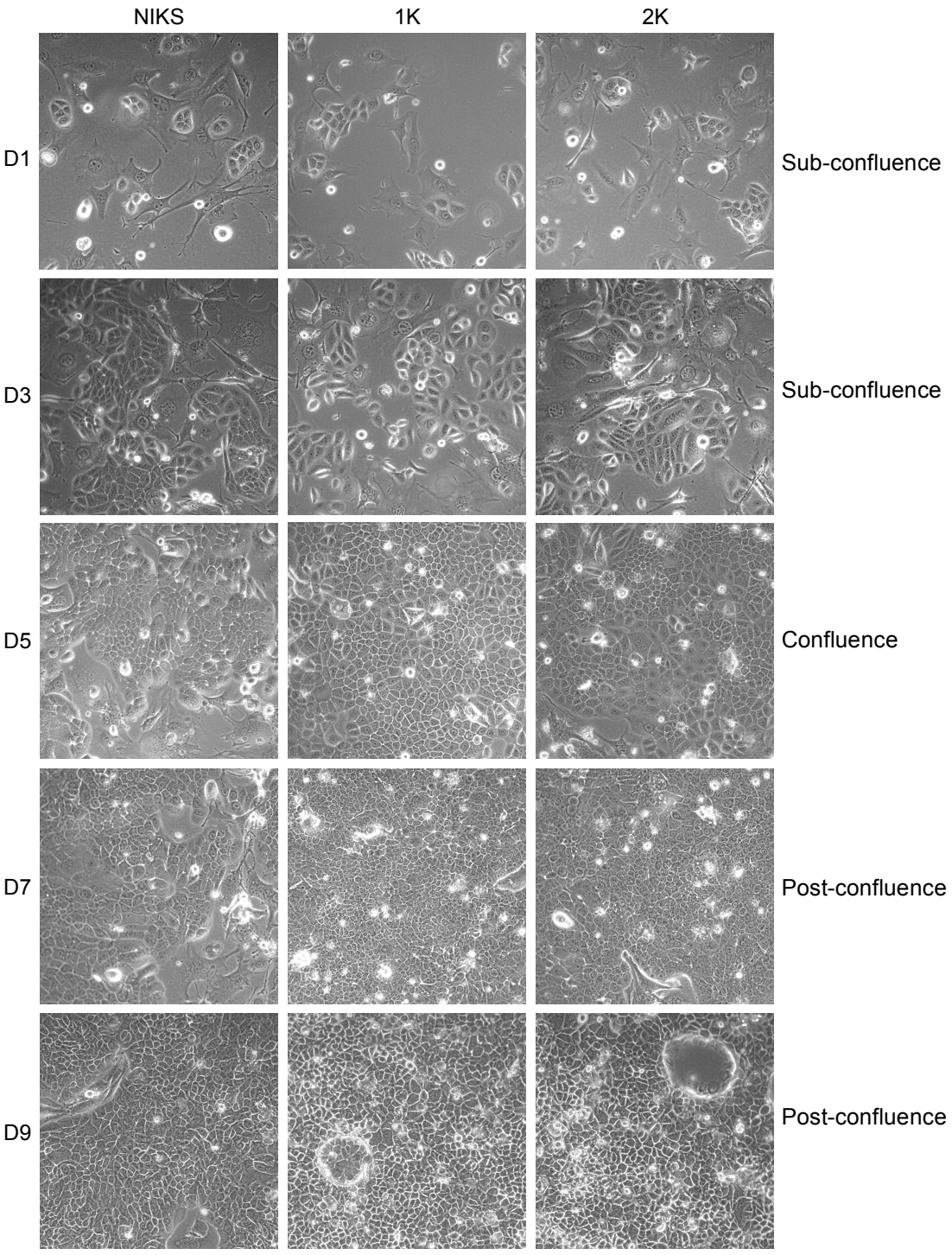

Figure 3.2: The difference in cell densities between NIKS and HPV16-containing clonal cells can be observed by microscopy

NIKS, 1K and 2K were cultured in duplicate wells in a growth assay format. Photographs were taken using brightfield microscopy at days 1, 3, 5, 7 and 9 post-seeding to visualize cells.

3.2.3 The LSIL- and HSIL-like growth phenotypes are not dependent on the specific stock of cells that is used for the different cell lines

As described in Section 3.2.1, my growth assays have shown me that the two proliferation phenotypes are reproducibly obtained. However, there are some differences between the growth patterns observed in Figure 3.1 and those previously found (Isaacson Wechsler et al., 2012). The current experiments show that the average number of cells per well are higher for all cell lines compared to the original data, and also that the LSIL-like 2K cell line, does not stop growing after reaching confluence.

To determine whether the differences between the current and previous experiments resulted from having to use higher passage cells, I did a proliferation assay using the HSIL and LSIL-like 1K and 2K cells from my current cell stock, and HSIL- and LSIL-like 1K and 4Q cell lines from the old stock (Fig. 3.3). As no early passage stocks of the 2K cell line were available, we used the 4Q cell line which had a very similar growth pattern to the original 2K cell line. As expected, the LSIL- and HSIL-like growth phenotypes emerge from the point of confluence at day 5 for cells from both the old and current cell stocks. Although the LSIL-like 4Q cells from the old stock grew slightly faster between days 3 and 7 than the 2K cell line, by day 9, both 2K and 4Q clones have reached the same cell number.

The proliferation assay suggests that the current and old stocks of cells have very similar growth patterns and grow to comparable densities. While the growth assay (Fig. 3.3) does show that 4Q cells from the old cell stock plateau between day 7 and 9, this is not the case between day 5 and 7. The original experiments were only taken out to day 7, and hence, I was expecting the 4Q cell line to plateau from day 5 onwards, as previously shown. Therefore the slight difference in growth patterns between the 2K cells from the current cell stock and 4Q cells from the old stock seems negligible. These data suggest that the current cell stock is suitable for all subsequent experiments and that any results obtained in past experiments should be replicable with these cells.

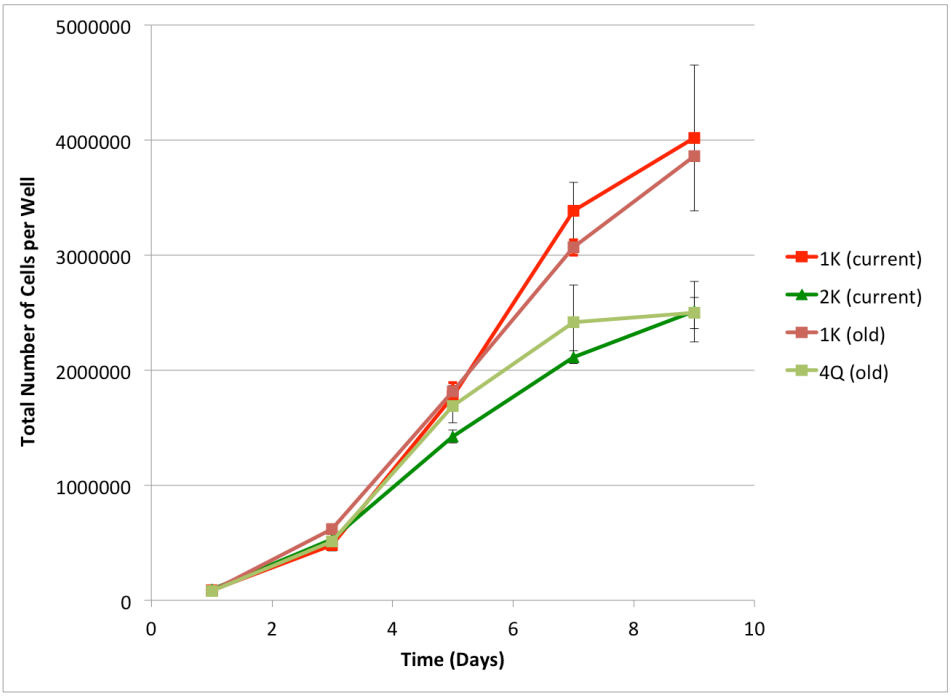

Figure 3.3: The LSIL- and HSIL-like growth phenotypes are not dependent on the specific stock of cells that is used for the different cell lines

Four clonal HPV16 cell lines were grown up in a 9-day growth assay. One LSIL- (2K and 4Q, respectively) and one HSIL-like clones (both are 1K) were taken from both the current and old stocks of cells. Cells were counted in duplicate at days 1, 3, 5, 7 and 9 post-seeding to assess the differential growth patterns. The clones that are colored red consistently grow to a high cell density whereas the cell lines marked in green reach a lower cell number. The average number of cells per 6-well plate well was plotted against the time in days. The error bars represent +/- the standard deviation of the duplicate wells.

3.2.4 The LSIL- and HSIL-like growth phenotypes are independent of the presence of feeder cells

Having shown that the decreased divergence in LSIL- and HSIL-like growth phenotypes is not a result of using higher cell passage numbers, I considered other factors that might be affecting proliferation. I speculated that decreasing the number of feeder cells could affect the growth of NIKS cells and the difference between phenotypes.

In an attempt to recreate the more extensive growth differential, I monitored the proliferation of HSIL- and LSIL-like 1K and 2K cells in the absence of feeder cells (Fig. 3.4). The results were plotted on a graph, with the 1K and 2K average cell counts presented in Figure 3.1 used as a reference for how these cells grow in normal culture conditions. The absence of feeder cells appears to decrease the proliferation rate of the cells, but does not seem to have a big effect on the LSIL- and HSIL-like growth phenotypes. The cell lines start to diverge in terms of their growth rate from day 3 onwards and by day 9 1K has grown to more than 1.5-fold the cell number of 2K.

These results seem to indicate that, although the overall rate of proliferation is affected by a lack of feeder cells, the LSIL- and HSIL-like growth phenotypes are not dependent on their presence. I hypothesize that the amount of growth factors supplied by the γ-irradiated feeders is so small compared to those supplemented in the media, that any dependence of the proliferation phenotype on growth factors may be masked in this experiment.

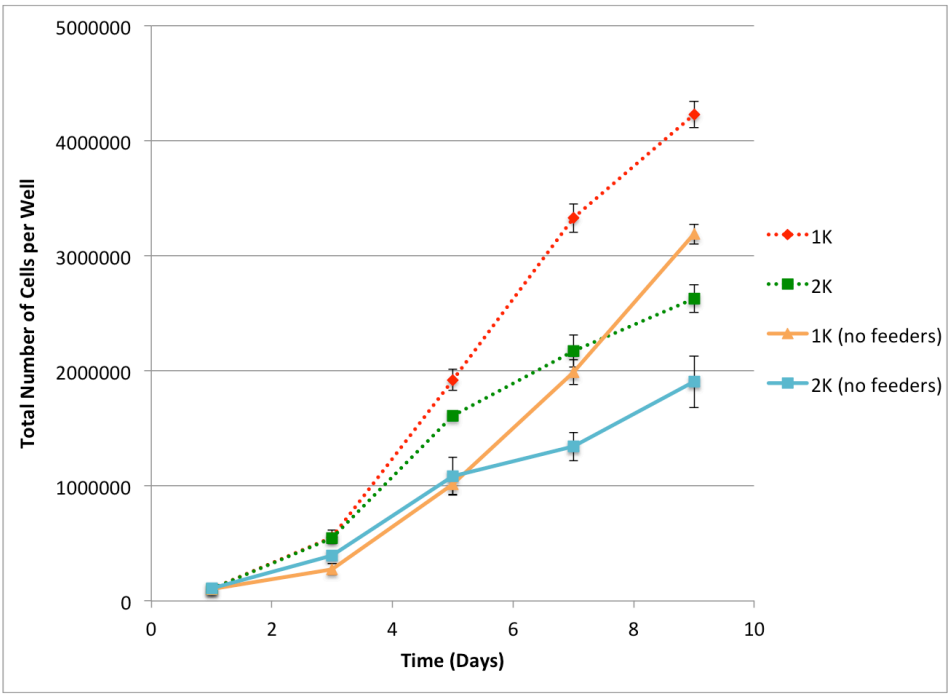

Figure 3.4: The LSIL- and HSIL-like growth phenotypes are independent of the presence of feeder cells

The growth of 1K and 2K cells was monitored for 9 days, according to standard protocol, but without the layer of γ-irradiated feeder cells. Cells were counted in duplicate at days 1, 3, 5, 7 and 9 post-seeding. In a standard growth assay, the clone that is colored orange consistently grows to a high cell density whereas the cell line marked in blue reaches a lower cell number. The average number of cells per 6-well plate well was plotted against the time in days. The error bars represent +/- the standard deviation of the duplicate wells. The cell counts for 1K and 2K, marked in dotted red and green lines, respectively, represent the growth patterns that are normally observed in the presence of feeder cells. These data have been presented previously in Figure 3.1.

3.2.5 The LSIL- and HSIL-like growth phenotypes arise even if significantly more LSIL-like cells are seeded at the beginning of the growth assay

To further confirm the phenotype, I wanted to ensure that the growth differentials did not result from the LSIL-like cells seeding less well than the HSIL cells in the growth assay. This was important, as I had noticed that the HSIL-like cells tended to survive the seeding procedure better than the LSIL-like cells.

To test whether differential seeding efficiency was causing the growth differences, I monitored 1K and 2K cells in a 9-day growth assay in which 50 % more 2K cells were seeded (Fig. 3.5). Cells were counted at days 1, 3, 5, 7 and 9 post-seeding to assess the proliferation patterns. The cell count at day 1 shows 37 % more 2K than 1K cells (140,000 and 103,000 cells, respectively) while the final cell count for 1K is more than 50 % higher than for 2K (3,320,000 and 2,220,000, respectively). This is consistent with previous growth assays, in which equivalent cell numbers were used for seeding, and shows that the two distinct growth phenotypes still emerge.

This experiment confirms that the HSIL-like phenotype is not a result of the greater seeding ability of the 1K cells.

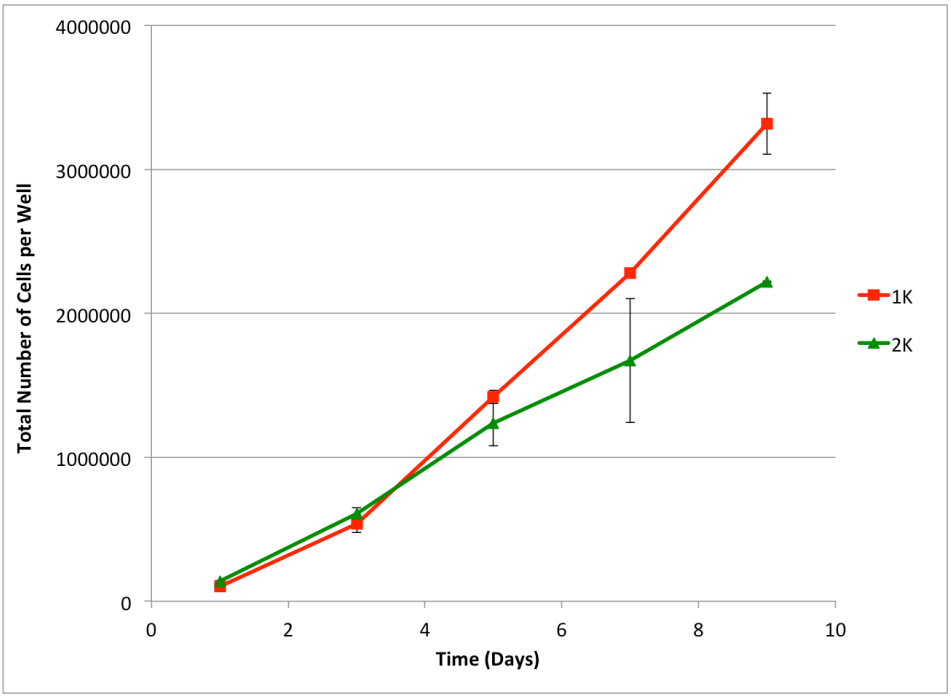

Figure 3.5: The LSIL- and HSIL-like growth phenotypes arise even if significantly more LSIL-like cells are seeded at the beginning of the growth assay

The growth of 1K and 2K cells was monitored for 9 days. The initial seeding densities were 150,000 1K and 100,000 2K cells and this resulted in 140,000 and 103,000 cells adhering, respectively; approximately 37 % more 2K than 1K cells. Cells were counted in duplicate at days 1, 3, 5, 7 and 9 post-seeding to characterize their proliferation patterns. In a standard growth assay, the clone that is colored red consistently grows to a high cell density whereas the cell line marked in green reaches a lower cell number. The mean number of cells per 6-well plate well was plotted against the time in days. The error bars represent +/- the standard deviation of the duplicate wells.

3.2.6 The HSIL-like growth phenotype does not arise from outgrowth within the population during the growth assay

It is known that cells containing HPV genomes can change their growth phenotype over time (Gray et al., 2010), for example in sub-optimal culturing conditions. Therefore, I routinely passaged my cells 1-2 times a week and did not let them grow to confluence. For this reason, I thought that it was important to determine whether the HSIL-like phenotype arises as a result of outgrowth of a fast-growing sub-population of the 1K cells.

The 1K and 2K clonal cell lines were cultured in a growth assay using the normal protocol, and counted every other day from day 1 to 21 post-seeding (Fig. 3.6A). The normal LSIL- and HSIL-like growth phenotypes are apparent between days 5, 7 and 9, as expected. From day 9 onwards, the cell numbers for both the LSIL- and HSIL-like clones continue increasing, albeit at a slower rate, up until day 17. It is only at this point that both cell lines cease growing. When looking at the cells down the microscope, I find that they look fairly healthy and normal up until day 17 and then look unhealthy at days 19 and 21. The number of cells floating in the media increases quite dramatically for these last two time-points. This led me to believe that both the 1K and 2K cell lines are still mitotically active at this time but that the number of cells dying is enough to offset the cell growth and give the false impression that overall the cells are not proliferating.

I have established so far, that both the LSIL- and HSIL like growth phenotypes are stable during an extended growth assay. To test whether the phenotypes result from outgrowth within the lines, I took cells from days 5 and 17 of the extended growth assay and reseeded them at low density in a standard growth assay (Fig. 3.6B and C). I hypothesized that if the lines were changing due to outgrowth, cells derived from day 5, when the cells first become confluent, and day 17, when the cells last look healthy, may show different growth characteristics.

Cells harvested at day 5 of the extended growth assay, give rise to normal LSIL- and HSIL-like growth phenotypes during the second growth assay (Fig. 3.6B). The 1K and 2K cell lines diverge in terms of their growth patterns from day 3 onwards and by day 9 the 1K clone has an almost 2-fold higher cell number than 2K. Similarly, Fig. 3.6C

shows that cells harvested at day 17 of the extended growth assay, also give rise to the normal LSIL- and HSIL-like growth phenotypes. The two cell lines only start to diverge from day 5 onwards but once again by day 9 the total cell number of 1K is considerably higher than for 2K.

When further assessing the actual cell numbers in the growth assays seeded with day 5 and day 17 cells, it becomes apparent that, overall, the rates of proliferation of the cell lines have not increased. At day 9 both batches of 2K cells have grown to a total of $2.5x10^6$ cells whereas 1K cells have grown to 4.5 and 4 $x10^6$ cells in the day 5 and 17 proliferations assays, respectively.

In conclusion, the results of the extended growth experiments suggest that no significant outgrowth occurs within the 21-day period measured. The LSIL- and HSIL-like proliferation patterns are reproducibly maintained even if cells are allowed to grow a long way past the point of post-confluence. Therefore outgrowth cannot be responsible for the appearance of the differential growth phenotypes.

A.

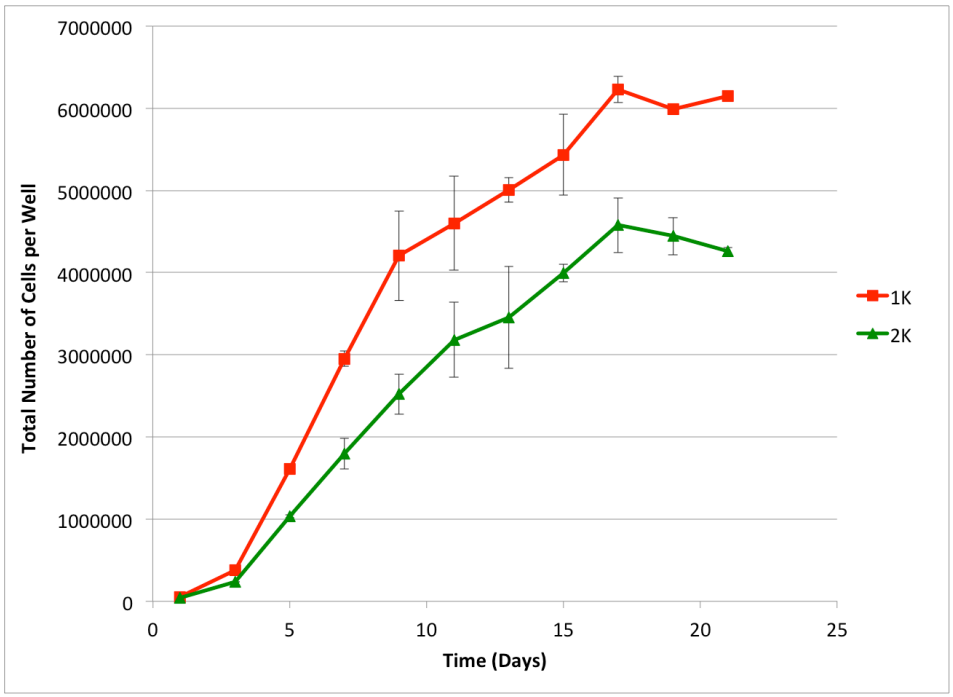
7000000
6000000
5000000
4000000
3000000
2000000
1000000
0
Total Number of Cells per Well
0
5
10
15
20
25
Time (Days)
1K
2K

B.

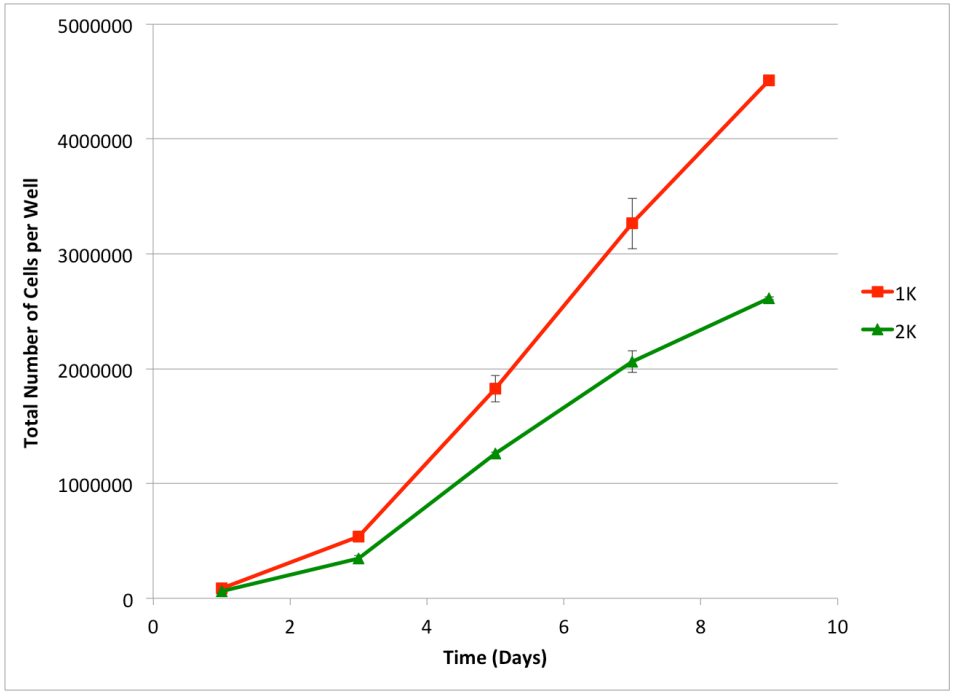
5000000
4000000
3000000
2000000
1000000
0
Total Number of Cells per Well
0
2
4
6
8
10
Time (Days)
1K
2K

C.

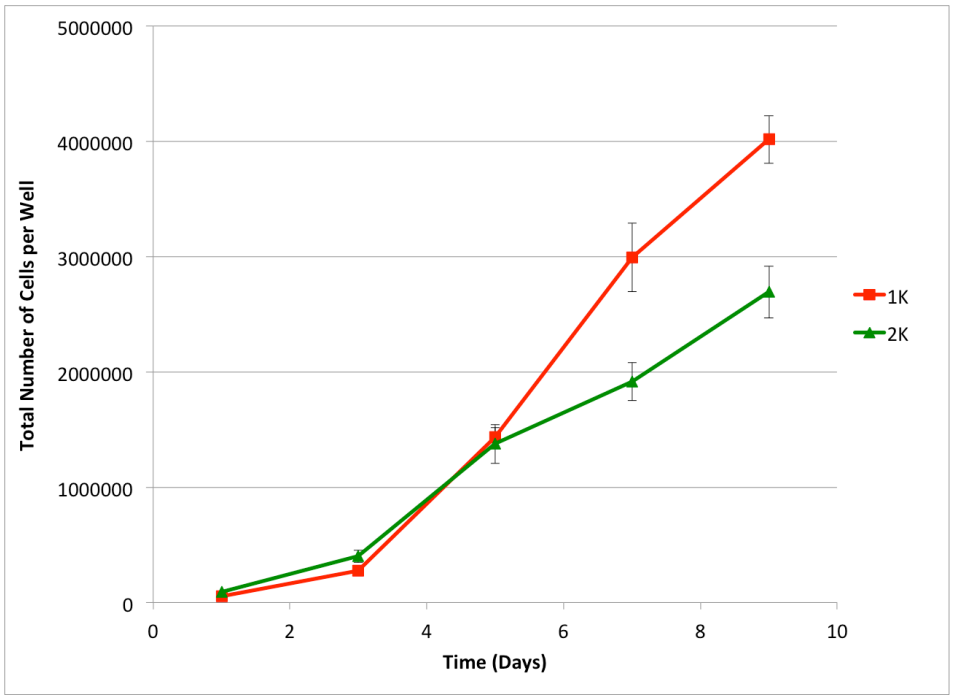

Figure 3.6: The HSIL-like growth phenotype does not arise from outgrowth within the population during the growth assay

A) 1K and 2K were grown up in a growth assay. Cells were counted in duplicate every other day from day 1 to 21 post-seeding to assess differential growth patterns. 1K and 2K cells harvested at day 5 **(B)**, or day 17 **(C)**, post-seeding from A) were reseeded in a new growth assay (identical to the first in terms of the set-up). Cells were counted in duplicate at days 1, 3, 5, 7, and 9 to reassess their growth patterns. Graphs show the mean number of cells per 6-well plate well, +/- the standard deviation of the duplicate wells.

3.2.7 HSIL-like cells are more mitotically active than LSIL-like cells when compared at both confluence and post-confluence

As mentioned before, the faster growing 1K cells are associated with an HSIL-like rafting phenotype whereas the slower 2K cells resemble a LSIL lesion in raft culture (Isaacson Wechsler et al., 2012). 1K epithelia have a larger number of cells in S phase than 2K, as determined by the amount of MCM staining. Therefore I hypothesized that the monolayer 1K HSIL-like phenotype similarly arises from an increased number of cycling cells, compared to the 2K LSIL-like cells.

To test this, I cultured parental NIKS, LSIL-like 2K and HSIL-like 1K cells on top of cover slips in a normal growth assay, and counted cells and harvested coverslips at days 1, 5, 9, 13, 17 and 21 post-seeding. From my previous experiments I know that my HPV16 clones reach confluence at day 5 and are post-confluent from day 7 onwards. However, the actual cell numbers that I measure at each time-point can be very different between cell lines, especially for NIKS which grow much slower. For this specific experiment it was important to compare cells at the same density (as determined by the exact cell count), as this is a major determinant of whether cells continue proliferating, and are therefore mitotically active. I found that at confluence at day 5, there are about $2x10^6$ cells per well for the HSIL-like 1K cells. In contrast, although the cells do not look very different microscopically, 2K only reach this cell number at day 9 and NIKS only reach this cell number at day 13. At day 9, I measure about $3x10^6$ cells for 1K, whilst NIKS and 2K only reach this cell number at days 21 and 13, respectively.

Having determined at which time-points to compare the lines, the cells were immunostained with antibodies to the mitotic marker anti-phospho-histone 3 (H3P) and also DAPI to detect their DNA, and analyzed by fluorescence microscopy (Fig. 3.7A and B). I used H3P as it is a highly specific cell cycle marker and only detects cells in prophase and metaphase (Gurley et al., 1978). It is clear that 1K cells are much more mitotically active than both NIKS and 2K, with a larger number of cells being positive for H3P at both cell densities.

I also observed when looking at the DAPI staining, especially at the later time-point, that 1K cells are all on the same plane, and becoming increasingly small, thereby

making space for new cells. This is consistent with my observations in Section 3.2.2. In contrast, for NIKS and 2K many of the nuclei are overlapping. This suggests that cells have starting growing on top of each other to accommodate the cell surplus. Hence, it seems that 1K is overcoming contact inhibition in a different way than NIKS and also 2K. I speculate that this difference may be allowing 1K cells to grow quicker than 2K (and NIKS) from the point of confluence.

This experiment has confirmed that the HSIL-like 1K cell line is more mitotically active than LSIL-like 2K cells when confluent, and this could account for their different growth phenotypes.

A. 2 million cells per well

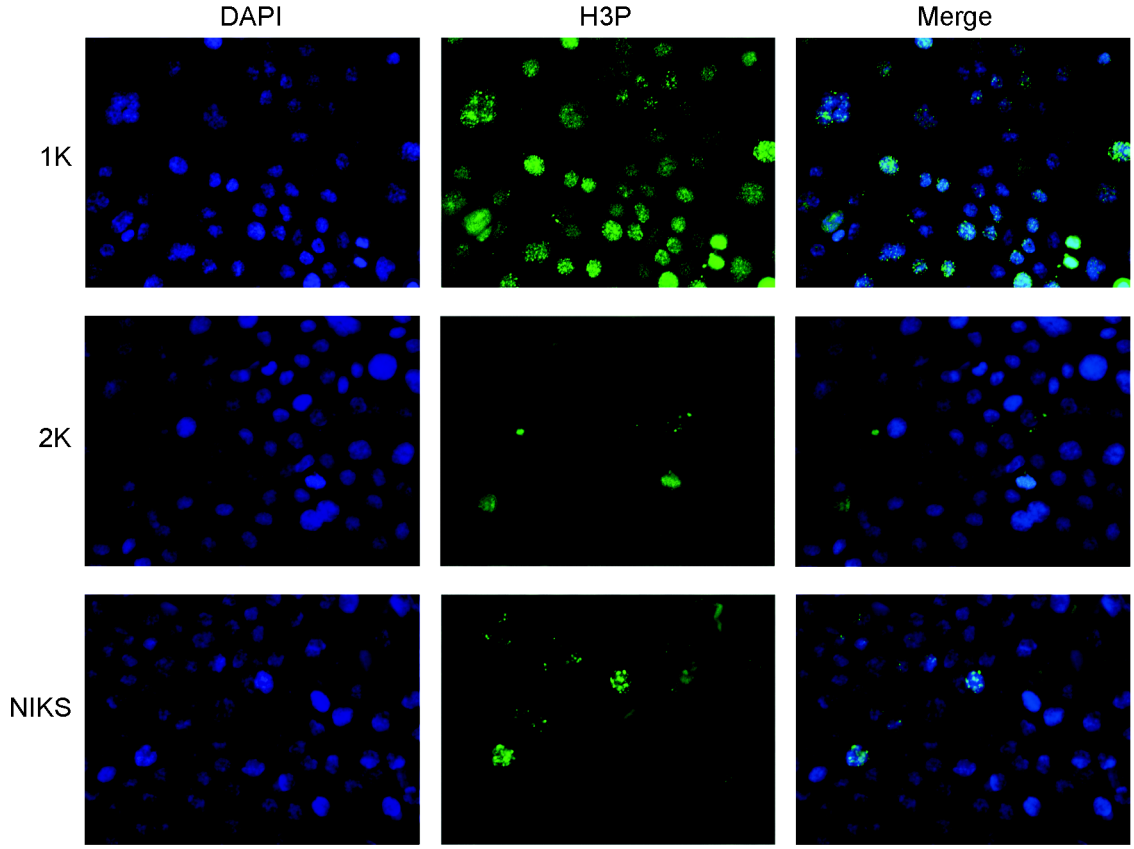

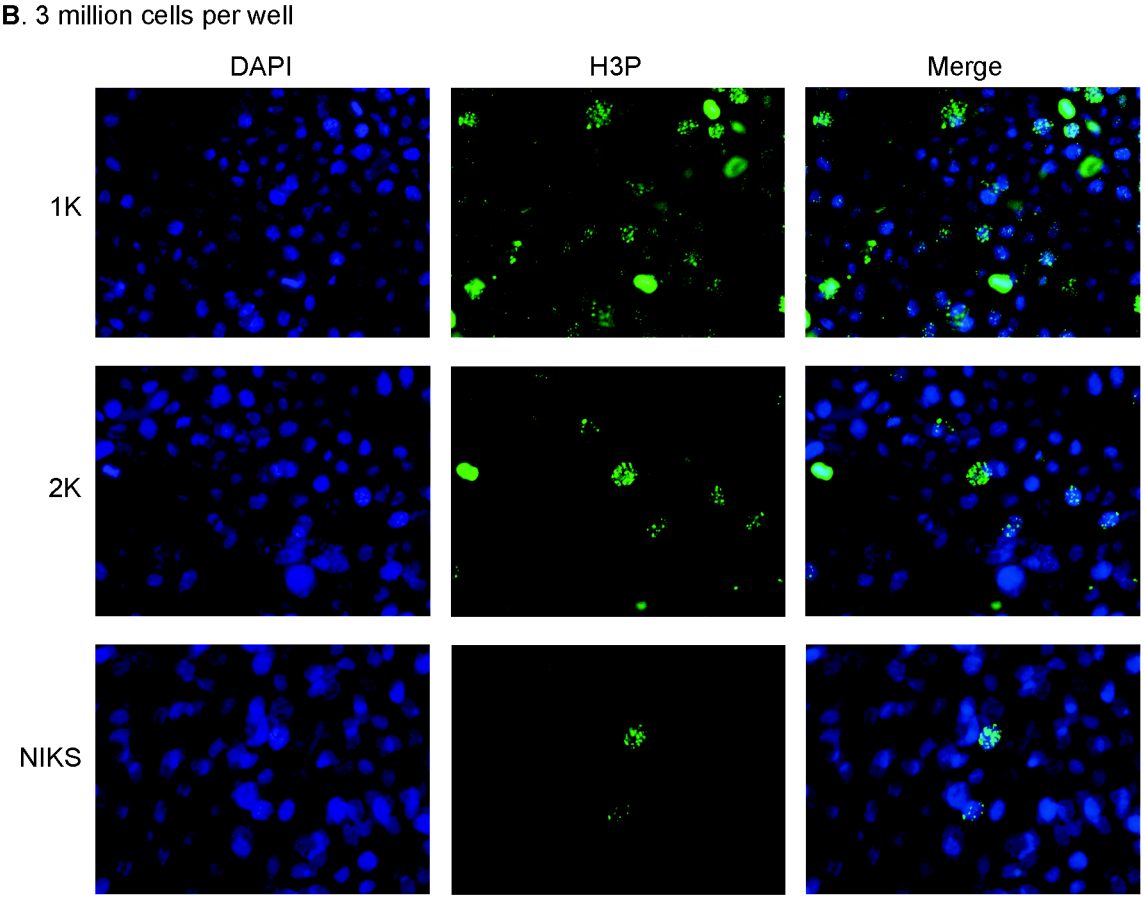

Figure 3.7: HSIL-like cells are more mitotically active than LSIL-like cells when compared at both confluence and post-confluence

NIKS, 1K and 2K cells were cultured on coverslips in an extended growth assay. Cells were counted in duplicate every other day from day 1 to 21 post-seeding. The lines were compared at two different cell densities ($2x10^6$and $3x10^6$cells per well) in terms of their expression levels of the mitotic marker H3P (green). Additionally, cells were stained with DAPI (blue) to detect their nuclei.

A) At confluence at day 5, there are approximately $2x10^6$ cells per well for the HSIL-like 1K cells. NIKS and 2K reach this cell number at days 13 and 9, respectively. **B)** At post-confluence at day 9, there are about $3x10^6$ cells for 1K. NIKS and 2K reach this cell number at days 21 and 13, respectively.

3.2.8 E6 transcript levels are similar for both LSIL- and HSIL-like cell lines at confluence

Having established in the previous sections that the phenotypic differences between 1K and 2K are inherent to these lines, and do not arise as a consequence of the growth assay procedure, I then wanted to characterize the reason for this. Preliminary data in the laboratory (Isaacson Wechsler et al., 2012) suggested that increased levels of E6 and E7 correlate with the HSIL-like growth phenotype from confluence. Therefore I wanted to assess whether differences in E6 transcript levels correlate with the phenotypes.

Since the growth phenotypes arise from the point of confluence at day 5 I decided to analyze this time-point in terms of E6 transcript levels. To do this I cultured two LSIL-like (4K and 4Q) and one HSIL-like (6K) clones to confluence (the equivalent of day 5 in a growth assay) in individual T75 flasks, according to standard laboratory protocol. During harvest the cells from each flask were split into three pellets, all of which were treated as individual samples. Subsequently I did RNA extraction and performed RT-qPCR to analyze E6 mRNA. Figure 3.8 shows that E6 transcript levels are not different between the two LSIL- and the HSIL-like clones at confluence. The bar chart indicates in fact that the levels are higher for the LSIL-like cell lines. As this experiment was repeated twice I performed two-tailed unpaired t-tests to assess these differences and found that they are not statistically significant with p values of 0.55 and 0.47 for 4K vs. 6K and 4Q vs. 6K, respectively.

My data show that E6 transcript levels are not significantly different between the LSIL- and HSIL-like clones at confluence when the differences in the proliferation patterns of these cells arise. This means that differential transcription of E6 (and presumably also E7) does not correlate with the two growth phenotypes.

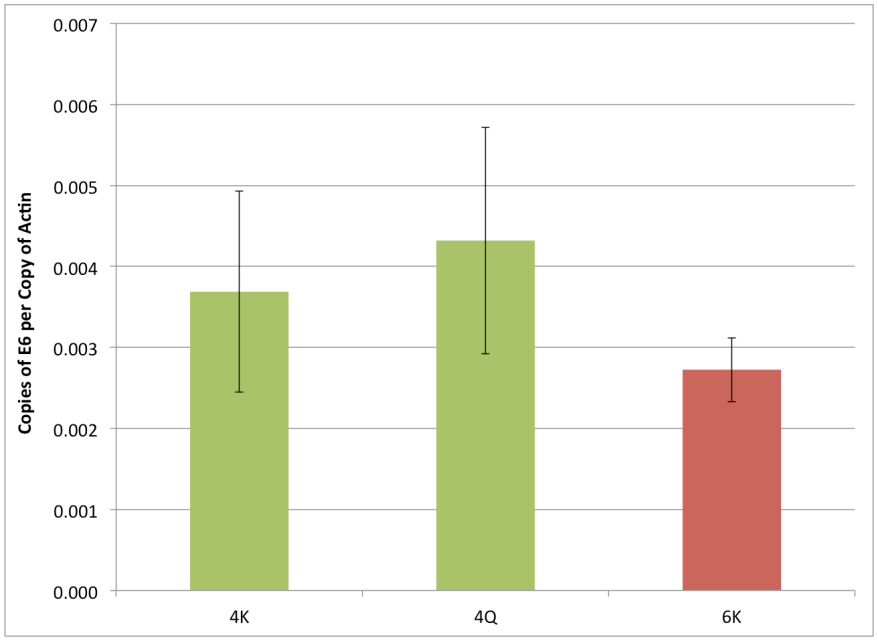

Figure 3.8: E6 transcript levels are similar for both LSIL- and HSIL-like cell lines at confluence

Two LSIL-like (4K and 4Q, in green) and one HSIL-like (6K, in red) clones were cultured to confluence in T75 flasks. During harvest each flask was split into three pellets, all of which were treated as individual samples. The levels of E6 mRNA for each clone were assessed by RNA extraction and RT-qPCR and normalized to the levels of actin. The experiment was repeated twice and the data compiled. Differences in E6 mRNA levels between the LSIL- and HSIL-like clones were assessed using two-tailed unpaired t-tests ($p=0.55$ for 4K vs. 6K and $p=0.47$ for 4Q vs. 6K). The error bars in the represent the standard error of the two repeats.

3.2.9 Assessment of a range of anti-E6 antibodies

Leading on from the qPCR work in the previous section, I wanted to assess E6 and E7 protein levels in both the LSIL- and HSIL-like clones. Although the laboratory has been using the same Euromedex HPV16 E6 antibody for some time, the newer batches do not work as well as the depleted original ones. When I run western blots there are very high levels of background and when I expose the membranes for a sufficient time to detect the E6 bands, the negative NIKS control is often positive. This non-specific band in the NIKS lane seems to be caused by the secondary antibody (data not shown). However, several different secondary antibodies tested give the same effect.

As a result of this I have tried to re-optimize western blotting conditions using different blocking buffers and different E6 antibodies. The gels for both new blocking buffers (Fig. 3.9A) look cleaner overall. However, lane A in both gels, in which I loaded lysate from a parental NIKS cell line, which I confirmed contains no HPV DNA, presents with a band that is as clear as the band in lane B from cells which actually express E6. Hence, these data indicate that using BSA to block gels enhances the problem of the negative control being positive.

I then tested several new E6 antibodies, one each from Abcam, Arbor Vita Corporation, Euromedex and two from Santa Cruz. For each I tested four different blocking buffers (5 % milk, 5 % BSA, 5 % milk and 2 % BSA, 5 % BSA and 2 % milk) and various concentrations of the antibody (ranging from 1:500 to 1:2000). The blots (Fig. 3.9B) show the best result for each of the antibodies. As can be seen, there are no bands in any of them that correspond to the known 15-16 kDa size of E6. Based on the results here I have decided to use p53 as an inverse marker of E6 levels for all further westerns.

A.

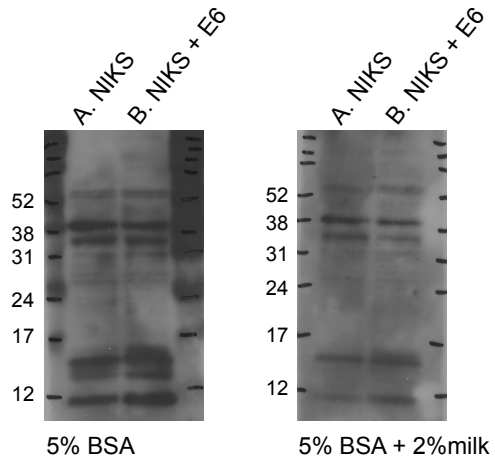

B.

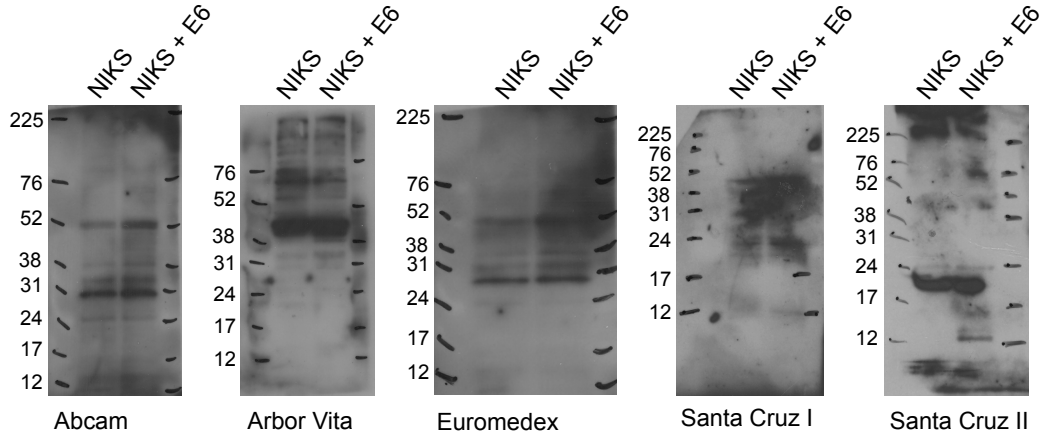

Figure 3.9: Assessment of a range of anti-E6 antibodies

Whole cell extracts from confluent wild type and E6-expressing NIKS cells were western blotted using the original Euromedex E6 antibody and different blocking buffers **(A),** and a range of different anti-E6 antibodies (Abcam: ab70; Arbor Vita Corporation: AVC#1007; Euromedex: 1E-6F4; Santa Cruz I: sc-460 and Santa Cruz II: sc-1584) **(B)**. E6 runs at approximately 15-16 kDa.

3.2.10 From the point of confluence, E6 activity appears higher for HSIL-like cells than LSIL-like cells

Having shown that differences in E6 transcript levels do not correlate with the LSIL- and HSIL-like growth patterns, I decided to determine whether the phenotypes correlate with protein levels of E6 and E7.

To assess protein levels, I cultured LSIL-like 2K and HSIL-like 1K clones in a growth assay and harvested cells at days 3, 5, 7 and 9 post-seeding. Cell pellets were prepared in duplicate throughout the proliferation assay and were stored at -80 °C. After the 10-day period all samples were lysed using a buffer containing 1 % NP-40. The levels of E6 and E7 were determined by western blot (Fig. 3.10A and B). In the blots, "a" and "b" samples from the four time-points were run on one gel for each clone separately to assess the overall trend in protein levels. For 1K, the levels of p53 is low at sub-confluence at day 3 and then consistently high from the point of confluence at day 5 onwards. This indicates that the levels of E6 are high at the beginning of the growth assay and then decrease with confluence. In contrast, the 2K blot shows that the levels of E6 are high at day 3, much lower at day 5 and then higher again at day 9. The levels of E7 are higher at post-confluence at both days 7 and 9 than at sub-confluence and confluence at days 3 and 5, respectively. This can be observed for both clones.

To enable a direct comparison of protein levels between the clones, the same samples were rerun in a different order (Fig. 3.10C and D). This time all the "a" samples from both clones were run on one gel and all the "b" samples on another. The p53 westerns show that E6 levels are significantly higher for 1K than for 2K, from the point of confluence at day 5 onwards. Unfortunately, the "a" and "b" replicates that were run on different gels are not always internally consistent. Regardless of this, the levels of E6 remain consistently higher for 1K than for 2K at days 5, 7 and 9. Again, I have found that the levels of E7 are the same for both clones at all time-points.

From the western blotting data there is a strong indication that the levels of E6 are higher in the HSIL-like clones as compared to the LSIL-like clone from the point of confluence at day 5 onwards. This suggests that it may be differences in the levels of E6, and not E7 that are giving rise to the two growth phenotypes.

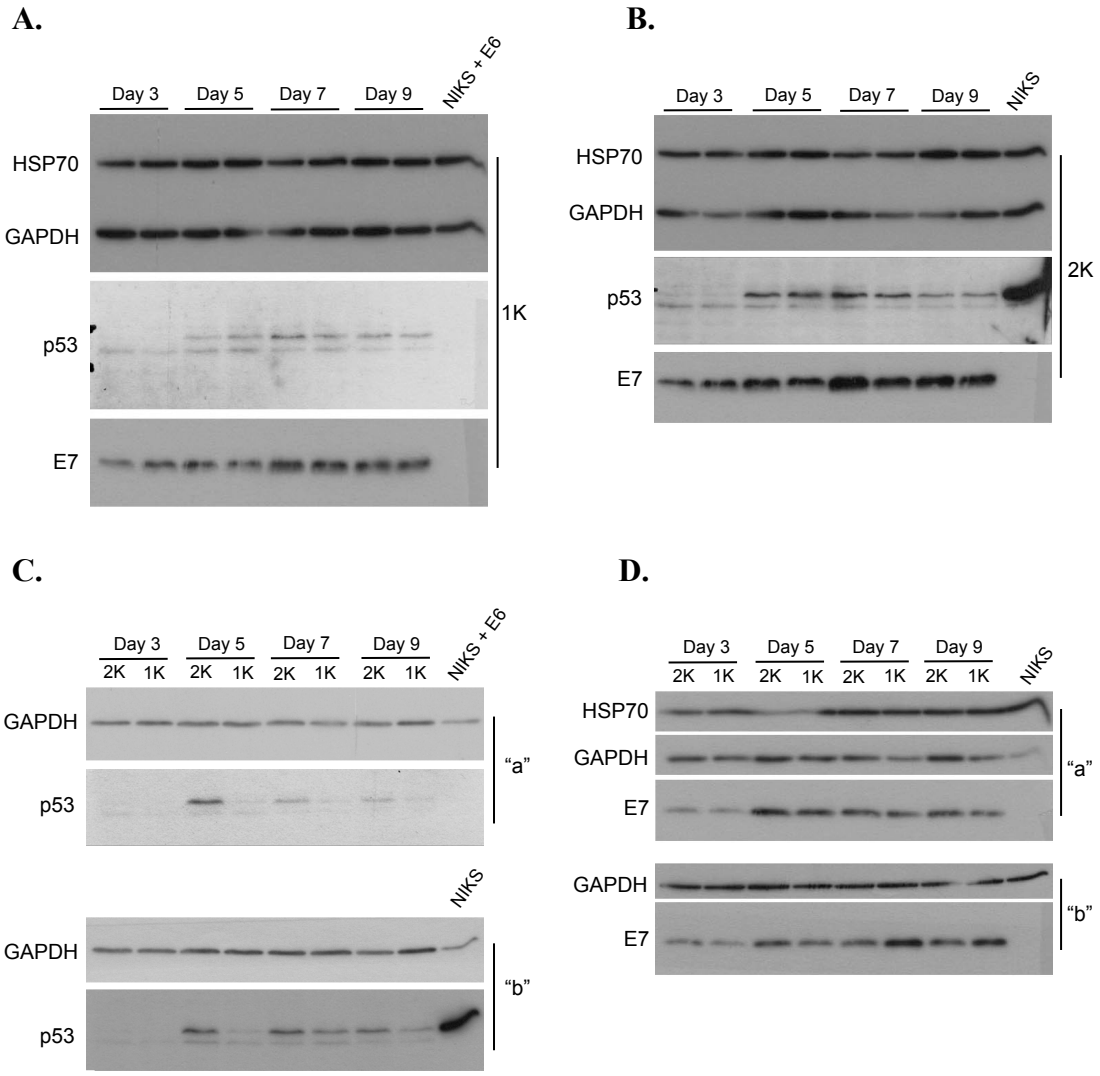

Figure 3.10: From the point of confluence, E6 activity appears higher for HSIL-like cells than LSIL-like cells

1K and 2K clones were cultured in a growth assay format and harvested on days 3, 5, 7 and 9 post-seeding. The levels of 1 % NP-40-soluble p53, used as an inverse marker of E6, and E7 were determined by western blot. Whole cell extracts from confluent wild type and E6-expressing NIKS cells were used as controls.
A) + B) Changes in the levels of p53 and E7 during the time-course for clones 1K and 2K, respectively.
C) + D) Absolute levels of both p53 and E7 for each time-point for duplicate "a" and "b" samples.

3.2.11 LXSN_E6 and LXSN_E6/E7 cells grow significantly faster than LXSN_E7 and control cells

As it appears that higher levels of E6 in the HSIL-like clone correlate with the fast growth phenotype, I wanted to test if E6 alone has the capacity to drive proliferation in such a way that would lead to the HSIL-like pattern of cell growth.

To do this LXSN retroviruses containing HPV16 E6, E7 or both E6 and E7 (Halbert et al., 1991) were used to infect NIKS cells. After infection, cells were selected using geneticin to make stable cell populations. Pellets of confluent cells were lysed using a RIPA buffer containing 6 % SDS, and these whole cell extracts were used in western blots (Fig. 3.11A). Each population expresses the expected proteins.

Subsequently the growth of LXSN, LXSN_E6, LXSN_E7 and LXSN_E6/E7 cells was assessed in a 9-day growth assay (Fig. 3.11B). Cells expressing E6 or both E6 and E7 grow considerably faster than both E7-only expressing and control cells. E7 alone does not stimulate these cells to proliferate faster than control cells. Overall between days 1 and 9 LXSN, E6-, E7- and E6/E7-expressing cells have increased their cell numbers 18-, 25-, 17-, and 23-fold, respectively. This means that E6- and E6/E7 expressing cells have grown to a density that is 1.8- and 1.7-fold fold higher, respectively, than that of LXSN controls cells while the difference in density at day 9 between E7-expressing and LXSN cells is negligible. The data in Figure 3.11 are an average of 8 individual experiments. Unpaired t-tests were used to compare the numbers of LXSN- and E6-expressing cells at each time-point. There is no significant difference at day 1 with a p value of 0.4. At days 3, 5, 7 and 9 the overall cell numbers are significantly different with p values of less than 0.01.

The experiment shows that E6 alone can push cells to proliferate. Hence, the higher levels of E6 in the HSIL-like clone from the point of confluence, may be the cause of the faster growth phenotype of this cell line.

A.

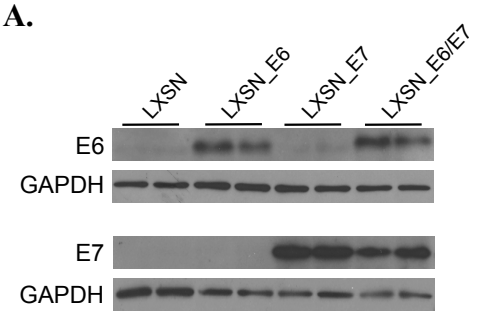

B.

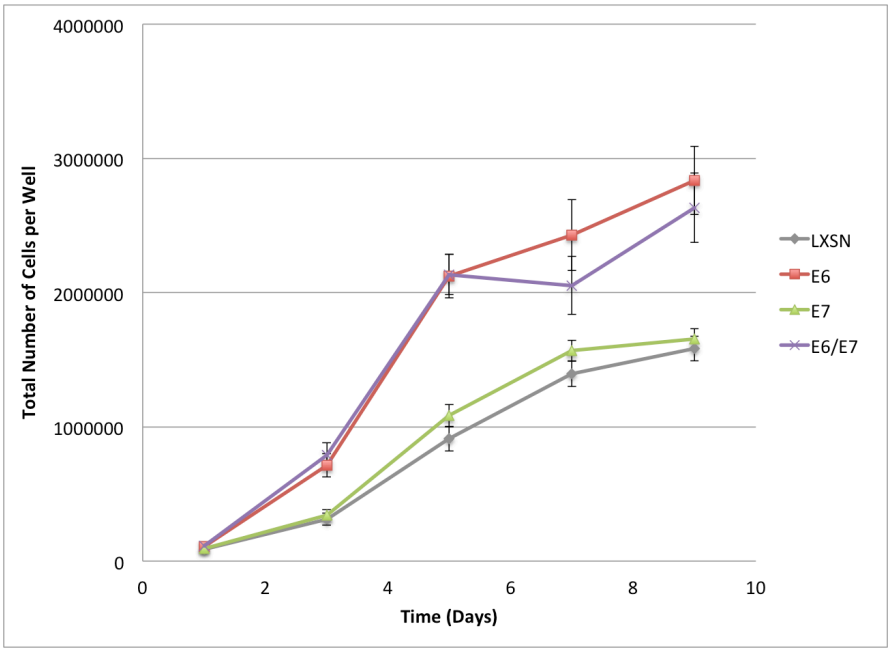

Figure 3.11: LXSN_E6 and LXSN_E6/E7 cells grow significantly faster than LXSN_E7 and control cells

LXSN retroviruses were used to make stable NIKS cell populations expressing only E6, E7 or both E6 and E7.

A) Cells were cultured to confluence, and lysed using a RIPA buffer containing 6 % SDS. Whole cell extracts were used to confirm by western blot that the cell lines express only E6, E7 or both proteins.

B) The growth patterns of LXSN-, E6-, E7- and E6/E7-expressing cells were compared in a 9-day growth assay. Cells from duplicate wells were counted at days 1, 3, 5, 7 and 9 post-seeding. The graph shows the mean number of cells per 6-well plate well. The error bars represent +/- the standard error of 8 individual experiments. Unpaired t-tests were used to compare LXSN and LXSN_E6 cell numbers at each time-point. At day 1 the p value obtained is 0.4. At days 3, 5, 7 and 9 the p values are less than 0.01.

3.2.12 Both E6 and E7 can stimulate cell proliferation in a growth factor-diminished monolayer environment

The growth data with E7-expressing cells in the previous section are surprising. Current literature suggests that E7, not E6, drives cell proliferation by degrading Rb (Dyson et al., 1989), causing release of E2F and hence transcription of many components required for G1/ S phase transition, including cyclin A and E (Zerfass et al., 1995). I came to the conclusion, that, in hindsight, one might expect the result obtained in the previous section. In monolayer culture, cells are provided with growth factors, from the media and also the feeder cells. Epidermal growth factor (EGF) is the main growth factor present when I culture cells. EGF family members activate a signaling cascade via the ErbB1 receptor (also known as epidermal growth factor receptor (EGFR)) that involves the ERK1/2 pathway of the Mitogen-activate protein kinase (MAPK) system (reviewed in (Shirakata, 2010)). This leads to, among other things, cyclin D activation (Dhillon et al., 2007). Cyclin D interacts with both cyclin-dependent kinase (CDK) 4 and CDK6 to bring about phosphorylation of Rb and release of E2F (reviewed in (Sherr, 1994)). E2F induces the expression of S phase promoting genes, such as cyclin A and CDK2 (Soucek et al., 1997), which promote further Rb phosphorylation and thereby enable cell cycle progression (reviewed in (Woo and Poon, 2003)). The function of E7 is to drive cells into cycle by degrading Rb (Dyson et al., 1989, Munger et al., 1989) and thereby releasing E2F (Boyer et al., 1996). However, since the growth factors in my medium are essentially targeting the same point in the cell cycle, the release of E2F from Rb, E7 cannot induce additional proliferation and thus its function is redundant. Based on this, I hypothesized that E7 may have a positive effect on the growth potential of cells in growth factor-diminished culture conditions.

To test this theory I assessed the growth of LXSN, LXSN_E6, LXSN_E7 and LXSN_E6/E7 cells in a 9-day growth assay, both in the presence and absence of growth factors (Fig. 3.12A and B, respectively). To remove growth factors I made media without supplemented FBS and EGF.

As expected, in the normal culture environment only E6-expressing cells drive proliferation. E7 alone cannot stimulate cells to grow significantly faster than control cells. In contrast, in a growth factor diminished environment, E7 is able to promote proliferation. E6- and E7-only expressing cells can drive cell proliferation to a very

similar extent while cells expressing both E6 and E7 present with even more cell growth.

Cell pellets prepared in duplicate at confluence at day 5 for both proliferation assays were lysed using a buffer containing 6 % SDS. Whole cell extracts were used to assess the levels of cyclin A and Rb by western blot (Fig. 3.12C). As expected the levels of Rb are lowest for E7-only expressing cells, irrespective of the presence of growth factors, with the higher levels in E6/E7-expressing cells presumably being caused by the generally lower levels of E7 (see Fig. 3.11A). While cyclin A levels are generally very low for cells expressing E7 in both proliferation time-courses, the levels are slightly higher than for LXSN control cells in the presence of growth factors. Since this is not associated with faster growth than LXSN cells, I speculate that there may be a threshold of cyclin A levels necessary for promoting fast growth (like that observed in cells expressing E6) that is not being met here. According to my model, I would expect E7 to bring about cyclin A activation in the absence of growth factors. However, this does not seem to be the case here. This may indicate that a different mechanism is driving E7-dependent cell growth. Rb and cyclin A levels are high for fast growing E6-expressing cells in both culture environments. This is in accordance with published data (Malanchi et al., 2002, Malanchi et al., 2004). For this reason I propose that E6 is targeting something other than the release of E2F from Rb to promote proliferation.

The data in Figure 3.12 seem to confirm my model in that the lack of enhanced growth of E7-expressing cells is a result of the normal cell culture environment. The proliferation assay without growth factors may indicate that E6 and E7 are affecting growth by two distinct mechanisms, as the presence of both proteins leads to a higher overall cell number than the presence of just one. However, the exact pathways through which proliferation is being induced need to be investigated further.

A.

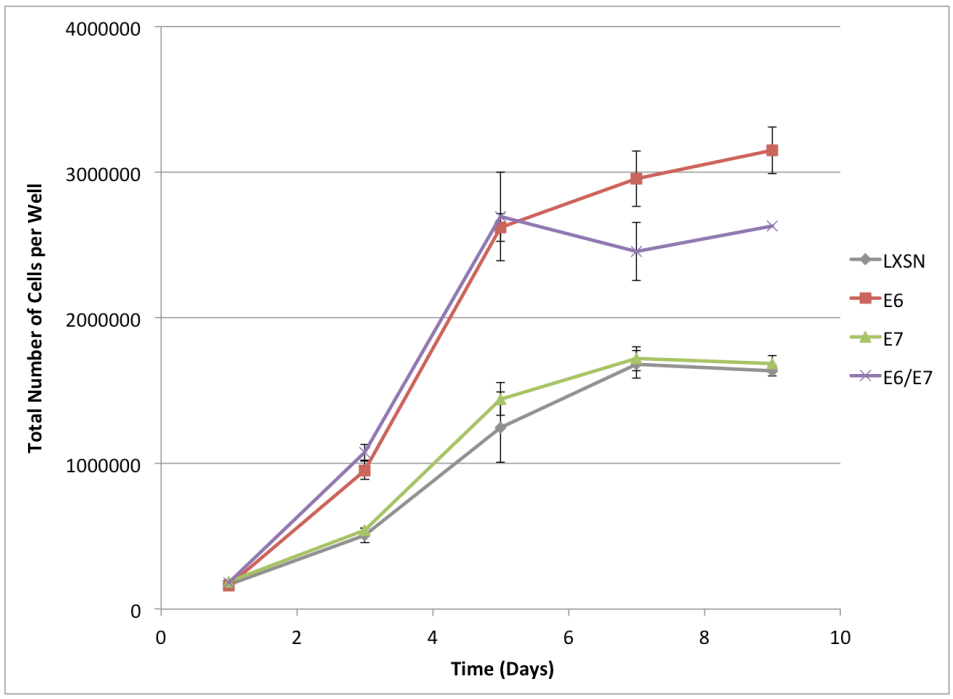
4000000
3000000
2000000
1000000
0
Total Number of Cells per Well
0
2
4
6
8
10
Time (Days)
LXSN
E6
E7
E6/E7

B.

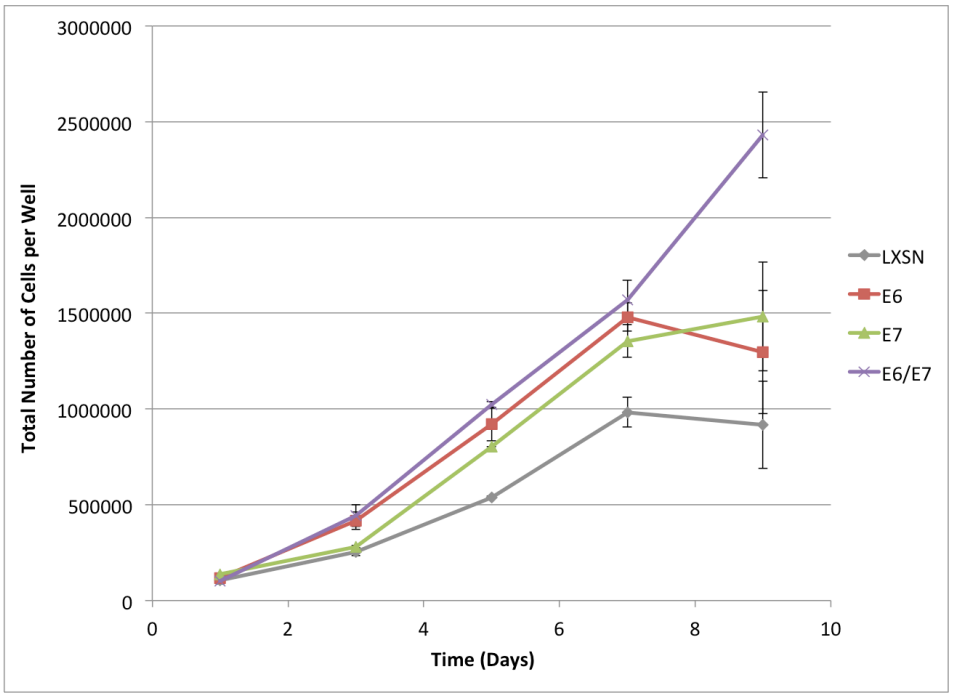
3000000
2500000
2000000
1500000
1000000
500000
0
Total Number of Cells per Well
0
2
4
6
8
10
Time (Days)
LXSN
E6
E7
E6/E7

C.

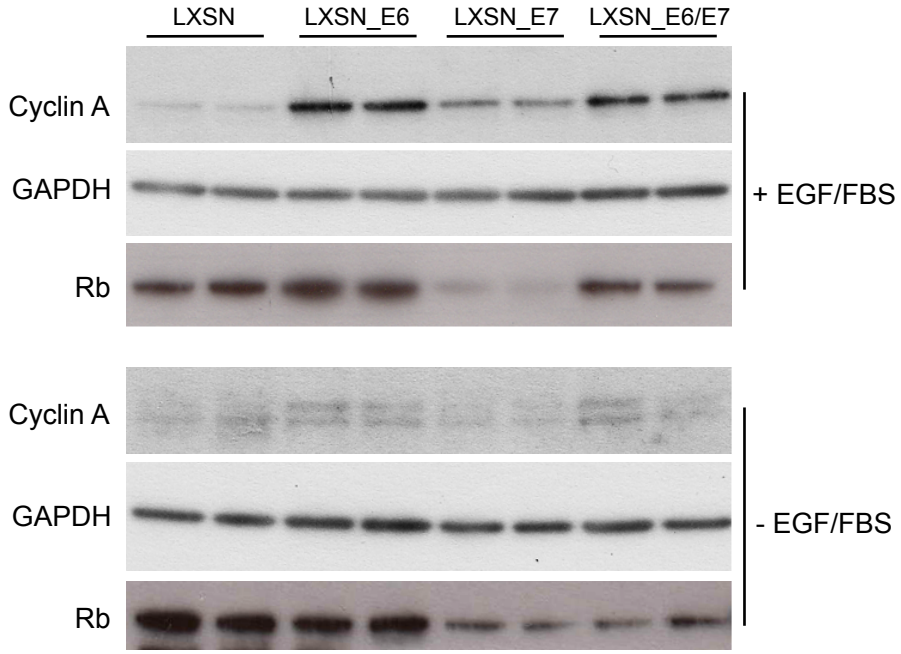

Figure 3.12: Both E6 and E7 can stimulate cell proliferation in a growth factor-diminished monolayer environment

The growth of LXSN, LXSN_E6, LXSN_E7 and LXSN_E6/E7 cells in the presence **(A)** and absence **(B)** of growth factors was assessed in a 9-day growth assay. Cells from duplicate wells were counted at days 1, 3, 5, 7 and 9 post-seeding. The error bars represent +/- the standard deviation of the duplicate wells and the graph is representative of multiple similar experiments.

C) Cell pellets prepared in duplicate at confluence at day 5 were lysed using a RIPA buffer containing 6 % SDS to prepare whole cell extracts. The levels of cyclin A and Rb were determined by western blot.

3.2.13 In organotypic raft cultures, more E6-expressing cells are in S phase in the basal and also suprabasal layers than in control cells

The 1K and 2K clonal cells not only give rise to two distinct proliferation patterns in monolayer growth assays, but also show distinct HSIL- and LSIL-like rafting phenotypes, respectively(Isaacson Wechsler et al., 2012). As the levels of E6 are higher for the HSIL-like clone from confluence onwards and E6 on its own may be driving these cells to grow faster than their LSIL-like counterparts, I speculated that I would also see differences between LXSN and LXSN_E6 rafts in terms of their MCM staining patterns.

To test this, LXSN and E6-expressing cells were grown in raft cultures that were left to differentiate for 12 days post-lifting. The normal protocol failed to produce good results. By re-attempting the rafts several times and tweaking the protocol I eventually found that supplementing the media with EGF, both prior to and post-lifting, produces good rafts with a properly stratified, differentiating epithelium.

In Figure 3.13A, cross sections of rafts were stained with MCM7 (red), to identify the S phase compartment, and DAPI (blue) was applied as a nuclear counterstain. The MCM7 expression patterns are quite different for the LXSN and E6-expressing cells. In the LXSN rafts, MCM7 positive cells, which are considered to be in S phase, are limited to mainly the basal layer. In contrast, for the E6 rafts the number of MCM7 positive cells is generally higher. Additionally, there are lots of cells that are in S phase in the suprabasal layers, up to five or even six cell layers above the basal cells.

Using the stained raft sections, I carried out some quantitative analysis (Fig. 3.13B) where I counted mitotically active cells in the basal layer. Approximately 13 % of E6-expressing cells are MCM7 positive whereas less than 7 % of LXSN controls cells express the S phase marker.

The rafting experiment indicates, that E6-expressing cells give rise to a more high-grade rafting phenotype than LXSN cells. This result further supports my on-going theory that differences in E6 levels (not E7) seem to be the underlying cause of not only the slow and fast monolayer growth patterns, but also the LSIL-and HSIL-like rafting phenotypes that have previously been described (Isaacson Wechsler et al., 2012).

A.

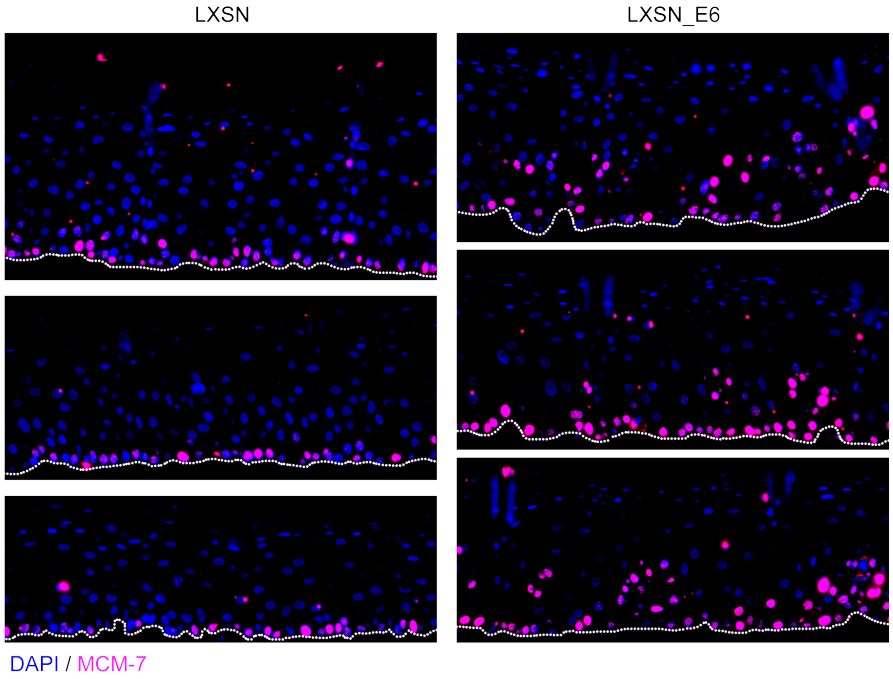

B.

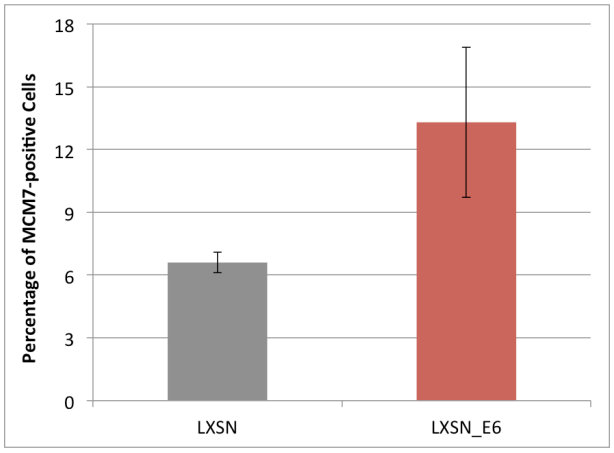

Figure 3.13: In organotypic raft cultures, more E6-expressing cells are in S phase in the basal and also suprabasal layers than in control cells

LXSN and LXSN_E6 cells were rafted in duplicate according to standard laboratory protocol. Media was supplemented with EGF both prior to and post-lifting. On day 12 post-lifting rafts were harvested and subsequently sectioned.

A) Raft sections were stained with MCM7 (red), to identify the S phase compartment, and DAPI (blue) as a nuclear counterstain. The broken white line indicates the basal layer of rafts.

B) MCM7-positive cells were counted in the basal layer and the mean numbers plotted in a bar chart. The error bars represent +/- the standard deviation of the mean.

3.3 Discussion

The work in this chapter is based on past findings in the laboratory that showed that HPV16-positive NIKS clonal cell lines spontaneously present with two growth phenotypes. One type of clone proliferates more quickly in monolayer culture from the point of confluence onwards. This fast growth pattern has previously been associated with an HSIL-like rafting phenotype whereas the slower cells consistently resemble LSILs (Isaacson Wechsler et al., 2012).

Using just one LSIL- and one HSIL-like clonal line I have found that the two distinct growth phenotypes are very reproducible and seem to correlate with higher E6 protein levels in the HSIL-like clone from confluence. My results also indicate that in the monolayer cell culture environment, which mimics the basal cell layer of a stratified epithelium, E6 on its own allows cells to proliferate rapidly while cells expressing only E7 do not have a growth advantage over control cells. When I assessed the growth of cells in a growth factor-diminished environment I found that in this situation, which mimics the upper layers of the epithelium, both E6 and E7 can drive cell proliferation. Additionally, the rafting experiment has shown me that E6 may delay differentiation and extend the period in which cells are actively cycling when allowed to stratify. All together, the data suggest that high levels of E6 in the HSIL-like clones do not merely correlate but may be directly involved in giving rise to both the rafting and the monolayer growth phenotypes.

At present I cannot explain why the LSIL- and HSIL-like cell lines are inherently different. I speculate that variations in episomal copy number or epigenetic differences in the viral genomes such as DNA methylation or histone acetylation may be involved.

The finding that E7 cannot stimulate cell proliferation in the normal culture environment is surprising. I hypothesized that the growth promoting function of E7 is rendered redundant by the presence of growth factors, as they target the same point in the cell cycle as E7 (the G1/S phase transition), and thereby do not allow the viral protein to induce additional proliferation. While removing growth factors does enable E7 to drive cell growth, this does not occur via the proposed pathway. Hence, the exact mechanism by which E7 promotes cells growth in my NIKS model needs to be further investigated. However, the theory that the pathways targeted by E7 and growth factors

seem to overlap, at least to some extent, is still applicable as otherwise the cells would not present with two distinct patterns of proliferation when cultured in the presence and absence of growth factors.

In NIKS, it seems that E6 can stimulate cells to grow faster by driving them into cycle and also by pushing them through the cell cycle more quickly. The data suggest that E6 and E7 are targeting distinct pathways to bring about their specific effects. This may explain why E6 can promote enhanced proliferation independent of the presence of growth factors. In a stratified epithelium, only the basal and the adjacent suprabasal layers are considered to be a growth factor-rich environment while in the upper layers the concentration of growth factors is low. Therefore I consider the two different culture conditions (high and low concentrations of growth factors) in the growth assays in Section 3.12 to mimic these environments. Based on the results, I hypothesize that in a stratified epithelium, E6 can induce rapid cell growth, and thus promote neoplasia in all cell layers, while the function of E7, to drive cells into cycle, may be limited to the upper layers where growth factors are sparse.

While E7 is the viral protein that is traditionally associated with induction of cell growth, there are several studies that have found that E6 can have a growth promoting effect. It was shown in 1994 that in human embryonic fibroblasts (HEF) the presence of only HPV16 E6 allows cells to proliferate to a two-fold higher density within six days than control cells (Ishiwatari et al., 1994). Hence, in HEF cells, E6 alone is sufficient to stimulate proliferation. Another study in the same year found that HPV16 E6 can stimulate mouse fibroblasts to grow slightly faster than control cells in a high-serum environment (Inoue et al., 1994) and that the positive effect of E6 on proliferation is enhanced in a low-serum environment. A few years later the same group showed that this function of E6 is independent of its ability to degrade p53, in both high- and low-serum conditions (Inoue et al., 1998). The authors of yet a further publication have established that E6 can bring about hyperproliferation of cells and also epidermal hyperdysplasia in transgenic mice and that this is associated with a delay in the normal cell differentiation program (Song et al., 1999). Furthermore this effect is independent of p53 (Nguyen et al., 2003).

A separate study has implicated E6 in the G1/S transition through activation of cyclin A and E (Malanchi et al., 2002). The authors suggest that E6 can alleviate the growth inhibitory effects of both p16 and p27 and that this is independent of p53 degradation. My results in Section 3.2.12 seem to confirm these findings, in that I too observe E6-dependent cyclin A activation. However, I have not yet investigated this further in my cell model.

When the authors continued this line of work (Malanchi et al., 2004) they found that in fibroblasts, E6 is able to promote proliferation by inducing the activation of CDK4/CDK6 complexes, which are involved in hyperphosphorylating Rb, by an unknown mechanism. Their E6-expressing cells present with high levels of phosphorylated Rb. A different group working with transgenic mouse models (Shai et al., 2007) further established that E6 can deregulate the p16/Rb pathway in mouse epithelium. E6 can inactivate Rb to induce E2F and its downstream targets, which leads to cell cycle progression. The mechanism by which E6 achieves this is different to that of E7. While the presence of E7 correlates with high levels p16 and low levels of Rb, there are low levels of p16 and high levels of hyperphosphorylated Rb in cells expressing E6. The authors proposed that E6 may deregulate Rb by inactivating p53, thereby hindering the expression of the CDK inhibitor p21. This causes higher CDK activity resulting in increased hyperphosphorylated Rb, E2F release and expression of E2F-responsive genes such as MCM7 and cyclin E. They also suggested another mechanism that is independent of p53. Hence, it seems that E6, much like E7, can deregulate the restriction point in G1 phase and promote cell cycle progression to induce proliferation.

All together these studies, that have analyzed the potentially growth promoting functions of E6, make it seem likely that the enhanced E6-dependent proliferation that I have observed in my cells is real and not just specific to NIKS cells or a result of the way they are cultured. Therefore it seems worthwhile to assess these pathways in my cells to determine, which of them, if any, and to what extent, are involved in giving rise to the LSIL- and HSIL-like growth phenotypes.

The work in this chapter has given me some important insight into the specific characteristics of the LSIL- and HSIL-like clonal cell lines. However, my progress has

been impeded considerably by reproducibility issues. Isaacson Wechsler *et al.* showed in 2012 that the 1K and 2K cell lines give rise to HSIL- and LSIL-like rafting phenotypes, respectively. Although I refer to these cell lines as LSIL- and HSIL-like in this chapter and also throughout the rest of this report, I (and other laboratory members) have not been able to reproduce these rafting phenotypes since my work with the cells began. I have carried out rafts to attempt to reproduce the phenotypes on three separate occasions, following the same protocol described in the study by Isaacson Wechsler and colleagues, and none of them have succeeded. I have consistently found that both 1K and 2K resemble LSIL epithelia, with abundant E4 expression detectable in the upper, differentiating layers. As the rafting protocol I used has not changed since the original study, I propose that changes in the various individual components of the FI medium used for culturing NIKS, and also for making the Keratinocyte plating and Cornification media for rafting, may be having an effect. Originally, my laboratory routinely mixed F12-Hams and high glucose DMEM media to obtain the required 3:1 ratio, respectively, for F Medium. However, throughout this study I have been using pre-mixed medium. Moreover, the laboratory supplier of fetal bovine serum (FBS) has also changed. As FBS is a natural product, there is variation between each batch and hence the FBS used presently may be quite different to that used at the time of the original study. Additionally, other laboratory members have shown that the duration of storage of collagen, used for making the dermal equivalent support structure for rafting, can have an impact on how well the cells differentiate into a stratified epithelium. This is often not something that can be controlled easily as, for cost reasons, collagen is generally bought in large batches. These three factors combined may be having a significant impact on the growth of the clonal cell lines. Hence, it seems reasonable to assume that they may be contributing, at least in part, to the reproducibility issues.

Another important issue to address is the obvious limitations of my model system. As discussed in Section 1.10 of the main Introduction, two big challenges of HPV research include host specificity of the virus and dependency of the viral life cycle on the stratified, differentiating epithelium. This has an impact on the models that can be used to study the virus and makes real *in vivo* work difficult. While raft cultures have proven very useful since they were first developed, it is still difficult to truly mimic real life epithelial conditions, for instance in terms of calcium and growth factor concentrations. Additionally, for the raft cultures produced in my laboratory, immortalized human

fibroblasts are used. Immortalization of these cells is necessary to allow them to grow to sufficiently high numbers, however, immortalized cells are not normally found in real epithelium.

There are also limitations of using specifically NIKS cells for our work. For one, as mentioned in Section 1.18 outlining the aims of my work, I am using foreskin cells to characterize cervical disease. Hence, I am using cutaneous skin cells to model mucosal conditions, which in itself poses a problem, not least because mucosal epithelia are not associated with a cornified layer while cutaneous epithelia are. Furthermore one problem of NIKS is that they are spontaneously immortalized cells (Allen-Hoffmann et al., 2000). While the fact that they are immortalized allows them to grow well in culture, it also means that there are inherent genetic differences (they are "near diploid") between normal foreskin and NIKS cells. One other limitation of my cell culture model is that I use immortalized J2-3T3 mouse fibroblasts as feeder cells for my work with NIKS. These immortalized cells grow very quickly and hence make experiments much easier than using human fibroblasts. However, as described above, the fact that they are immortalized means that real life conditions are not being mimicked. Additionally, the fact the they are mouse cells means that the signals they provide and growth factors they express may be different to those from human cells.

The work in this chapter has laid the foundations for the rest of the project. I have found that the precise levels of E6 seem to dictate how quickly cells containing viral episomes can proliferate. The data suggest that HSIL-like cells grow faster than LSIL-like cells from the point of confluence and that this correlates with higher E6 levels in the HSIL-like cells. Hence, logic dictates, that if I reduce the levels of E6 in the HSIL-like cells I should see a slower growth phenotype, while increasing E6 in the LSIL-like cells should lead to faster proliferation. For this reason the next chapter will focus primarily on the manipulation of E6 levels in the cells to determine whether this has these corresponding growth effects.

Chapter 4: Manipulating the levels of E6 and/or E7 in LSIL- and HSIL-like clonal cell lines is associated with a corresponding change in proliferation

4.1 Introduction

The data presented in the previous chapter have shown that the two growth patterns that arise in clonal NIKS cell lines stably expressing HPV16 episomes correlate with E6 protein levels from the point of confluence. I have also shown that E6, when overexpressed, on its own can drive proliferation of keratinocytes in my monolayer cultures.

In this chapter I wanted to further address the exact role of E6 in promoting growth. I used RNA interference (RNAi) to knock-down E6 and/or E7 in HSIL-like 1K cells. Based on my working hypothesis, that high levels of E6 are pivotal in bringing about enhanced proliferation, I expected to find that the cells would grow much slower than before. Depending on the extent levels knock-down, I hoped to show that they would present with a more LSIL-like growth phenotype. As a complementary method, I used a plasmid vector to increase the levels of E6 in the LSIL-like 2K clone.

Fire and Mello first described RNA interference (RNAi) in *Caenorhabditis elegans* (Fire et al., 1998) and presented a novel method by which endogenous mRNA could be degraded by the introduction of complementary double stranded RNA into cells. The use of RNAi to silence genes was later also found to be effective in mammals (Elbashir et al., 2001) and most other animals, plants, fungi and metazoans (Hammond et al., 2001). The RNAi pathway is used for regulating endogenous genes during plant and metazoan development (Hannon, 2002) and is thought to have come about in eukaryotes as a form of cell-based immunity against viruses and other microbes (Paddison and Hannon, 2002). Originally, small interfering RNAs (siRNAs) were developed for research and therapeutic purposes, followed later by short hairpin RNAs (shRNAs), which can be used for a stable knock-down of target genes.

The discovery of RNAi brought with it immense therapeutic potential, as cells could now be easily treated with siRNAs to bring about inhibition of disease-specific genes

(Phalon et al., 2010). To this end several siRNA molecules are now in clinical trials (reviewed in (Burnett et al., 2011)). However, the introduction of siRNA into cells brings with it some major side effects, for instance on non-target gene transcription patterns and also activation of the innate immune response (Robbins et al., 2009). To solve the issue of lack of precise sequence specificity, online tools have been developed that not only facilitate the design of efficient siRNA sequences but also make predictions about off-target effects (Boese et al., 2005), though these efforts are still ongoing. Additionally, to avoid an immune response a better form of delivery of the siRNA into target cells is being developed. Currently the most common form of siRNA uptake is the use of positively charged lipids that complex with negatively charged RNA and are subsequently endocytosed by cells. Other delivery methods that have shown some success include targeted nanoparticles (Davis et al., 2010) and inhalation (Moschos et al., 2011).

In the treatment of cervical cancer the HPV E6 and E7 oncoproteins make ideal targets for RNAi as they promote cell proliferation and prevent apoptosis. Hence, if their silencing does not bring about cell death it should at the very least induce growth arrest. Additionally, by targeting viral proteins, only diseased cells will be affected, as healthy cells surrounding the site of infection do not contain any viral mRNAs. The problem of siRNA delivery could be resolved very soon, when it comes to RNAi targeting HPV, as topical delivery to the cervix may be possible through PEGylated Lipoplex-entrapped Alginate Scaffold (PLAS) (Singhania et al., 2012).

The exact effects of the knock-down of E6 and E7, although shown to be effective, differ from study to study. Some groups have shown that their knock-down in SiHa and HeLa cells is associated with growth inhibition and a decrease in cell viability (Putral et al., 2005, Sima et al., 2008, Qi et al., 2010, Zhou et al., 2012). In contrast, other groups have found that, in these same cell lines, E6 and E7 knock-down is not associated with apoptosis but instead that cells have reduced invasive ability and growth potential (Yoshinouchi et al., 2003, Bai et al., 2006).

Since E6 and E7 are transcribed together and only spliced prior to translation, most si- or shRNAs target both genes. Nevertheless, depending on the exact sequence used, some groups have managed to achieve a knock-down of just one of the oncogenes.

Several studies have made use of these si- and shRNAs, targeting either E6 or E7 on its own, and again their results are not in agreement. The authors of one publication show quite convincingly that use of siE6 leads to the induction of apoptosis (Butz et al., 2003). In contrast, Jiang and Milner showed in 2002 that siRNA targeting E7 leads to apoptosis while treatment with siE6 only results in slower cell growth. In contrast, another group found that use of shE6 results in a minor retardation on growth while shE7 results in a more pronounced decrease in cell proliferation without any associated apoptosis (Bousarghin et al., 2009).

One common theme in all of these studies, is that they have found that either E6 or E7 or both seem to be involved in promoting proliferation, as their knock-down leads to the loss of cellular growth potential. The point where they seem to conflict most is whether cell viability is affected. Additionally, there is disagreement as to the extent to which the individual oncogenes drive cell proliferation. The lack of agreement means that the effect of E6 and E7 knock-down in these cells needs to be further characterized.

I hypothesized that in HPV-positive NIKS cells growing in monolayer culture, knock-down of E6 alone would be able to reduce proliferation. Based on the literature it was difficult to predict the exact effects that a knock-down would have in the HPV16-expressing cell lines. Most previous studies have used SiHa, HeLa or CaSki, which are cervical carcinoma cells with integrated viral genomes, while only a small amount of RNAi work has been done in episomal keratinocyte cell lines. The levels of viral and cellular proteins and, consequently, some of the downstream pathways that are affected to promote growth, are very different in my cells. Hence, I speculated that the results of RNAi in NIKS would differ substantially from those observed in cervical carcinoma cells.

Importantly, the dependence of the LSIL- and HSIL-like growth phenotypes on the confluence of cells makes my monolayer model very relevant in terms of studying the virus in the context of its normal environment. As described earlier, I consider a confluent monolayer to represent a reasonable model of the basal layer in real stratified epithelium because the cells are probably equally dense. Based on this, I propose that any effects observed as a consequence of E6/E7 knock-down in my cells, should be similar to the effects that would be observed in the basal cells of a lesion.

4.2 Results

4.2.1 Knock-down of E6 and /or E7 using siRNA in SiHa was not achieved in the monolayer cell culture environment

My data in Chapter 3 have conclusively shown that E6 on its own has the capacity to increase cell growth and that higher levels of E6 seem to correlate with enhanced proliferation. I wanted to assess whether knocking down the levels of E6 using siRNA would lead to a corresponding decrease in growth in the HSIL-like clonal 1K cell line. As NIKS cells are not easily transfectable I decided to test various E6 and/or E7 siRNA sequences in SiHa cells first. Although I primarily wanted to target E6, as mentioned earlier, the majority of siRNAs will knock-down both oncogenes. The sequences tested here were synthesized as duplexes by Dharmacon and have all been published previously and shown to successfully reduce E6 and/or E7 levels.

The siE6 and both siE7 sequences were previously shown to be specific for their respective mRNAs, and a 70 % reduction in E6 levels and 50-60 % reduction in E7 levels has been described in CaSki and SiHa cells (Jiang and Milner, 2002, Allison et al., 2009, Jiang and Milner, 2005). The siE6/E7-1, -2, -3 and -4 sequences do not differentiate between E6 and E7. The siE6/E7-1 sequence was originally published as an shRNA (Gu et al., 2009) and I ordered the corresponding siRNA for my experiments. The siE6/E7-2 oligo has been shown to reduce mRNA levels by up to 81 % in CaSki cells (Putral et al., 2005, Gu et al., 2008). The siE6/E7-3 sequence was shown to reduce E6 and E7 mRNA levels by about 60 % in CaSki cells (Ben Khalifa et al., 2011), and siE6/E7-4 was shown to work well in SiHa cells (Accardi et al., 2011).

One day after seeding, SiHa were transfected with various siRNAs targeting E6 and/or E7, siGAPDH and one siNon-target (siNT) control sequence. Quadruplicate cell pellets were harvested 48 hours later. Whole cell extracts were prepared for two pellets per transfection condition, using a buffer containing 6 % SDS, and the levels of E6, E7 and GAPDH were assessed by western blot (Fig. 4.1A and B). The remaining two pellets were used for RNA extraction and subsequent RT-qPCR to quantify the levels of E6 mRNA (Fig. 4.1C and D).

Treating SiHa cells with siGAPDH (Fig. 4.1A) shows that the transfection procedure itself is working. The levels of GAPDH in the siGAPDH-treated cells are low compared to both untreated control and siNT-treated cells. As expected, siNT does not significantly reduce the levels of E6 or E7 (Fig. 4.1B). However, neither do the siE6, siE7 or siE6/E7 sequences, irrespective of whether they target just one or both mRNAs. The protein levels of E6 and E7 remain as high as in the untreated control, for all cells transfected with siRNA.

In addition to its effects on protein levels, transfection of SiHa with siGAPDH also reduces the amount of GAPDH transcript (Fig. 4.1C). This is a further confirmation that the experiment itself is working and that GAPDH mRNA is being degraded in the presence of its siRNA counterpart. The siE6 and siE6/E7-1 oligos, the effects of which were shown to be negligible by western blot (see Figure 4. 1A and B), also do not seem to induce a measurable decrease in E6 mRNA levels (Fig. 4D). The effects of three further siE6/E7 sequences (siE6/E7-2, -3 and -4) were also assessed by qPCR. While treatment with siE6/E7-4 does not result in any decrease in E6 transcript levels, both siE6/E7-2 and -3 do. However, after several repeats of this experiment, the effects were still not significant, and no corresponding change in protein was observed. This suggests that any effect is marginal, and may be insufficient to significantly affect protein level.

These experiments show that SiHa cells can be transfected with siRNA, and that the correct pathways that reduce mRNA levels, and subsequently protein levels, are activated. However, siRNAs targeting E6 and E7 do not deplete corresponding RNAs. Only two siE6/E7 sequences seem to reduce, to some extent, the levels of E6 transcript levels in cells. While this is promising, the effect is not significant enough to warrant further siRNA experiments. As cells with high levels of E6 grow faster than cells with low levels, using these two siRNAs to reduce E6 in cells may still not result in an overall slower growth of cells. The faster, lesser transfected or completely untransfected cells with high levels of E6 would outgrow the slower, well-transfected ones with low E6. Hence, to measure a corresponding reduction in E6-dependent proliferation of cells, I need to knock-down the levels of E6 with a much higher efficiency.

A.

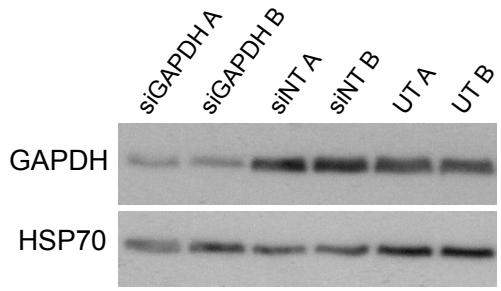
siGAPDH A
siGAPDH B
siNT A
siNT B
UT A
UT B
GAPDH
HSP70

B.

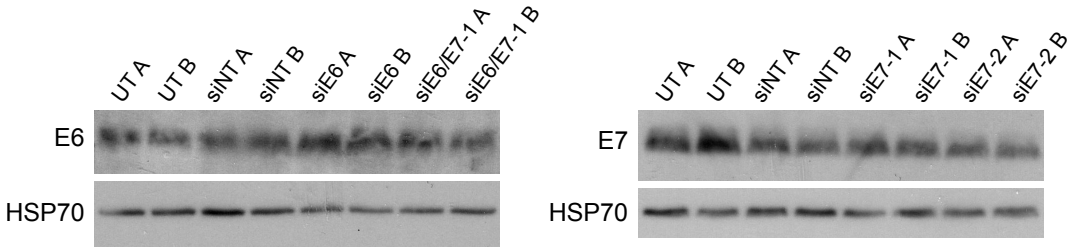
UT A
UT B
siNT A
siNT B
siE6 A
siE6 B
siE6/E7-1 A
siE6/E7-1 B
E6
HSP70
UT A
UT B
siNT A
siNT B
siE7-1 A
siE7-1 B
siE7-2 A
siE7-2 B
E7
HSP70

C.

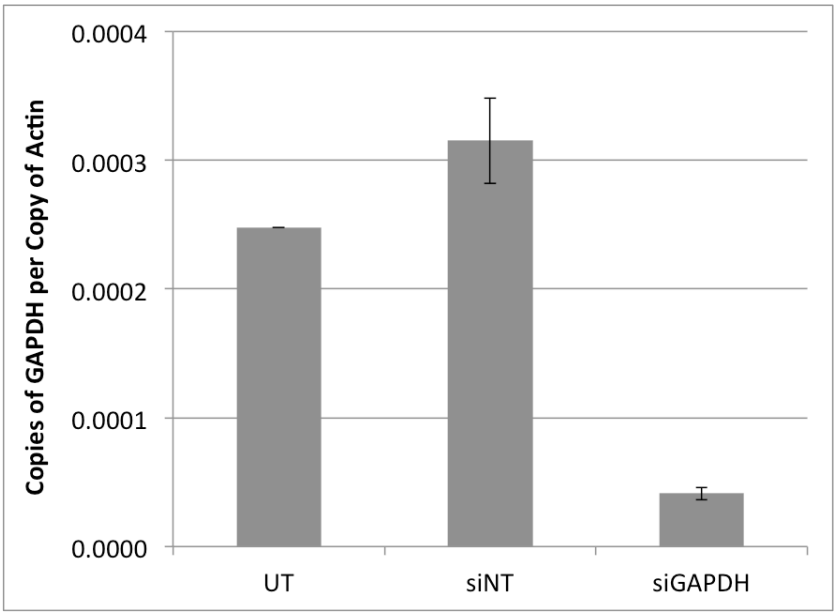
Copies of GAPDH per Copy of Actin
0.0004
0.0003
0.0002
0.0001
0.0000
UT
siNT
siGAPDH

D.

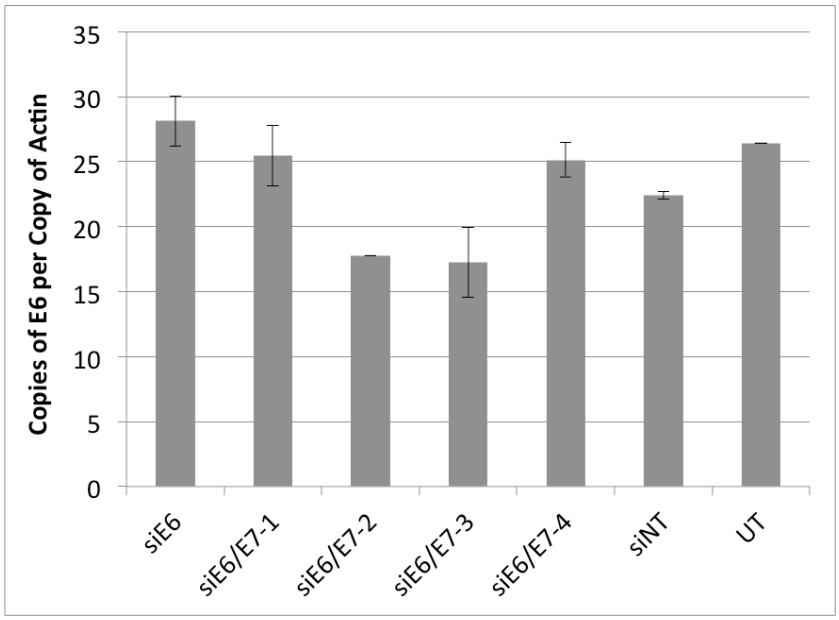

Figure 4.1: Knock-down of E6 and /or E7 using siRNA in SiHa was not achieved in the monolayer cell culture environment

SiHa cells were transfected with various siRNA sequences and harvested 48 hours later**.** UT (untreated), siNT- (non-target) and siGAPDH-transfected cells were used as controls. One E6 specific (siE6), two E7 specific (siE7-1 and -2) and four siE6/E7 (siE6/E7-1, -2, -3 and -4) sequences were tested.

A + B) Whole cell extracts were prepared and western blotted for GAPDH, E6 and E7. HSP70 was used as a loading control.

C + D) The levels of GAPDH and E6 mRNA were assessed by RT-qPCR and normalized to the levels of actin. The error bars in the bar charts represent the standard deviation of qPCR triplicates.

4.2.2 Commercially available shE6 lentiviral particles do not knock-down the levels of E6 in my cells

It is not clear why the knock-down of E6 and E7 was unsuccessful. It may be that the siRNAs were insufficiently transfected or that they were not stable in my cells. Therefore, I decided to use shE6 and shE6/E7 to reattempt a knock-down of E6 and/or E7, as unlike siRNA, the effects of shRNA are not transient. I hoped that using shRNA, would allow me to create stable cell lines with permanently low levels of E6. I decided to use the clonal HPV16-expressing NIKS cell lines for the shRNA work as, to truly test my hypothesis, I needed the cell line model. Hence, it seemed simpler to attempt a knock-down in the HSIL-like 1K cell line. Based on my previous data, I speculated that this would result in a more LSIL-like growth phenotype.

In this experiment, I used commercially available E6 lentiviral particles (Santa Cruz, USA) that were developed using published siRNA sequences targeting E6 (Niu et al., 2006). The sequence targets both E6 and E7 mRNAs and therefore I expected a decrease in both E6 and E7 levels. The HSIL-like 1K clone was infected with the lentiviral particles on the day post-seeding. In addition to shE6, two sets of control shRNA lentiviral particles were used; shScrambled, is the same as a non-target control, and shGFP, should essentially also function as a non-target control as my cells do not express GFP. I tested three different multiplicities of infection (MOIs), however, due to the small volume of lentiviral supernatant supplied by the company, these were limited to MOIs of 1, 2 and 3. After selection, 1K shRNA populations were grown to the point of confluence at which point cells were harvested and lysed using a buffer containing 6 % SDS. The whole cell extracts were used to assess the levels of E6 and E7 by western blot. I found that untreated 1K and cells infected with either of the shRNA controls have high E6 and E7 levels (Fig. 4.2). However, cells infected with shE6 lentiviral particles have equally high levels, irrespective of the amount of viral particles (as measured by MOI) used during the infection.

These results indicate, that although the infection itself was successful, as cells were selected with puromycin, this shE6 sequence does not work in the cells. Hence, I will pursue my work with shRNA and use other sequences to hopefully achieve a knock-down of E6 levels.

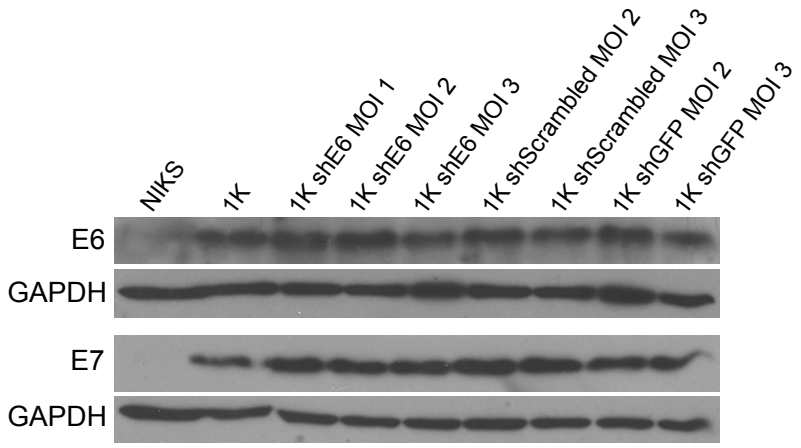

Figure 4.2: Commercially available shE6 lentiviral particles do not knock-down the levels of E6 in my cells

1K cells were infected with shRNA lentiviral particles targeting E6 and E7. Cell populations stably expressing shE6, shScrambled or shGFP were grown to confluence. Cell pellets were lysed and total levels of E6 and E7 were assessed by western blot.

4.2.3 Cells infected with custom-made shE6 lentiviral particles present with a modest decrease in E6 transcript levels

In the previous section, I found that the shE6 sequence that was tested, was ineffective at reducing the levels of both E6 and E7. Hence I ordered custom-made shE6 and shE6/E7 lentiviral particles (Mission®, Sigma-Aldrich, USA) using other sequences that were previously published and found to work. As I wanted to achieve a knock-down of just E6 levels, I ordered one shE6, that was based on the siE6 sequence tested in Section 4.2.1 (Jiang and Milner, 2002, Jiang and Milner, 2005, Allison et al., 2009). Previously, this siE6 was shown to reduce E6 levels by about 70 % without affecting E7. I also ordered a shE6/E7 based on the siE6/E7-1 sequence tested in Section 4.2.1. This sequence was originally published as an shRNA (Gu et al., 2009) that seemed to work really well. Therefore, I was optimistic that lentiviral particles based on this would result in a reduction of E6 and also E7 levels.

To test the efficacy of the two shRNAs, the HSIL-like 1K clone was infected with the lentiviral particles, including an shNT control, on the day after seeding. After antibiotic selection, the new 1K shRNA populations were left to grow to the point of confluence. Cell pellets were used to do RNA extraction and subsequently RT-qPCR was carried out to assess the levels of E6 mRNA. The qPCR results (Fig. 4.3) show that E6 transcript levels are high in both untreated 1K and 1K infected with shNT lentiviral particles. While cells stably expressing shE6/E7 do not show a decrease in E6 level, cells with shE6 do. Based on this, I decided to further characterize these cells.

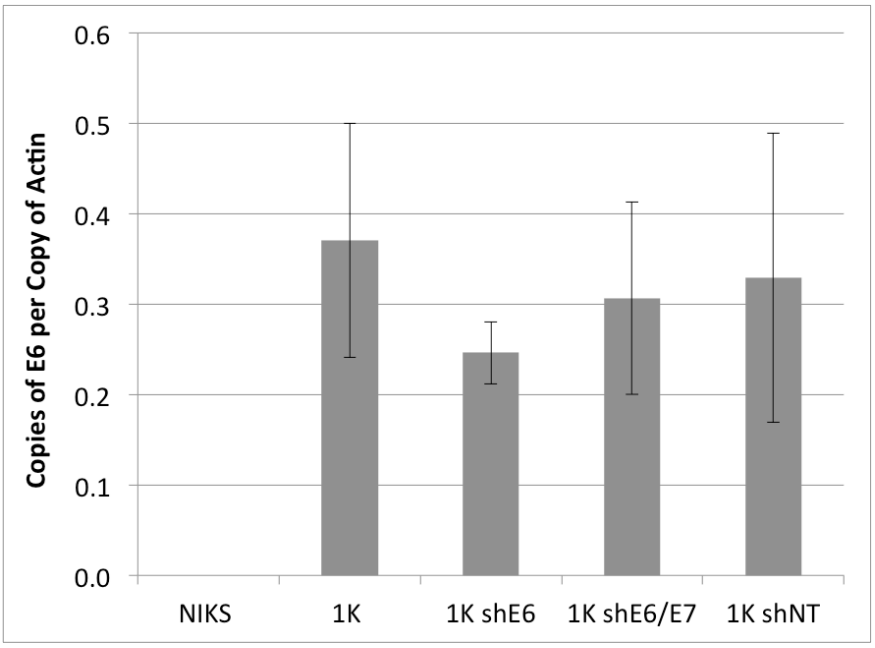

Figure 4.3: Cells infected with custom-made shE6 lentiviral particles present with a modest decrease in E6 transcript levels

1K cells were infected with shRNA lentiviral particles targeting E6 or both E6 and E7. Cell populations stably expressing shE6, shE6/E7 or shNT were grown to confluence. The levels of E6 mRNA were assessed by RT-qPCR and normalized to actin. The error bars in the graph represent the standard deviation of qPCR triplicates. The data here are representative of multiple similar experiments.

4.2.4 Cells infected with custom-made shE6 lentiviral particles do not grow slower than control cells

In this section I assessed the specific growth patterns of ushE6-expressing 1K. I found that the level of E6 transcript in these cells is slightly decreased as compared to 1K shNT control cells and hoped to show that even a very modest reduction in E6 levels could bring about a corresponding decrease in cell growth. As described earlier, my concerns was that within a heterogeneous population of transfected cells, such as in my siRNA experiments in Section 4.2.1, cells with higher levels of E6, which had been transfected with a low efficiency or not at all, would outgrow cells that had taken up the siE6 well and expressed low levels of E6. However, as these 1K shE6 cells had been selected with puromycin, I expected to have a more homogeneous population of cells. Hence, I speculated that shE6-expressing 1K would grow slower than 1K shNT cells.

Untreated 1K, 1K shNT and 1K shE6 cells were cultured in a 9-day growth assay along with untreated 2K and 2K shNT cells. 2K shNT cells were prepared following the same protocol as the corresponding 1K cells (see Section 4.2.3) using the same lentiviral particles. The two 2K infected cell populations were used for comparisons with the 1K populations. Cells were counted at days 1, 3, 5, 7 and 9 post-seeding to assess the growth patterns (Fig. 4.4). The graph shows that the 1K and 2K clonal cell lines give rise to their normal HSIL- and LSIL-like growth phenotypes, respectively. As expected, 2K shNT cells present with a similar growth phenotype as wild type 2K cells and can grow to same overall cell density within the time-course. However, 1K shE6-expressing cells grow slightly faster than their uninfected counterparts. The same effect can be observed for 1K shNT control cells.

The assessment of the proliferation of these cell populations has shown me that a minor decrease in E6 mRNA is not enough to significantly reduce the growth of cells. It seems that the process of infecting cells with lentiviruses and subsequently selecting them has the capacity to make cells grow more quickly. Therefore any growth decrease brought about by the knock-down of E6, would have to negate this increase first before any "real" effect can be observed.

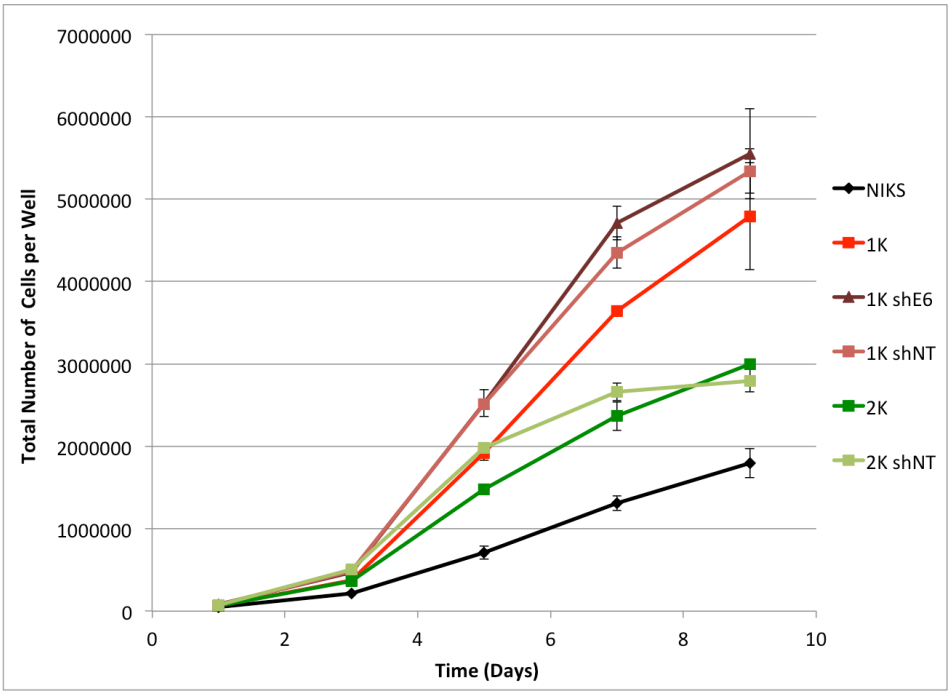

Figure 4.4: Cells infected with custom-made shE6 lentiviral particles do not grow slower than control cells

NIKS, untreated 1K, 1K shNT, 1K shE6, untreated 2K and 2K shNT cells were counted in duplicate at days 1, 3, 5, 7 and 9 post-seeding and compared in terms of their growth phenotypes. The average number of cells per 6-well plate well was plotted against the time in days. The error bars represent +/- the standard deviation of the duplicate wells.

4.2.5 Infection of LSIL- and HSIL-like cells with LXSN_E6 retrovirus does not bring about higher E6 levels

The experiments in this chapter so far have shown me that using RNAi to knock-down the levels of E6 and/or E7 in both SiHa and HSIL-like 1K cells does not work well. When I did see modest reductions in the level of E6 transcript, this did not lead to slower growth. Therefore I decided to attempt to change E6 levels by using the opposite approach; increase the levels of E6 in the slower growing 2K cells and investigate whether the LSIL-like pattern of proliferation could be transformed into an HSIL-like phenotype.

Having worked with the LXSN vector system before (in Chapter 3), I used LXSN_E6 retroviruses to infect both HSIL-like 1K and LSIL-like 2K cells. I decided to infect 1K in addition to 2K to assess whether this would result in even faster growth of these cells. Following antibiotic selection, 1K and 2K cells, now stably expressing LXSN_E6, were seeded in a growth assay. Cells were counted at days 1, 3, 5, 7 and 9 post-seeding to assess the differential patterns of proliferation (Fig. 4.5A). Cell pellets harvested at confluence at day 5 were lysed using a RIPA buffer containing 6 % SDS and used to assess the levels of E6 by western blot (Fig. 4.5B)

The proliferation data show that both 1K and 2K expressing LXSN_E6 do not have any growth advantage whatsoever over wild type 1K and 2K cells, respectively. Untreated 1K cells are actually growing slightly faster than 1K E6 cells. The western blotting data seem to correlate with this. Neither 1K E6 nor 2K E6 present with higher levels of E6 than wild type 1K and 2K.

The western blots do show that the levels of E6 for 1K are higher than for 2K. This is good as, on this rare occasion where the E6 antibody has worked, these results confirm what the p53 western blots in Chapter 3 suggest; that the levels of E6 are higher in 1K than 2K at confluence.

It seems that over-expressing E6 using the LXSN vector system does not work. While I am unsure as to why this is, I do think that testing a different vector is worthwhile.

A.

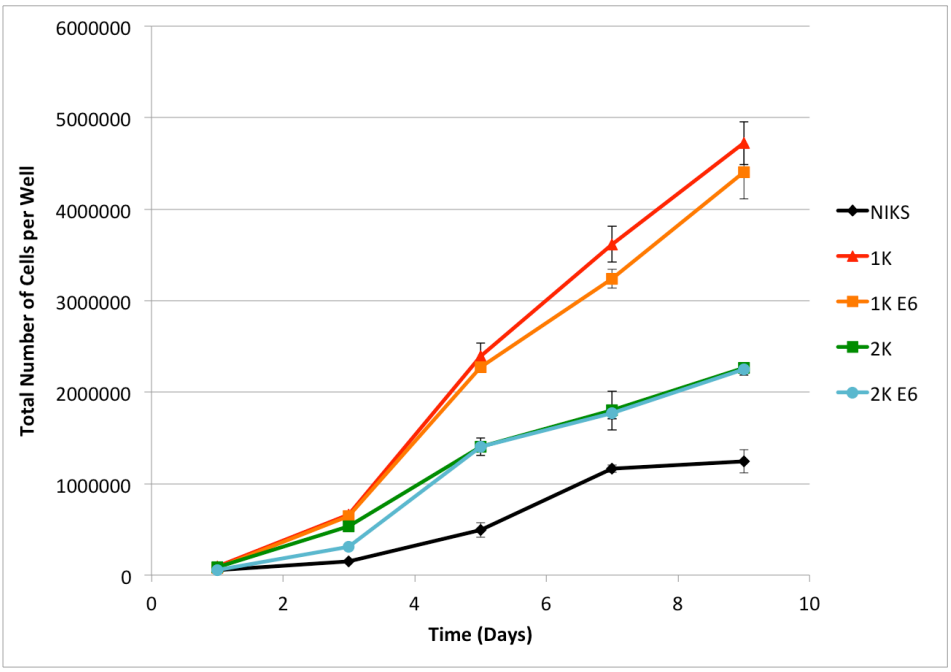

B.

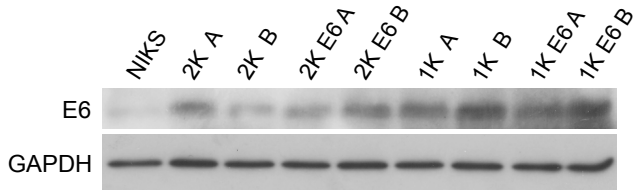

Figure 4.5: Infection of LSIL- and HSIL-like cells with LXSN_E6 retrovirus does not bring about higher E6 levels

LXSN_E6 retroviruses were used to infect 1K and 2K clonal cell lines. **A)** The growth patterns of NIKS, 1K, 1K E6, 2K and 2K E6 cells were compared in a 9-day growth assay. Cells from duplicate wells were counted at days 1, 3, 5, 7 and 9 post-seeding. The average number of cells per 6-well plate well was plotted against the time in days. The error bars represent +/- the standard deviation of the duplicate wells. **B)** Cells were cultured to confluence at day 5, and lysed using a RIPA buffer containing 6 % SDS. Whole cell extracts were used to assess the levels of E6 by western blot.

4.2.6 Testing of two vectors to over-express E6 in LSIL-like cells

Other laboratory members have previously used both pMV11 and pcDNA3.1 to express HPV16 E6 in cells and found that both of them work quite well. For this reason, I decided to repeat the experiment with these two vectors. (The pcDNA vector used here (pcDNA_E6SD) contains a splice defective form of E6. This means that only full-length E6 is expressed and none of the truncated E6* species).

Further personal communication with my colleagues suggested that integration of vector DNA into host chromosomes, which is necessary for the production of stable cell populations, is more efficient if DNA is transfected in the linear format. Therefore I digested vectors with an appropriate restriction enzyme prior to use.

LSIL-like 2K cells were transfected with pMV11_E6 (together with pBABE_puromycin) or pcDNA_E6SD plasmids on the day after seeding. The pBABE plasmid had to be used alongside pMV11_E6, as this vector itself does not contain an antibiotic resistance gene. Following antibiotic selection, cells were grown to confluence, harvested and then lysed using a RIPA buffer containing 6 % SDS. Whole cell extracts were used to assess the levels of p53, an inverse marker for E6, by western blot (Fig. 4.6). The results show that, as expected, compared to wild type NIKS cells, the levels of p53 are much lower in 2K cells. While 2K MV11_E6 cells present with considerably lower p53 levels, 2K pcDNA_E6SD cells do not show a further decrease. This indicates that only MV11_E6 seems to be increasing E6 levels successfully. I am unsure whether the pcDNA vector itself is less efficient at expressing E6, as compared to pMV11, or whether the fact that only full-length E6 is being expressed contributes to the lack of increased E6 levels.

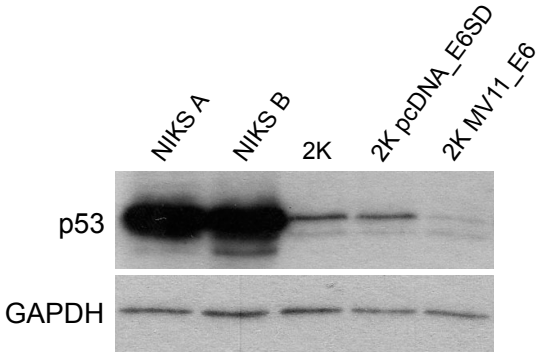

Figure 4.6: Testing of two vectors to over-express E6 in LSIL-like cells

LSIL-like 2K cells were transfected with linearized pcDNA_E6SD (splice-defective E6) or pMV11_E6. Stable cell populations were seeded in 6-well plates and cultured to confluence. Cells were lysed using a RIPA buffer containing 6 % SDS and whole cell extracts used to assess the levels of p53, an inverse marker of E6, by western blot.

4.2.7 LSIL-like cells over-expressing E6 grow faster than HSIL-like cells

LSIL-like 2K cells stably expressing MV11_E6 were shown in the previous section to present with higher levels of E6 as compared to wild type 2K cells. Here I continued the work with these cell populations and characterized their growth characteristics.

Untreated 1K, 2K and 2K MV11_E6 cells were counted at days 1, 3, 5, 7 and 9 post-seeding to assess their differential patterns of proliferation (Fig. 4.7A). Cell pellets harvested at each of the time-points were lysed using a RIPA buffer containing 6 % SDS. Whole cell extracts were used to assess the levels of p53, an inverse marker of E6, and also E7 by western blot (Fig. 4.7B).

The growth curve shows that 1K and 2K cells present with the normal LSIL- and HSIL-like phenotypes from the point of confluence at day 5 onwards. Surprisingly, 2K MV11_E6 cells not only grow faster than their wild type 2K counterparts but also than 1K cells.

The western blot data for p53 inversely correlate well with the ability of these cells to grow. Wild type 2K have much lower levels of p53 than NIKS at all time-points. Furthermore, as expected, they are higher than in 1K, suggesting that the levels of E6 are higher in 1K than 2K. Importantly, at all time-points analyzed, except at day 9, the levels of p53 in 2K MV11_E6 are as low as for 1K. At day 7, they are much lower in 2K MV11_E6 than in 2K. The levels of E7 are similar for 1K, 2K and 2K MV11_E6 throughout the growth assay. These were measured to ensure that the levels of p53 are not merely being altered by differences in E7. The results indicate that the variation in p53 levels observed is due to E6.

The data together seem to suggest that high levels of E6 in 2K MV11_E6 allow these cells to grow faster than untreated 2K. This further supports my theory that E6 on its own can enhance cell growth, suggesting that higher levels in HSIL-like cells cause these cells to proliferate more rapidly than LSIL-like cells.

A.

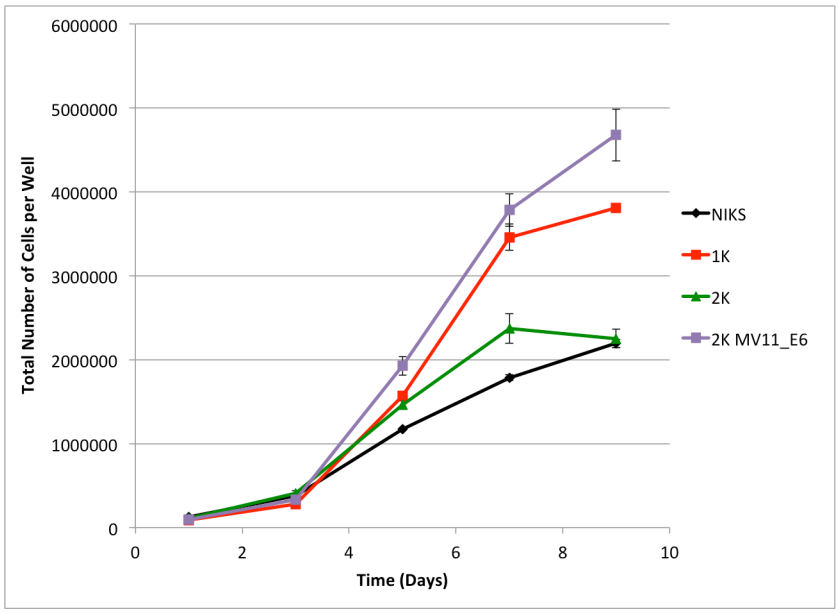

B.

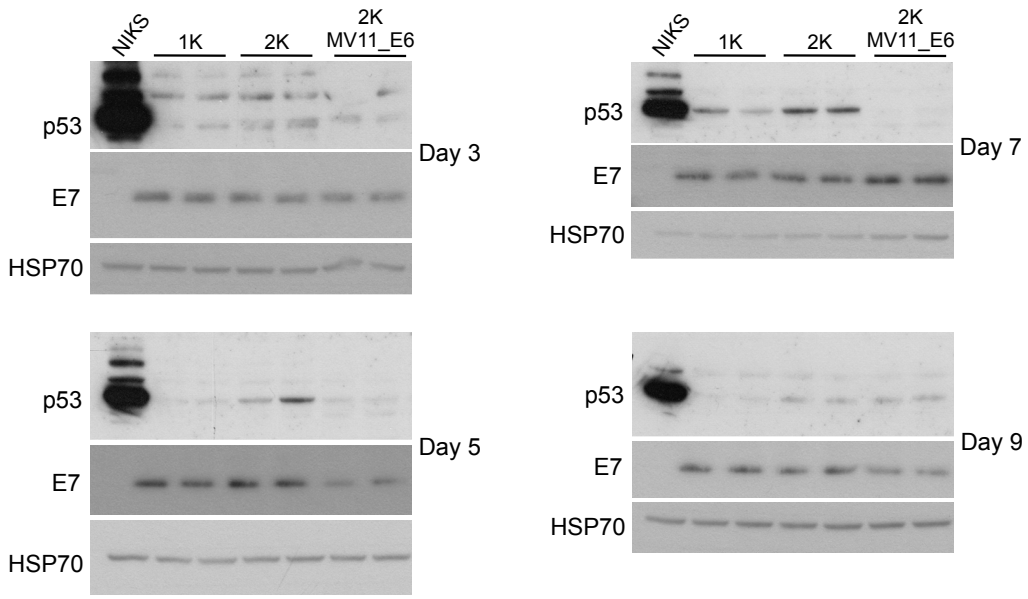

Figure 4.7: LSIL-like cells over-expressing E6 grow faster than HSIL-like cells **A)** The growth patterns of NIKS, 1K, 2K and 2K MV11_E6 were compared in a 9-day growth assay. Cells from duplicate wells were counted at days 1, 3, 5, 7 and 9 post-seeding. The average number of cells per 6-well plate well was plotted against the time in days. The error bars represent +/- the standard deviation of the duplicate wells. **B)** Cells were harvested at day 3, 5, 7 and 9 and lysed using a RIPA buffer containing 6 % SDS. Whole cell extracts were used to assess the levels of p53, an inverse marker of E6, and E7 by western blot.

4.2.8 Assessment of new endogenous controls for normalization of qPCR

Work in the previous two sections showed that 2K MV11_E6 cells express higher levels of E6 and that this leads to faster proliferation. As a direct consequence of the presence of more E6 in the infected 2K cells, this cell population could grow to a much higher cell density than not only its parental 2K counterpart, but also HSIL-like 1K cells. In Chapter 3 I showed that the differences in p53 protein levels, which I use to inversely measure E6, were not reflected in the E6 transcript levels of LSIL- and HSIL-like clones. Hence, it seems that in wild type 1K and 2K the differences in protein levels are caused by post-transcriptional modifications. To assess this I aimed to determine whether increasing the levels of E6 using pMV11_E6 in 2K cells would correlate with higher E6 transcript levels. I hypothesized that since E6 in these cells is being expressed from a separate source and is not under the control of the HPV promoter, the transcript levels may as a result be higher.

Having done a considerable amount of RNA work to this point in the project I found that the transcript levels of actin, the endogenous housekeeping control used for normalization during most of the qPCR experiments, and also GAPDH, vary significantly throughout a proliferation time-course. As shown in Figure 4.8A and B, respectively, the levels of actin and GAPDH mRNA fluctuate substantially between sub-confluence, confluence and post-confluence at days 3, 5 and 7.

Therefore I decided to find a better control that would allow me to make more accurate conclusions about the transcript levels of E6. I used a TaqMan® Express Human Endogenous Control 96-well plate (Life Technologies; 4396840) with three sets of 32 different housekeeping genes to assess the levels in one sub-confluent and one post-confluent cDNA sample from HSIL-like 1K cells and one post-confluent NIKS cDNA sample. After performing the qPCR according to the manufacturer's instructions, the data were analyzed and I determined which of the 32 controls had the least amount of variation (as measured by the standard deviation of the Ct values obtained) across the three samples that I had run. I found that *RPL30*, *RPS17*, *ELF1* and *E1F2B1* were the best housekeeping genes to consider for my experiments. The standard deviations for some of the other genes were up to 12-fold higher. I carried out qPCR with 2K day 3 and 7 (sub-confluence and post-confluence) cDNA, 2K MV11_E6 day 3 and day 7 cDNA and wild type NIKS day 7 cDNA and compared E1F2B1, ELF1, RPL30 and

RPS17 levels in terms of Ct value variation across these samples (Fig 4.9A-D, respectively). I tested each primer set with two dilutions (1:50 and 1:500) of each cDNA sample. As some genes are expressed at much higher levels than others, and it is important to keep linear amplification of each cDNA within the optimum range of qPCR (Ct values in the high 20s or low 30s), I wanted to establish which dilution was best for each primer pair. The copy numbers that I calculated based on the 1:500 dilution Ct values were multiplied by 10 so that they could be plotted on the same graph as the copy numbers calculated for the 1:50 dilution results.

The data show that the control with the least variability is ELF1 or E74-Like Factor 1 (Ets Domain Transcription Factor), a transcription factor. Regardless of the presence of HPV and whether cells are sub-confluent or post-confluent, the levels of ELF1 do not fluctuate very much. Furthermore in terms of the optimum range of qPCR the 1:50 dilution of cDNA is better than 1:500.

A.

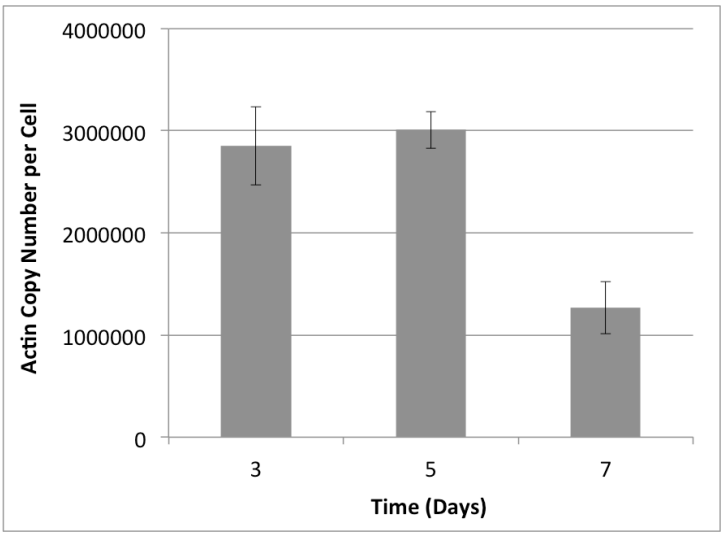

B.

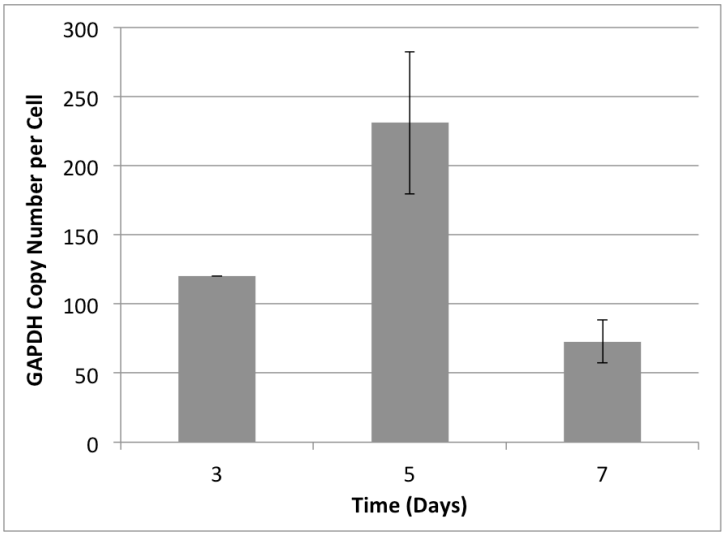

Figure 4.8: The transcript levels of the endogenous qPCR controls actin and GAPDH fluctuate substantially during a growth assay

1K cells were cultured in a growth assay format and harvested at sub-confluence at day 3, confluence at day 5 and post-confluence at day 7 post-seeding. The levels of actin **(A)** and GAPDH **(B)** mRNA were assessed by RNA extraction and RT-qPCR. The error bars in the graph represent the standard deviation of qPCR triplicates.

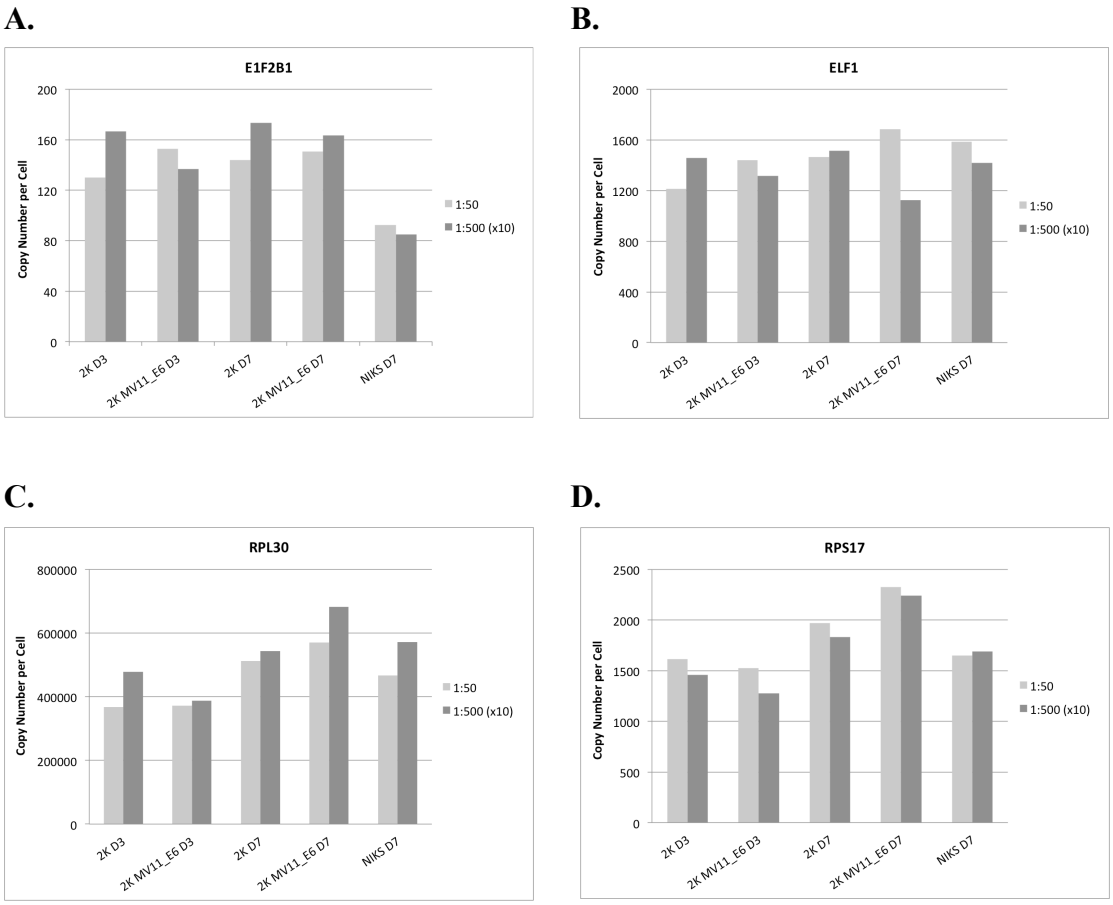

Figure 4.9: Assessment of new endogenous controls for normalization of qPCR

Sub- and post-confluent 2K and 2K MV11_E6 cDNAs from days 3 and 7 and post-confluent NIKS cDNA from day 7 were used to do qPCR with E1F2B1 **(A),** ELF1 **(B),** RPL30 **(C)** and RPS17 **(D)** primer sets. Copy number variation across the cDNA samples is shown in the bar charts. Each primer set was tested with two dilutions (1:50 and 1:500) of each cDNA sample. The copy numbers calculated based on the 1:500 dilution Ct values were multiplied by 10 so that the values could be plotted on the same graph as the 1:50 dilution results.

4.2.9 LSIL-like cells over-expressing the E6 protein present with increased E6 transcript levels

In the previous section I addressed an ongoing issue with my qPCR and found that ELF1 is a much better endogenous control for use in my experiments than both actin and GAPDH. Having established this, I decided to measure whether the higher levels of E6 protein in 2K MV11_E6 cells correspond with elevated E6 transcript levels.

To test this I cultured 1K, 2K and 2K MV11_E6 cells in a growth assay format, extracted RNA at sub-confluence at day 3 and post-confluence at day 7 post-seeding, and assessed the levels of E6 mRNA, relative to ELF1, using RT-qPCR (Fig. 4.10A and B, respectively). At day 3 the levels of E6 mRNA in 1K are slightly higher than for 2K, with levels in 2K MV11_E6 being higher still. At day 7, E6 mRNA levels are slightly lower for 2K than for 1K, more so than at day 3. The levels in 2K MV11_E6 appear to be similar to those measured in 1K.

The levels of E6 transcript do not correlate exactly with E6 protein levels. I found in Figure 4.7B that the levels of E6, as inversely measured by p53, are similar for 1K and 2K MV11_E6 at sub-confluence at day 3 and higher for the latter at post-confluence at day 7. The results here show the opposite trend for E6 mRNA. From this I conclude, that the higher protein levels of E6 in this cell population must be brought about by post-transcriptional regulation. However, the data confirm that the levels of E6 transcript are higher in 2K MV11_E6 cells than for the 2K clone.

Moreover, at both days 3 and 7 the levels of E6 mRNA in HSIL-like 1K cells are higher than in LSIL-like 2K cells. This is in contrast to what I found in Section 3.2.8 where the levels in the HSIL-like clone where not significantly different to the levels in the LSIL-like clones. I believe that this difference in results, was brought about by using the new superior ELF1 endogenous control for my qPCR experiments. This means that the LSIL- and HSIL-growth phenotypes correlate with both the transcript and protein levels of E6.

A.

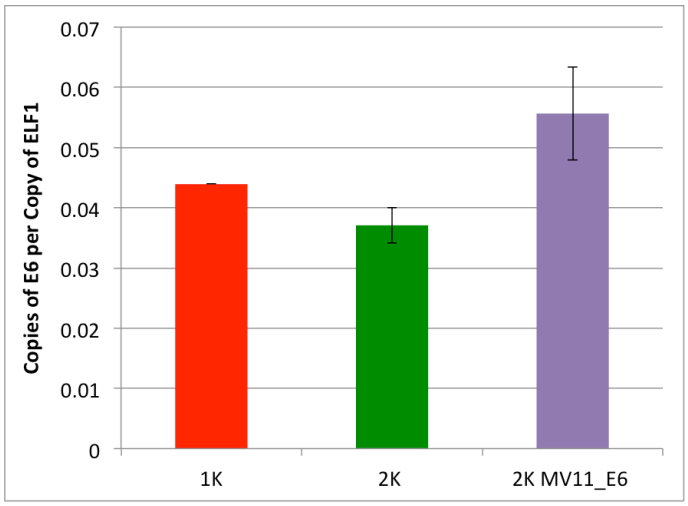

B.

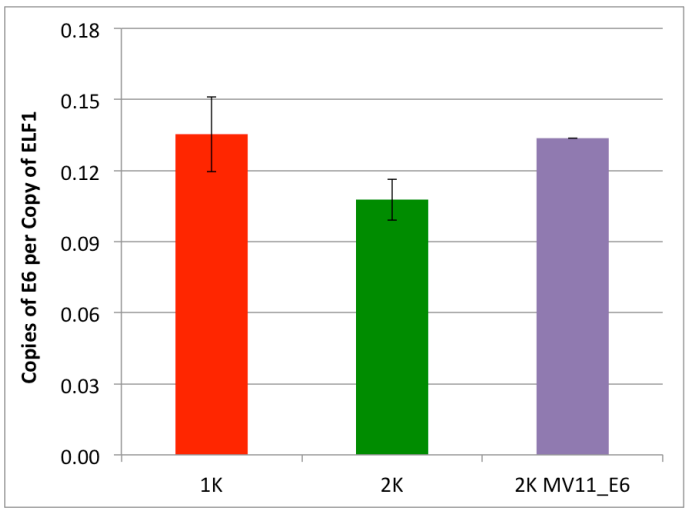

Figure 4.10: LSIL-like cells over-expressing the E6 protein present with increased E6 transcript levels

1K, 2K and 2K MV11_E6 cells were cultured in a growth assay format and harvested at sub-confluence at day 3 and post-confluence at day 7 post-seeding. The levels of E6 mRNA for each clone were assessed by RNA extraction and RT-qPCR and normalized to the levels of ELF1 at day 3 **(A)** and day 7 **(B)**. The error bars in the graph represent the standard deviation of qPCR triplicates.

4.2.10 Generation of cell populations expressing E6 from plasmid vectors can lead to integration of the original viral episomes into the cellular genome

Having established that high E6 levels seem to be involved in giving rise to fast monolayer proliferation, I hypothesized that 2K MV11_E6 cells would, as a result of their increased E6 levels, also give rise to a high-grade raft phenotype.

To test this, 2K and 2K MV11_E6 cells were rafted using the procedure outlined in Chapter 2. Raft cultures were left to differentiate for 12 days post-lifting. Cross sections of rafts were stained with MCM7 (red), to identify the S phase compartment, E4 (green), to detect late viral gene expression and DAPI (blue) was applied as a nuclear counterstain (Fig. 4.11A). The results of the experiment show that, as expected, wild type 2K cells give rise to a LSIL-like rafting phenotype. There is quite a large S phase compartment, with many cells in the upper half/upper third of the epithelium positive for MCM7. Furthermore, there is abundant E4 expression in the upper layers. For 2K MV11_E6 cells E4 expression cannot be detected. In terms of MCM7 expression, the 2K MV11_E6 and wild type 2K rafts are very similar, with the S phase compartment comprising comparable portions of the epithelium.

A phenotype like this, with absence of E4 yet no HSIL-like MCM7 expression pattern, suggests that the viral episomes may have integrated into the host genomes. To test this, I carried out Southern blot analysis of total genomic DNA extracted from confluent monolayer cultures for 2K, 2K MV11_E6 and 2K INT, which is a 2K population with fully integrated viral genomes. For 2K MV11_E6 both low and high-passage cell populations were used.

DNA was digested with BamHI or HindIII and hybridized to a [^{32}P] radioactively-labeled full-length HPV16 genome probe. BamHI cuts the HPV16 genome only once and therefore digestion of episomes with this enzyme produces a single 8kb linear band. HindIII does not cut within the genome and, hence, the bands represent open circular and supercoiled DNA normally associated with episomes. To allow me to establish the episomal copy numbers of my cells, I also loaded varying amounts of linearized HPV16 plasmid DNA of a known concentration. The Southern blot analysis (Fig. 4.11B) shows that 2K cells contain only episomal viral DNA, as there is just one 8kb band in the lane

where BamHI-treated cut DNA was loaded. In contrast, for 2K MV11_E6, at both low and high passage, and 2K INT cells there are bands of varying sizes within the lanes of cut DNA. This shows that the viral genome has integrated, with the different integration events in the cell populations giving rise to different sized fragments. Additionally, due to the integration, HindIII no longer does not cut the DNA. In the lanes that should represent uncut DNA for these three cell populations, there are now bands that are not associated with episomes. The arrows labeled "A" and "B" show the positions of faint bands in BamHI (cut) and HindIII (uncut) lanes, respectively, for 2K MV11_E6 at both low and high passages.

The experiments here have shown that, although 2K MV11_E6 cells have higher levels of E6 than their wild type 2K counterparts, these cells now have integrated viral DNA. I am unsure what specifically has lead to the integration of episomes. It may have been the process of making the populations, for instance the antibiotic selection. Alternatively, it could be that the act of putting additional E6 into the cells, the expression of which is not under the control of the HPV promoter.

Regardless of why the integration has occurred, these findings put an end to my work with the 2K MV11_E6 population. My earlier observation that higher E6 levels lead to faster growth still stands. However, comparing episomal and integrated lines is generally difficult as integration leads to many changes within the cells, with levels of both viral and cellular proteins being altered. Hence, using these populations to study the underlying mechanism that is giving rise to the LSIL- and HSIL-growth phenotypes may be very challenging.

A.

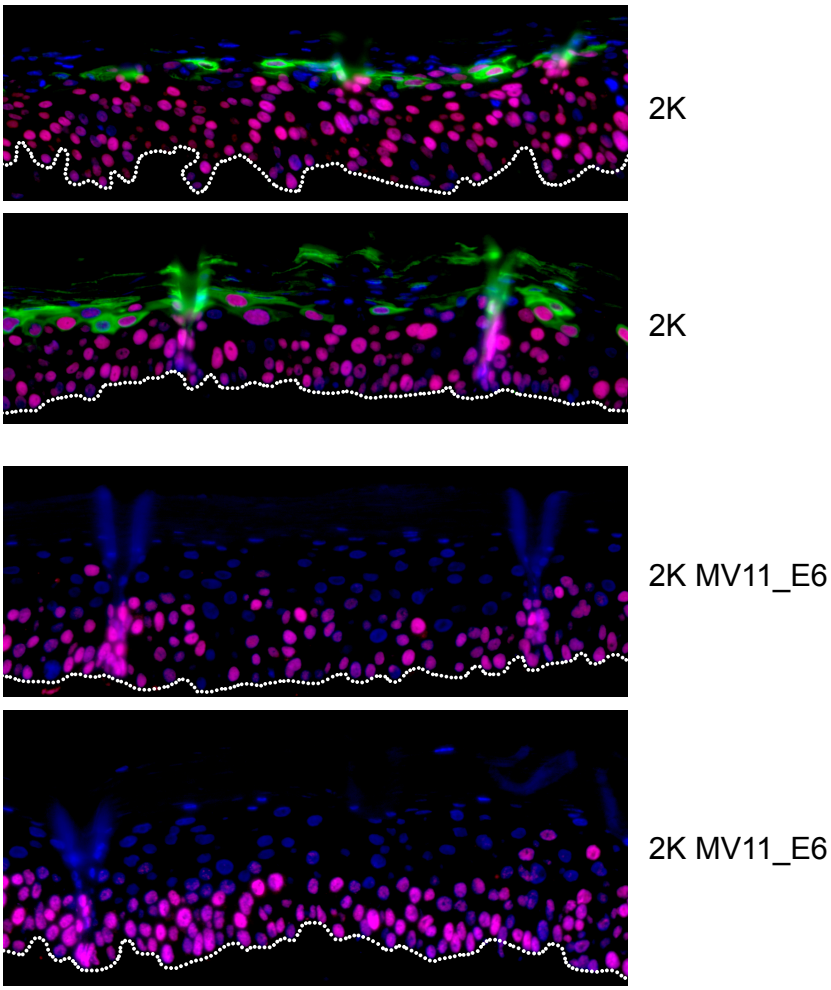

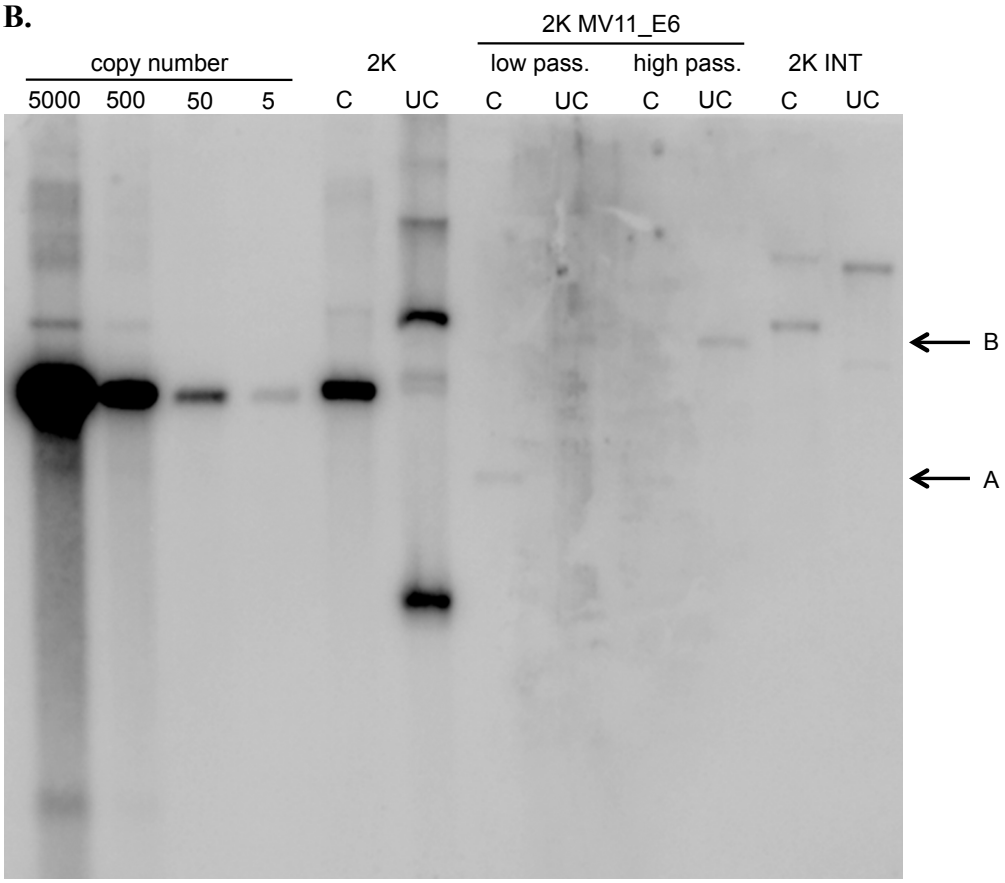

Figure 4.11: Generation of cell populations expressing E6 from plasmid vectors can lead to integration of the original viral episomes into the cellular genome

A) 2K and 2K MV11_E6 cells were rafted in duplicate according to standard laboratory protocol. On day 12 post-lifting rafts were harvested and subsequently sectioned. Raft sections were stained with MCM7 (red), to identify the S phase compartment, E4 (green), to detect late viral gene expression, and DAPI (blue) as a nuclear counterstain. The broken white line indicates the basal layer of rafts.

B) Southern blot analysis was carried out of total genomic DNA extracted from confluent monolayer cultures for 2K, 2K MV11_E6 (low and high passage) and 2K INT (a fully integrated sub-population of 2K). DNA was digested with BamHI or HindIII and hybridized to a [^{32}P] radioactively-labeled full-length HPV16 genome probe. BamHI (C) cuts the HPV16 genome only once and produces a single 8kb linear band. HindIII (UC) does not cut within the genome; bands represent open circular and supercoiled DNA. Control DNA was loaded at varying concentrations to establish viral copy number of cells. The arrows labeled "A" and "B" show the positions of faint bands in BamHI and HindIII lanes, respectively, for 2K MV11_E6 at both low and high passage.

4.2.11 Optimization of conditions for treatment with siRNA in LSIL- and HSIL-like clonal cell lines

The work in this chapter so far has focused on manipulating the levels of E6 in LSIL-like 2K and HSIL-like 1K cells to show that this would result in a corresponding change in the specific growth phenotypes of these cell lines. In Section 4.1 I tested various siE6, siE7 and siE6/E7 sequences in SiHa cells, found that they did not work and decided not to test the siRNA in NIKS, as NIKS are much less transfectable than SiHa. In the meantime other laboratory members have tested a 4D Nucleofector® X Unit for electroporating cells and found that the transfection efficiency of NIKS using this approach is much higher than using standard laboratory protocol; up to 60 or 70 % instead of less than 1 %. Therefore, to achieve a better knock-down of E6 and/or E7, I decided to electroporate NIKS HPV-containing clones with siRNA.

I began by testing the efficiency of siGAPDH. I electroporated $1x10^6$ 1K cells and seeded them into 6-well plates. I tested two different concentrations of siRNA, 66 and 100 nM. At 48 hours post-transfection cell pellets were harvested and lysed using a RIPA buffer containing 6 % SDS. Whole cell extracts were used to assess the levels of GAPDH by western blot (Fig. 4.12A). I found that the siRNA treatment had worked very well. When 66 nM was used, I found a small decrease in GAPDH levels whereas a concentration of 100 nM of siRNA reduced the levels more substantially.

One reason why use of siRNA in these cells is challenging is because the growth assays go on for longer than the effect of siRNA. Generally, most siRNA treatment analysis is done 48 or 72 hours post-transfection, with the upper limit being 4 days or 96 hours, before the effect deteriorates. However, my growth assays go on for 9 days. Since the preliminary results with the siGAPDH looked convincing, I decided to try to adapt my growth assay to a shorter time span. I hypothesized that if I seeded more cells at day 0, so that cells reach confluence earlier, and hence start to diverge into their respective growth phenotypes earlier, I could reduce the length of the growth assays. Generally, cells need 24 hours after seeding to adapt to the 6-well plate and start to grow normally. Hence, for optimum growth conditions and to allow cells to recover, cells should be approaching confluence about two days post-seeding. When I examined growth data for 1K and 2K, I found that at confluence at day 5 there are approximately $1.5x10^6$ cells in each well. Based on this I speculated that seeding $6x10^5$ cells at day 0 would result in

approximately $1.5x10^6$ cells per well on day 2 post-seeding, the equivalent of day 5 of a normal growth assay.

To test this I seeded 1K and 2K at this higher cell density in a growth assay format. At day 1 I counted cells to check their seeding efficiency. At days 2, 4 and 6 I counted cells to assess their growth patterns (Fig 4.11B). These time-points should be the equivalent of days 5, 7 and 9, respectively, of the normal growth assay. A bar chart showing fold-increase relative to the previous time-point is shown in Figure 4.11C. The data show that 1K and 2K start to diverge and give rise to their normal growth phenotypes from confluence at day 2 onwards. While the difference between the cell lines is much smaller than in a normal time-course, it is highly reproducible. The bar chart shows, that at each time-point 1K cell numbers have increased more than for 2K. NIKS take longer to recover from the seeding process and therefore only start to grow rapidly from day 2 onwards. Hence, the increase in NIKS cell numbers is higher than for both clones prior to the last time-point although overall 2K, and especially 1K, can grow to a much higher cell density. Throughout the duration of the growth assay NIKS have increased their cell numbers 3-fold, while 1K and 2K have done so 6- and 4-fold, respectively. This means that 1K have grown to a density that is 2-fold higher than that of NIKS while 2K have reached a 1.5-fold higher cell density. The data in Figure 4.11B are an average of 8 individual experiments. Unpaired t-tests were used to compare 1K and 2K cell numbers at each time-point. There is no significant difference at confluence at day 2 with a p value of 0.47. At post-confluence at days 4 and 6, the overall cell numbers are significantly different with p values of 0.031 and 0.0031, respectively.

The shortened growth assay shows that the LSIL- and HSIL-like growth phenotypes arise as normal. Hence, I can use this format for siRNA experiments. This set-up should allow me to detect any growth effects resulting from treatment with siRNA targeting E6.

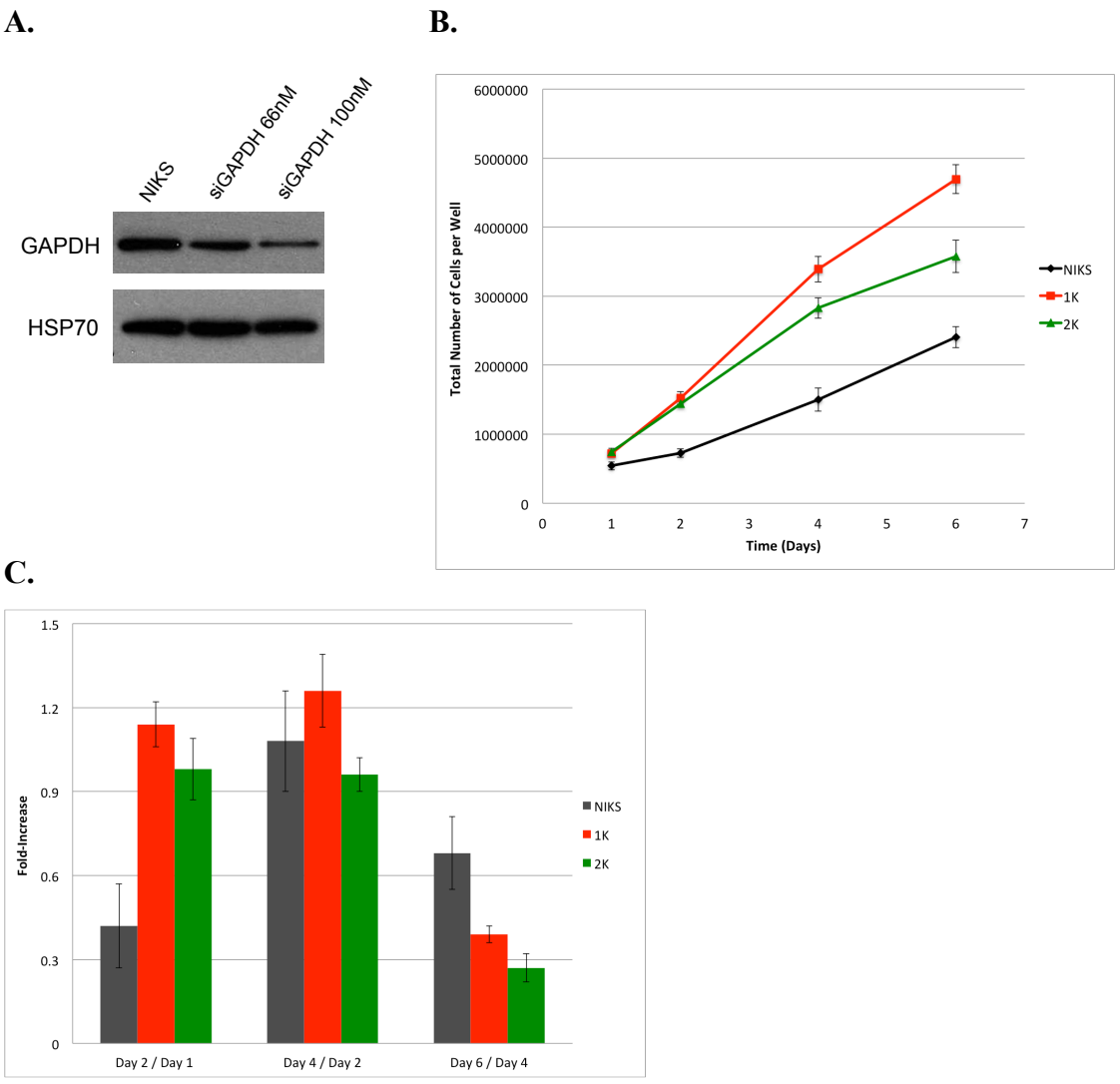

Figure 4.12: Optimization of conditions for treatment with siRNA in LSIL- and HSIL-like clonal cell lines

A) 1K cells were transfected with 66 or 100 nM of siGAPDH and harvested 48 hours later. Untreated NIKS cells were used as controls. Whole cell extracts were prepared and western blotted for GAPDH.

B + C) NIKS, 1K and 2K were seeded at a high density ($6x10^5$) in 6-well plates and counted in duplicate at days 1, 2, 4 and 6 post-seeding. Day 2 corresponds to confluence at day 5 of a normal growth assay, while days 4 and 6 correspond to post-confluence at days 7 and 9. Cells were compared in terms of their growth phenotypes. Unpaired t-tests were used to compare 1K and 2K cell numbers at each time-point. The p values at day 2, 4 and 6 are 0.47, 0.031 and 0.0031, respectively.

B) The average number of cells per 6-well plate well was plotted against the time in days. The error bars represent +/- the standard error of 8 individual experiments.

C) Fold-increase relative to the previous time-point was calculated and plotted in a bar chart. The error bars represent +/- the standard error of 8 individual experiments.

4.2.12 The knock-down of E6 using siRNA by electroporation in HSIL-like cells results in slower proliferation

The work in the previous section has shown that siGAPDH is successful at reducing the levels of GAPDH protein in 1K using electroporation. I also optimized the conditions for a short growth assay so that LSIL- and HSIL-like cells diverge into their respective growth phenotypes from day 2 onwards. Hence, the growth effects of any siRNAs should now be observable in this format. In this section I will use siE6/E7-3, the sequence that looked most promising in SiHa cells in Section 4.2.1, to reattempt the knock-down of E6 and E7.

When I first tested the Nucleofector® I found that, although, the transfection efficiency is quite high, many cells, up to 60 or 70 %, die as a result of the electroporation process. Therefore I decided to increase the number of cells per individual electroporation from 1 to $1.5x10^6$ cells per cuvette. This way I hoped to end up with at least $6x10^5$ adhering cells per well, with about 60-70 % successfully transfected. Hence, if any of the siRNA sequences work, I should be able to measure a reduction in E6 or E6 and E7 levels and see a corresponding growth effect.

NIKS and 1K cells were electroporated with siNT (non-target) and 1K with siE6/E7-3. Cells were plated and subsequently counted on the day after to check their seeding efficiency. Cells were counted to assess their proliferation patterns at 48, 72 and 96 hours after siRNA treatment, which corresponds to days 2 (confluence), 3 and 4 (both post-confluence) (Fig 4.12A). Cell pellets were prepared in duplicate throughout the growth assay and the day 3 pellets lysed using a RIPA buffer containing 6 % SDS. The levels of p53, used as an inverse marker of E6, were determined by western blot (Fig 4.13B).

The growth results in Figure 4.13A show that compared to 1K cells treated with siNT, siE6/E7-3 treated cells present with much slower cell growth at all stages of the short growth assay. Although 1K siNT cells seeded better, which means that I would expect them to outgrow 1K siE6/E7-3 cells, the latter no longer have the capacity to grow to a higher overall density than NIKS electroporated with siNT cells.

Additionally, the western blot results in Figure 4.13B show that the levels of p53 are

much higher in 1K siE6/E7-3 than 1K siNT cells. This suggests that the levels of E6 are much lower in the former than the latter and that the growth effects observed are a direct consequence of these diminished E6 levels.

The data in this section indicate that knock-down of E6, and presumably E7, using siRNA by means of electroporation leads to a dramatic reduction in the growth potential of 1K cells. All in all, I have further confirmed my working hypothesis that E6 on its own has the capacity to increase the proliferation of cells.

A.

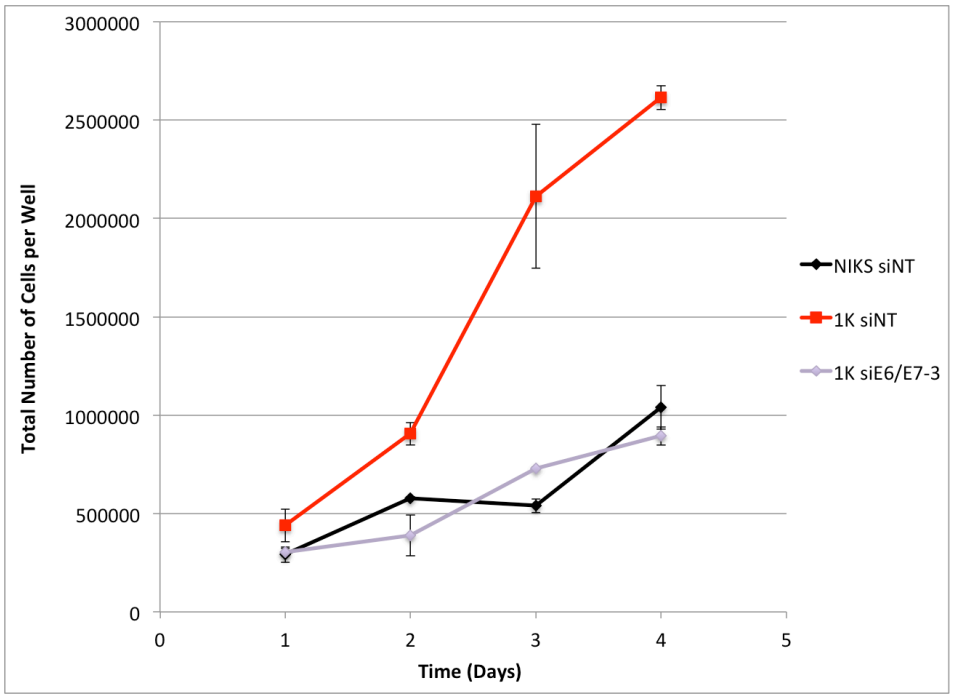

B.

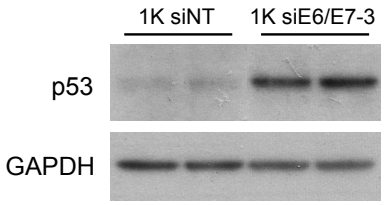

Figure 4.13: The knock-down of E6 using siRNA by electroporation in HSIL-like cells results in slower proliferation

The growth of 1K cells electroporated with siE6/E7-3 or siNT (non-target) and NIKS treated with siNT was assessed in a short growth assay. Approximately $1.5x10^6$ cells were electroporated per well with 100 nM of siRNA. Cells were counted at days 1, 2, 3 and 4 post-electroporation.

A) The average number of cells per 6-well plate well was plotted against the time in days. The error bars represent +/- the standard deviation of the duplicate wells. **B)** Cell pellets were prepared in duplicate at day 3 for 1K siE6/E7-3- and siNT-treated cells and lysed using a RIPA buffer containing 6 % SDS. The levels of p53, used as an inverse marker of E6, were determined by western blot.

4.3 Discussion

The work in this chapter aimed to determine whether altering the levels of E6 in the HPV positive cells lines, would convert the phenotype of the LSIL- to that of the HSIL-like cells. Initially, I found, using several previously published siE6, siE7 and siE6/E7 sequences, that the knock-down of E6 and/or E7 in SiHa did not work. Subsequently I attempted to reduce E6 and E7 levels using shRNA in HSIL-like 1K cells. Although two different retroviral delivery systems were tested, the experiment was unsuccessful. Hence, I decided to use a different approach and tried to increase the levels of E6 in LSIL-like 2K cells using a plasmid vector. This experiment was successful and I not only detected high levels of the E6 protein but also found that 2K cells now grew more rapidly than 1K cells. However, when I carried out raft cultures and Southern blot analysis I found that the transfection of cells with additional E6 had lead to the integration into the host chromosomes of the viral genomes. I then revisited my RNAi approach and this time electroporated HSIL-like 1K cells with a si6/E7 oligo. By using this method, the knock-down of E6 was successful. 1K cells expressing low levels of E6, as a result of the siRNA treatment, were only able to grow as quickly as NIKS control cells.

Two separate plasmid infections, subsequent selections, rafting and Southern blot analysis have confirmed that 2K MV11_E6-expressing cells had fully integrated viral genomes. This finding, that cells expressing additional E6 cannot maintain their viral episomes, is interesting. Previous work in the laboratory has shown that when cells already expressing E6 (LXSN_E6) are transfected with the full HPV16 genome, the genome cannot persist. While some integration into host chromosomes occurs, most episomes are lost from the cells (Nicolaides, 2011). This was shown on multiple occasions. Therefore it was hypothesized that E6 has a role in preventing the "super-infection" of cells, so that when one type of HPV is present in a cell, another type cannot infect the same cell and persist additionally. This hypothesis makes sense, as generally two different types of virus, although it has been reported (Egawa et al., 1993, McLaughlin-Drubin and Meyers, 2004), are not found within a single cell. Approximately 10 % of clinical lesions contain two or even multiple HPV types (Kalantari et al., 1997, Brown et al., 1999, Silins et al., 1999, Bachtiary et al., 2002) but this is likely associated with the regional separation of the various infections within the lesion (Christensen et al., 1997). While my experiments in this chapter were different to

the ones that gave rise to the "super-infection" theory, I still think that my findings complement the original ones. In the original study, integration occurred in cells with lots of E6. My data also show that integration was brought about in cells with high levels of E6. Hence, I propose that integration is E6 dose-dependent. Although, this concept is interesting I have not investigated this further.

As discussed in the main introduction and at the end of Chapter 3, although E7 is classically associated with driving cell growth, there are numerous studies that have attributed this function to E6. E6 can interfere with the canonical Wnt pathway through the degradation of hDlg and hScrib via its PDZ motif (Ishidate et al., 2000, Nagasaka et al., 2006). E6 can also deregulate the Notch pathway, though there is disagreement in the field as to, how, and to what extent this occurs (Henken et al., 2012). Furthermore E6 can interfere with the regulation of the G1/S phase checkpoint and promote cell cycle progression and growth (Malanchi et al., 2002, Malanchi et al., 2004, Shai et al., 2007). Hence, based on current literature, it seems likely that the E6-dependent growth effects I have consistently been observing are real.

My results suggest that the next logical step is to determine the mechanism by which E6 can bring about enhanced cell proliferation. The LSIL- and HSIL-like cell lines start to diverge in terms of their growth patterns from the point of confluence onwards. This also correlates with differences in the levels of E6. Hence, the HSIL-like cells may be able to more easily overcome the contact inhibition pathways that normally prevent cell growth when sufficient cell-to-cell contact has been established. Neither wild type NIKS nor LSIL-like cells contact inhibit completely upon reaching confluence, i.e. they do not cease growing. However, in Section 3.2.7 I observed that the mechanism through which the HSIL-like cell lines make room for additional cells is very different to NIKS and LSIL-like cells. While the former become increasingly smaller and stay within a single plane, the latter, though they also decrease in size, grow on top of each other and form cell piles. These observations suggest that contact inhibition pathways may be differentially regulated in the various cell lines. Based on my results so far I hypothesize that this may be brought about by E6. The contact inhibition pathways within cells are complex and there is a lot of overlap between them. One of the key ones in epithelial cells is the Notch signal transduction pathway and this will be analyzed in more detail in the next chapter.

Chapter 5: Investigation of the Pathways Targeted by E6 to Enhance Cell Proliferation

5.1 Introduction

The work in the previous two chapters has shown that HPV16 E6 alone can up-regulate cell proliferation, and that high levels of this protein correlate with the enhanced ability of the cells to grow to high density. The LSIL- and HSIL-like growth phenotypes emerge from the point of confluence onwards and this correlates with high E6 levels in the latter. This chapter aims to address how E6 leads to the increased cell numbers, in particular how it appears to overcome the NIKS contact inhibition pathways.

In Chapter 3 I showed that the growth of E6-expressing cells is associated with cyclin A activation. These results are in agreement with published findings (Malanchi et al., 2002, Malanchi et al., 2004). However, neither I nor the authors of those studies have determined the mechanism by which E6 is bringing about this effect. Furthermore, I want to characterize how E6 is specifically overcoming contact inhibition. Malanchi *et al.* were characterizing overall growth of fibroblasts, not growth in a high cell density environment. As outlined in Chapter 3 I believe that the confluent monolayer has a similar cell density as the basal layer of a raft culture or a real epithelium. This means that the pathways affected by viral proteins to drive proliferation past the point of confluence, should be reflective of their role in basal cells. Hence, unlike studies in fibroblasts, my cell line model can be used to characterize the signaling systems deregulated by the virus in its natural environment, which may make my findings more relevant to the HPV field on the whole.

One of the most well characterized functions of high risk E6 is its ability to bind to and target p53 for proteasomal degradation (Werness et al., 1990, Scheffner et al., 1990) in an E6-AP-dependent manner (Huibregtse et al., 1991, Scheffner et al., 1993). There are numerous publications suggesting that degradation of p53 is essential to allow HPV-infected cells to proliferate (Ishiwatari et al., 1994, Horner et al., 2004). Since p53 is a crucial regulator of the cell cycle and I observe differential cyclin A activation in my experiments, p53 inactivation by E6 in NIKS cells may be involved in allowing cells to proliferate.

The PDZ-binding motif of the high-risk E6 protein enables E6 to bind to PDZ proteins such as hDlg (Lee et al., 1997, Kiyono et al., 1997), and hScrib (Nakagawa and Huibregtse, 2000), and target them for degradation. It has been shown that the interaction of E6 with PDZ binding partners is required for its ability to induce epithelial hyperplasia (Nguyen et al., 2003). Additionally the PDZ motif of E6 may drive cell proliferation by increasing β-catenin activity in the canonical Wnt pathway. Both hDlg and hScrib, can bind to the adenomatous polyposis coli (APC) protein (Matsumine et al., 1996, Takizawa et al., 2006), which also contains a PDZ binding motif. APC forms part of the destruction complex of the canonical Wnt pathway that actively degrades β-catenin in the absence of Wnt ligands, to prevent activation of β-catenin transcriptional targets (Logan and Nusse, 2004). Binding of both hDlg and hScrib to APC has been shown to be involved in this cell cycle inhibitory function (Ishidate et al., 2000, Nagasaka et al., 2006). Hence, degradation of these PDZ proteins by E6 may lead to deregulated growth through Wnt signaling.

Some of the PDZ proteins bound by E6 also have a role in maintaining adherens junctions. The main component of adherens junctions, found at certain cell-cell contact sites in the epithelium, is the cell adhesion receptor E-cadherin (Jeanes et al., 2008). These junctions allow adjacent cells to bind to each other and form connections and play essential roles in cell adhesion, recognition and motility, epithelial polarity, contact inhibition and differentiation. E-cadherin is linked to intracellular networks such as the actin cytoskeleton, via its direct association with β-catenin and the association of β-catenin with α-catenin. Both hDlg and hScrib are recruited to adherens junctions in an E-cadherin-dependent manner (Bilder et al., 2000, Firestein and Rongo, 2001, Navarro et al., 2005) and function to stabilize the linkage between E-cadherin and α-catenin (Qin et al., 2005). Furthermore, E6 has been shown to reduce surface E-cadherin and hence interfere with its function (Matthews et al., 2003). This means that in my cells, E6 may deregulate adherens junctions and promote proliferation in this way.

As described in more detail in the main Introduction, the Notch pathway is one of the main players involved in regulating contact inhibition of cells. In the epithelium, Notch is implicated mainly in cell cycle withdrawal and keratinocyte differentiation (reviewed in (Watt et al., 2008, Dotto, 2008)), though some of its targets are involved in actively

promoting cell growth. Notch receptor activation generally requires cell-cell contact because its ligands (Delta-like1, -3, -4 and Jagged1, -2) are cell surface anchored molecules (Kolly et al., 2005). Upon activation Notch gets sequentially cleaved to give rise to Notch IntraCellular Domain (NICD), which translocates to the nucleus and associates with RBPJ (Recombining binding protein suppressor of hairless). In the absence of Notch, RBPJ is a repressor complex (Dou et al., 1994). However when NICD is bound, other proteins such as MAML1 (Mastermind-like protein 1) and p300 (E1A binding protein p300) are recruited to the, now, activator complex and this enables transcriptional regulation of Notch targets including, amongst many others, HES1, p21 and AP-1 (Borggrefe and Liefke, 2012). The p21 protein (Cyclin-dependent kinase inhibitor 1) is activated by Notch and is involved in mediating its growth inhibitory and differentiation promoting effects (Abbas and Dutta, 2009). Several groups (Weijzen et al., 2003, Brimer et al., 2012, Henken et al., 2012, Tan et al., 2012, Meyers et al., 2013) have shown that E6 can interfere with the Notch pathway and thereby inhibit transcriptional activation of certain Notch targets. While the exact mechanism by which E6 affects Notch has yet to be determined, with much data contradicting each other, it seems that depending on the precise expression levels and cell environment (Henken et al., 2012), Notch, as deregulated by E6, can have growth promoting effects. Accordingly high expression of Notch1 has been shown to lead to growth arrest of cervical tumor-derived cells (Talora et al., 2002, Talora et al., 2005, Wang et al., 2007).

Gamma secretase is a membrane complex involved in cleaving single-pass type I transmembrane proteins (reviewed in (Strooper and Annaert, 2001)). One of the main substrates of the complex is the Notch receptor. Upon binding an active ligand the receptor is cleaved twice, with the second cleavage giving rise to the NICD that can subsequently move to the nucleus and activate transcription of downstream Notch targets (reviewed in (Borggrefe and Liefke, 2012)). The gamma secretase complex consists of four essential proteins; presenilin (PS), presenilin enhancer-2 (PEN-2), nicastrin (Nct) and anterior pharynx-defective-1 (APH-1) (reviewed in (Kaether et al., 2006)). In addition to a role in proteolytic activity, APH-1 promotes the assembly of all the components into the gamma secretase complex (Lee et al., 2004). Once it is fully formed the complex is activated through autocatalytic processing of PS-1, which is the

essential proteolytic component. The main role of both Nct and PEN-2 is to stabilize the whole assembled complex (Prokop et al., 2004, Zhang et al., 2005).

Another substrate of the gamma secretase complex is amyloid precursor protein (APP). Its cleaved product, amyloid beta (Aβ) (Selkoe, 2001), is processed abnormally in people with Alzheimer's disease and this is associated with amyloid plaques in their brain (Hardy and Allsop, 1991). Due to this condition being very widespread, several drugs and inhibitors against the gamma secretase complex have been developed to prevent the formation of amyloid plaques. Many of them do not distinguish between APP and other gamma secretase substrates, such as Notch, and therefore they can be used for studying signaling pathways that are not necessarily involved in Alzheimer's disease.

In this chapter I will address the roles of p53 degradation, the PDZ-binding motif and Notch signaling in promoting E6-dependent growth in a high cell-density environment.

5.2 Results

5.2.1 E6ΔPDZ- but not E6SAT-expressing cells grow slower than wild type E6-expressing cells

Having shown that E6 can induce cells to proliferate faster, I next wanted to determine what specific function(s) of E6 is involved in cell proliferation. The ability of high-risk E6 to degrade both p53 and several PDZ proteins has been characterized very well and shown to be important for the overall function of this protein. Thus I decided to first assess these two functions of E6 and determine whether they contribute to the enhanced cell proliferation observed in my cells.

I made two E6 mutant cell lines using LXSN retroviruses (Halbert et al., 1991); LXSN_E6SAT (8S9A10T mutant) is unable to bind to and bring about the degradation of p53 while LXSN_E6ΔPDZ (a truncated form of E6 with the ETQL PDZ-binding motif, located on the extreme C-terminus, cut off) cannot bind to and target PDZ proteins for degradation. The mutants were made by Lietta Nicolaides (NIMR) using site-directed mutagenesis in the wild type E6 retroviral LXSN vector. NIKS cells were infected and cells containing the retroviruses were selected with geneticin, in order to make stable cell populations. Pellets of confluent LXSN-, E6-, E7-, E6/E7-, E6SAT- and E6ΔPDZ-expressing cells were lysed using a RIPA buffer containing 6 % SDS, and these whole cell extracts were used in western blot analysis (Fig. 5.1A). Each population expresses the expected proteins. Predictably, E6ΔPDZ migrates slightly faster than wild type E6 due its truncated C-terminus. Moreover, it seems that the E6ΔPDZ protein is less abundant in cells than wild type E6 or E6SAT proteins. This can be explained by a recent study showing that the stability of the E6 protein is dependent on its PDZ motif (Nicolaides et al., 2011).

E6SAT- and E6ΔPDZ-expressing cells were cultured alongside E6-, E7- and E6/E7-expressing cells in a 9-day growth assay. Cells were counted at days 1, 3, 5 and 9 post-seeding to assess the differential growth phenotypes (Fig. 5.1B). As usual, I find that E6-expressing cells have the capacity to grow much quicker than E7-expressing and control cells, and that the cell population with both E6/E7 does not have a growth advantage over E6 only-expressing cells. While cells expressing E6SAT grow to the

same cell density as the wild type E6 population, E6ΔPDZ-expressing cells grow slower. However, the E6ΔPDZ population still grows much faster than cells expressing only E7 and control cells. Overall, this suggests that whereas the degradation of p53 by E6 does not affect growth, the PDZ binding motif may be involved in, but is not the sole contributor to E6-dependent enhanced proliferation. Due to the impaired stability of the E6ΔPDZ protein and its resultant lower levels within the cell, it is difficult to say for certain that this is the case.

These results suggest that there may be a further pathway(s) that E6 is regulating to bring about its effect on proliferation.

A.

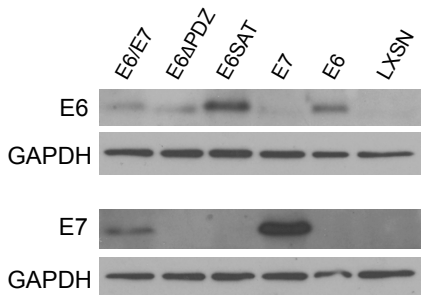

B.

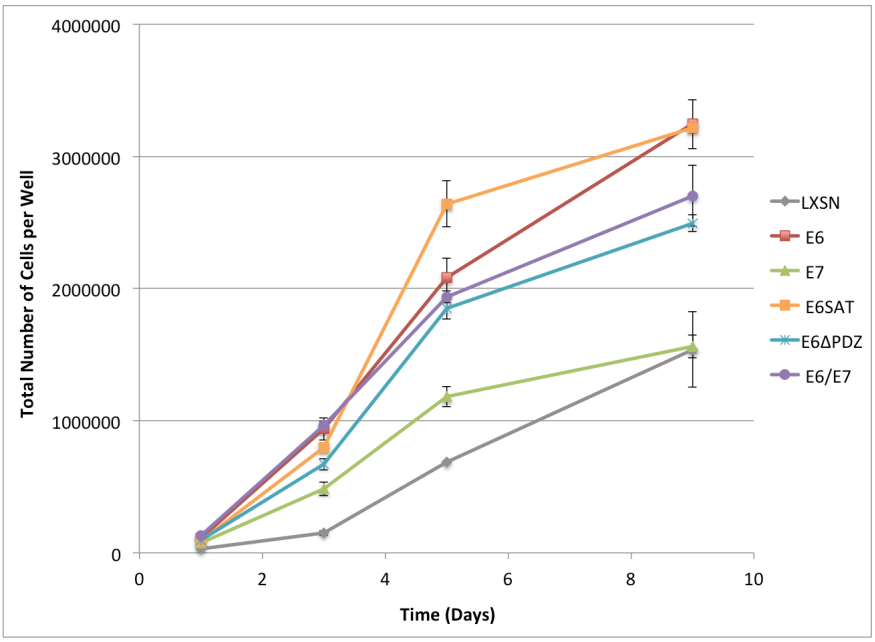

Figure 5.1: E6ΔPDZ- but not E6SAT-expressing cells grow slower than wild type E6-expressing cells

LXSN retroviruses were used to make stable NIKS cell populations expressing either an E6 8S9A10T mutant deficient for p53 degradation (E6SAT) or a truncated E6 mutant, with the ETQL PDZ-binding motif cut off, which is unable to bind and bring about degradation of PDZ proteins (E6ΔPDZ).

A) LXSN-, E6-, E7-, E6/E7-, E6SAT- and E6ΔPDZ-expressing cells were cultured to confluence, and lysed using a RIPA buffer containing 6 % SDS. Whole cell extracts were used to detect E6 and E7 by western blot.

B) The growth patterns of LXSN-, E6-, E7-, E6/E7-, E6SAT- and E6ΔPDZ-expressing cells were compared in a growth assay. Cells from duplicate wells were counted at days 1, 3, 5 and 9 post-seeding. The mean number of cells per 6-well plate well was plotted against the time in days. The error bars represent +/- the standard deviation of the duplicate wells.

5.2.2 The levels of NICD are lower in E6-expressing than control cells

In epithelial cells, Notch signaling is involved in regulating cell proliferation and differentiation. Levels of active Notch (NICD) increase when cells reach confluence, thereby initiating cell cycle arrest and the onset of terminal differentiation (reviewed in (Watt et al., 2008, Dotto, 2008)). As the LSIL- and HSIL-like growth phenotypes displayed by my cells are very much dependent on confluence, I decided to assess whether the Notch pathway is involved in mediating E6-dependent growth. I opted to use the LXSN populations first as with these cells an effect that is caused by E6, as opposed to other viral proteins, can be easily distinguished.

E6-expressing and LXSN control NIKS cells were cultured in a 9-day growth assay and counted at days 1, 3, 5, 7 and 9 to assess their differential proliferation patterns (Fig 5.2A). Cell pellets harvested in duplicate at each of the time-points were lysed using a RIPA buffer containing 6 % SDS. Whole cell extracts were used to assess the levels of p53, an inverse marker of E6 levels, and NICD by western blot (Fig. 5.2B).

As expected, the presence of E6 allows cells to proliferate to a much higher density than control cells, with the overall cell number at day 9 being almost 2-fold higher.

The western blot analysis has shown that while p53 is abundant in control cells it is undetectable in cells expressing E6. The levels of NICD are low for both populations at sub-confluence at day 3, high for both at confluence at day 5. They stay elevated in control cells at post-confluence at days 7 and 9 while the E6 population has no detectable levels of NICD at these time-points. These results are highly reproducible between the two replicates of each cell population at each time-point analyzed. It seems reasonable that NICD is undetectable when cells are sub-confluent, as current literature suggests that Notch signaling, which triggers NICD expression, is dependent on confluence (Kolly et al., 2005). Therefore it also makes sense that NICD levels are high for both cell populations at confluence. However, only E6-expressing cells are then able to repress NICD levels allowing proliferation to a much higher cell density.

Based on my work so far, I hypothesize that this differential regulation of Notch signaling may be involved in facilitating E6-mediated cell growth.

A.

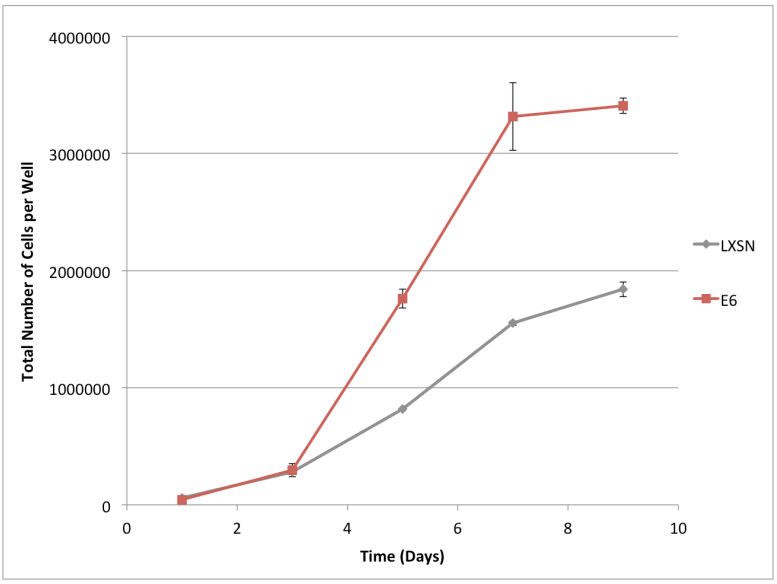

B.

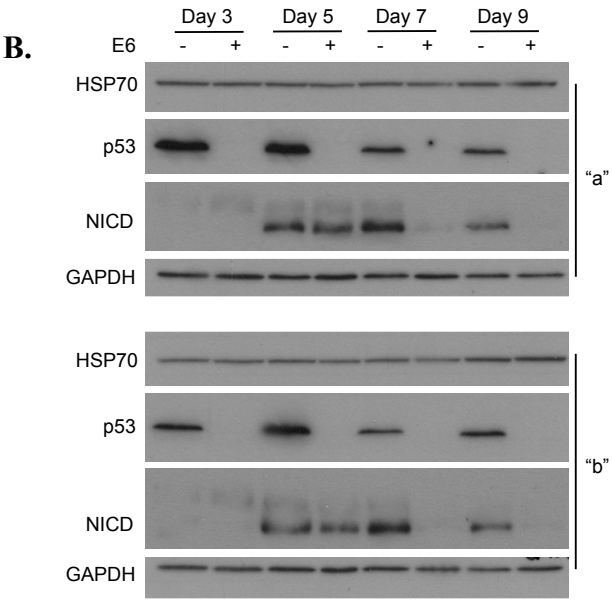

Figure 5.2: The levels of NICD are lower in E6-expressing than control cells

LXSN- and E6-expressing cells were cultured in a 9-day growth assay and counted at days 1, 3, 5, 7 and 9 to assess their differential proliferation patterns.

A) The average number of cells per 6-well plate well was plotted against the time in days. The error bars represent +/- the standard deviation of the duplicate wells.

B) Cell pellets harvested in duplicate at each of the time-points were lysed using a RIPA buffer containing 6 % SDS. Whole cell extracts were used to assess the levels of p53, used as an inverse marker of E6, and NICD by western blot. The pellets harvested from duplicate wells at each time-point, are represented by "a" and "b".

5.2.3 The levels of NICD are lower in HSIL-like cells than LSIL-like cells

Having found that E6 can disrupt NICD levels of the Notch pathway, I wanted to test if this effect would also be observed in the NIKS HPV16-expressing clonal cells. Based on my data, I hypothesized that LSIL-like cells would have higher levels of NICD than the HSIL-like clone from confluence onwards.

To this end, HSIL-like 1K and LSIL-like 2K cells were cultured in a growth assay format and counted at days 1, 3, 5, 7 and 9 to establish their patterns of proliferation (Fig 5.3A). Cell pellets harvested in duplicate at each of the time-points were lysed using a RIPA buffer containing 6 % SDS. Whole cell extracts were used to assess the levels of p53, an inverse marker of E6 levels, and NICD by western blot (Fig. 5.3B).

As usual, the cell lines diverge in terms of their proliferation pattern from the point of confluence at day 5 onwards, with the HSIL-like cells growing to a much higher cell density than the LSIL-like cells. NIKS grow to a much lower cell number, presumably due to absence of E6.

In accordance with this, the levels of p53 are consistently very high for NIKS, much lower for 2K and barely detectable for 1K. The levels of NICD are lowest in HSIL-like 1K cells at all time-points assessed. I interpret this to mean that, much like in E6-expressing cells, Notch signaling is repressed in 1K, leading to reduced NICD levels and rapid cell proliferation. Hence, this effect may be involved in giving rise to the HSIL-like phenotype. The low levels of NICD in NIKS at days 7 and 9, are probably reflective of their slower growth and the resulting overall lower cell density at all time-points as compared to the clonal HPV16-expressing cell lines. E7 levels are the same for 1K and 2K and are unchanging throughout the growth assay. This means that E7 is not involved in bringing about any aspect of the differential proliferation patterns observed.

All together my results suggest that E6 can down-regulate NICD levels and that this correlates with growth. Generally, the higher the levels of E6, the more repression of NICD can be measured.

A.

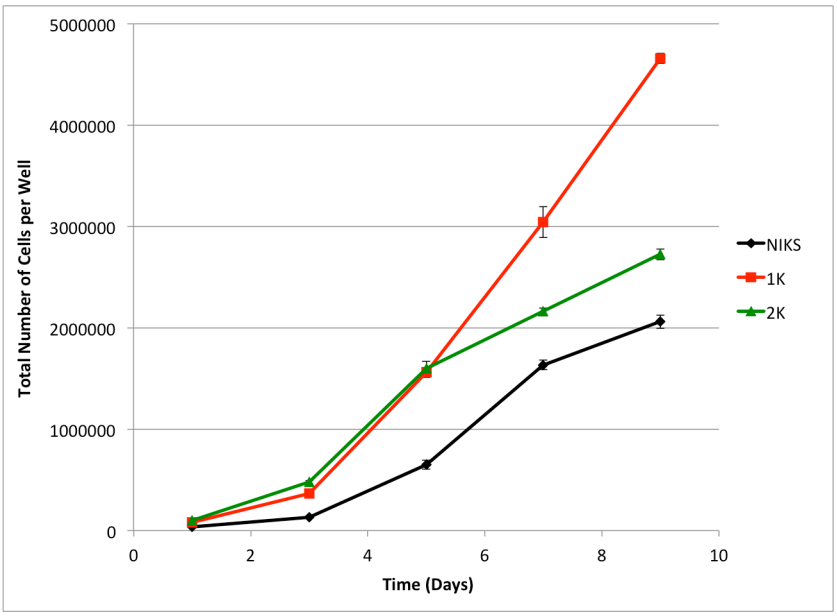

B.

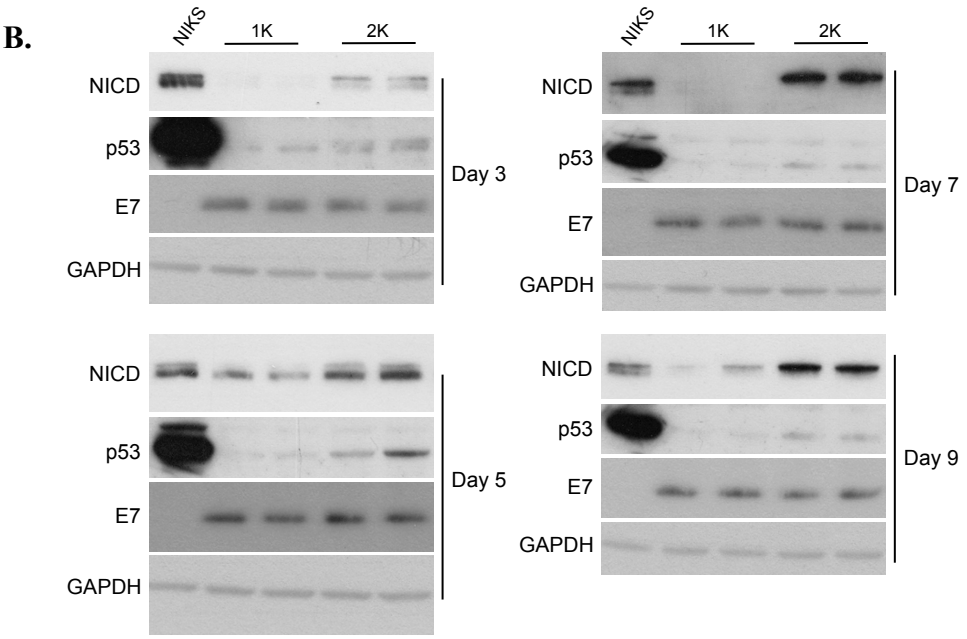

Figure 5.3: The levels of NICD are lower in HSIL-like cells than LSIL-like cells

NIKS, 1K and 2K cell lines were cultured in a 9-day growth assay and counted at days 1, 3, 5, 7 and 9 to assess their differential proliferation patterns.

A) The mean number of cells per 6-well plate well was plotted against the time in days. The error bars represent +/- the standard deviation of the duplicate wells.

B) Cell pellets harvested from duplicate wells at each of the time-points were lysed using a RIPA buffer containing 6 % SDS. Whole cell extracts were used to assess the levels of p53, used as an inverse marker of E6, E7 and NICD by western blot.

5.2.4 The p21 protein, a downstream effector of Notch signaling, is expressed at lower levels in HSIL-like cells than LSIL-like cells in an E6-dependent manner

The p21 protein is a cyclin-dependent kinase inhibitor that is a key regulator of cell cycle progression in G1 phase. It acts by inhibiting CDK1 and CDK2 and also by abrogating the activity of PCNA (reviewed in (Abbas and Dutta, 2009)). Due to its cytostatic effects, p21 also promotes terminal differentiation of cells. Notch1 can stimulate p21 expression by binding of RBPJ directly to the p21 (*CDKN1A* gene) promoter (Rangarajan et al., 2001b). I hypothesized that low levels of NICD, mediated by the presence of E6 in my cells would result in diminished p21 levels, and hence that E6 could promote cell growth by indirectly inhibiting p21 via Notch.

To determine whether E6-induced repression of Notch signaling has a corresponding effect on p21 levels, I assessed p21 levels in my cells by western blot. I used the whole cell extracts prepared in Section 5.2 for LXSN- and LXSN_E6 cells and in Section 5.3 for NIKS, 1K and 2K clonal cell line (Fig 5.4A and B, respectively).

For LXSN control cells, the levels of p21, although generally very low and hard to detect, are consistently higher throughout the time-course than for cells expressing E6.

For parental NIKS, p21 levels are higher at sub-confluence at day 3 and confluence at day 5 but seem to be lower at post-confluence at days 7 and 9 than for both 1K and 2K cell lines. These different kinetics in protein expression are reflective of the slower rate of proliferation of NIKS and the resulting overall lower cell density at all time-points as compared to both clonal HPV16-expressing cell lines. More importantly, the levels of p21 are much lower for HSIL-like 1K cells than for LSIL-2K cells at days 3 and 5. At days 7 and 9 the levels are the same for both clones.

My results confirm that p21 levels are diminished in the presence of E6. However, the kinetics of p21 levels during the time course do not fit with my hypothesis that this protein is regulated solely by Notch signaling. In Figure 5.2B I showed that the levels of NICD between E6-expressing and control cells are only different at days 7 and 9. Here I showed that p21 levels are different from day 3 onwards. For the clonal cell lines, I observed in Figure 5.3B that NICD levels are consistently lower for 1K than for 2K at all time-points, yet p21 levels assessed here are only different at days 3 and 5.

The data seem to suggest that low levels of p21, mediated by E6, are not necessary to allow cells to continue growing after reaching confluence. Nevertheless, p21 inhibition may be involved in promoting sub-confluent proliferation, as cells with lower levels of p21 grow faster than cells with higher levels at the beginning of the growth assay. Hence, I propose that differences in p21 levels may allow E6-expressing cells and 1K and 2K clonal lines to grow faster than their respective LXSN and NIKS control cells. However, the growth differences between 1K and 2K, which give rise to the LSIL- and HSIL-like phenotypes, are mediated by a different mechanism that may involve repression of Notch signaling.

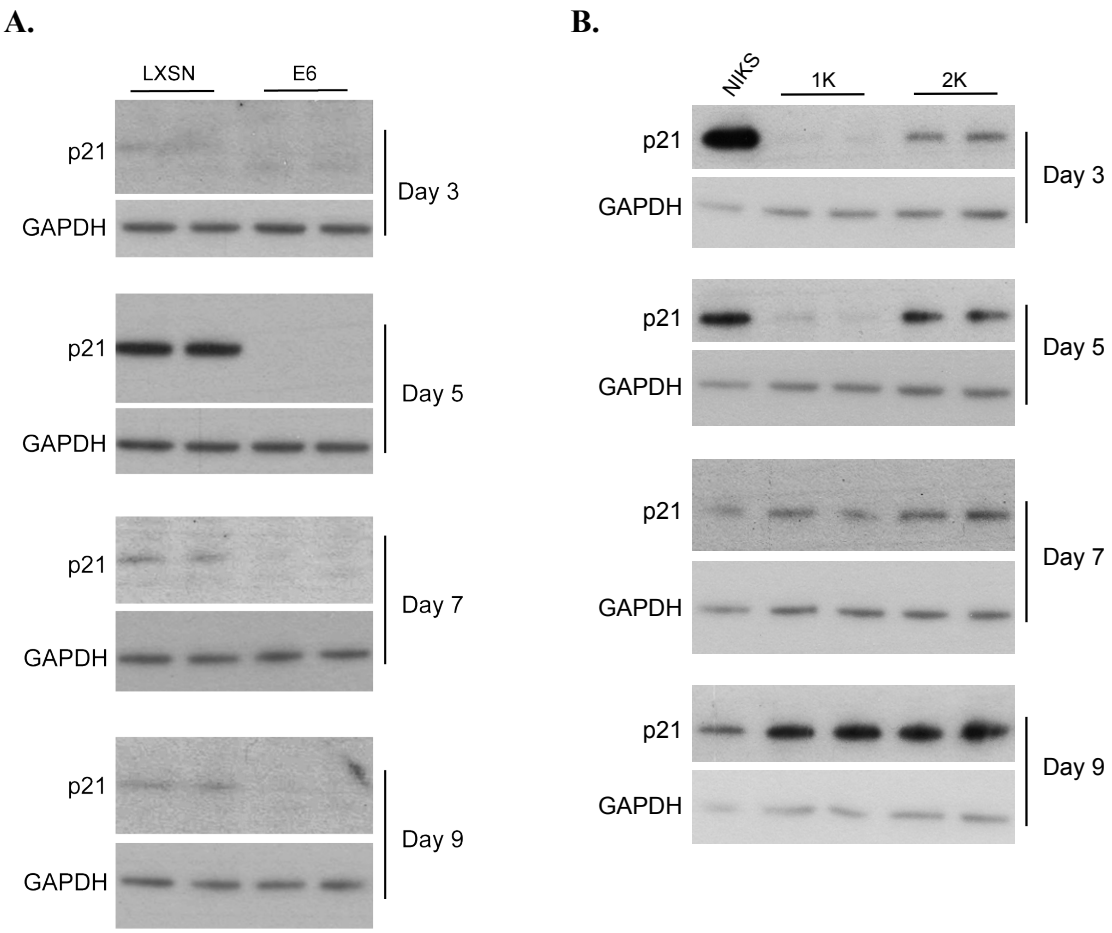

Figure 5.4: The p21 protein, a downstream effector of Notch signaling, is expressed at lower levels in HSIL-like cells than LSIL-like cells in an E6-dependent manner
LXSN- and E6-expressing cells **(A)** and NIKS, 1K and 2K cell lines **(B)** were cultured in a 9-day growth assay. Cell pellets were harvested in duplicate at days 1, 3, 5, 7 and 9 and lysed using a RIPA buffer containing 6 % SDS. Whole cell extracts were used to assess the levels of p21 by western blot.

5.2.5 The effects of E6 on p21 levels are Notch-independent and are not involved in cell growth at a high density

In the previous section I showed that p21 may be involved in regulating proliferation of cells. I wanted to further analyze whether E6 disruption of Notch signaling affects p21. NICD forms a complex with, amongst other proteins, RBPJ and MAML1, and directly binds to the p21 (*CDKN1A* gene) promoter (Rangarajan et al., 2001b) to activate its transcription.

To test this, I seeded 1K and 2K cells in growth assay format and harvested cells from duplicate wells at sub-confluence at day 3 and post-confluence at day 7. Pellets were used for RNA extraction and subsequent RT-qPCR to analyze the levels of p21 mRNA. Figure 5.5Ai and ii show the results of my analyses at day 3 and day 7, respectively. The data suggest that at both sub- and post-confluence the levels of p21 are not different between HSIL-like 1K and LSIL-like 2K cells. These results further suggest that p21 is not regulated by NICD-dependent direct transcriptional activation via E6.

To further investigate whether E6 can, in fact, affect p21 independently of Notch I decided to use a gamma secretase inhibitor (GSI). Upon binding of a ligand from an adjacent cell, the Notch receptor protease cleavage site is exposed. This allows it to be cleaved by ADAM-proteases, which subsequently leads to an intracellular cleavage by the gamma secretase complex (reviewed in (Borggrefe and Liefke, 2012)). This second proteolytic cleavage event ultimately gives rise to the NICD. Treating cells with a GSI inhibits this cleavage and, hence, leads to reduced NICD levels. I hypothesized that in this situation, if p21 is a downstream effector of Notch signaling, I would find low p21 levels, as NICD activity would be necessary to activate its expression. However, if p21 was regulated by E6 independently of the Notch pathway, then I would expect to see that p21 is expressed normally, even in the absence of NICD.

E6-expressing and LXSN control cells were seeded in 6-well plates in a growth assay format and grown to confluence at day 5. As induction of Notch signaling seems to occur primarily from the point of confluence, growing cells to this point is an important aspect of the experiment. Subsequently, cells were treated with 10 μM DAPT or an equivalent volume of DMSO for 24 hours, and then harvested. Cell pellets were lysed using a RIPA buffer containing 6 % SDS and subsequently the levels of NICD and p21

were assessed by western blot (Fig. 5.5B). As hypothesized, both NICD and p21 are high in LXSN cells treated with just DMSO. After treatment with DAPT the levels of NICD are diminished, yet p21 levels remain as high as in control cells. For E6-expressing cells treated with DMSO the levels of both NICD and p21 are much lower generally than in LXSN cells. Treatment with DAPT results in even lower NICD levels. Yet, as with LXSN cells, the levels of p21 are not affected. The observation that after DAPT treatment NICD levels are diminished without a corresponding reduction in p21 levels, further suggests that p21 is not predominantly regulated by E6 via Notch signaling in these cells. However, in both the LXSN population and clonal cell line model systems, p21 protein levels are lower for fast-growing cells with high levels of E6 (Fig. 5.4A and B). As p21 levels do correlate with enhanced proliferation, I speculated that E6 may be involved in post-translational regulation of p21.

In Section 5.2.1 I showed that cells expressing the E6SAT mutant are deficient for p53 degradation and that they can grow to a high density. The data in the previous section suggest that diminished p21, mediated by E6, seems to be involved in promoting cell growth in general. If low p21 levels are in fact a requirement for proliferation I would expect that E6SAT-expressing cells could bring about degradation of p21 in a p53-independent manner. I wanted to determine whether high cyclin A levels (shown in Chapter 3 to correlate with E6-dependent proliferation) are involved in promoting proliferation in E6SAT-expressing cells. Based on my results and current literature, I hypothesized that these cells can degrade p21 as this is necessary to promote high levels of cyclin A and thus proliferation.

To this end LXSN-, E6-, E6SAT- and E6ΔPDZ-expressing cells were cultured to post-confluence at day 7. Cell pellets were harvested and subsequently lysed using a RIPA buffer containing 6 %SDS. Whole cell extracts were used to assess the levels of cyclin A, p21 and p53, an inverse marker of E6, by western blot (Fig. 5.5C). The protein analysis shows that the levels of p53 are high in LXSN and E6SAT-expressing cells and much lower in cells with wild type E6 or E6ΔPDZ. The levels of p21 are high in cells with E6SAT and undetectable in the other cell populations. Furthermore, cyclin A levels are undetectable in E6 SAT-expressing cells and abundant in all other cells. These results suggest that in the E6-expressing cells p21 regulation is brought about in a p53-dependent manner. However, degradation of p21 and high levels of cyclin A appear

not to be necessary for cells to grow rapidly post-confluence, as E6SAT cannot bring about either of them, but can still drive cells to grow to as high of a density as cells with wild type E6 (shown in Section 5.2.1). Additionally, the fact that even LXSN control cells have high levels of cyclin A but are still associated with slow proliferation shows that the growth of my cells in these conditions is not dependent on cyclin A activation.

All in all, the experiments in this section have shown that p21 is not a direct effector of E6-dependent Notch signaling and that its repression is not essential in allowing growth post-confluence. This is in stark contrast to the Shai *et al.* study (discussed in Section 3.3) where the authors proposed that E6 represses p21 by inactivating p53 to bring about growth. Additionally, to complement my findings at the end of Chapter 3 and those of Malanchi *et al*. in 2002 and 2004 in fibroblasts, I have extended my knowledge and have shown that high cyclin A levels are dependent on the down-regulation of p53. This is supported by published data showing that cyclin A is inhibited by p53 (Yamamoto et al., 1994). Additionally, it seems that cyclin A is not involved in driving the growth of NIKS at a high cell density. As cyclins are known to be able to compensate for one another (Geng et al., 1999, Masamha and Benbrook, 2009), I propose that the low cyclin A levels measured here in E6SAT-expressing cells may indicate that other cyclins are present in high levels to promote cell cycle progression and proliferation.

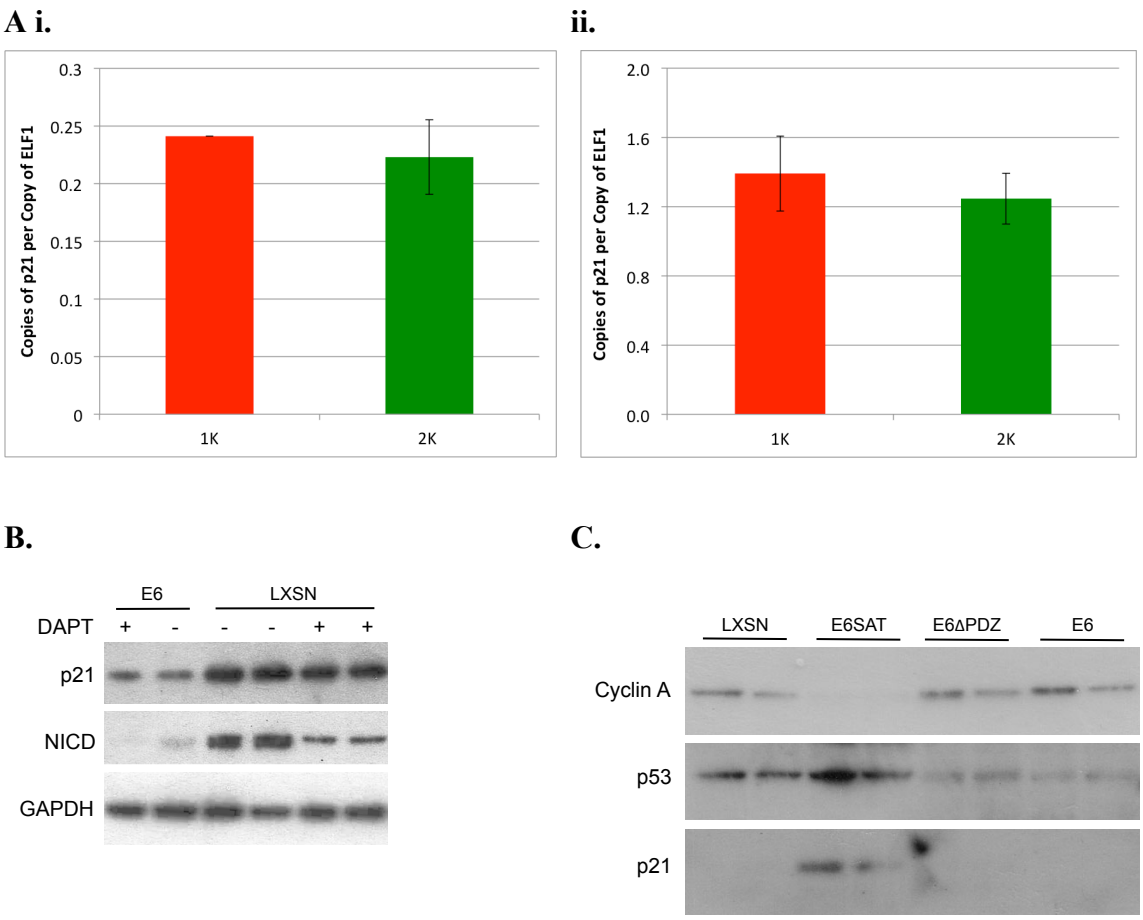

Figure 5.5: The effects of E6 on p21 levels are Notch- independent and are not involved in cell growth at a high density

A) 1K and 2K cells were cultured in a growth assay format and harvested in duplicate at sub-confluence at day 3 **(i)** and post-confluence at day 7 **(ii)**. Subsequently RNA was extracted, RT-qPCR carried out and the levels of p21 mRNA assessed relative to ELF1. The error bars represent the standard deviation of duplicate wells.

B) E6-expressing and LXSN control cells were seeded in 6-well plates in a growth assay format and grown to confluence at day 5. Cells were treated with 10 μM of the gamma secretase inhibitor DAPT or DMSO for 24 hours and then harvested. Cell pellets were lysed using a RIPA buffer containing 6 % SDS and subsequently the levels of NICD and p21 were assessed by western blot.

C) LXSN-, E6-, E6SAT- and E6ΔPDZ-expressing cells were cultured to post-confluence at day 7. Cells pellets were harvested and subsequently lysed using a RIPA buffer containing 6 %SDS. Whole cell extracts were used to assess the levels of cyclin A, p53 and p21 by western blot.

5.2.6 Use of RNAi to knock-down Notch1 or gamma secretase is unsuccessful in LSIL- and HSIL-like cells

Much of my work in this chapter to this point has focused on establishing that Notch signaling is disrupted by E6 and that this is necessary to allow cells to grow rapidly. Here I wanted to test whether reducing the expression levels of genes involved in Notch signaling would have a similar effect to knocking down E6/E7 using siRNA, as described in Section 4.2.12. In that section I found that a reduction in E6/E7 levels has a big negative effect on overall proliferation of NIKS. By only reducing the levels of members of the Notch pathway, I hypothesized that cells would only gain a growth advantage after reaching confluence, and thereby confirm that Notch signaling is specifically involved in allowing cells to grow in a high cell density environment. Hence, I speculated that by treating LSIL-like 2K cells with shRNA targeting the Notch pathway, these cells could grow to a density similar to that associated with 1K.

I ordered commercially available TRC lentiviral shRNA vectors targeting either Notch1 or both the APH-1α and PS-1 subunits of the gamma secretase complex. I also acquired an shGFP vector to use as a control during my experiment. I transfected 293TT cells with appropriate packaging and lentiviral vectors, and harvested viruses 48 hours later. The virus mix was used to directly infect 2K cells. After antibiotic selection, cells were seeded in 6-well plates for a 9-day growth assay and counted in duplicate at each time-point to assess differential proliferation patterns (Fig 5.6A). As usual, the normal HSIL-like 1K and LSIL-like 2K growth phenotypes become apparent from the point of confluence at day 5 onwards. Both 2K shγ-secretase- and 2K shNotch-expressing cells can grow faster than the wild type 2K clone. However, shGFP-treated cells can grow even faster, suggesting that this enhanced proliferation effect is a consequence of the infection and/or selection process and not the knock-down of Notch1 or gamma secretase. Additionally, both 2K shγ-secretase- and 2K shNotch-treated cells seem to have a growth advantage even at early time-points. As Notch pathway repression should result in fast growth only from the point of confluence onwards, this observation further suggests that the rapid proliferation is a side effect of my experiment and not a direct result of attenuating Notch signaling. All in all, my attempt to reduce the levels of Notch1 and gamma secretase in LSIL-like 2K cells has been unsuccessful.

Looking back over some of my old data I realized that I generally seem to observe this adverse effect on proliferation when using antibiotics to select cells after transfection or infection (Fig. 5.6Bi-iii). The shNT control cell populations used in the growth assay in Figure 5.6Bi were made in Section 4.4, when I tried to knock-down E6 levels using custom-made shE6 lentiviruses. The 1K and 2K cells with LXSN in Figure 5.6Bii were originally used as controls for the experiment in Section 4.5 where I tried to increase the levels of E6 in the clonal cell lines by infecting them with LXSN_E6 retroviruses. And the cells assessed in terms of their proliferation in Figure 5.6Biii where made as controls as part of the experiments in Sections 4.6 and 4.7 when I over-expressed E6 in 2K cells using pMV11 and pcDNA3.1 vectors.

The enhanced growth of these cells seems to result from the experimental procedure. To make the populations used in the various growth assays in Figure 5.6B, cells were both infected and transfected and selected with either puromycin or geneticin. Hence, I speculate that these fast-growing populations may be selected while treating cells with antibiotics. As I generally have to select cells for 7 to 10 days, due to the nature of NIKS cells, it seems reasonable that in this time fast cells, that are not adversely affected by the antibiotics, have a chance to outgrow slower cells that are struggling to survive. Based on my findings so far I propose that the cells that are outgrowing during the selection process have high E6 levels and that, as a result of this, the viral genomes may have integrated in host cell chromosomes.

A.

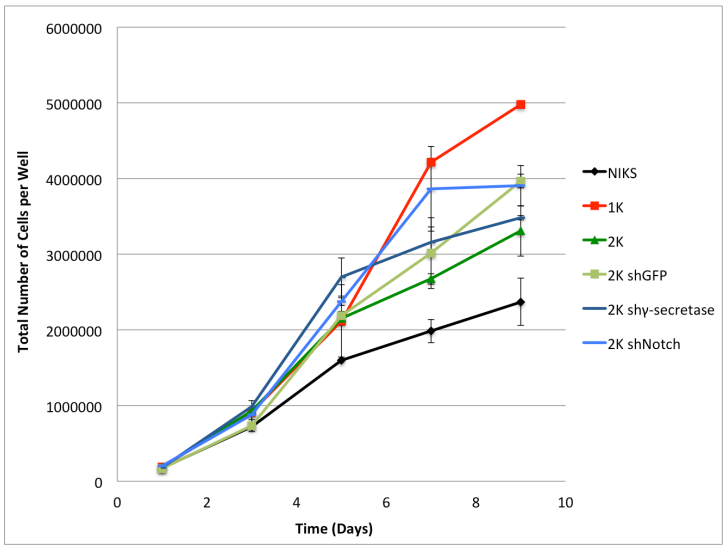
6000000
5000000
4000000
3000000
2000000
1000000
0
Total Number of Cells per Well
0
2
4
6
8
10
Time (Days)
NIKS
1K
2K
2K shGFP
2K shy-secretase
2K shNotch

B i.

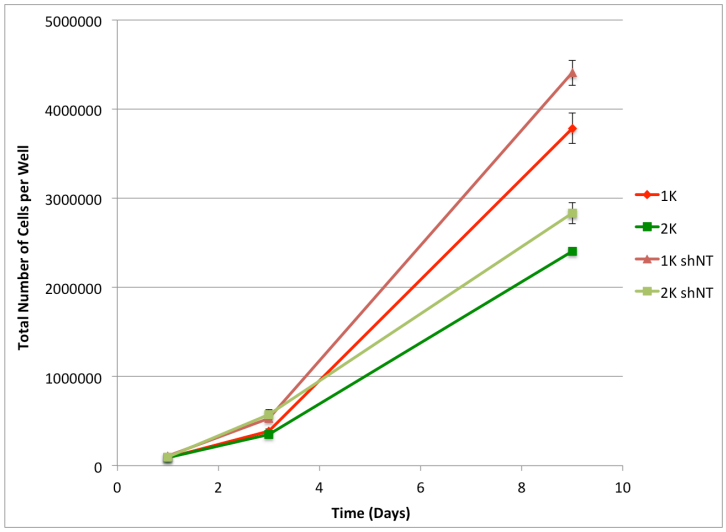
5000000
4000000
3000000
2000000
1000000
0
Total Number of Cells per Well
0
2
4
6
8
10
Time (Days)
1K
2K
1K shNT
2K shNT

ii.

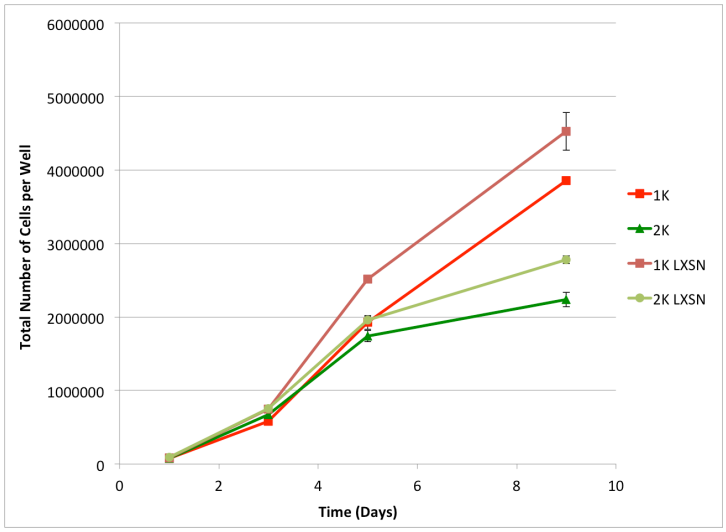
6000000
5000000
4000000
3000000
2000000
1000000
0
Total Number of Cells per Well
0
2
4
6
8
10
Time (Days)
1K
2K
1K LXSN
2K LXSN

iii.

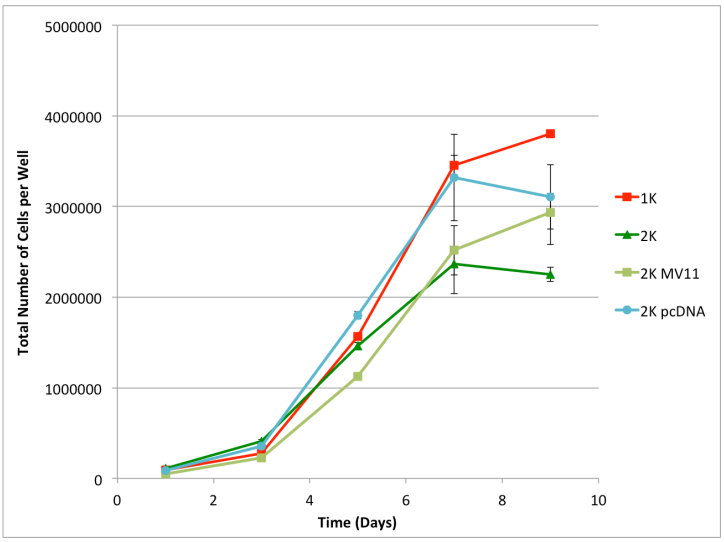

Figure 5.6: Use of RNAi to knock-down Notch1 or gamma secretase is unsuccessful in LSIL- and HSIL-like cells

A) NIKS, 1K, 2K and 2K shGFP-, 2K shNotch- and 2K shγ-secretase-expressing cells were counted in duplicate at days 1, 3, 5, 7 and 9 post-seeding and compared in terms of their growth phenotypes. The average number of cells per 6-well plate well was plotted against the time in days. The error bars represent +/- the standard deviation of the duplicate wells.

B i-iii) Growth assays using control cells originally made in previous transfection or infection experiments, that involved an antibiotic selection step, were reanalyzed in terms of their rate of proliferation. The average number of cells per 6-well plate well was plotted against the time in days. The error bars represent +/- the standard deviation of the duplicate wells.

i) 1K and 2K cells were infected with shRNA lentiviral particles. 1K, 1K shNT, 2K and 2K shNT cells were counted in duplicate at days 1, 3, 5, 7 and 9 post-seeding.

ii) LXSN_E6 retroviruses were used to infect 1K and 2K clonal cell lines. 1K, 1K LXSN, 2K and 2K LXSN cells were compared in a 9-day growth assay. Cells from duplicate wells were counted at days 1, 3, 5, 7 and 9 post-seeding.

iii) 2K cells were transfected with linearized pcDNA3.1 or pMV11. 1K, 2K, 2K MV11 and 2K pcDNA were counted in duplicate at days 1, 3, 5, 7 and 9 post-seeding.

5.2.7 Treating LSIL- and HSIL-like cells with DAPT results in a collapse of the differential growth phenotypes

The use of shRNA to reduce Notch signaling in the cells has proven unsuccessful. However, I still felt that it was very important to establish if Notch is specifically involved in allowing cells to overcome contact inhibition. Therefore I decided to use a different approach to manipulate Notch signaling. DAPT, the GSI used in Section 5.2.5, inhibits the final cleavage of the Notch receptor that gives rise to NICD. I speculated that by treating cells with DAPT to block NICD formation, I would see a corresponding positive growth effect.

When using DAPT I treat control cells with DMSO. NIKS suffer considerably when DMSO is present and therefore I decided to use my short growth assay format (for assessing the effect of DAPT on cell growth) so as to reduce the exposure time to the treatment. The short growth assay was fully optimized for NIKS, 1K and 2K in Section 4.12. However, I also wanted to treat the LXSN populations with DAPT/DMSO during a time-course. Hence I decided to optimize the short growth assay conditions for the LXSN populations. To do this, I seeded $6x10^5$ LXSN- and LXSN_E6-expressing cells. At day 1 I counted cells to check their seeding efficiency. At days 2, 4 and 6 I counted cells to assess their growth patterns (Fig 5.7Ai). These time-points should equate to days 5, 7 and 9, respectively, in my normal time-courses. A bar chart showing fold-increase relative to the previous time-point is shown in Figure 5.7Aii.

The data show that, as normal, control and E6-expressing cells start to diverge in terms of their growth from day 1 onwards. At the end of a normal growth assay, I generally see a 2-fold difference in cell number between LXSN- and E6-expressing cells. In this format, the difference is slightly less but still very big. The bar chart shows that at day 2, cells with E6 have increased their numbers much more than the control cells. Same as wild type NIKS, NIKS with LXSN take longer to recover from the seeding process and therefore only start to grow rapidly from day 2 onwards. Hence, the increase in LXSN control cell numbers is bigger than for E6-expressing cells prior to the last time point, although overall the latter can grow to a much higher cell density. Between days 1 and 6 LXSN have increased their total cell number 2.5-fold whilst E6-expressing cells have have done so 5-fold. This means that all in all, E6-expressing cells have reached a 1.8-fold higher cell density than LXSN control cells. The data are an average of 7

individual experiments. Unpaired s were used to compare LXSN and E6 cell numbers at each time-point. There are significant differences between them at confluence at day 2 and post-confluence at days 4 and 6 with p values of 0.0043, 0.0005 and 0.0002, respectively.

I hypothesized that, if repression of Notch signaling by E6 is indeed involved in driving proliferation, then inhibition of the gamma secretase complex (by using DAPT) and the resulting low levels of NICD would promote faster cell growth. I expected this effect to be bigger in control cells without E6 as the NICD levels here are much higher to begin with. Hence, I predicted that DAPT would only have a minor positive effect on the growth of cells that express high levels of E6, such as LXSN_E6 and HSIL-like 1K cells. In contrast, the growth of cells expressing little or no E6, such as LSIL-like 2K and NIKS or LXSN cells, respectively, would be enhanced considerably. Based on this, I further hypothesized that use of DAPT would result in a collapse of the LSIL- and HSIL-like growth phenotypes as all cells would be able to grow to a high density due to the presence of DAPT.

To test my theory I seeded LXSN- and LXSN_E6-expressing cells and in parallel NIKS, 1K and 2K in a short growth assay. From the day after seeding onwards cells were treated with 10 μM of DAPT or DMSO that was replaced every 24 hours. Cells are normally only given fresh FC medium (with EGF) every second day of the short growth assay (on days 2, 4, and 6). To allow me to change the medium every day, and thereby replace the DMSO or DAPT, I prepared conditioned medium for the changes at days 3 and 5 to ensure that the growth conditions, in terms of growth factor concentrations, throughout the experiment remained consistent. The cells were counted in duplicate at days 1, 2, 4 and 6 to assess their differential proliferation patterns. The results are shown in Figure 5.7B and C for LXSN and E6-expressing cell populations and NIKS, 1K, and 2K cell lines, respectively.

Surprisingly, treating cells with DAPT has a huge negative impact on their growth. The effect of DAPT seems to be much bigger for the E6-expressing population as compared to the one without. Due to this, E6-expressing cells treated with the drug can grow at a comparable rate to untreated LXSN cells. DAPT works on the gamma secretase complex, which is involved in negatively regulating cell growth through Notch

signaling at a high cell density. Hence, this difference in the effect of the drug is presumably caused by the fact that E6 allows cells to proliferate rapidly and reach confluence more quickly. This means that while DMSO-treated E6-expressing cells grow to a density that is almost 2-fold higher than that of LXSN cells, this difference is only approximately 1.4-fold for DAPT-treated cells. For the clonal cell lines I see a similar negative effect on growth with DAPT. While untreated 1K and 2K diverge from day 2 onwards to give rise to their normal HSIL- and LSIL-like growth phenotypes, DAPT-treated 1K and 2K do not diverge significantly throughout the time-course. These cells now grow to an overall density that is only slightly higher than that of untreated NIKS. Similarly to the LXSN populations, the effect of DAPT is bigger for cells with higher levels of E6.

The results of the DAPT growth assays are unexpected. My hypothesis that the 1K and 2K growth phenotypes will collapse holds true. I also see a similar effect for LXSN and E6-expressing cells. However, I hypothesized that the effect of the drug may be smaller for cells with high levels of E6 as they have lower NICD levels to begin with; I have observed the opposite here. The biggest surprise is that according to my hypothesis DAPT-treated cells should grow to a higher, not lower, cell density than their untreated counterparts.

Other members of my laboratory have found that DMSO has effects on the expression of viral proteins, such as E4, in NIKS (personal communication with Clare Davy and Qian Wang; NIMR, London, UK). I speculate that DMSO could be having effects on the expression levels of not only viral but also cellular proteins and that this may be causing these unforeseen effects. For this reason I have decided to re-optimize the conditions of this experiment.

A i.

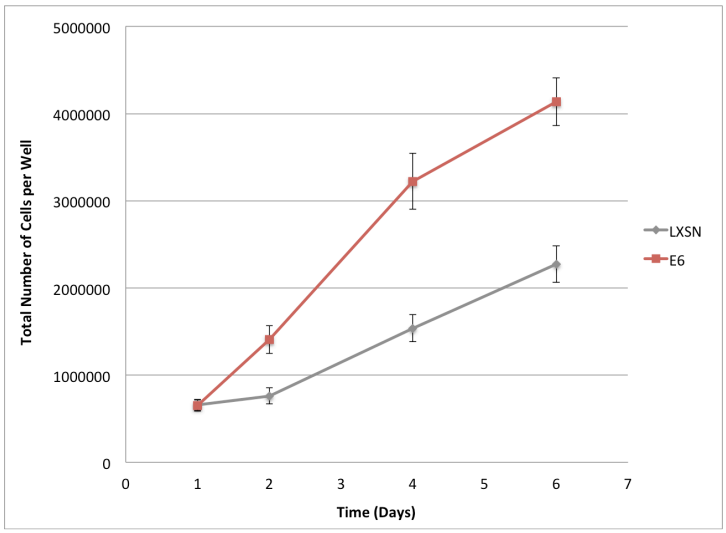
5000000
4000000
3000000
2000000
1000000
0
Total Number of Cells per Well
0
1
2
3
4
5
6
7
Time (Days)
LXSN
E6

ii.

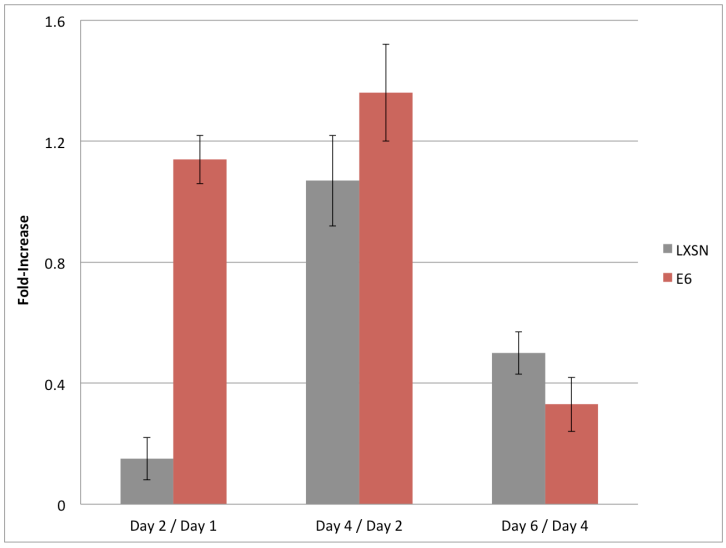
1.6
1.2
0.8
0.4
0
Fold-Increase
Day 2 / Day 1
Day 4 / Day 2
Day 6 / Day 4
LXSN
E6

B.

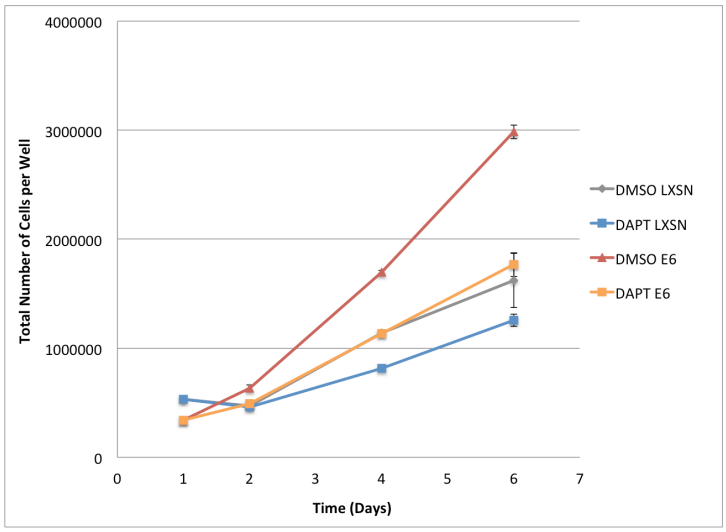
4000000
3000000
2000000
1000000
0
Total Number of Cells per Well
0
1
2
3
4
5
6
7
Time (Days)
DMSO LXSN
DAPT LXSN
DMSO E6
DAPT E6

C.

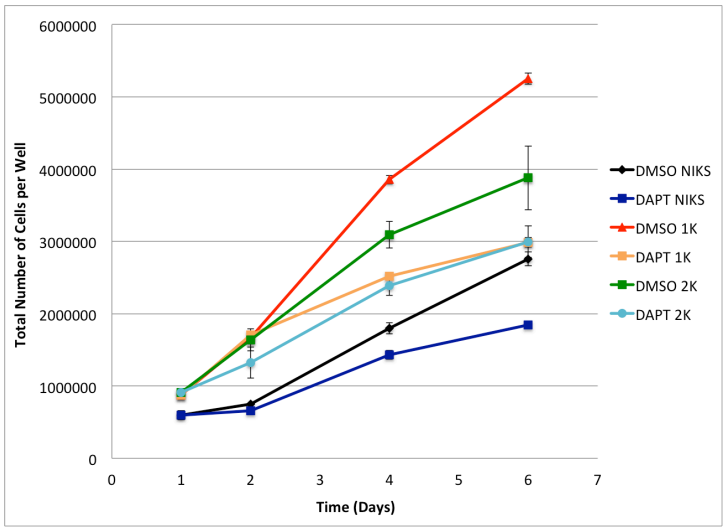

Figure 5.7: Treating LSIL- and HSIL-like cells with DAPT results in a collapse of the differential growth phenotypes

A) E6-expressing and LXSN control cells were seeded at a high density ($6x10^5$) in 6-well plates and counted in duplicate at days 1, 2, 4 and 6 post-seeding. Day 2 corresponds to confluence at day 5 of a normal growth assay while days 4 and 6 correspond to post-confluence at days 7 and 9. Cells were compared in terms of their growth phenotypes.

i) The average number of cells per 6-well plate well was plotted against the time in days. The error bars represent +/- the standard error of 7 individual experiments. Unpaired t-tests were used to compare LXSN- and E6-expressing cell numbers at each time-point. The p values at day 2, 4 and 6 are 0.0043, 0.0005 and 0.0002, respectively.

ii) Fold-increase relative to the previous time-point was calculated and plotted in a bar chart. The error bars represent +/- the standard error of 7 individual experiments. A short growth assay was done with LXSN- and E6-expressing cells **(B)** or NIKS, 1K and 2K **(C)**. From day 1 onwards cells were treated with 10 μM of DAPT or DMSO that was replaced every 24 hours. Cells were counted in duplicate at days 1, 2, 4 and 6 post-seeding and compared in terms of their growth phenotypes. The average number of cells per 6-well plate well was plotted against the time in days. The error bars represent +/- the standard deviation of the duplicate wells.

5.2.8 Treating cells with DAPT dissolved in ethanol brings about a negative effect on growth

In the previous section I postulated that the growth inhibitory effect of DAPT on all my cells may be a brought about by the presence of DMSO as opposed to being a direct effect of the drug itself. To resolve the issue I decided to repeat the experiment using DAPT dissolved in ethanol.

To this end I seeded LXSN- and E6-expressing cells and in parallel NIKS, 1K and 2K in a short growth assay. From the day after seeding onwards cells were treated with 10 μM of DAPT or ethanol that was replaced every 24 hours. Similarly to the growth assays in the previous section I used conditioned media to feed cells on days 3 and 5 to ensure that the growth conditions throughout the experiment remained consistent. The cells were counted in duplicate at days 1, 2, 4 and 6 to assess their differential proliferation patterns. The results are shown in Figure 5.8A and B for LXSN and E6-expressing cell populations and NIKS, 1K, and 2K cell lines, respectively.

Even when dissolved in ethanol, DAPT has a negative effect on the growth of all the cells. Once again, the effect of the drug is bigger for E6-expressing than LXSN cells due to the former being able to grow to a higher cell density. Hence, while DAPT-treated LXSN cells show the same growth pattern as untreated cells, untreated E6-expressing cells have increased their numbers 1.5-fold more than DAPT-treated ones. For 1K and 2K clones I see the normal HSIL- and LSIL-like growth phenotypes. After treatment with DAPT the difference between 1K and 2K is slightly diminished. As found previously, the growth effect of the drug is bigger for 1K than for 2K.

The data here suggest that the growth inhibitory effect of DAPT is caused by the drug itself as opposed to what it is dissolved in. Looking through the literature I have found that DAPT does not specifically block the Notch receptor cleavage function of gamma secretase, but that it is an inhibitor of the complex on the whole. I speculate that DAPT may be inhibiting other functions of gamma secretase and that this is bringing about the unexpected growth effects observed in the growth assays.

A.

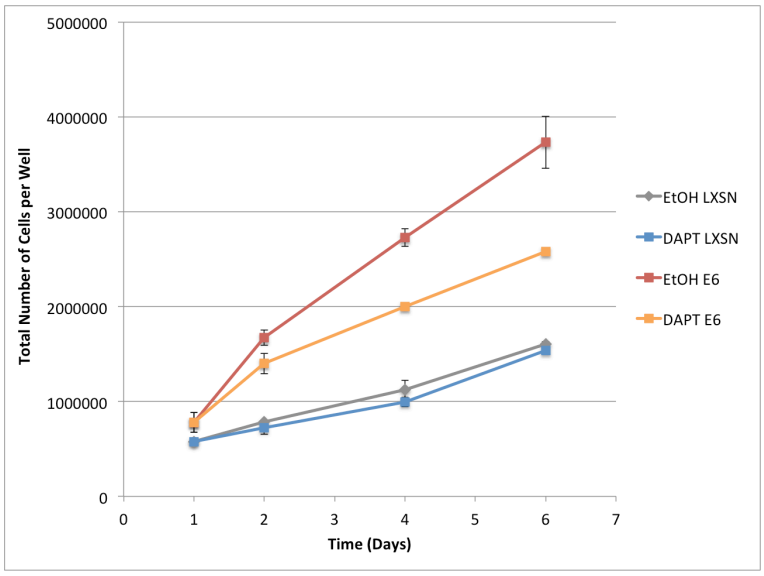

B.

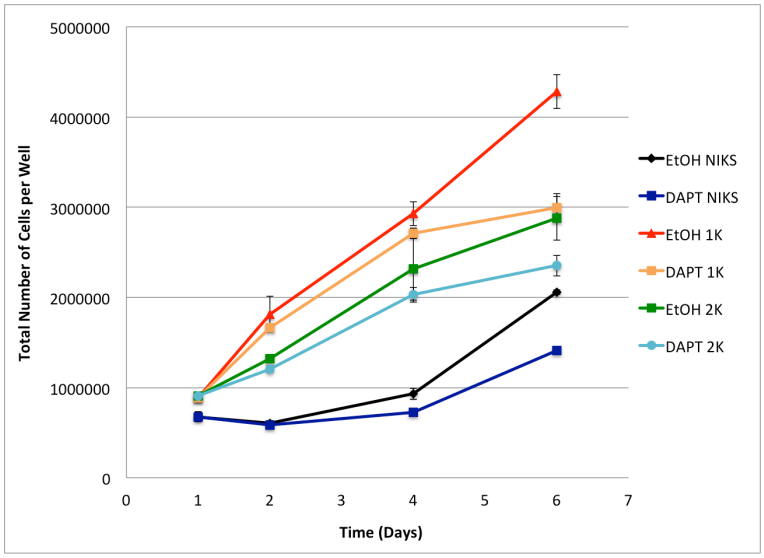

Figure 5.8: Treating cells with DAPT dissolved in ethanol brings about a negative effect on growth

A short growth assay was done with LXSN- and E6-expressing cells **(A)** or NIKS, 1K and 2K **(B)**. From day 1 onwards cells were treated with 10 µM of DAPT or ethanol that was replaced every 24 hours. Cells were counted in duplicate at days 1, 2, 4 and 6 post-seeding and compared in terms of their growth phenotypes. The average number of cells per 6-well plate well was plotted against the time in days. The error bars represent +/- the standard deviation of the duplicate wells.

5.2.9 Treating cells with R04929097 brings about a negative effect on growth

My work using the gamma secretase inhibitor DAPT has shown that the drug has a growth inhibitory, as opposed to growth promoting effect on NIKS cells. DAPT is a general inhibitor of the gamma secretase complex, not just its Notch receptor cleavage function. A well-known substrate of gamma secretase is amyloid precursor protein (APP). In Alzheimer's disease, cleaved amyloid beta (Aβ) is processed abnormally and its accumulation is associated with the amyloid plaques in the brain (Hardy and Allsop, 1991). Furthermore, presenilin-1 (PS-1), one of the subunits of the gamma secretase complex, has been implicated in Wnt/β-catenin signaling. PS-1 can bind to β-catenin and bring about its phosphorylation and subsequent degradation (Kang et al., 2002). β-catenin is a transcription factor that is a key component of the Wnt pathway. Canonical Wnt pathway activation, which leads to the formation of the active β-catenin transcription complex, has been associated with HPV-dependent transformation of cells (Uren et al., 2005), with a more recent study showing that E6 alone can augment Wnt signaling (Lichtig et al., 2009). Additionally, PS-1 can control cleavage by gamma secretase of the E-cadherin receptor (Marambaud et al., 2002). E-cadherin, along with β-catenin, is a major component of adherens junctions that are found at cell-cell contact sites in the epithelium and play an important role in, amongst other things, contact inhibition. The cleavage of E-cadherin by gamma secretase leads to the disassembly of the adherens junction complex, and release of β-catenin into the cytoplasm that can then, as part of canonical Wnt signaling, activate transcription. Due to the variety of functions of the gamma secretase complex described here, and many others that have not been considered, I decided that it was important to use a GSI specific to Notch signaling during my experiments. I purchased an inhibitor called R04929097 that reduces Notch processing with a much higher affinity and at a much lower concentration than APP cleavage and other functions of gamma secretase.

I seeded LXSN- and E6-expressing cells and in parallel NIKS, 1K and 2K in a short growth assay. From the day after seeding onwards cells were treated with 8 nM of R04929097 or DMSO that was replaced every 24 hours. I used conditioned media to feed cells on days 3 and 5 to ensure consistent growth conditions throughout the experiment. The cells were counted in duplicate at days 1, 2, 4 and 6 to assess their differential proliferation patterns. The results are shown in Figure 5.9A and B for LXSN and E6-expressing cell populations and NIKS, 1K, and 2K cell lines, respectively.

Much like DAPT, R04929097 reduces the growth potential of all the cells. Once again, the effect of the drug on E6-expressing cells is much bigger than for LXSN cells, with the former now growing to a lower density than untreated LXSN cells. For untreated 1K and 2K, I get the normal LSIL- and HSIL-like growth phenotype. The extent of the negative effect of R04929097 seems to be the same for NIKS, 1K and 2K, regardless of the levels of E6. This means that even in the presence of the drug, the normal LSIL- and HSIL-like proliferation patterns emerge.

The results here indicate that blocking gamma secretase has a growth inhibitory effect on cells, regardless of whether the GSI specifically targets Notch processing or not. Additionally, due to the pleiotropic effects of gamma secretase, it is difficult to fully interpret my data. The issue of affecting both growth promoting and suppressing pathways should have been solved by using R04929097. However, the overall outcome of my experiment has not changed. Some studies have shown that Insulin-like growth factor 1 (IGF-1), EGFR and also ErbB4, a receptor tyrosine-protein kinase that is a member of the EGFR subfamily, are substrates of gamma secretase (Ni et al., 2001, Li et al., 2007, McElroy et al., 2007). My medium contains supplemented FBS (providing growth factors), EGF and also insulin. Therefore I speculate that this may be interfering with gamma secretase and causing, at least in part, the growth effects that I observe here.

A.

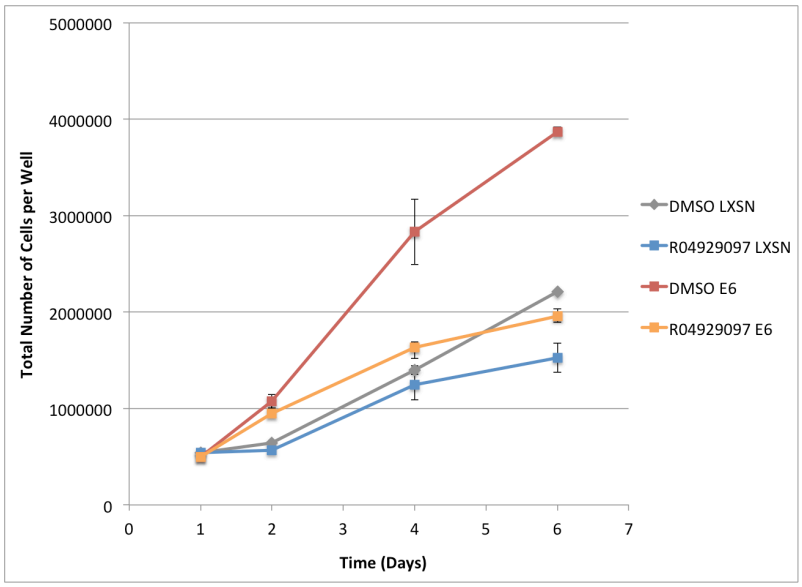

B.

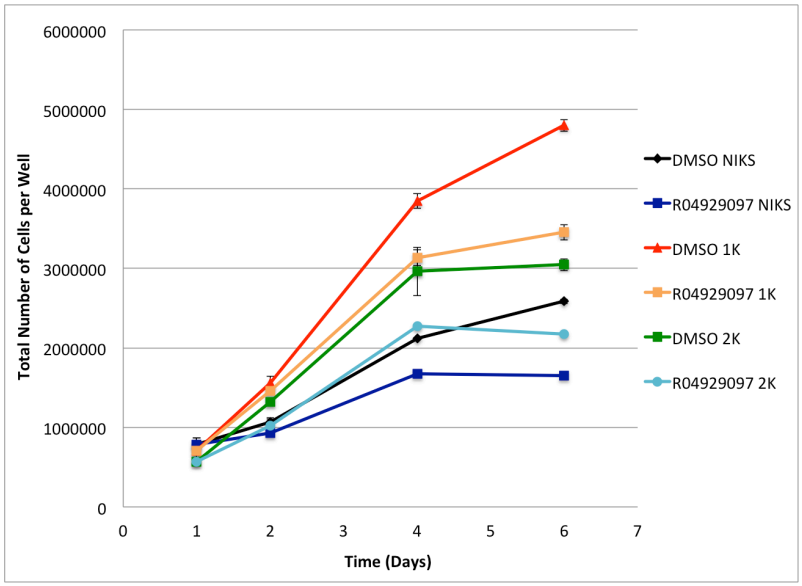

Figure 5.9: Treating cells with R04929097 brings about a negative effect on growth

A short growth assay was done with LXSN- and E6-expressing cells **(A)** or NIKS, 1K and 2K **(B)**. From day 1 onwards cells were treated with 8 nM of R04929097 or DMSO that was replaced every 24 hours. Cells were counted in duplicate at days 1, 2, 4 and 6 post-seeding and compared in terms of their growth phenotypes. The average number of cells per 6-well plate well was plotted against the time in days. The error bars represent +/- the standard deviation of the duplicate wells.

5.2.10 E6 up-regulates Notch signal transduction via RBPJ

In the previous sections I manipulated Notch signaling to attempt to show that regulation of this pathway by E6 is essential for overcoming contact inhibition. Unfortunately my various approaches have not worked well and I do not have conclusive data. Therefore, I decided to use a completely different approach and measure the activity of the Notch promoter using a transcription transactivation assay. By using this technique I was hoping to directly monitor the activity of the Notch pathway. E6 from βHPVs, has recently been shown to bind MAML1, which forms part of the transcriptional activation complex with RBPJ and NICD, and thereby reduce Notch signaling (Brimer et al., 2012, Tan et al., 2012, Meyers et al., 2013). Based on this I speculated that Notch activation would be reduced in high level E6-expressing cells as compare to the LXSN control.

To do this LXSN- and E6-expressing NIKS cells were electroporated in triplicate with the Topflash *Photinus* luciferase reporter plasmid containing either the specific RBPJ binding site of NICD (including the tandem repeats of the RBPJ transcriptional response element (TRE)) or a mutant version used as a negative control. This RBPJ-responsive construct encodes the firefly luciferase reporter gene under the control of a minimal (m)CMV promoter. The *Renilla* luciferase reporter plasmid was co-electroporated and serves as an internal control for normalizing transfection efficiencies. Cells were seeded in 6-well plates and allowed to grow to confluence for 5 days. To assess Notch activity, cells were lysed and the *Photinus* luciferase levels were quantified and normalized to the luminescence levels of the *Renilla* plasmid (Fig 5.10A). My results show that the levels of RBPJ activity are approximately 2.6-fold higher in E6-expressing as compared to LXSN cells. This suggests that E6 can up-regulate RBPJ activation.

These data are surprising in that I was expecting Notch signaling to be reduced in the presence of high levels of E6, yet I have observed the opposite. To further confirm my results I decided to carry out some RT-qPCR analysis to establish whether HES1 transcript levels correlate with RBPJ activation. HES1 is one of the main downstream effectors of the Notch pathway. Having seen more RBPJ-responsive promoter activity in E6-expressing cells, I also expected higher HES1 mRNA levels in these cells.

HSIL-like 1K and LSIL-like 2K cells were cultured in a growth assay format and harvested from duplicate wells at sub-confluence at day 3 and post-confluence at day 7. Subsequently I extracted RNA and performed RT-qPCR to assess HES1 transcript levels. Figure 5.10Bi and ii show that at both days 3 and 7, respectively, the levels of HES1 mRNA are higher for 1K than 2K cells.

The results of the transactivation assay and the qPCR experiments are compatible with each other and show that Notch signaling via RBPJ is elevated in cells with high levels of E6 as compared to cells with lower levels. This suggests that high E6 levels correlate with Notch pathway activation. It is interesting that E6 is apparently having opposing effects; it can down-regulate NICD levels but at the same time increase activation of the Notch responsive promoter.

A.

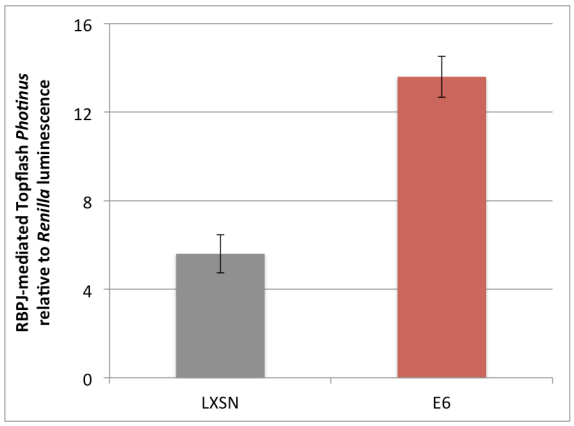

B i. **ii.**

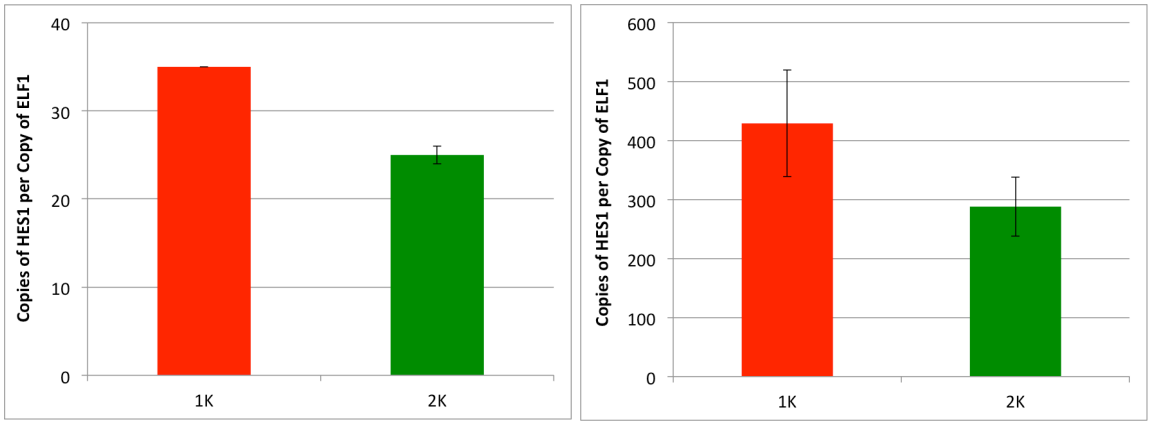

Figure 5.10: E6 up-regulates Notch signal transduction via RBPJ

A) LXSN- and E6-expressing cells were electroporated in triplicate with the Topflash *Photinus* luciferase reporter plasmid containing the specific RBPJ binding site of NICD. The *Renilla* luciferase reporter plasmid was co-electroporated and used as an internal control. Cells were seeded in 6-well plates and allowed to grow to confluence for 5 days. To assess Notch activity, cells were lysed and the *Photinus* luciferase levels were quantified and normalized to the luminescence levels of the *Renilla* plasmid (arbitrary units). The error bars represent the standard deviation of triplicate wells. **B)** 1K and 2K cells were cultured in a growth assay format and harvested in duplicate at sub-confluence at day 3 **(i)** and post-confluence at day 7 **(ii)**. Subsequently RNA was extracted, RT-qPCR performed and the levels of HES1 mRNA assessed relative to ELF1. The error bars represent the standard deviation of duplicate wells.

5.2.11 E6-dependent growth correlates with the levels of a putative truncated form of NICD

In Section 5.2.8 when I assessed the growth of my cells treated with DAPT dissolved in ethanol, I prepared cell pellets at each of the time points. I lysed cells with a RIPA buffer containing 6 % SDS and carried out some western blot analysis with the whole cell extracts from day 6 to test whether the levels of NICD were diminished in the presence of the GSI (data not shown). As part of these routine westerns I found that my NICD antibody can detect a small band of approximately 17 kDA with a much higher affinity than NICD. As NICD is a big protein that runs at 102 kDa, many of the low molecular weight proteins are routinely run off the bottom of low percentage gels and hence, I had never detected this other NICD species before. I hypothesized, based on the antibody's specificity and the size of the fragment, that the small band is the RAM domain of NICD. When an active ligand binds to the Notch receptor on the cell surface, gamma secretase cleavage gives rise to active NICD that can translocate to the nucleus. Once there, it can associate with RBPJ through an interaction involving both the RAM (RBPJ Associated Molecule) and ANK domains of NICD (Johnson and Barrick, 2012), leading to transactivation of Notch target genes. Biochemical analysis has shown that the RAM domain is also involved in displacing co-repressor proteins from the promoters of target genes to give rise to the transcriptional activation complex of Notch (Johnson and Barrick, 2012). To the best of my knowledge a stand-alone RAM domain has not been described *in vivo* in other studies. Surprisingly, I found that the levels of this truncated form of NICD correlate with E6-dependent growth of cells (Fig. 5.11A). LXSN control cells have no E6, express high levels of NICD and low levels of the putative "RAM" domain. In contrast, E6-expressing cells have low levels of NICD and high levels of the proposed "RAM" at the time-point analyzed. In both LXSN and E6-expressing cells, DAPT can reduce the levels of both full-length and "truncated NICD".

Leading on from this experiment I wanted to ensure that this stand-alone expression of the proposed "RAM" domain is not specific to NIKS cells. To do this I cultured primary cervical cells (PHKS) (isolated by Deborah Jackson in the laboratory) and also 1321 keratinocytes (that contain β-actin promoter driven HPV16 E6/E7) to confluence and prepared cell pellets. Cells were lysed with a RIPA buffer containing 6 % SDS and whole cell extracts were used to assess the levels of "truncated NICD" (Fig. 5.11B). The western blot shows that both the primary cells and 1321s express "truncated NICD".

Similarly to the patterns of expression observed in NIKS, E6- and E7-expressing1321 cells have low levels of NICD and high levels of the putative "RAM" domain while PHKS, without the oncogenes, show the opposite.

A.

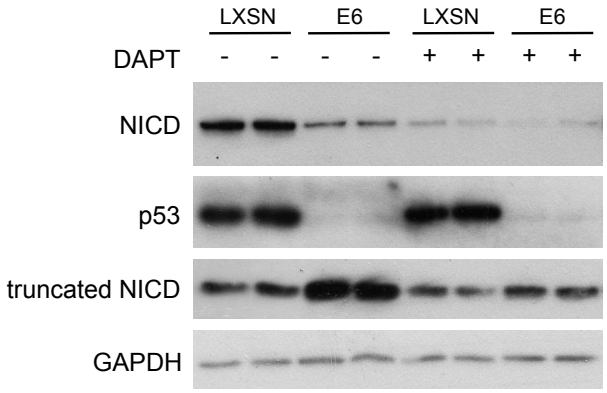

B.

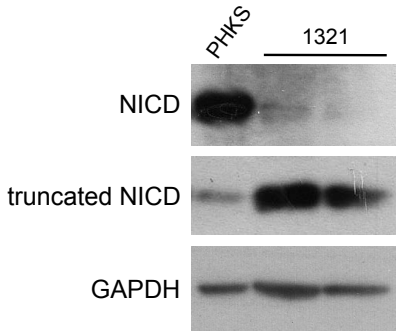

Figure 5.11: E6-dependent growth correlates with the levels of a putative truncated form of NICD

A) LXSN and E6-expressing cells were cultured in a short growth assay. From day 1 onwards cells were treated with 10 μM of DAPT or ethanol that was replaced every 24 hours. Cells were harvested in duplicate at day 6 post-seeding and lysed using a RIPA buffer containing 6 % SDS. Whole cell extracts were used to detect both full-length NICD and "truncated NICD" by western blot.

B) Primary human cervical cells (PHKS) and 1321 keratinocytes (expressing both E6 and E7) were cultured to confluence. Cells were harvested and lysed using a RIPA buffer containing 6 % SDS. Whole cell extracts were used to detect both full-length NICD and "truncated NICD" by western blot.

5.3 Discussion

In this chapter I have examined the underlying mechanism that is giving rise to the LSIL- and HSIL-like growth phenotypes. The different proliferation patterns of these cells correlate with high E6 levels in the latter from the point of confluence onwards. I first assessed whether degradation of p53 or PDZ proteins by E6 is involved in growth. I found that the PDZ motif seems to promote rapid proliferation but is not the sole contributor to cell growth. I then established that Notch signaling is involved in mediating growth in a high-density cell environment, though p21, a key effector of the pathway, is not activated in my cells in a Notch-dependent manner. Subsequently I moved on to show that use of a gamma secretase inhibitor (GSI) leads to a collapse of the phenotypic differences between HSIL-like 1K and LSIL-like 2K cells. Although the exact kinetics of the experiment appear wrong, this result shows that signaling through gamma secretase, which plays a crucial role in the Notch pathway, is involved in giving rise to the growth differences between these clonal cell lines. Further analysis of the Notch pathway showed, surprisingly, that high E6 levels are associated with increased RBPJ activation, as reflected in the transcript levels of HES1. This result is in accordance with a further experiment where I found that the putative "RAM" domain, may be expressed on its own in NIKS and also other keratinocytes, and that the levels of this small fragment of the protein correlate with E6-dependent proliferation.

Some of my Notch-related results, and those of others are contradictory. It is unexpected that E6 can bring about such a big reduction in NICD levels but at the same increase transcriptional activation of Notch targets. I speculate that the two mechanisms work in tandem to bring about growth of cells. The main role of Notch in epithelial cells is to promote growth arrest and commitment to the cellular differentiation program (Dotto, 2008). However, Notch may also have tumorigenic, and hence growth promoting effects, as shown in a recent study focusing on AP-1, yet another effector of the pathway. AP-1 is a dimeric transcription factor complex consisting of one Jun family member (cJun, JunD or JunB) and also a Fos family member (Fra1, Fra2, cFos or FosB) (Eferl and Wagner, 2003). It was previously shown that cancer cells such as SiHa and HeLa contain primarily cJun/cFos dimers while non-tumorigenic HPV-immortalized keratinocytes and other similar cells contain cJun/Fra1 dimers (Soto et al., 2000, de Wilde et al., 2008). In the study at hand (Henken et al., 2012), two sets of SiHa cells expressing exogenous Notch were assessed, with increased AP-1 activity measured

in both. Moderate levels of Notch were associated with cJun/cFos dimers normally found in SiHa, whereas high levels of Notch lead to a change in AP-1 complex composition to cJun/Fra1, which is associated with non-tumorigenic cells. This suggests that the effects of Notch on transformation are dosage dependent. While I have not looked at AP-1 activation in my cells, or dimer composition for that matter, I speculate, based on the Henken *et al.* study, that I might also be seeing a dose dependent effect of Notch signal transduction. I postulate that in my cell line model, low levels of NICD and high transcriptional activation through RBPJ, associated with high E6 levels in the HSIL-like clone, contribute to increased proliferation. In contrast, high levels of NICD and lower levels of transcriptional activation in the LSIL-like cell line, with less E6, are associated with slow growth and reduced capacity to overcome contact inhibition.

Furthermore, the growth effects I have observed in my cells, that seem to correlate with differential Notch signaling, could also be caused by the regulation of Notch transcriptional activation itself. NICD has the capacity to bind to thousands of gene promoters with only a small subset of these being fully activated in its presence (Margolin et al., 2009). Activation seems to be dependent on the cellular context, with RBPJ binding to DNA in a cell type specific manner (Meier-Stiegen et al., 2010). Moreover, activation is heavily regulated by histone acetylation (Mulligan et al., 2011) and DNA methylation (Deaton and Bird, 2011). Additionally, histone modifications like methylation and ubiquitinylation also play major roles in regulating Notch-dependent transcriptional activation (Borggrefe and Liefke, 2012).

Yet another publication has shown that HES1 can interact with RBPJ and thereby reduce the transcriptional activation of Notch targets, including the *HES1* gene itself (King et al., 2006). I have shown that HSIL-like cells have higher levels of HES1 transcript than the LSIL-like cell line. Therefore I speculate that HES1 could be involved in down regulating those targets of Notch that can have growth inhibitory effects.

The discovery that a peptide, that is recognized by the NICD antibody, and that is of a size consistent with the RAM domain of NICD, is present as a stand-alone fragment in my cells is unexpected. The finding that the levels of this putative truncated form of NICD correlate with the growth of cells is surprising and may suggest that this fragment

is involved in promoting cell growth. Johnson *et al.* from the Barrick laboratory at Johns Hopkins University in Baltimore, have shown that the main role of the RAM domain is to displace co-repressors from RBPJ upon NICD binding. This then enables the RBPJ/NICD complex (along with other co-activators such as MAML1 and p300) to activate Notch transcriptional targets (Borggrefe and Liefke, 2012). I propose that the stand-alone "RAM" domain could be removing repressors of RBPJ in my cells, more so in HSIL-like cells with high levels of "RAM" than in LSIL-like cells with low levels. This may lead to the activation of growth-promoting Notch targets (discussed above) and thereby allow cells to overcome contact inhibition.

I also have a second "RAM"-related growth theory. While E6 can only reduce the levels of full-length NICD (and thereby increase levels of the truncated form), Figure 5.11A shows that DAPT decreases both full-length and "truncated NICD". Based on this, I speculate that the growth effects observed in my cells may be dependent on the "RAM" vs. NICD ratio as opposed to the precise levels of each protein itself. However, this needs to be investigated further.

In this chapter I have shown that the negative effect of E6 on NICD levels is very big, with an approximate 50 to 100-fold decrease in levels, while all the downstream targets are associated with much smaller effects. For instance, RBPJ promoter activity is enhanced 2.6-fold in the presence of E6 while HES1 mRNA levels, between LSIL- and HSIL-like cells, are even less different. These distinct results together might indicate that E6 is having other growth-promoting effects that I have not yet considered. Recent findings (Howie et al., 2011) have shown that E6 from primarily HPV5 and 8, but also type 16, can bring about degradation of the tumor suppressor p300. This is achieved by binding of E6 directly to the protein and inhibiting its interaction with AKT. AKT phosphorylates p300 and this is essential for maintaining the stability of the latter. As p300 is associated with various signaling pathways, including some that are involved in proliferation and cellular differentiation, even small changes in its levels are associated with profound effects on the whole cell. For instance, it has been shown in human foreskin keratinocytes, that loss of p300 is associated with delayed onset of differentiation, the ability of cells to re-enter the cell cycle and also increased growth potential (Wong et al., 2010). Another study has found that cell-cell adhesion is also lost (Krubasik et al., 2006). Furthermore, for 16E6 specifically, it has been proposed

that shRNA-mediated knock-down of p300 is associated with the transcription of hTERT and subsequent telomerase activity (James et al., 2006). Hence, based on this, it seems reasonable to test in my cell lines whether this specific effect of E6 is involved in giving rise to the distinct patterns of proliferation I have observed.

All in all, the data have shown that high levels of E6 lead to rapid proliferation in the context of cell-cell contact. This is associated with up-regulation of RBPJ-dependent transcription and also down-regulation of NICD. I hypothesize that increased transcription arises because of the ability of the putative "RAM" domain to displace repressors from the RBPJ complex (Johnson and Barrick, 2012). This enables transcriptional activation of growth promoting Notch targets, such as AP-1, which may be involved in bringing about the differential proliferation phenotypes between LSIL-like cells, with low E6 levels, and HSIL-like cells, with high E6 levels.

Chapter 6: Final Discussion

6.1 Project background and rationale

Previous work by Isaacson Wechsler *et al.* in 2012 showed that HPV16-containing episomal NIKS cell lines spontaneously present with two rafting phenotypes; one set of cell lines has a gene expression pattern that resembles a LSIL lesion while the others are reminiscent of an HSIL, according to the viral gene expression patterns which were previously characterized by Middleton *et al.* in 2003. The authors further showed that in monolayer culture, the HSIL-like cells have the capacity to grow faster than LSIL-like cells from the point of confluence onwards when cell-cell contact is abundant. The aim of my work was to further characterize these cell lines and to investigate the underlying mechanism causing the differences between them. I anticipated that this could provide a useful insight into neoplastic progression: the changes that occur as a lesion develops from a low-grade infection associated with a productive viral life cycle, to a high-grade one with an abortive life cycle.

6.2 The HPV16 E6 protein on its own can drive keratinocytes to proliferate in a monolayer growth environment

The first aim of this study was to determine whether differences in E6/E7 levels are responsible for the LSIL- and HSIL-like phenotypes. I show here, surprisingly, that E6 on its own can cause the enhanced growth of keratinocytes, whilst E7 is unable to increase proliferation of my cells in normal culture conditions. E7 is the oncoprotein that is classically associated with driving cell cycle progression due to its well characterized ability to bind to and degrade the Rb protein (Dyson et al., 1989, Munger et al., 1989) and thereby bring about release of E2F (Boyer et al., 1996) and components required for G1/S transition (Zerfass et al., 1995). However in my model system, the levels of E7 protein are not different between the two types of cells that show different growth rates. In contrast, the levels of E6 are elevated in the HSIL-like cells compared to the LSIL-like cells, from confluence onwards. I further tested this growth-promoting function of E6 using cells expressing either one of the two oncoproteins individually in the absence of the viral genome. This confirmed that in my standard cell culture conditions, E6 on its own has the capacity to enhance proliferation.

To investigate the inability of E7 to drive proliferation of my cells, I considered the normal environment of HPV, the stratified epithelium. E7 generally fulfills its growth-promoting role in the suprabasal layers of the epithelium, where cells would normally be differentiating. In these cell layers the levels of growth factors are much lower than in the basal layer, where many cells are mitotically active even in the absence of the virus. During normal cell culture, cells are surrounded by a high concentration of growth factors due to the inclusion of FBS and EGF in my keratinocyte growth medium. EGF signals through the ERK1/2 pathway of the MAPK system (reviewed in (Shirakata, 2010)), which leads to cyclin D activation (Dhillon et al., 2007). Cyclin D then interacts with both CDK4 and CDK6 to, bring about the release of E2F from Rb (reviewed in (Sherr, 1994)). E2F induces the expression of other S phase promoting genes, such as cyclin A and CDK2 (Soucek et al., 1997), leading to cell cycle progression (reviewed in (Woo and Poon, 2003)). Hence I hypothesized that in the normal monolayer environment, the high concentration of growth factors, reminiscent of the basal layer, makes the function of E7 largely redundant as E2F is already fully released. Based on this I showed that in a growth-factor diminished environment, which resembles the suprabasal layers, E7 can promote cell proliferation because in this situation the degradation of Rb, brought about by E7, leads to the release of E2F. Hence, I conclude that cell culture conditions have to mimic the normal environment of the virus in order for the normal growth-promoting function of E7 to be observed. Interestingly, the effects of E6 are independent of the presence of growth factors, suggesting that E6- and E7-induced growth effects occur through different mechanisms.

While the role of aberrant E6 levels in promoting malignancy has been studied extensively, this has predominantly been done in transformed cells and non-keratinocytes. In contrast, this study uses non-transformed keratinocytes, which can support the full viral life cycle in raft culture (Flores et al., 1999) and, importantly, contain viral episomes. This is in contrast to fibroblasts that cannot stratify into an epithelium, and also cervical cancer cell lines such as CaSki, SiHa and HeLa that are associated with integrated HPV genomes. This means that I could the cell line model to characterize the full productive life cycle and also early events during life cycle deregulation.

My data show that the induction of proliferation by E6 is associated with increased cyclin A levels, which is in accordance with published findings in fibroblasts by Malanchi *et al.* in 2002 and 2004. However, my work with the E6SAT mutant, which is unable to bring about the degradation of p53, has shown that cyclin A is not always found at high levels in E6-stimulated cells. While E6SAT-expressing cells have the same growth potential as wild type E6-expressing cells they do not express high levels of cyclin A. This suggests that whilst cyclin A activation may correlate with wild type E6-induced proliferation, it is not in itself causative of the increased proliferation. That cyclin A appears elevated in the presence of increased cell proliferation, is perhaps not surprising, as any mechanism that drives cells either to transit G1 faster, or have a greater propensity to enter S phase, will result in elevated cyclin A. It is not clear why cyclin A is not elevated by the E6SAT mutant, but may be due to suppression of cyclin A expression by p53 (Yamamoto et al., 1994). Since the different cyclins are known to be able to substitute for each other (Geng et al., 1999, Masamha and Benbrook, 2009), lack of cyclin A, per se, is not a problem for cell cycle progression, and this indeed appears to be the case in the NIKS SAT mutant.

My work further shows that NIKS cells expressing only E6 and also HSIL-like cells, have lower levels of p21 than the empty vector LXSN control and the LSIL-like clone, respectively. This suggested initially that p21 levels might correlate with cell growth as shown by Malanchi *et al.* in 2004 and also Shai *et al.* in 2007. However, the E6SAT mutant showed not only that the expression of p21 is dependent on p53, but also that in these p53-degradation deficient cells, the levels of p21 are high. Again this suggests that whilst decreased p21 levels can appear to correlate with wild type E6-induced proliferation, the decrease in p21 levels is not necessarily causative of increased growth potential. While most work focusing on p21 has shown that it negatively regulates cell cycle progression and, hence, inhibits growth (reviewed in (Abbas and Dutta, 2009)), in certain situations it has been attributed oncogenic activities. The protein is over-expressed in a variety of human cancers, including that of the cervix (Cheung et al., 2001). Moreover, other studies suggest that p21 localization can have an effect on its precise function. While the growth-repressive role of p21 is carried out predominantly by its nuclear fraction, the cytoplasmic pool has oncogenic potential, for instance during breast carcinogenesis (Zhou et al., 2001, Winters et al., 2003). All these observations together are supportive of my data and show that even in the presence of high levels of

p21, proliferation of cells is possible in certain situations. Hence, the fact that E6SAT-expressing cells are associated with both fast growth potential and high p21 levels does not pose a problem in that respect.

My data are in accordance with previous work that showed almost 20 years ago, that E6 can enhance cell growth (Ishiwatari et al., 1994, Inoue et al., 1994, Inoue et al., 1998, Song et al., 1999), and that various cell cycle proteins are affected, (Malanchi et al., 2002, Malanchi et al., 2004, Shai et al., 2007). However my analysis has extended what is known by showing that it is not necessarily the effects on cyclin A and p21 that are responsible for E6-induced proliferation in keratinocytes.

As discussed throughout this study, I believe that in my cell culture model a confluent monolayer resembles the basal layer of the epidermis in terms of cell density. This theory and the dependency of LSIL- and HSIL-like growth phenotypes on cell-cell contact add a great deal of significance to my model. I speculate that the effects of E6 and E7 observed in the various monolayer conditions can be used to infer the functions of the oncoproteins in the epithelium. Hence, I hypothesize that in a stratified epithelium, E6 can induce rapid cell growth, and thus promote neoplasia in many cells layers, irrespective of the presence of extracellular growth factors, while the function of E7 may be limited to the upper layers where growth factors are sparse. My raft culture data with cells expressing only E6 seem to support this theory. Compared to empty vector control rafts, the number of MCM7-positive cells (delineating cells that are in S phase) in both the basal and suprabasal layers, is much higher for E6-expressing cells.

6.3 The manipulation of E6 levels has a corresponding effect on proliferation

Having shown that the underlying difference between the LSIL- and HSIL-like cells is the E6 level, I then wanted to move on to my second objective and test whether changing the levels of E6 would have the predicted effect on cell growth. To this end I transfected cells with a plasmid vector expressing high levels of E6 and showed that the resulting populations grew to a higher density than HSIL-like cells. While doing these experiments I also showed that, in accordance with a previously postulated hypothesis in my laboratory (Nicolaides, 2011), high levels of E6 seem to promote loss of the viral episomes. This observation has recently been reported in the literature (Kho et al., 2013).

Subsequently, I used RNAi to knock-down E6 levels in HSIL-like cells and showed that when levels of E6 are very low, these cells do not have the capacity to grow significantly faster than NIKS cells treated with control siRNA. This line of work further confirmed that high E6 levels do not merely correlate with a high growth potential of cells but seem to be the underlying cause of the observed phenotypes.

6.4 Notch signaling, as perturbed by E6, is involved in overcoming cell-cell contact inhibition

The third and final aim of my work was to investigate which function of E6 is involved in promoting proliferation. I decided to assess the Notch pathway due to its known role in repressing epithelial cell growth and initiating differentiation (reviewed in (Watt et al., 2008)).

I found that the high levels of E6 associated with the fast growing HSIL-like cells, correlate with low levels of NICD. An inhibitory effect of E6 proteins from other HPV types on Notch signaling has previously been found in several independent studies (Brimer et al., 2012, Tan et al., 2012, Meyers et al., 2013). Using gamma secretase inhibitors (GSIs), to block formation of NICD, I found that the precise kinetics of cell growth resulting from Notch inhibition are not as anticipated. However, the GSIs cause a reduction in the divergence between the LSIL- and HSIL-like growth phenotypes. Notch signaling, as regulated by gamma secretase, is involved in negatively controlling cell proliferation at a high cell density. Hence, the effects of both GSIs used seem to be greater in cells that, as a result of high E6 levels, grow more rapidly. These results confirm that low NICD levels correlate with high E6 levels in such a way that is conducive to rapid proliferation, though I have not yet shown that repressed Notch signaling is the underlying cause of cell growth.

The work of the other groups that have assessed the effect of E6 on the Notch pathway (Brimer et al., 2012, Tan et al., 2012, Meyers et al., 2013) has shown that E6 from bovine papillomaviruses (BPV) and/or βHPV8 can bind MAML1 (one of the transcriptional co-activators of NICD) and thereby negatively affect activation of Notch target genes. None of these studies have found a direct association between NICD and E6. Additionally, one group (Tan et al., 2012) has carried out some preliminary analyses with 16E6 and shown that this protein is not associated with the same mechanism.

Based on this I decided to assess Notch promoter activity in the NIKS cells to determine whether 16E6 could regulate transcriptional activation of Notch targets by reducing NICD levels. Surprisingly, my results indicate that in HSIL-like cells Notch signaling through the RBPJ promoter is significantly enhanced by E6. Additionally, the levels of HES1 mRNA, one of the targets of the NICD transcriptional activation complex, are higher in HSIL-like cells with high levels of E6, than in LSIL-like cells that are associated with less E6. Hence, the results of my experiments to this point seem to be in direct conflict with each other. On the one hand, E6 can reduce NICD, which should repress Notch signaling, while on the other hand, E6 seems to augment Notch promoter activity. As discussed above, the lack of HPV16 E6-dependent repression of Notch transcriptional targets has previously been reported (Tan et al., 2012) and my data support this view. This suggests that 16E6 has evolved a different mechanism for disrupting the Notch pathway.

The presence of an apparent truncated form of NICD, the putative "RAM" domain, may yet resolve the issue of my seemingly contradicting data. My results show that the levels of this putative "RAM" domain correlate with the growth of cells, in that high-level E6-expressing cells are associated with more "RAM" than LXSN control cells. This suggests that in fast-growing cells, high E6 levels may promote degradation of NICD in favor of the stand-alone putative "RAM" domain. This then leads to increased transcriptional activation of Notch target genes, presumably due to the higher levels of "RAM". There are several ways by which high levels of the "RAM" domain could theoretically promote transcription of Notch target genes. The first possibility, discussed briefly at the end of Chapter 5, is based on findings by Johnson *et al.* in 2012. In the absence of Notch, RBPJ is a repressor complex (Dou et al., 1994) and can inhibit transcription of its target genes through the recruitment of histone deacetylase HDAC1 (Kao et al., 1998). The role of RAM is to bind with high affinity to RBPJ and displace co-repressors, to promote formation of the activator complex (Johnson and Barrick, 2012). In this first scenario, the binding of "RAM" to RBPJ would not allow the full length NICD protein (containing both RAM and ANK domains necessary for promoting transcriptional activation) to bind to RBPJ. While the "RAM" domain alone may not actively drive transcription, it could still bring about de-repression of transcription of growth promoting Notch target genes, leading to proliferation. A second option is that the "RAM" domain, which I estimate to be approximately 50- to 100-fold more

abundant than full-length NICD, can bind to RBPJ and thereby inhibit NICD from binding and recruiting MAML1 and other co-activators to growth-repressing Notch target genes. Without further analysis, I cannot rule out the possibility that, as the putative "RAM" domain arises from cleavage of full-length NICD, it may actually be the other half of the NICD (i.e. the ANK domain, which my antibody does not detect) that is the active fragment. Based on my results to date I propose that the first option, in which "RAM" leads to de-repression of the activation of transcriptional targets, is most likely. It seems that in NIKS cells, Notch signaling can bring about expression of genes that actively promote growth. Growth promoting effects of the Notch pathway have been described through activation of AP-1 (Henken et al., 2012), histone methyltransferases (Hsu et al., 2012) and also by the activation of a subset of Notch targets through HES1 (Dudley et al., 2009).

I also detected the putative "RAM" domain in another keratinocyte cell line and also in primary cervical cells, and I speculate that the fragment may play a significant role in Notch signaling in many other cell types. Hence, assessing the expression patterns of the putative "RAM" domain as part of all experiments investigating Notch signal transduction, may help shed light on the divide in the HPV field pertaining to the exact involvement of this pathway in cervical neoplasia.

6.5 The role of adherens junctions in deregulating Notch signaling

As explained in more detail in the Introduction, one of the main types of adhesive junctions, which are found at cell-cell contact sites, is the adherens junction, whose main component is the cell receptor E-cadherin (reviewed in (Balda and Matter, 2003)). Adherens junctions allow adjacent cells to bind to each other and are implicated in roles such as contact inhibition, cell polarity and adhesion. Both E6 and E7 can reduce the levels of E-cadherin (Matthews et al., 2003, Yuan et al., 2009, Laurson et al., 2010) and as such affect the overall formation and efficacy of the junction and hence downstream pathways. Two other components of the junctions are α- and β-catenin, with the latter also being an important cellular transcription factor. Both hDlg and hScrib, two PDZ proteins that high-risk E6 can associate with and target for degradation, localize to adherens junctions to stabilize the link between the catenins and E-cadherin (Qin et al., 2005). Additionally, the PDZ protein MAGI-1 can also be found at the site of adherens

junctions (Dobrosotskaya and James, 2000, Ivanova et al., 2007). While I have not assessed the levels of E-cadherin in my cells in this study, I have done some work with an E6 mutant (E6ΔPDZ) that lacks the PDZ motif and is unable to bind these proteins. During a growth assay with this cell population I found that it grows slower than wild type E6-expressing cells. Although this difference may result from the lower stability of the mutant E6 protein, it might also reflect a role for PDZ proteins in E6-induced proliferation. Reduced PDZ protein degradation by this E6 mutant could result in more intact cell polarity, adhesion and cell-cell contact inhibition pathways. As both hDlg and hScrib localize to adherens junctions and enable their correct formation, I speculate that degradation of these two proteins by E6 promotes abnormalities in junction formation and hence contact inhibition, thereby contributing to the ability of E6 to allow cells to proliferate to a high cell density.

Additionally, based on the known effects of E6 on E-cadherin (Matthews et al., 2003), I hypothesize that this interaction further destabilizes adherens junctions. According to this theory and my observations with the E6ΔPDZ mutant, I suggest that the presence of E6 prevents normal junction formation or, at the very least, significantly slows down the process. This has negative effects on cell adhesion, polarity and cell-cell contact recognition and hence the normal downstream pathways associated with high cell density. Hence I propose that the effects of E6 on Notch signaling that I have described here may not be brought about directly by the interaction of E6 with components of the Notch pathway, but as a downstream result of disrupted adherens junctions. A study showing that the Delta-like 1 ligand of Notch can localize to adherens junctions in a MAGI-1-dependent manner to activate Notch signaling in adjacent cells (Mizuhara et al., 2005) seems to be supportive of this theory. It would suggest that degradation of the MAGI-1 protein by E6 and subsequent lack of Delta-like 1 presentation on the cell surface can lead to reduced Notch activation and hence promote proliferation.

6.6 Overall conclusions

E6 is a viral protein that is necessary for the productive viral life cycle. When expressed aberrantly it can contribute to neoplastic progression and malignant transformation of cells. In this study I have used a unique monolayer cell line system to show that the HPV16 E6 oncoprotein on its own can promote keratinocyte cell growth and that high levels of E6 seem to be associated with the progression from a LSIL- to an HSIL-like

growth phenotype. My data also suggest that E6-dependent proliferation correlates with high levels of a putative truncated form of NICD and also augmented activity of Notch-responsive promoters. Moreover, my experiments using gamma secretase inhibitors indicate that the gamma secretase complex itself, and downstream targets other than those involved in Notch signaling, have strong effects on cell proliferation. Hence, I propose that signaling through gamma secretase and the Notch pathway is involved, at least in part, in giving rise to the growth patterns, although I have not yet established whether it is the underlying cause.

Based on my data and the known effects of E6 on adhesive junctions, I further hypothesize that the growth phenotypes may not only be brought about directly by the interaction of E6 with components of the Notch pathway, but as a downstream result of disrupted adherens junctions. According to this theory, HSIL-like clonal cell lines, due to the higher levels of E6 associated with these cells from confluence onwards, have a less intact apical junctional complex than LSIL-like cells, leading to their differential responses to contact inhibition. This is manifest through an effect on Notch signaling. According to this model, it is likely that deregulation of the Notch pathway directly by E6 is not the only underlying cause of high cell density proliferation. This means that, although not investigated here, other pathways involved in contact inhibition, for instance the Hippo pathway (discussed in the Introduction), may also be affected. This theory, if proven to be correct, may explain some of the more multi-faceted results associated with Notch signaling that I have not been able to explain in full so far.

The monolayer experiments in high and low level growth factor environments seem to suggest that the role of HPV16 E7 is redundant in the presence of high concentrations of growth factors, as both E7 and growth factors target the same point in the cell cycle. However, in a growth factor diminished environment, which is reminiscent of the suprabasal layers of the epithelium, E7 is able to fulfill its normal function. Based on current literature, and the fact that in my experiments E6 can drive growth irrespective of the presence of growth factors, I hypothesize that E6 and E7 have distinct effects on proliferation. E6 can push cells through the cell cycle more quickly, via the pathways proposed above, to bring about enhanced proliferation while the role of E7 is to push quiescent cells into cycle, in an environment that is associated with low levels of growth factors, such as the suprabasal layers.

Due to the established role of aberrant E6 expression in promoting HPV-dependent malignancy, the E6 protein has been subject of considerable work. Moreover, a role of E6 in driving the proliferation of cells specifically has been described before. However, in most cases these observations have been made by overexpressing E6 alone either in cervical carcinoma cells, fibroblasts or transgenic mice. This study has uniquely modeled this function of E6 in episomal HPV16-expressing keratinocytes. The fact that I am using LSIL- and HSIL-like cell lines that consistently give rise to distinct growth patterns, due to differences in E6 protein levels, in a cell-cell contact dependent manner, means that they can be used to model neoplastic progression.

6.7 Future work

6.7.1 Investigating whether the pathways disturbed by E6 in monolayer are also increasingly deregulated during neoplastic progression

The aim of my future work is to determine by which mechanism(s) E6 can drive cell growth in monolayer. Once that has been established, I want to show that the pathways disrupted in this environment are also affected in a similar way in a stratified epithelium and, hence, the site of HPV infection. This involves several different approaches:

1) To show that the pathways deregulated by E6 to give rise to the LSIL- and HSIL-like growth patterns are also instrumental in driving the corresponding rafting phenotypes, I will use the LSIL- and HSIL-like rafts (Isaacson Wechsler et al., 2012) to stain for NICD levels and also adherens junction formation using E-cadherin.

2) To ensure that the pathways affected by E6 in NIKS are not part of a cell-type specific effect, I will use other cells, including primary cervical keratinocytes, to show that the same pathways are similarly altered.

This line of investigation is also important as it was shown recently that a specific population of cells at the squamo-columnar junction of the cervix, is associated with most, if not all, cervical carcinomas (Herfs et al., 2012). This suggests that neoplastic progression and HPV-associated malignancy may be dependent on the precise cellular environment.

3) I will test whether the same pathways perturbed in the monolayer environment, and presumably LSIL- and HSIL-like raft cultures, are also altered in real cervical biopsies. According to my model the level of deregulation should be higher in high-grade cervical lesions than in low-grade lesions.

6.7.2 Gaining more insight into the role E7

My results suggest that the ability of E7 to carry out its main role, of bringing about the release of E2F from Rb, is dependent on its precise extracellular environment. I want to test my hypothesis and confirm that the role of E7 is limited to suprabasal layers of the epithelium. The experiments to further my knowledge in this respect include:

1) Attempting the knock-down of cyclin D by RNAi. This will allow me to test my theory that both E7 and growth factors bring about the expression of cyclin D by releasing E2F from Rb.

2) I will try to establish which type of growth factor(s) is involved in mediating cell growth. I supplement my NIKS growth medium with pure EGF and IGF. However, FBS, that is also included, contains a variety of growth factors that could be involved in promoting proliferation.

3) I speculate that the effect of growth factors is dose-dependent. Therefore I will use various different concentrations of EGF, IGF and/or FBS, mimicking the different cell layers of the epithelium that are associated with a growth factor gradient, to determine at which concentration E7 is able to fulfill its role, at least in part.

4) To further assess whether the growth factors in the growth medium and E7 are in fact targeting the same downstream effectors, I will use an E7 mutant that is unable to bind to and bring about the degradation of Rb. If my hypothesis is correct then this mutant form of E7 should not be able to promote cell cycle entry even in a growth-factor diminished environment.

6.7.3 Characterization of the putative "truncated NICD"

It remains important to conclusively establish whether the putative "RAM" domain, is a truncated form of NICD and whether it is pivotal in bringing about the LSIL- and HSIL-like growth phenotypes. Doing this involves a number of different experiments:

1) To further characterize the putative "RAM" domain I will be challenging my western blots with other anti-NICD antibodies to different sites on the RAM domain, and using mass spectrometry to analyze the fragments immunoprecipitated by my antibody.

2) To determine whether the "RAM" domain can enhance proliferation and/or transcription in cells, I will be expressing the RAM domain from a plasmid vector that I have obtained from Doug Barrick (Johns Hopkins University, Baltimore, USA). Initially this will be done in easily transfectable cells, but with the aim of eventually analyzing the effect in NIKS.

3) The presence and levels of other truncated NICD species will also be assessed using antibodies to sites external to the RAM domain. In particular, as the ANK domain is the main player involved in binding to RBPJ, it is of interest to investigate whether this domain too is found on its own and the extent to which it correlates with E6-dependent cell growth.

4) It has been shown that in certain situations the NICD can be cleaved at other proteolytic cleavage sites (Cohen et al., 2005, van Tetering et al., 2011), giving rise to various different species, and it is hypothesized that these may have different biological properties. It will be interesting to see if the apparent lack of NICD in the presence of E6 is in fact just a failure of my antibody, which is specific to a particular cleavage event, to recognize other forms of NICD that may be present.

5) I have some additional preliminary observations (data not shown) that suggest that the levels of the putative "RAM" domain are affected by proteasome inhibition (with MG132), in an E6-dependent manner. This suggests that E6 may direct the NICD to the proteasome to bring about degradation of NICD and increase the levels of the "RAM" domain, and it will be important to further test this.

6) Additionally, if I can find a protease inhibitor that specifically blocks "RAM" formation without having any adverse effects on cells, this would be another way of assessing whether high levels of the putative "RAM" domain are causative in the rapid proliferation of high-level E6-expressing cells. I could start, for instance, by inhibiting the granzyme B (van Tetering et al., 2011) and caspase-3 and -6 (Cohen et al., 2005) proteolytic cleavage sites between the ANK and RAM domains.

6.7.4 Dissecting the role of adherens junctions in mediating the effects of E6 on Notch signaling

I hypothesized earlier that the effects of E6 on the Notch pathway may not be brought about by E6 directly affecting Notch signaling but actually as a consequence of disrupted adherens junctions. I now want to investigate this further and determine whether in the LSIL- and HSIL-like cells adherens junctions are differentially intact.

1) To determine whether the junctions are disrupted I will stain confluent E6-expressing monolayer cells with antibodies to adherens junction proteins, starting with E-cadherin, as it has been shown to be affected by the presence of E6 in previously published studies. Additionally I will also assess β-catenin levels, as β-catenin signaling may be altered by the effects of E6 on E-cadherin or though Wnt signaling, via both PDZ-motif dependent (Matsumine et al., 1996, Ishidate et al., 2000, Takizawa et al., 2006, Nagasaka et al., 2006) and independent (Lichtig et al., 2009) mechanisms.

Other targets for staining would include the PDZ proteins hDlg, hScrib and MAGI-1. Most studies looking at the effect of high-risk E6 on these PDZ proteins have been done *in vitro* or using over-expression systems. However, other work that has assessed the levels of endogenous PDZ proteins in response to HPV31 genome transfection has shown no effect on E6 (Lee and Laimins, 2004). Therefore, the function of the PDZ-binding motif of E6 *in vivo* remains unclear and hence interpreting the results of immunofluorescence with antibodies against these PDZ proteins may prove challenging.

2) I will also assess the levels of adherens junction proteins by western blot. If I find that E-cadherin levels are affected by E6 in my cells then I can increase them using drugs, such as Indole-3-carbinol and 5-Aza-2'-deoxycytidin. These have been shown to reinstate normal levels of E-cadherin (D'Costa et al., 2012a, D'Costa et al., 2012b) in response to HPV-dependent depletion. I expect that this would have a negative effect on the growth potential of cells.

3) To determine whether E6-mediated disruption of the Notch pathway is indirectly caused by its effects on adherens junctions, I will activate the Notch pathway independently of cell-cell contact. To do this I will introduce active Jagged and/or Delta ligands to sub-confluent E6-expressing and control cells. If E6 is acting directly on the Notch pathway then I should find low levels of NICD, whilst if it is acting via effects on adherens junctions, and hence high cell density, then I should find high levels of NICD.

4) The negative effect of E6 on E-cadherin (Matthews et al., 2003) seems to be mediated by DNA methyltransferase (DNMT) (D'Costa et al., 2012a). DNMT activity is elevated in cells expressing E6 (Au Yeung et al., 2010), and when repressed, normal E-cadherin transcription is restored (D'Costa et al., 2012a). Based on these findings, it seems worthwhile to assess DNMT levels in my NIKS cells to determine whether downstream effects of DNMT could be involved in modulating proliferation.

References

ABBAS, T. & DUTTA, A. 2009. p21 in cancer: intricate networks and multiple activities. *Nat Rev Cancer,* 9**,** 400-14.

ACCARDI, R., RUBINO, R., SCALISE, M., GHEIT, T., SHAHZAD, N., THOMAS, M., BANKS, L., INDIVERI, C., SYLLA, B. S., CARDONE, R. A., RESHKIN, S. J. & TOMMASINO, M. 2011. E6 and E7 from human papillomavirus type 16 cooperate to target the PDZ protein Na/H exchange regulatory factor 1. *J Virol,* 85**,** 8208-16.

AGOSTI, J. M. & GOLDIE, S. J. 2007. Introducing HPV vaccine in developing countries--key challenges and issues. *N Engl J Med,* 356**,** 1908-10.

ALAZAWI, W., PETT, M., ARCH, B., SCOTT, L., FREEMAN, T., STANLEY, M. A. & COLEMAN, N. 2002. Changes in cervical keratinocyte gene expression associated with integration of human papillomavirus 16. *Cancer Res,* 62**,** 6959-65.

ALLEN-HOFFMANN, B. L., SCHLOSSER, S. J., IVARIE, C. A., SATTLER, C. A., MEISNER, L. F. & O'CONNOR, S. L. 2000. Normal growth and differentiation in a spontaneously immortalized near-diploid human keratinocyte cell line, NIKS. *J Invest Dermatol,* 114**,** 444-55.

ALLISON, S. J., JIANG, M. & MILNER, J. 2009. Oncogenic viral protein HPV E7 up-regulates the SIRT1 longevity protein in human cervical cancer cells. *Aging (Albany NY),* 1**,** 316-27.

AMORNPHIMOLTHAM, P., PATEL, V., SODHI, A., NIKITAKIS, N. G., SAUK, J. J., SAUSVILLE, E. A., MOLINOLO, A. A. & GUTKIND, J. S. 2005. Mammalian target of rapamycin, a molecular target in squamous cell carcinomas of the head and neck. *Cancer Res,* 65**,** 9953-61.

ANDJELKOVIC, M., JAKUBOWICZ, T., CRON, P., MING, X. F., HAN, J. W. & HEMMINGS, B. A. 1996. Activation and phosphorylation of a pleckstrin homology domain containing protein kinase (RAC-PK/PKB) promoted by serum and protein phosphatase inhibitors. *Proc Natl Acad Sci U S A,* 93**,** 5699-704.

ANDROPHY, E. J., LOWY, D. R. & SCHILLER, J. T. 1987. Bovine papillomavirus E2 trans-activating gene product binds to specific sites in papillomavirus DNA. *Nature,* 325**,** 70-3.

ANTINORE, M. J., BIRRER, M. J., PATEL, D., NADER, L. & MCCANCE, D. J. 1996. The human papillomavirus type 16 E7 gene product interacts with and trans-activates the AP1 family of transcription factors. *EMBO J,* 15**,** 1950-60.

ARBEIT, J. M., HOWLEY, P. M. & HANAHAN, D. 1996. Chronic estrogen-induced cervical and vaginal squamous carcinogenesis in human papillomavirus type 16 transgenic mice. *Proc Natl Acad Sci U S A,* 93**,** 2930-5.

ARENDS, M. J., BUCKLEY, C. H. & WELLS, M. 1998. Aetiology, pathogenesis, and pathology of cervical neoplasia. *J Clin Pathol,* 51**,** 96-103.

ARROYO, M., BAGCHI, S. & RAYCHAUDHURI, P. 1993. Association of the human papillomavirus type 16 E7 protein with the S-phase-specific E2F-cyclin A complex. *Mol Cell Biol,* 13**,** 6537-46.

ARTAVANIS-TSAKONAS, S., RAND, M. D. & LAKE, R. J. 1999. Notch signaling: cell fate control and signal integration in development. *Science,* 284**,** 770-6.

AU YEUNG, C. L., TSANG, W. P., TSANG, T. Y., CO, N. N., YAU, P. L. & KWOK, T. T. 2010. HPV-16 E6 upregulation of DNMT1 through repression of tumor suppressor p53. *Oncol Rep,* 24**,** 1599-604.

AUSTIN, J. & KIMBLE, J. 1987. glp-1 is required in the germ line for regulation of the decision between mitosis and meiosis in C. elegans. *Cell,* 51**,** 589-99.

BACHTIARY, B., OBERMAIR, A., DREIER, B., BIRNER, P., BREITENECKER, G., KNOCKE, T. H., SELZER, E. & POTTER, R. 2002. Impact of multiple HPV infection on response to treatment and survival in patients receiving radical radiotherapy for cervical cancer. *Int J Cancer,* 102**,** 237-43.

BAI, L., WEI, L., WANG, J., LI, X. & HE, P. 2006. Extended effects of human papillomavirus 16 E6-specific short hairpin RNA on cervical carcinoma cells. *Int J Gynecol Cancer,* 16**,** 718-29.

BALDA, M. S. & MATTER, K. 2003. Epithelial cell adhesion and the regulation of gene expression. *Trends Cell Biol,* 13**,** 310-8.

BALDWIN, P., LASKEY, R. & COLEMAN, N. 2003. Translational approaches to improving cervical screening. *Nat Rev Cancer,* 3**,** 217-26.

BAND, V., DE CAPRIO, J. A., DELMOLINO, L., KULESA, V. & SAGER, R. 1991. Loss of p53 protein in human papillomavirus type 16 E6-immortalized human mammary epithelial cells. *J Virol,* 65**,** 6671-6.

BARBARESI, S., CORTESE, M. S., QUINN, J., ASHRAFI, G. H., GRAHAM, S. V. & CAMPO, M. S. 2010. Effects of human papillomavirus type 16 E5 deletion mutants on epithelial morphology: functional characterization of each transmembrane domain. *J Gen Virol,* 91**,** 521-30.

BARNARD, P. & MCMILLAN, N. A. 1999. The human papillomavirus E7 oncoprotein abrogates signaling mediated by interferon-alpha. *Virology,* 259**,** 305-13.

BARON, M. 2003. An overview of the Notch signalling pathway. *Semin Cell Dev Biol,* 14**,** 113-9.

BASEMAN, J. G. & KOUTSKY, L. A. 2005. The epidemiology of human papillomavirus infections. *J Clin Virol,* 32 Suppl 1**,** S16-24.

BECHTOLD, V., BEARD, P. & RAJ, K. 2003. Human papillomavirus type 16 E2 protein has no effect on transcription from episomal viral DNA. *J Virol,* 77**,** 2021-8.

BEDELL, M. A., HUDSON, J. B., GOLUB, T. R., TURYK, M. E., HOSKEN, M., WILBANKS, G. D. & LAIMINS, L. A. 1991. Amplification of human papillomavirus genomes in vitro is dependent on epithelial differentiation. *J Virol,* 65**,** 2254-60.

BELLACOSA, A., TESTA, J. R., STAAL, S. P. & TSICHLIS, P. N. 1991. A retroviral oncogene, akt, encoding a serine-threonine kinase containing an SH2-like region. *Science,* 254**,** 274-7.

BEN KHALIFA, Y., TEISSIER, S., TAN, M. K., PHAN, Q. T., DAYNAC, M., WONG, W. Q. & THIERRY, F. 2011. The human papillomavirus E6 oncogene represses a cell adhesion pathway and disrupts focal adhesion through degradation of TAp63beta upon transformation. *PLoS Pathog,* 7**,** e1002256.

BERNARD, B. A., BAILLY, C., LENOIR, M. C., DARMON, M., THIERRY, F. & YANIV, M. 1989. The human papillomavirus type 18 (HPV18) E2 gene product is a repressor of the HPV18 regulatory region in human keratinocytes. *J Virol,* 63**,** 4317-24.

BERNARD, H. U., BURK, R. D., CHEN, Z., VAN DOORSLAER, K., ZUR HAUSEN, H. & DE VILLIERS, E. M. 2010. Classification of papillomaviruses (PVs) based on 189 PV types and proposal of taxonomic amendments. *Virology,* 401**,** 70-9.

BERNARD, H. U., CALLEJA-MACIAS, I. E. & DUNN, S. T. 2006. Genome variation of human papillomavirus types: phylogenetic and medical implications. *Int J Cancer,* 118**,** 1071-6.

BIKLE, D. D., XIE, Z. & TU, C. L. 2012. Calcium regulation of keratinocyte differentiation. *Expert Rev Endocrinol Metab,* 7**,** 461-472.

BILDER, D. 2004. Epithelial polarity and proliferation control: links from the Drosophila neoplastic tumor suppressors. *Genes Dev,* 18**,** 1909-25.

BILDER, D., LI, M. & PERRIMON, N. 2000. Cooperative regulation of cell polarity and growth by Drosophila tumor suppressors. *Science,* 289**,** 113-6.

BLACK, A. R. & AZIZKHAN-CLIFFORD, J. 1999. Regulation of E2F: a family of transcription factors involved in proliferation control. *Gene,* 237**,** 281-302.

BOCK, M., BISHOP, K. N., TOWERS, G. & STOYE, J. P. 2000. Use of a transient assay for studying the genetic determinants of Fv1 restriction. *J Virol,* 74**,** 7422-30.

BOESE, Q., LEAKE, D., REYNOLDS, A., READ, S., SCARINGE, S. A., MARSHALL, W. S. & KHVOROVA, A. 2005. Mechanistic insights aid computational short interfering RNA design. *Methods Enzymol,* 392**,** 73-96.

BORGGREFE, T. & LIEFKE, R. 2012. Fine-tuning of the intracellular canonical Notch signaling pathway. *Cell Cycle,* 11**,** 264-76.

BOSCH, F. X., MANOS, M. M., MUNOZ, N., SHERMAN, M., JANSEN, A. M., PETO, J., SCHIFFMAN, M. H., MORENO, V., KURMAN, R. & SHAH, K. V. 1995. Prevalence of human papillomavirus in cervical cancer: a worldwide perspective. International biological study on cervical cancer (IBSCC) Study Group. *J Natl Cancer Inst,* 87**,** 796-802.

BOUSARGHIN, L., TOUZE, A., GAUD, G., IOCHMANN, S., ALVAREZ, E., REVERDIAU, P., GAITAN, J., JOURDAN, M. L., SIZARET, P. Y. & COURSAGET, P. L. 2009. Inhibition of cervical cancer cell growth by human papillomavirus virus-like particles packaged with human papillomavirus oncoprotein short hairpin RNAs. *Mol Cancer Ther,* 8**,** 357-65.

BOUSARGHIN, L., TOUZE, A., SIZARET, P. Y. & COURSAGET, P. 2003. Human papillomavirus types 16, 31, and 58 use different endocytosis pathways to enter cells. *J Virol,* 77**,** 3846-50.

BOUVARD, V., STOREY, A., PIM, D. & BANKS, L. 1994. Characterization of the human papillomavirus E2 protein: evidence of trans-activation and trans-repression in cervical keratinocytes. *EMBO J,* 13**,** 5451-9.

BOYER, S. N., WAZER, D. E. & BAND, V. 1996. E7 protein of human papilloma virus-16 induces degradation of retinoblastoma protein through the ubiquitin-proteasome pathway. *Cancer Res,* 56**,** 4620-4.

BRAKE, T. & LAMBERT, P. F. 2005. Estrogen contributes to the onset, persistence, and malignant progression of cervical cancer in a human papillomavirus-transgenic mouse model. *Proc Natl Acad Sci U S A,* 102**,** 2490-5.

BRAY, S. J. 2006. Notch signalling: a simple pathway becomes complex. *Nat Rev Mol Cell Biol,* 7**,** 678-89.

BRAZIL, D. P. & HEMMINGS, B. A. 2001. Ten years of protein kinase B signalling: a hard Akt to follow. *Trends Biochem Sci,* 26**,** 657-64.

BREHM, A., NIELSEN, S. J., MISKA, E. A., MCCANCE, D. J., REID, J. L., BANNISTER, A. J. & KOUZARIDES, T. 1999. The E7 oncoprotein associates with Mi2 and histone deacetylase activity to promote cell growth. *EMBO J,* 18**,** 2449-58.

BRIMER, N., LYONS, C., WALLBERG, A. E. & VANDE POL, S. B. 2012. Cutaneous papillomavirus E6 oncoproteins associate with MAML1 to repress transactivation and NOTCH signaling. *Oncogene,* 31**,** 4639-46.

BROGNARD, J., SIERECKI, E., GAO, T. & NEWTON, A. C. 2007. PHLPP and a second isoform, PHLPP2, differentially attenuate the amplitude of Akt signaling by regulating distinct Akt isoforms. *Mol Cell,* 25**,** 917-31.

BROOKMEYER, R., JOHNSON, E., ZIEGLER-GRAHAM, K. & ARRIGHI, H. M. 2007. Forecasting the global burden of Alzheimer's disease. *Alzheimers Dement,* 3**,** 186-91.

BROWN, D. R., BRYAN, J. T., SCHROEDER, J. M., ROBINSON, T. S., FIFE, K. H., WHEELER, C. M., BARR, E., SMITH, P. R., CHIACCHIERINI, L., DICELLO, A. & JANSEN, K. U. 2001. Neutralization of human papillomavirus type 11 (HPV-11) by serum from women vaccinated with yeast-derived HPV-11 L1 virus-like particles: correlation with competitive radioimmunoassay titer. *J Infect Dis,* 184**,** 1183-6.

BROWN, D. R., SCHROEDER, J. M., BRYAN, J. T., STOLER, M. H. & FIFE, K. H. 1999. Detection of multiple human papillomavirus types in Condylomata acuminata lesions from otherwise healthy and immunosuppressed patients. *J Clin Microbiol,* 37**,** 3316-22.

BRYAN, J. T. & BROWN, D. R. 2001. Transmission of human papillomavirus type 11 infection by desquamated cornified cells. *Virology,* 281**,** 35-42.

BUCK, C. B., PASTRANA, D. V., LOWY, D. R. & SCHILLER, J. T. 2005. Generation of HPV pseudovirions using transfection and their use in neutralization assays. *Methods Mol Med,* 119**,** 445-62.

BUITRAGO-PEREZ, A., HACHIMI, M., DUENAS, M., LLOVERAS, B., SANTOS, A., HOLGUIN, A., DUARTE, B., SANTIAGO, J. L., AKGUL, B., RODRIGUEZ-PERALTO, J. L., STOREY, A., RIBAS, C., LARCHER, F., DEL RIO, M., PARAMIO, J. M. & GARCIA-ESCUDERO, R. 2012. A humanized mouse model of HPV-associated pathology driven by E7 expression. *PLoS One,* 7**,** e41743.

BURGHARDT, E. & OSTOR, A. G. 1983. Site and origin of squamous cervical cancer: a histomorphologic study. *Obstet Gynecol,* 62**,** 117-27.

BURNETT, J. C., ROSSI, J. J. & TIEMANN, K. 2011. Current progress of siRNA/shRNA therapeutics in clinical trials. *Biotechnol J,* 6**,** 1130-46.

BUTZ, K., RISTRIANI, T., HENGSTERMANN, A., DENK, C., SCHEFFNER, M. & HOPPE-SEYLER, F. 2003. siRNA targeting of the viral E6 oncogene efficiently kills human papillomavirus-positive cancer cells. *Oncogene,* 22**,** 5938-45.

CABERG, J. H., HUBERT, P. M., BEGON, D. Y., HERFS, M. F., RONCARATI, P. J., BONIVER, J. J. & DELVENNE, P. O. 2008. Silencing of E7 oncogene restores functional E-cadherin expression in human papillomavirus 16-transformed keratinocytes. *Carcinogenesis,* 29**,** 1441-7.

CALAUTTI, E., LI, J., SAONCELLA, S., BRISSETTE, J. L. & GOETINCK, P. F. 2005. Phosphoinositide 3-kinase signaling to Akt promotes keratinocyte differentiation versus death. *J Biol Chem,* 280**,** 32856-65.

CAPELL, A., GRUNBERG, J., PESOLD, B., DIEHLMANN, A., CITRON, M., NIXON, R., BEYREUTHER, K., SELKOE, D. J. & HAASS, C. 1998. The

proteolytic fragments of the Alzheimer's disease-associated presenilin-1 form heterodimers and occur as a 100-150-kDa molecular mass complex. *J Biol Chem,* 273**,** 3205-11.

CHAN, E. F., GAT, U., MCNIFF, J. M. & FUCHS, E. 1999. A common human skin tumour is caused by activating mutations in beta-catenin. *Nat Genet,* 21**,** 410-3.

CHANG, Y. E. & LAIMINS, L. A. 2000. Microarray analysis identifies interferon-inducible genes and Stat-1 as major transcriptional targets of human papillomavirus type 31. *J Virol,* 74**,** 4174-82.

CHARETTE, S. T. & MCCANCE, D. J. 2007. The E7 protein from human papillomavirus type 16 enhances keratinocyte migration in an Akt-dependent manner. *Oncogene,* 26**,** 7386-90.

CHELLAPPAN, S. P., HIEBERT, S., MUDRYJ, M., HOROWITZ, J. M. & NEVINS, J. R. 1991. The E2F transcription factor is a cellular target for the RB protein. *Cell,* 65**,** 1053-61.

CHEN, Z., TROTMAN, L. C., SHAFFER, D., LIN, H. K., DOTAN, Z. A., NIKI, M., KOUTCHER, J. A., SCHER, H. I., LUDWIG, T., GERALD, W., CORDON-CARDO, C. & PANDOLFI, P. P. 2005. Crucial role of p53-dependent cellular senescence in suppression of Pten-deficient tumorigenesis. *Nature,* 436**,** 725-30.

CHENG, S., SCHMIDT-GRIMMINGER, D. C., MURANT, T., BROKER, T. R. & CHOW, L. T. 1995. Differentiation-dependent up-regulation of the human papillomavirus E7 gene reactivates cellular DNA replication in suprabasal differentiated keratinocytes. *Genes Dev,* 9**,** 2335-49.

CHEUNG, T. H., LO, K. W., YU, M. M., YIM, S. F., POON, C. S., CHUNG, T. K. & WONG, Y. F. 2001. Aberrant expression of p21(WAF1/CIP1) and p27(KIP1) in cervical carcinoma. *Cancer Lett,* 172**,** 93-8.

CHIANG, C. M., DONG, G., BROKER, T. R. & CHOW, L. T. 1992. Control of human papillomavirus type 11 origin of replication by the E2 family of transcription regulatory proteins. *J Virol,* 66**,** 5224-31.

CHIEN, W. M., PARKER, J. N., SCHMIDT-GRIMMINGER, D. C., BROKER, T. R. & CHOW, L. T. 2000. Casein kinase II phosphorylation of the human papillomavirus-18 E7 protein is critical for promoting S-phase entry. *Cell Growth Differ,* 11**,** 425-35.

CHONG, J. P., THOMMES, P. & BLOW, J. J. 1996. The role of MCM/P1 proteins in the licensing of DNA replication. *Trends Biochem Sci,* 21**,** 102-6.

CHONG, T., APT, D., GLOSS, B., ISA, M. & BERNARD, H. U. 1991. The enhancer of human papillomavirus type 16: binding sites for the ubiquitous transcription factors oct-1, NFA, TEF-2, NF1, and AP-1 participate in epithelial cell-specific transcription. *J Virol,* 65**,** 5933-43.

CHRISTENSEN, N. D., KOLTUN, W. A., CLADEL, N. M., BUDGEON, L. R., REED, C. A., KREIDER, J. W., WELSH, P. A., PATRICK, S. D. & YANG, H.

1997. Coinfection of human foreskin fragments with multiple human papillomavirus types (HPV-11, -40, and -LVX82/MM7) produces regionally separate HPV infections within the same athymic mouse xenograft. *J Virol,* 71**,** 7337-44.

COBRINIK, D. 2005. Pocket proteins and cell cycle control. *Oncogene,* 24**,** 2796-809.

COFFER, P. J. & WOODGETT, J. R. 1991. Molecular cloning and characterisation of a novel putative protein-serine kinase related to the cAMP-dependent and protein kinase C families. *Eur J Biochem,* 201**,** 475-81.

COHEN, L. Y., BOURBONNIERE, M., SABBAGH, L., BOUCHARD, A., CHEW, T., JEANNEQUIN, P., LAZURE, C. & SEKALY, R. P. 2005. Notch1 antiapoptotic activity is abrogated by caspase cleavage in dying T lymphocytes. *Cell Death Differ,* 12**,** 243-54.

COLEMAN, N. & STANLEY, M. A. 1994. Characterization and functional analysis of the expression of vascular adhesion molecules in human papillomavirus-related disease of the cervix. *Cancer,* 74**,** 884-92.

COLLINS, A. S., NAKAHARA, T., DO, A. & LAMBERT, P. F. 2005. Interactions with pocket proteins contribute to the role of human papillomavirus type 16 E7 in the papillomavirus life cycle. *J Virol,* 79**,** 14769-80.

CORNELISSEN, M. T., SMITS, H. L., BRIET, M. A., VAN DEN TWEEL, J. G., STRUYK, A. P., VAN DER NOORDAA, J. & TER SCHEGGET, J. 1990. Uniformity of the splicing pattern of the E6/E7 transcripts in human papillomavirus type 16-transformed human fibroblasts, human cervical premalignant lesions and carcinomas. *J Gen Virol,* 71 (Pt 5)**,** 1243-6.

D'COSTA, Z. J., JOLLY, C., ANDROPHY, E. J., MERCER, A., MATTHEWS, C. M. & HIBMA, M. H. 2012a. Transcriptional repression of E-cadherin by human papillomavirus type 16 E6. *PLoS One,* 7**,** e48954.

D'COSTA, Z. J., LEONG, C. M., SHIELDS, J., MATTHEWS, C. & HIBMA, M. H. 2012b. Screening of drugs to counteract human papillomavirus 16 E6 repression of E-cadherin expression. *Invest New Drugs,* 30**,** 2236-51.

DANIEL, B., RANGARAJAN, A., MUKHERJEE, G., VALLIKAD, E. & KRISHNA, S. 1997. The link between integration and expression of human papillomavirus type 16 genomes and cellular changes in the evolution of cervical intraepithelial neoplastic lesions. *J Gen Virol,* 78 (Pt 5)**,** 1095-101.

DAVIES, R., HICKS, R., CROOK, T., MORRIS, J. & VOUSDEN, K. 1993. Human papillomavirus type 16 E7 associates with a histone H1 kinase and with p107 through sequences necessary for transformation. *J Virol,* 67**,** 2521-8.

DAVIS, M. E., ZUCKERMAN, J. E., CHOI, C. H., SELIGSON, D., TOLCHER, A., ALABI, C. A., YEN, Y., HEIDEL, J. D. & RIBAS, A. 2010. Evidence of RNAi in humans from systemically administered siRNA via targeted nanoparticles. *Nature,* 464**,** 1067-70.

DAVY, C. E., JACKSON, D. J., RAJ, K., PEH, W. L., SOUTHERN, S. A., DAS, P., SORATHIA, R., LASKEY, P., MIDDLETON, K., NAKAHARA, T., WANG, Q., MASTERSON, P. J., LAMBERT, P. F., CUTHILL, S., MILLAR, J. B. & DOORBAR, J. 2005. Human papillomavirus type 16 E1 E4-induced G2 arrest is associated with cytoplasmic retention of active Cdk1/cyclin B1 complexes. *J Virol,* 79**,** 3998-4011.

DAVY, C. E., JACKSON, D. J., WANG, Q., RAJ, K., MASTERSON, P. J., FENNER, N. F., SOUTHERN, S., CUTHILL, S., MILLAR, J. B. & DOORBAR, J. 2002. Identification of a G(2) arrest domain in the E1 wedge E4 protein of human papillomavirus type 16. *J Virol,* 76**,** 9806-18.

DAY, P. M., RODEN, R. B., LOWY, D. R. & SCHILLER, J. T. 1998. The papillomavirus minor capsid protein, L2, induces localization of the major capsid protein, L1, and the viral transcription/replication protein, E2, to PML oncogenic domains. *J Virol,* 72**,** 142-50.

DE GEEST, K., TURYK, M. E., HOSKEN, M. I., HUDSON, J. B., LAIMINS, L. A. & WILBANKS, G. D. 1993. Growth and differentiation of human papillomavirus type 31b positive human cervical cell lines. *Gynecol Oncol,* 49**,** 303-10.

DE RUIJTER, A. J., VAN GENNIP, A. H., CARON, H. N., KEMP, S. & VAN KUILENBURG, A. B. 2003. Histone deacetylases (HDACs): characterization of the classical HDAC family. *Biochem J,* 370**,** 737-49.

DE VILLIERS, E. M., FAUQUET, C., BROKER, T. R., BERNARD, H. U. & ZUR HAUSEN, H. 2004. Classification of papillomaviruses. *Virology,* 324**,** 17-27.

DE WILDE, J., DE-CASTRO ARCE, J., SNIJDERS, P. J., MEIJER, C. J., ROSL, F. & STEENBERGEN, R. D. 2008. Alterations in AP-1 and AP-1 regulatory genes during HPV-induced carcinogenesis. *Cell Oncol,* 30**,** 77-87.

DEATON, A. M. & BIRD, A. 2011. CpG islands and the regulation of transcription. *Genes Dev,* 25**,** 1010-22.

DECAPRIO, J. A., LUDLOW, J. W., FIGGE, J., SHEW, J. Y., HUANG, C. M., LEE, W. H., MARSILIO, E., PAUCHA, E. & LIVINGSTON, D. M. 1988. SV40 large tumor antigen forms a specific complex with the product of the retinoblastoma susceptibility gene. *Cell,* 54**,** 275-83.

DEMERS, G. W., HALBERT, C. L. & GALLOWAY, D. A. 1994. Elevated wild-type p53 protein levels in human epithelial cell lines immortalized by the human papillomavirus type 16 E7 gene. *Virology,* 198**,** 169-74.

DENG, W., LIN, B. Y., JIN, G., WHEELER, C. G., MA, T., HARPER, J. W., BROKER, T. R. & CHOW, L. T. 2004. Cyclin/CDK regulates the nucleocytoplasmic localization of the human papillomavirus E1 DNA helicase. *J Virol,* 78**,** 13954-65.

DERKAY, C. S. 1995. Task force on recurrent respiratory papillomas. A preliminary report. *Arch Otolaryngol Head Neck Surg,* 121**,** 1386-91.

DESAINTES, C. & DEMERET, C. 1996. Control of papillomavirus DNA replication and transcription. *Semin Cancer Biol,* 7**,** 339-47.

DHILLON, A. S., HAGAN, S., RATH, O. & KOLCH, W. 2007. MAP kinase signalling pathways in cancer. *Oncogene,* 26**,** 3279-90.

DIMAIO, D. & MATTOON, D. 2001. Mechanisms of cell transformation by papillomavirus E5 proteins. *Oncogene,* 20**,** 7866-73.

DOBROSOTSKAYA, I. Y. & JAMES, G. L. 2000. MAGI-1 interacts with beta-catenin and is associated with cell-cell adhesion structures. *Biochem Biophys Res Commun,* 270**,** 903-9.

DOLLARD, S. C., WILSON, J. L., DEMETER, L. M., BONNEZ, W., REICHMAN, R. C., BROKER, T. R. & CHOW, L. T. 1992. Production of human papillomavirus and modulation of the infectious program in epithelial raft cultures. OFF. *Genes Dev,* 6**,** 1131-42.

DONG, G., BROKER, T. R. & CHOW, L. T. 1994. Human papillomavirus type 11 E2 proteins repress the homologous E6 promoter by interfering with the binding of host transcription factors to adjacent elements. *J Virol,* 68**,** 1115-27.

DONJERKOVIC, D. & SCOTT, D. W. 2000. Regulation of the G1 phase of the mammalian cell cycle. *Cell Res,* 10**,** 1-16.

DOORBAR, J. 2006. Molecular biology of human papillomavirus infection and cervical cancer. *Clinical Science,* 110**,** 525-541.

DOORBAR, J. 2007. Papillomavirus life cycle organization and biomarker selection. *Dis Markers,* 23**,** 297-313.

DOORBAR, J., ELSTON, R. C., NAPTHINE, S., RAJ, K., MEDCALF, E., JACKSON, D., COLEMAN, N., GRIFFIN, H. M., MASTERSON, P., STACEY, S., MENGISTU, Y. & DUNLOP, J. 2000. The E1E4 protein of human papillomavirus type 16 associates with a putative RNA helicase through sequences in its C terminus. *J Virol,* 74**,** 10081-95.

DOORBAR, J., ELY, S., STERLING, J., MCLEAN, C. & CRAWFORD, L. 1991. Specific interaction between HPV-16 E1-E4 and cytokeratins results in collapse of the epithelial cell intermediate filament network. *Nature,* 352**,** 824-7.

DOORBAR, J., FOO, C., COLEMAN, N., MEDCALF, L., HARTLEY, O., PROSPERO, T., NAPTHINE, S., STERLING, J., WINTER, G. & GRIFFIN, H. 1997. Characterization of events during the late stages of HPV16 infection in vivo using high-affinity synthetic Fabs to E4. *Virology,* 238**,** 40-52.

DOORBAR, J. & GALLIMORE, P. H. 1987. Identification of proteins encoded by the L1 and L2 open reading frames of human papillomavirus 1a. *J Virol,* 61**,** 2793-9.

DOORBAR, J., PARTON, A., HARTLEY, K., BANKS, L., CROOK, T., STANLEY, M. & CRAWFORD, L. 1990. Detection of novel splicing patterns in a HPV16-containing keratinocyte cell line. *Virology,* 178**,** 254-62.

DOORBAR, J., QUINT, W., BANKS, L., BRAVO, I. G., STOLER, M., BROKER, T. R. & STANLEY, M. A. 2012. The biology and life-cycle of human papillomaviruses. *Vaccine,* 30 Suppl 5**,** F55-70.

DOTTO, G. P. 2008. Notch tumor suppressor function. *Oncogene,* 27**,** 5115-23.

DOU, S., ZENG, X., CORTES, P., ERDJUMENT-BROMAGE, H., TEMPST, P., HONJO, T. & VALES, L. D. 1994. The recombination signal sequence-binding protein RBP-2N functions as a transcriptional repressor. *Mol Cell Biol,* 14**,** 3310-9.

DOW, L. E., BRUMBY, A. M., MURATORE, R., COOMBE, M. L., SEDELIES, K. A., TRAPANI, J. A., RUSSELL, S. M., RICHARDSON, H. E. & HUMBERT, P. O. 2003. hScrib is a functional homologue of the Drosophila tumour suppressor Scribble. *Oncogene,* 22**,** 9225-30.

DUDLEY, D. D., WANG, H. C. & SUN, X. H. 2009. Hes1 potentiates T cell lymphomagenesis by up-regulating a subset of notch target genes. *PLoS One,* 4**,** e6678.

DYSON, N., HOWLEY, P. M., MUNGER, K. & HARLOW, E. 1989. The human papilloma virus-16 E7 oncoprotein is able to bind to the retinoblastoma gene product. *Science,* 243**,** 934-7.

EFERL, R. & WAGNER, E. F. 2003. AP-1: a double-edged sword in tumorigenesis. *Nat Rev Cancer,* 3**,** 859-68.

EGAWA, K. 2003. Do human papillomaviruses target epidermal stem cells? *Dermatology,* 207**,** 251-4.

EGAWA, K., SHIBASAKI, Y. & DE VILLIERS, E. M. 1993. Double infection with human papillomavirus 1 and human papillomavirus 63 in single cells of a lesion displaying only an human papillomavirus 63-induced cytopathogenic effect. *Lab Invest,* 69**,** 583-8.

EKEOWA-ANDERSON, A. L., PURDIE, K. J., GIBBON, K., BYRNE, C. R., ARBEIT, J. M., HARWOOD, C. A. & O'SHAUGHNESSY, R. F. 2012. AKT1 loss correlates with episomal HPV16 in vulval intraepithelial neoplasia. *PLoS One,* 7**,** e38608.

ELBASHIR, S. M., LENDECKEL, W. & TUSCHL, T. 2001. RNA interference is mediated by 21- and 22-nucleotide RNAs. *Genes Dev,* 15**,** 188-200.

ELLISEN, L. W., BIRD, J., WEST, D. C., SORENG, A. L., REYNOLDS, T. C., SMITH, S. D. & SKLAR, J. 1991. TAN-1, the human homolog of the Drosophila notch gene, is broken by chromosomal translocations in T lymphoblastic neoplasms. *Cell,* 66**,** 649-61.

ELSTON, R. C. 1996. *Identification of cellular proteins which interact with the human papillomavirus E6 protein.* Doctoral thesis, Darwin College, University of Cambridge, Cambridge, United Kingdom.

EMENY, R. T., WHEELER, C. M., JANSEN, K. U., HUNT, W. C., FU, T. M., SMITH, J. F., MACMULLEN, S., ESSER, M. T. & PALIARD, X. 2002. Priming of human papillomavirus type 11-specific humoral and cellular immune responses in college-aged women with a virus-like particle vaccine. *J Virol,* 76**,** 7832-42.

EVANDER, M., FRAZER, I. H., PAYNE, E., QI, Y. M., HENGST, K. & MCMILLAN, N. A. 1997. Identification of the alpha6 integrin as a candidate receptor for papillomaviruses. *J Virol,* 71**,** 2449-56.

EVANS, T. G., BONNEZ, W., ROSE, R. C., KOENIG, S., DEMETER, L., SUZICH, J. A., O'BRIEN, D., CAMPBELL, M., WHITE, W. I., BALSLEY, J. & REICHMAN, R. C. 2001. A Phase 1 study of a recombinant viruslike particle vaccine against human papillomavirus type 11 in healthy adult volunteers. *J Infect Dis,* 183**,** 1485-93.

FAHRAEUS, R., CHEN, W., TRIVEDI, P., KLEIN, G. & OBRINK, B. 1992. Decreased expression of E-cadherin and increased invasive capacity in EBV-LMP-transfected human epithelial and murine adenocarcinoma cells. *Int J Cancer,* 52**,** 834-8.

FAVRE, M., RAMOZ, N. & ORTH, G. 1997. Human papillomaviruses: general features. *Clin Dermatol,* 15**,** 181-98.

FEENEY, K. M. & PARISH, J. L. 2009. Targeting mitotic chromosomes: a conserved mechanism to ensure viral genome persistence. *Proc Biol Sci,* 276**,** 1535-44.

FEHRMANN, F., KLUMPP, D. J. & LAIMINS, L. A. 2003. Human papillomavirus type 31 E5 protein supports cell cycle progression and activates late viral functions upon epithelial differentiation. *J Virol,* 77**,** 2819-31.

FILIPPOVA, M., PARKHURST, L. & DUERKSEN-HUGHES, P. J. 2004. The human papillomavirus 16 E6 protein binds to Fas-associated death domain and protects cells from Fas-triggered apoptosis. *J Biol Chem,* 279**,** 25729-44.

FIRE, A., XU, S., MONTGOMERY, M. K., KOSTAS, S. A., DRIVER, S. E. & MELLO, C. C. 1998. Potent and specific genetic interference by double-stranded RNA in Caenorhabditis elegans. *Nature,* 391**,** 806-11.

FIRESTEIN, B. L. & RONGO, C. 2001. DLG-1 is a MAGUK similar to SAP97 and is required for adherens junction formation. *Mol Biol Cell,* 12**,** 3465-75.

FLORES, E. R., ALLEN-HOFFMANN, B. L., LEE, D. & LAMBERT, P. F. 2000. The human papillomavirus type 16 E7 oncogene is required for the productive stage of the viral life cycle. *J Virol,* 74**,** 6622-31.

FLORES, E. R., ALLEN-HOFFMANN, B. L., LEE, D., SATTLER, C. A. & LAMBERT, P. F. 1999. Establishment of the human papillomavirus type 16

(HPV-16) life cycle in an immortalized human foreskin keratinocyte cell line. *Virology,* 262**,** 344-54.

FLORES, E. R. & LAMBERT, P. F. 1997. Evidence for a switch in the mode of human papillomavirus type 16 DNA replication during the viral life cycle. *J Virol,* 71**,** 7167-79.

FOSTER, S. A., DEMERS, G. W., ETSCHEID, B. G. & GALLOWAY, D. A. 1994. The ability of human papillomavirus E6 proteins to target p53 for degradation in vivo correlates with their ability to abrogate actinomycin D-induced growth arrest. *J Virol,* 68**,** 5698-705.

FRANCIS, R., MCGRATH, G., ZHANG, J., RUDDY, D. A., SYM, M., APFELD, J., NICOLL, M., MAXWELL, M., HAI, B., ELLIS, M. C., PARKS, A. L., XU, W., LI, J., GURNEY, M., MYERS, R. L., HIMES, C. S., HIEBSCH, R., RUBLE, C., NYE, J. S. & CURTIS, D. 2002. aph-1 and pen-2 are required for Notch pathway signaling, gamma-secretase cleavage of betaAPP, and presenilin protein accumulation. *Dev Cell,* 3**,** 85-97.

FRIEDL, F., KIMURA, I., OSATO, T. & ITO, Y. 1970. Studies on a new human cell line (SiHa) derived from carcinoma of uterus. I. Its establishment and morphology. *Proc Soc Exp Biol Med,* 135**,** 543-5.

FUCHS, E., TUMBAR, T. & GUASCH, G. 2004. Socializing with the neighbors: stem cells and their niche. *Cell,* 116**,** 769-78.

FUNK, J. O., WAGA, S., HARRY, J. B., ESPLING, E., STILLMAN, B. & GALLOWAY, D. A. 1997. Inhibition of CDK activity and PCNA-dependent DNA replication by p21 is blocked by interaction with the HPV-16 E7 oncoprotein. *Genes Dev,* 11**,** 2090-100.

GAGE, J. R., MEYERS, C. & WETTSTEIN, F. O. 1990. The E7 proteins of the nononcogenic human papillomavirus type 6b (HPV-6b) and of the oncogenic HPV-16 differ in retinoblastoma protein binding and other properties. *J Virol,* 64**,** 723-30.

GAILANI, M. R. & BALE, A. E. 1999. Acquired and inherited basal cell carcinomas and the patched gene. *Adv Dermatol,* 14**,** 261-83; discussion 284.

GAO, Q., KUMAR, A., SINGH, L., HUIBREGTSE, J. M., BEAUDENON, S., SRINIVASAN, S., WAZER, D. E., BAND, H. & BAND, V. 2002. Human papillomavirus E6-induced degradation of E6TP1 is mediated by E6AP ubiquitin ligase. *Cancer Res,* 62**,** 3315-21.

GAO, Q., SRINIVASAN, S., BOYER, S. N., WAZER, D. E. & BAND, V. 1999. The E6 oncoproteins of high-risk papillomaviruses bind to a novel putative GAP protein, E6TP1, and target it for degradation. *Mol Cell Biol,* 19**,** 733-44.

GARCIA-MATA, R., DUBASH, A. D., SHAREK, L., CARR, H. S., FROST, J. A. & BURRIDGE, K. 2007. The nuclear RhoA exchange factor Net1 interacts with

proteins of the Dlg family, affects their localization, and influences their tumor suppressor activity. *Mol Cell Biol,* 27**,** 8683-97.

GARDIOL, D., KUHNE, C., GLAUNSINGER, B., LEE, S. S., JAVIER, R. & BANKS, L. 1999. Oncogenic human papillomavirus E6 proteins target the discs large tumour suppressor for proteasome-mediated degradation. *Oncogene,* 18**,** 5487-96.

GARLAND, S. M., HERNANDEZ-AVILA, M., WHEELER, C. M., PEREZ, G., HARPER, D. M., LEODOLTER, S., TANG, G. W., FERRIS, D. G., STEBEN, M., BRYAN, J., TADDEO, F. J., RAILKAR, R., ESSER, M. T., SINGS, H. L., NELSON, M., BOSLEGO, J., SATTLER, C., BARR, E. & KOUTSKY, L. A. 2007. Quadrivalent vaccine against human papillomavirus to prevent anogenital diseases. *N Engl J Med,* 356**,** 1928-43.

GARNETT, T. O., FILIPPOVA, M. & DUERKSEN-HUGHES, P. J. 2006. Accelerated degradation of FADD and procaspase 8 in cells expressing human papilloma virus 16 E6 impairs TRAIL-mediated apoptosis. *Cell Death Differ,* 13**,** 1915-26.

GENG, Y., WHORISKEY, W., PARK, M. Y., BRONSON, R. T., MEDEMA, R. H., LI, T., WEINBERG, R. A. & SICINSKI, P. 1999. Rescue of cyclin D1 deficiency by knockin cyclin E. *Cell,* 97**,** 767-77.

GIANNINI, S. L., HUBERT, P., DOYEN, J., BONIVER, J. & DELVENNE, P. 2002. Influence of the mucosal epithelium microenvironment on Langerhans cells: implications for the development of squamous intraepithelial lesions of the cervix. *Int J Cancer,* 97**,** 654-9.

GISSMANN, L., DIEHL, V., SCHULTZ-COULON, H. J. & ZUR HAUSEN, H. 1982. Molecular cloning and characterization of human papilloma virus DNA derived from a laryngeal papilloma. *J Virol,* 44**,** 393-400.

GLAHDER, J. A., HANSEN, C. N., VINTHER, J., MADSEN, B. S. & NORRILD, B. 2003. A promoter within the E6 ORF of human papillomavirus type 16 contributes to the expression of the E7 oncoprotein from a monocistronic mRNA. *J Gen Virol,* 84**,** 3429-41.

GLAUNSINGER, B. A., LEE, S. S., THOMAS, M., BANKS, L. & JAVIER, R. 2000. Interactions of the PDZ-protein MAGI-1 with adenovirus E4-ORF1 and high-risk papillomavirus E6 oncoproteins. *Oncogene,* 19**,** 5270-80.

GLOSS, B. & BERNARD, H. U. 1990. The E6/E7 promoter of human papillomavirus type 16 is activated in the absence of E2 proteins by a sequence-aberrant Sp1 distal element. *J Virol,* 64**,** 5577-84.

GORRINI, C., SQUATRITO, M., LUISE, C., SYED, N., PERNA, D., WARK, L., MARTINATO, F., SARDELLA, D., VERRECCHIA, A., BENNETT, S., CONFALONIERI, S., CESARONI, M., MARCHESI, F., GASCO, M., SCANZIANI, E., CAPRA, M., MAI, S., NUCIFORO, P., CROOK, T., LOUGH, J. & AMATI, B. 2007. Tip60 is a haplo-insufficient tumour suppressor required for an oncogene-induced DNA damage response. *Nature,* 448**,** 1063-7.

GOTTLIEB, T. M. & OREN, M. 1996. p53 in growth control and neoplasia. *Biochim Biophys Acta,* 1287**,** 77-102.

GRAHAM, F. L., SMILEY, J., RUSSELL, W. C. & NAIRN, R. 1977. Characteristics of a human cell line transformed by DNA from human adenovirus type 5. *J Gen Virol,* 36**,** 59-74.

GRAHAM, S. V. 2010. Human papillomavirus: gene expression, regulation and prospects for novel diagnostic methods and antiviral therapies. *Future Microbiol,* 5**,** 1493-506.

GRASSMANN, K., RAPP, B., MASCHEK, H., PETRY, K. U. & IFTNER, T. 1996. Identification of a differentiation-inducible promoter in the E7 open reading frame of human papillomavirus type 16 (HPV-16) in raft cultures of a new cell line containing high copy numbers of episomal HPV-16 DNA. *J Virol,* 70**,** 2339-49.

GRAY, E., PETT, M. R., WARD, D., WINDER, D. M., STANLEY, M. A., ROBERTS, I., SCARPINI, C. G. & COLEMAN, N. 2010. In vitro progression of human papillomavirus 16 episome-associated cervical neoplasia displays fundamental similarities to integrant-associated carcinogenesis. *Cancer Res,* 70**,** 4081-91.

GREENWALD, I. 1998. LIN-12/Notch signaling: lessons from worms and flies. *Genes Dev,* 12**,** 1751-62.

GU, W., COCHRANE, M., LEGGATT, G. R., PAYNE, E., CHOYCE, A., ZHOU, F., TINDLE, R. & MCMILLAN, N. A. 2009. Both treated and untreated tumors are eliminated by short hairpin RNA-based induction of target-specific immune responses. *Proc Natl Acad Sci U S A,* 106**,** 8314-9.

GU, W., PUTRAL, L. & MCMILLAN, N. 2008. siRNA and shRNA as anticancer agents in a cervical cancer model. *Methods Mol Biol,* 442**,** 159-72.

GURLEY, L. R., D'ANNA, J. A., BARHAM, S. S., DEAVEN, L. L. & TOBEY, R. A. 1978. Histone phosphorylation and chromatin structure during mitosis in Chinese hamster cells. *Eur J Biochem,* 84**,** 1-15.

HAFNER, N., DRIESCH, C., GAJDA, M., JANSEN, L., KIRCHMAYR, R., RUNNEBAUM, I. B. & DURST, M. 2008. Integration of the HPV16 genome does not invariably result in high levels of viral oncogene transcripts. *Oncogene,* 27**,** 1610-7.

HALBERT, C. L., DEMERS, G. W. & GALLOWAY, D. A. 1991. The E7 gene of human papillomavirus type 16 is sufficient for immortalization of human epithelial cells. *J Virol,* 65**,** 473-8.

HAMMOND, S. M., CAUDY, A. A. & HANNON, G. J. 2001. Post-transcriptional gene silencing by double-stranded RNA. *Nat Rev Genet,* 2**,** 110-9.

HANNON, G. J. 2002. RNA interference. *Nature,* 418**,** 244-51.

HANSEN, C. N., NIELSEN, L. & NORRILD, B. 2010. Activities of E7 promoters in the human papillomavirus type 16 genome during cell differentiation. *Virus Res,* 150**,** 34-42.

HARDY, J. & ALLSOP, D. 1991. Amyloid deposition as the central event in the aetiology of Alzheimer's disease. *Trends Pharmacol Sci,* 12**,** 383-8.

HARRO, C. D., PANG, Y. Y., RODEN, R. B., HILDESHEIM, A., WANG, Z., REYNOLDS, M. J., MAST, T. C., ROBINSON, R., MURPHY, B. R., KARRON, R. A., DILLNER, J., SCHILLER, J. T. & LOWY, D. R. 2001. Safety and immunogenicity trial in adult volunteers of a human papillomavirus 16 L1 virus-like particle vaccine. *J Natl Cancer Inst,* 93**,** 284-92.

HARWOOD, C. A. & PROBY, C. M. 2002. Human papillomaviruses and non-melanoma skin cancer. *Curr Opin Infect Dis,* 15**,** 101-14.

HAUPT, Y., MAYA, R., KAZAZ, A. & OREN, M. 1997. Mdm2 promotes the rapid degradation of p53. *Nature,* 387**,** 296-9.

HAYFLICK, L. 1965. THE LIMITED IN VITRO LIFETIME OF HUMAN DIPLOID CELL STRAINS. *Exp Cell Res,* 37**,** 614-36.

HE, W., STAPLES, D., SMITH, C. & FISHER, C. 2003. Direct activation of cyclin-dependent kinase 2 by human papillomavirus E7. *J Virol,* 77**,** 10566-74.

HECK, D. V., YEE, C. L., HOWLEY, P. M. & MUNGER, K. 1992. Efficiency of binding the retinoblastoma protein correlates with the transforming capacity of the E7 oncoproteins of the human papillomaviruses. *Proc Natl Acad Sci U S A,* 89**,** 4442-6.

HEMMINGS, B. A. & RESTUCCIA, D. F. 2012. PI3K-PKB/Akt pathway. *Cold Spring Harb Perspect Biol,* 4**,** a011189.

HENKEN, F. E., DE-CASTRO ARCE, J., ROSL, F., BOSCH, L., MEIJER, C. J., SNIJDERS, P. J. & STEENBERGEN, R. D. 2012. The functional role of Notch signaling in HPV-mediated transformation is dose-dependent and linked to AP-1 alterations. *Cell Oncol (Dordr),* 35**,** 77-84.

HENNINGS, H., MICHAEL, D., CHENG, C., STEINERT, P., HOLBROOK, K. & YUSPA, S. H. 1980. Calcium regulation of growth and differentiation of mouse epidermal cells in culture. *Cell,* 19**,** 245-54.

HENRIQUE, D., HIRSINGER, E., ADAM, J., LE ROUX, I., POURQUIE, O., ISH-HOROWICZ, D. & LEWIS, J. 1997. Maintenance of neuroepithelial progenitor cells by Delta-Notch signalling in the embryonic chick retina. *Curr Biol,* 7**,** 661-70.

HERBER, R., LIEM, A., PITOT, H. & LAMBERT, P. F. 1996. Squamous epithelial hyperplasia and carcinoma in mice transgenic for the human papillomavirus type 16 E7 oncogene. *J Virol,* 70**,** 1873-81.

HERBST, L. H., LENZ, J., VAN DOORSLAER, K., CHEN, Z., STACY, B. A., WELLEHAN, J. F., JR., MANIRE, C. A. & BURK, R. D. 2009. Genomic characterization of two novel reptilian papillomaviruses, Chelonia mydas papillomavirus 1 and Caretta caretta papillomavirus 1. *Virology,* 383**,** 131-5.

HERFS, M., VARGAS, S. O., YAMAMOTO, Y., HOWITT, B. E., NUCCI, M. R., HORNICK, J. L., MCKEON, F. D., XIAN, W. & CRUM, C. P. 2013. A novel blueprint for 'top down' differentiation defines the cervical squamocolumnar junction during development, reproductive life, and neoplasia. *J Pathol,* 229**,** 460-8.

HERFS, M., YAMAMOTO, Y., LAURY, A., WANG, X., NUCCI, M. R., MCLAUGHLIN-DRUBIN, M. E., MUNGER, K., FELDMAN, S., MCKEON, F. D., XIAN, W. & CRUM, C. P. 2012. A discrete population of squamocolumnar junction cells implicated in the pathogenesis of cervical cancer. *Proc Natl Acad Sci U S A,* 109**,** 10516-21.

HERREMAN, A., HARTMANN, D., ANNAERT, W., SAFTIG, P., CRAESSAERTS, K., SERNEELS, L., UMANS, L., SCHRIJVERS, V., CHECLER, F., VANDERSTICHELE, H., BAEKELANDT, V., DRESSEL, R., CUPERS, P., HUYLEBROECK, D., ZWIJSEN, A., VAN LEUVEN, F. & DE STROOPER, B. 1999. Presenilin 2 deficiency causes a mild pulmonary phenotype and no changes in amyloid precursor protein processing but enhances the embryonic lethal phenotype of presenilin 1 deficiency. *Proc Natl Acad Sci U S A,* 96**,** 11872-7.

HERRERO, R., HILDESHEIM, A., BRATTI, C., SHERMAN, M. E., HUTCHINSON, M., MORALES, J., BALMACEDA, I., GREENBERG, M. D., ALFARO, M., BURK, R. D., WACHOLDER, S., PLUMMER, M. & SCHIFFMAN, M. 2000. Population-based study of human papillomavirus infection and cervical neoplasia in rural Costa Rica. *J Natl Cancer Inst,* 92**,** 464-74.

HESS, J., ANGEL, P. & SCHORPP-KISTNER, M. 2004. AP-1 subunits: quarrel and harmony among siblings. *J Cell Sci,* 117**,** 5965-73.

HO, G. Y., BIERMAN, R., BEARDSLEY, L., CHANG, C. J. & BURK, R. D. 1998. Natural history of cervicovaginal papillomavirus infection in young women. *N Engl J Med,* 338**,** 423-8.

HORI, K., SEN, A. & ARTAVANIS-TSAKONAS, S. 2013. Notch signaling at a glance. *J Cell Sci,* 126**,** 2135-40.

HORIGUCHI-YAMADA, J., FUKUMI, S., SAITO, S., NAKAYAMA, R., IWASE, S. & YAMADA, H. 2002. DNA topoisomerase II inhibitor, etoposide, induces p21WAF1/CIP1 through down-regulation of c-Myc in K562 cells. *Anticancer Res,* 22**,** 3827-32.

HORNER, S. M., DEFILIPPIS, R. A., MANUELIDIS, L. & DIMAIO, D. 2004. Repression of the human papillomavirus E6 gene initiates p53-dependent, telomerase-independent senescence and apoptosis in HeLa cervical carcinoma cells. *J Virol,* 78**,** 4063-73.

HOWIE, H. L., KOOP, J. I., WEESE, J., ROBINSON, K., WIPF, G., KIM, L. & GALLOWAY, D. A. 2011. Beta-HPV 5 and 8 E6 promote p300 degradation by blocking AKT/p300 association. *PLoS Pathog,* 7**,** e1002211.

HOWLEY, P. M. 1996. Papillomaviridae: the viruses and their replication. *In:* FIELDS, B. N., KNIPE, D. M. & HOWLEY, P. M. (eds.) *Fields Virology.* 3rd ed. Philadelphia, Pa: Lippincott-Raven Publishers.

HSU, C. H., PENG, K. L., JHANG, H. C., LIN, C. H., WU, S. Y., CHIANG, C. M., LEE, S. C., YU, W. C. & JUAN, L. J. 2012. The HPV E6 oncoprotein targets histone methyltransferases for modulating specific gene transcription. *Oncogene,* 31**,** 2335-49.

HSUEH, P. R. 2009. Human papillomavirus, genital warts, and vaccines. *J Microbiol Immunol Infect,* 42**,** 101-6.

HU, J., BUDGEON, L. R., CLADEL, N. M., CULP, T. D., BALOGH, K. K. & CHRISTENSEN, N. D. 2007. Detection of L1, infectious virions and anti-L1 antibody in domestic rabbits infected with cottontail rabbit papillomavirus. *J Gen Virol,* 88**,** 3286-93.

HUBERT, P., CABERG, J. H., GILLES, C., BOUSARGHIN, L., FRANZEN-DETROOZ, E., BONIVER, J. & DELVENNE, P. 2005. E-cadherin-dependent adhesion of dendritic and Langerhans cells to keratinocytes is defective in cervical human papillomavirus-associated (pre)neoplastic lesions. *J Pathol,* 206**,** 346-55.

HUELSKEN, J. & BEHRENS, J. 2002. The Wnt signalling pathway. *J Cell Sci,* 115**,** 3977-8.

HUIBREGTSE, J. M., SCHEFFNER, M. & HOWLEY, P. M. 1991. A cellular protein mediates association of p53 with the E6 oncoprotein of human papillomavirus types 16 or 18. *EMBO J,* 10**,** 4129-35.

HUMMEL, M., HUDSON, J. B. & LAIMINS, L. A. 1992. Differentiation-induced and constitutive transcription of human papillomavirus type 31b in cell lines containing viral episomes. *J Virol,* 66**,** 6070-80.

IFTNER, T., ELBEL, M., SCHOPP, B., HILLER, T., LOIZOU, J. I., CALDECOTT, K. W. & STUBENRAUCH, F. 2002. Interference of papillomavirus E6 protein with single-strand break repair by interaction with XRCC1. *EMBO J,* 21**,** 4741-8.

INGLE, A., GHIM, S., JOH, J., CHEPKOECH, I., BENNETT JENSON, A. & SUNDBERG, J. P. 2011. Novel laboratory mouse papillomavirus (MusPV) infection. *Vet Pathol,* 48**,** 500-5.

INOUE, T., KYO, S., KIYONO, T., ISHIBASHI, M., ISHIWATARI, H., HWANG, Y. I., YUTSUDO, M. & HAKURA, A. 1994. Correlation between tumorigenicity and expression levels or splicing patterns of transcripts of the human papillomavirus type 16 E6 gene. *Jpn J Cancer Res,* 85**,** 357-63.

INOUE, T., OKA, K., YONG-IL, H., VOUSDEN, K. H., KYO, S., JING, P., HAKURA, A. & YUTSUDO, M. 1998. Dispensability of p53 degradation for tumorigenicity and decreased serum requirement of human papillomavirus type 16 E6. *Mol Carcinog,* 21**,** 215-22.

ISAACSON WECHSLER, E., WANG, Q., ROBERTS, I., PAGLIARULO, E., JACKSON, D., UNTERSPERGER, C., COLEMAN, N., GRIFFIN, H. & DOORBAR, J. 2012. Reconstruction of human papillomavirus type 16-mediated early-stage neoplasia implicates E6/E7 deregulation and the loss of contact inhibition in neoplastic progression. *J Virol,* 86**,** 6358-64.

ISHIDATE, T., MATSUMINE, A., TOYOSHIMA, K. & AKIYAMA, T. 2000. The APC-hDLG complex negatively regulates cell cycle progression from the G0/G1 to S phase. *Oncogene,* 19**,** 365-72.

ISHIWATARI, H., HAYASAKA, N., INOUE, H., YUTSUDO, M. & HAKURA, A. 1994. Degradation of p53 only is not sufficient for the growth stimulatory effect of human papillomavirus 16 E6 oncoprotein in human embryonic fibroblasts. *J Med Virol,* 44**,** 243-9.

ISO, T., KEDES, L. & HAMAMORI, Y. 2003. HES and HERP families: multiple effectors of the Notch signaling pathway. *J Cell Physiol,* 194**,** 237-55.

ISO, Y., SAWADA, T., OKADA, T. & KUBOTA, K. 2005. Loss of E-cadherin mRNA and gain of osteopontin mRNA are useful markers for detecting early recurrence of HCV-related hepatocellular carcinoma. *J Surg Oncol,* 92**,** 304-11.

IVANOVA, S., REPNIK, U., BANKS, L., TURK, V. & TURK, B. 2007. Cellular localization of MAGI-1 caspase cleavage products and their role in apoptosis. *Biol Chem,* 388**,** 1195-8.

JACKSON, S., HARWOOD, C., THOMAS, M., BANKS, L. & STOREY, A. 2000. Role of Bak in UV-induced apoptosis in skin cancer and abrogation by HPV E6 proteins. *Genes Dev,* 14**,** 3065-73.

JAMES, M. A., LEE, J. H. & KLINGELHUTZ, A. J. 2006. HPV16-E6 associated hTERT promoter acetylation is E6AP dependent, increased in later passage cells and enhanced by loss of p300. *Int J Cancer,* 119**,** 1878-85.

JANES, S. M., OFSTAD, T. A., CAMPBELL, D. H., WATT, F. M. & PROWSE, D. M. 2004. Transient activation of FOXN1 in keratinocytes induces a transcriptional programme that promotes terminal differentiation: contrasting roles of FOXN1 and Akt. *J Cell Sci,* 117**,** 4157-68.

JEANES, A., GOTTARDI, C. J. & YAP, A. S. 2008. Cadherins and cancer: how does cadherin dysfunction promote tumor progression? *Oncogene,* 27**,** 6920-9.

JEON, S. & LAMBERT, P. F. 1995. Integration of human papillomavirus type 16 DNA into the human genome leads to increased stability of E6 and E7 mRNAs: implications for cervical carcinogenesis. *Proc Natl Acad Sci U S A,* 92**,** 1654-8.

JHA, S., VANDE POL, S., BANERJEE, N. S., DUTTA, A. B., CHOW, L. T. & DUTTA, A. 2010. Destabilization of TIP60 by human papillomavirus E6 results in attenuation of TIP60-dependent transcriptional regulation and apoptotic pathway. *Mol Cell,* 38**,** 700-11.

JIANG, M. & MILNER, J. 2002. Selective silencing of viral gene expression in HPV-positive human cervical carcinoma cells treated with siRNA, a primer of RNA interference. *Oncogene,* 21**,** 6041-8.

JIANG, M. & MILNER, J. 2005. Selective silencing of viral gene E6 and E7 expression in HPV-positive human cervical carcinoma cells using small interfering RNAs. *Methods Mol Biol,* 292**,** 401-20.

JOHANSSON, C. & SCHWARTZ, S. 2013. Regulation of human papillomavirus gene expression by splicing and polyadenylation. *Nat Rev Micro,* 11**,** 239-251.

JOHNSON, S. E. & BARRICK, D. 2012. Dissecting and circumventing the requirement for RAM in CSL-dependent Notch signaling. *PLoS One,* 7**,** e39093.

JONES, D. L. & MUNGER, K. 1996. Interactions of the human papillomavirus E7 protein with cell cycle regulators. *Semin Cancer Biol,* 7**,** 327-37.

JONES, P. F., JAKUBOWICZ, T., PITOSSI, F. J., MAURER, F. & HEMMINGS, B. A. 1991. Molecular cloning and identification of a serine/threonine protein kinase of the second-messenger subfamily. *Proc Natl Acad Sci U S A,* 88**,** 4171-5.

JONES, S. B. 1999. Cancer in the developing world: a call to action. *BMJ,* 319**,** 505-8.

JOYCE, J. G., TUNG, J. S., PRZYSIECKI, C. T., COOK, J. C., LEHMAN, E. D., SANDS, J. A., JANSEN, K. U. & KELLER, P. M. 1999. The L1 major capsid protein of human papillomavirus type 11 recombinant virus-like particles interacts with heparin and cell-surface glycosaminoglycans on human keratinocytes. *J Biol Chem,* 274**,** 5810-22.

KADAJA, M., SILLA, T., USTAV, E. & USTAV, M. 2009. Papillomavirus DNA replication - from initiation to genomic instability. *Virology,* 384**,** 360-8.

KAETHER, C., HAASS, C. & STEINER, H. 2006. Assembly, trafficking and function of gamma-secretase. *Neurodegener Dis,* 3**,** 275-83.

KALANTARI, M., KARLSEN, F., JOHANSSON, B., SIGURJONSSON, T., WARLEBY, B. & HAGMAR, B. 1997. Human papillomavirus findings in relation to cervical intraepithelial neoplasia grade: a study on 476 Stockholm women, using PCR for detection and typing of HPV. *Hum Pathol,* 28**,** 899-904.

KANG, D. E., SORIANO, S., XIA, X., EBERHART, C. G., DE STROOPER, B., ZHENG, H. & KOO, E. H. 2002. Presenilin couples the paired phosphorylation of beta-catenin independent of axin: implications for beta-catenin activation in tumorigenesis. *Cell,* 110**,** 751-62.

KAO, H. Y., ORDENTLICH, P., KOYANO-NAKAGAWA, N., TANG, Z., DOWNES, M., KINTNER, C. R., EVANS, R. M. & KADESCH, T. 1998. A histone deacetylase corepressor complex regulates the Notch signal transduction pathway. *Genes Dev,* 12**,** 2269-77.

KAO, W. H., BEAUDENON, S. L., TALIS, A. L., HUIBREGTSE, J. M. & HOWLEY, P. M. 2000. Human papillomavirus type 16 E6 induces self-ubiquitination of the E6AP ubiquitin-protein ligase. *J Virol,* 74**,** 6408-17.

KARANU, F. N., MURDOCH, B., GALLACHER, L., WU, D. M., KOREMOTO, M., SAKANO, S. & BHATIA, M. 2000. The notch ligand jagged-1 represents a novel growth factor of human hematopoietic stem cells. *J Exp Med,* 192**,** 1365-72.

KENNEDY, M. B. 1995. Origin of PDZ (DHR, GLGF) domains. *Trends Biochem Sci,* 20**,** 350.

KHO, E. Y., WANG, H. K., BANERJEE, N. S., BROKER, T. R. & CHOW, L. T. 2013. HPV-18 E6 mutants reveal p53 modulation of viral DNA amplification in organotypic cultures. *Proc Natl Acad Sci U S A,* 110**,** 7542-9.

KIM, N. G., KOH, E., CHEN, X. & GUMBINER, B. M. 2011. E-cadherin mediates contact inhibition of proliferation through Hippo signaling-pathway components. *Proc Natl Acad Sci U S A,* 108**,** 11930-5.

KING, I. N., KATHIRIYA, I. S., MURAKAMI, M., NAKAGAWA, M., GARDNER, K. A., SRIVASTAVA, D. & NAKAGAWA, O. 2006. Hrt and Hes negatively regulate Notch signaling through interactions with RBP-Jkappa. *Biochem Biophys Res Commun,* 345**,** 446-52.

KIRNBAUER, R., BOOY, F., CHENG, N., LOWY, D. R. & SCHILLER, J. T. 1992. Papillomavirus L1 major capsid protein self-assembles into virus-like particles that are highly immunogenic. *Proc Natl Acad Sci U S A,* 89**,** 12180-4.

KIYONO, T., HIRAIWA, A., FUJITA, M., HAYASHI, Y., AKIYAMA, T. & ISHIBASHI, M. 1997. Binding of high-risk human papillomavirus E6 oncoproteins to the human homologue of the Drosophila discs large tumor suppressor protein. *Proc Natl Acad Sci U S A,* 94**,** 11612-6.

KLAES, R., WOERNER, S. M., RIDDER, R., WENTZENSEN, N., DUERST, M., SCHNEIDER, A., LOTZ, B., MELSHEIMER, P. & VON KNEBEL DOEBERITZ, M. 1999. Detection of high-risk cervical intraepithelial neoplasia and cervical cancer by amplification of transcripts derived from integrated papillomavirus oncogenes. *Cancer Res,* 59**,** 6132-6.

KLINGELHUTZ, A. J., FOSTER, S. A. & MCDOUGALL, J. K. 1996. Telomerase activation by the E6 gene product of human papillomavirus type 16. *Nature,* 380**,** 79-82.

KLUMPP, D. J. & LAIMINS, L. A. 1999. Differentiation-induced changes in promoter usage for transcripts encoding the human papillomavirus type 31 replication protein E1. *Virology,* 257**,** 239-46.

KOLLY, C., SUTER, M. M. & MULLER, E. J. 2005. Proliferation, cell cycle exit, and onset of terminal differentiation in cultured keratinocytes: pre-programmed pathways in control of C-Myc and Notch1 prevail over extracellular calcium signals. *J Invest Dermatol,* 124**,** 1014-25.

KORINEK, V., BARKER, N., MOERER, P., VAN DONSELAAR, E., HULS, G., PETERS, P. J. & CLEVERS, H. 1998. Depletion of epithelial stem-cell compartments in the small intestine of mice lacking Tcf-4. *Nat Genet,* 19**,** 379-83.

KRUBASIK, D., IYER, N. G., ENGLISH, W. R., AHMED, A. A., VIAS, M., ROSKELLEY, C., BRENTON, J. D., CALDAS, C. & MURPHY, G. 2006. Absence of p300 induces cellular phenotypic changes characteristic of epithelial to mesenchyme transition. *Br J Cancer,* 94**,** 1326-32.

KUHNE, C. & BANKS, L. 1998. E3-ubiquitin ligase/E6-AP links multicopy maintenance protein 7 to the ubiquitination pathway by a novel motif, the L2G box. *J Biol Chem,* 273**,** 34302-9.

KUKIMOTO, I., AIHARA, S., YOSHIIKE, K. & KANDA, T. 1998. Human papillomavirus oncoprotein E6 binds to the C-terminal region of human minichromosome maintenance 7 protein. *Biochem Biophys Res Commun,* 249**,** 258-62.

LACE, M. J., YAMAKAWA, Y., USHIKAI, M., ANSON, J. R., HAUGEN, T. H. & TUREK, L. P. 2009. Cellular factor YY1 downregulates the human papillomavirus 16 E6/E7 promoter, P97, in vivo and in vitro from a negative element overlapping the transcription-initiation site. *J Gen Virol,* 90**,** 2402-12.

LAIMINS, L. A. 1993. The biology of human papillomaviruses: from warts to cancer. *Infect Agents Dis,* 2**,** 74-86.

LAMBERT, P. F., OZBUN, M. A., COLLINS, A., HOLMGREN, S., LEE, D. & NAKAHARA, T. 2005. Using an immortalized cell line to study the HPV life cycle in organotypic "raft" cultures. *Methods Mol Med,* 119**,** 141-55.

LANE, D. P. & CRAWFORD, L. V. 1979. T antigen is bound to a host protein in SV40-transformed cells. *Nature,* 278**,** 261-3.

LAURSON, J., KHAN, S., CHUNG, R., CROSS, K. & RAJ, K. 2010. Epigenetic repression of E-cadherin by human papillomavirus 16 E7 protein. *Carcinogenesis,* 31**,** 918-26.

LEE, C. & LAIMINS, L. A. 2004. Role of the PDZ domain-binding motif of the oncoprotein E6 in the pathogenesis of human papillomavirus type 31. *J Virol,* 78**,** 12366-77.

LEE, S. F., SHAH, S., YU, C., WIGLEY, W. C., LI, H., LIM, M., PEDERSEN, K., HAN, W., THOMAS, P., LUNDKVIST, J., HAO, Y. H. & YU, G. 2004. A conserved GXXXG motif in APH-1 is critical for assembly and activity of the gamma-secretase complex. *J Biol Chem,* 279**,** 4144-52.

LEE, S. S., WEISS, R. S. & JAVIER, R. T. 1997. Binding of human virus oncoproteins to hDlg/SAP97, a mammalian homolog of the Drosophila discs large tumor suppressor protein. *Proc Natl Acad Sci U S A,* 94**,** 6670-5.

LEFORT, K., MANDINOVA, A., OSTANO, P., KOLEV, V., CALPINI, V., KOLFSCHOTEN, I., DEVGAN, V., LIEB, J., RAFFOUL, W., HOHL, D., NEEL, V., GARLICK, J., CHIORINO, G. & DOTTO, G. P. 2007. Notch1 is a p53 target gene involved in human keratinocyte tumor suppression through negative regulation of ROCK1/2 and MRCKalpha kinases. *Genes Dev,* 21**,** 562-77.

LEONE, G., DEGREGORI, J., YAN, Z., JAKOI, L., ISHIDA, S., WILLIAMS, R. S. & NEVINS, J. R. 1998. E2F3 activity is regulated during the cell cycle and is required for the induction of S phase. *Genes Dev,* 12**,** 2120-30.

LEVY-LAHAD, E., WIJSMAN, E. M., NEMENS, E., ANDERSON, L., GODDARD, K. A., WEBER, J. L., BIRD, T. D. & SCHELLENBERG, G. D. 1995. A familial Alzheimer's disease locus on chromosome 1. *Science,* 269**,** 970-3.

LI, T., WEN, H., BRAYTON, C., DAS, P., SMITHSON, L. A., FAUQ, A., FAN, X., CRAIN, B. J., PRICE, D. L., GOLDE, T. E., EBERHART, C. G. & WONG, P. C. 2007. Epidermal growth factor receptor and notch pathways participate in the tumor suppressor function of gamma-secretase. *J Biol Chem,* 282**,** 32264-73.

LI, X. & COFFINO, P. 1996. High-risk human papillomavirus E6 protein has two distinct binding sites within p53, of which only one determines degradation. *J Virol,* 70**,** 4509-16.

LICHTIG, H., GILBOA, D. A., JACKMAN, A., GONEN, P., LEVAV-COHEN, Y., HAUPT, Y. & SHERMAN, L. 2009. HPV16 E6 augments Wnt signaling in an E6AP-dependent manner. *Virology,* 396**,** 47-58.

LIM, J., KIM, J. H., PAENG, J. Y., KIM, M. J., HONG, S. D., LEE, J. I. & HONG, S. P. 2005. Prognostic value of activated Akt expression in oral squamous cell carcinoma. *J Clin Pathol,* 58**,** 1199-205.

LIU, J., LIAN, Z., HAN, S., WAYE, M. M., WANG, H., WU, M. C., WU, K., DING, J., ARBUTHNOT, P., KEW, M., FAN, D. & FEITELSON, M. A. 2006. Downregulation of E-cadherin by hepatitis B virus X antigen in hepatocellullar carcinoma. *Oncogene,* 25**,** 1008-17.

LIU, X., DAKIC, A., ZHANG, Y., DAI, Y., CHEN, R. & SCHLEGEL, R. 2009. HPV E6 protein interacts physically and functionally with the cellular telomerase complex. *Proc Natl Acad Sci U S A,* 106**,** 18780-5.

LIU, X., YUAN, H., FU, B., DISBROW, G. L., APOLINARIO, T., TOMAIC, V., KELLEY, M. L., BAKER, C. C., HUIBREGTSE, J. & SCHLEGEL, R. 2005. The E6AP ubiquitin ligase is required for transactivation of the hTERT promoter by the human papillomavirus E6 oncoprotein. *J Biol Chem,* 280**,** 10807-16.

LOGAN, C. Y. & NUSSE, R. 2004. The Wnt signaling pathway in development and disease. *Annu Rev Cell Dev Biol,* 20**,** 781-810.

LONGWORTH, M. S. & LAIMINS, L. A. 2004. Pathogenesis of human papillomaviruses in differentiating epithelia. *Microbiol Mol Biol Rev,* 68**,** 362-72.

LONGWORTH, M. S., WILSON, R. & LAIMINS, L. A. 2005. HPV31 E7 facilitates replication by activating E2F2 transcription through its interaction with HDACs. *EMBO J,* 24**,** 1821-30.

LOWELL, S., JONES, P., LE ROUX, I., DUNNE, J. & WATT, F. M. 2000. Stimulation of human epidermal differentiation by delta-notch signalling at the boundaries of stem-cell clusters. *Curr Biol,* 10**,** 491-500.

LUE, R. A., MARFATIA, S. M., BRANTON, D. & CHISHTI, A. H. 1994. Cloning and characterization of hdlg: the human homologue of the Drosophila discs large tumor suppressor binds to protein 4.1. *Proc Natl Acad Sci U S A,* 91**,** 9818-22.

MAJOR, T., SZARKA, K., SZIKLAI, I., GERGELY, L. & CZEGLEDY, J. 2005. The characteristics of human papillomavirus DNA in head and neck cancers and papillomas. *J Clin Pathol,* 58**,** 51-5.

MALANCHI, I., ACCARDI, R., DIEHL, F., SMET, A., ANDROPHY, E., HOHEISEL, J. & TOMMASINO, M. 2004. Human papillomavirus type 16 E6 promotes retinoblastoma protein phosphorylation and cell cycle progression. *J Virol,* 78**,** 13769-78.

MALANCHI, I., CALDEIRA, S., KRUTZFELDT, M., GIARRE, M., ALUNNI-FABBRONI, M. & TOMMASINO, M. 2002. Identification of a novel activity of human papillomavirus type 16 E6 protein in deregulating the G1/S transition. *Oncogene,* 21**,** 5665-72.

MAMMAS, I. N., SOURVINOS, G. & SPANDIDOS, D. A. 2009. Human papilloma virus (HPV) infection in children and adolescents. *Eur J Pediatr,* 168**,** 267-73.

MANTOVANI, F., MASSIMI, P. & BANKS, L. 2001. Proteasome-mediated regulation of the hDlg tumour suppressor protein. *J Cell Sci,* 114**,** 4285-92.

MAO, J. H., TO, M. D., PEREZ-LOSADA, J., WU, D., DEL ROSARIO, R. & BALMAIN, A. 2004. Mutually exclusive mutations of the Pten and ras pathways in skin tumor progression. *Genes Dev,* 18**,** 1800-5.

MARAMBAUD, P., SHIOI, J., SERBAN, G., GEORGAKOPOULOS, A., SARNER, S., NAGY, V., BAKI, L., WEN, P., EFTHIMIOPOULOS, S., SHAO, Z., WISNIEWSKI, T. & ROBAKIS, N. K. 2002. A presenilin-1/gamma-secretase

cleavage releases the E-cadherin intracellular domain and regulates disassembly of adherens junctions. *EMBO J,* 21**,** 1948-56.

MARGOLIN, A. A., PALOMERO, T., SUMAZIN, P., CALIFANO, A., FERRANDO, A. A. & STOLOVITZKY, G. 2009. ChIP-on-chip significance analysis reveals large-scale binding and regulation by human transcription factor oncogenes. *Proc Natl Acad Sci U S A,* 106**,** 244-9.

MASAMHA, C. P. & BENBROOK, D. M. 2009. Cyclin D1 degradation is sufficient to induce G1 cell cycle arrest despite constitutive expression of cyclin E2 in ovarian cancer cells. *Cancer Res,* 69**,** 6565-72.

MASSIMI, P., NARAYAN, N., CUENDA, A. & BANKS, L. 2006. Phosphorylation of the discs large tumour suppressor protein controls its membrane localisation and enhances its susceptibility to HPV E6-induced degradation. *Oncogene,* 25**,** 4276-85.

MASTERSON, P. J., STANLEY, M. A., LEWIS, A. P. & ROMANOS, M. A. 1998. A C-terminal helicase domain of the human papillomavirus E1 protein binds E2 and the DNA polymerase alpha-primase p68 subunit. *J Virol,* 72**,** 7407-19.

MATSUMINE, A., OGAI, A., SENDA, T., OKUMURA, N., SATOH, K., BAEG, G. H., KAWAHARA, T., KOBAYASHI, S., OKADA, M., TOYOSHIMA, K. & AKIYAMA, T. 1996. Binding of APC to the human homolog of the Drosophila discs large tumor suppressor protein. *Science,* 272**,** 1020-3.

MATTHEWS, K., LEONG, C. M., BAXTER, L., INGLIS, E., YUN, K., BACKSTROM, B. T., DOORBAR, J. & HIBMA, M. 2003. Depletion of Langerhans cells in human papillomavirus type 16-infected skin is associated with E6-mediated down regulation of E-cadherin. *J Virol,* 77**,** 8378-85.

MCBRIDE, A. A. 2008. Replication and partitioning of papillomavirus genomes. *Adv Virus Res,* 72**,** 155-205.

MCCLATCHEY, A. I. & YAP, A. S. 2012. Contact inhibition (of proliferation) redux. *Curr Opin Cell Biol,* 24**,** 685-94.

MCCUSKER, S. M., MACQUEEN, I., LOUGH, G., MACDONALD, A. I., CAMPBELL, C. & GRAHAM, S. V. 2013. Gaps in detailed knowledge of human papillomavirus (HPV) and the HPV vaccine among medical students in Scotland. *BMC Public Health,* 13**,** 264.

MCELROY, B., POWELL, J. C. & MCCARTHY, J. V. 2007. The insulin-like growth factor 1 (IGF-1) receptor is a substrate for gamma-secretase-mediated intramembrane proteolysis. *Biochem Biophys Res Commun,* 358**,** 1136-41.

MCINTOSH, P. B., LASKEY, P., SULLIVAN, K., DAVY, C., WANG, Q., JACKSON, D. J., GRIFFIN, H. M. & DOORBAR, J. 2010. E1--E4-mediated keratin phosphorylation and ubiquitylation: a mechanism for keratin depletion in HPV16-infected epithelium. *J Cell Sci,* 123**,** 2810-22.

MCLAUGHLIN, M., HALE, R., ELLSTON, D., GAUDET, S., LUE, R. A. & VIEL, A. 2002. The distribution and function of alternatively spliced insertions in hDlg. *J Biol Chem,* 277**,** 6406-12.

MCLAUGHLIN-DRUBIN, M. E., CHRISTENSEN, N. D. & MEYERS, C. 2004. Propagation, infection, and neutralization of authentic HPV16 virus. *Virology,* 322**,** 213-9.

MCLAUGHLIN-DRUBIN, M. E. & MEYERS, C. 2004. Evidence for the coexistence of two genital HPV types within the same host cell in vitro. *Virology,* 321**,** 173-80.

MCLAUGHLIN-DRUBIN, M. E. & MUNGER, K. 2009. Oncogenic activities of human papillomaviruses. *Virus Res,* 143**,** 195-208.

MEIER-STIEGEN, F., SCHWANBECK, R., BERNOTH, K., MARTINI, S., HIERONYMUS, T., RUAU, D., ZENKE, M. & JUST, U. 2010. Activated Notch1 target genes during embryonic cell differentiation depend on the cellular context and include lineage determinants and inhibitors. *PLoS One,* 5**,** e11481.

MENGES, C. W., BAGLIA, L. A., LAPOINT, R. & MCCANCE, D. J. 2006. Human papillomavirus type 16 E7 up-regulates AKT activity through the retinoblastoma protein. *Cancer Res,* 66**,** 5555-9.

MEYERS, J. M., SPANGLE, J. M. & MUNGER, K. 2013. The Human Papillomavirus Type 8 E6 Protein Interferes with NOTCH Activation during Keratinocyte Differentiation. *J Virol,* 87**,** 4762-7.

MIDDLETON, K., PEH, W., SOUTHERN, S., GRIFFIN, H., SOTLAR, K., NAKAHARA, T., EL-SHERIF, A., MORRIS, L., SETH, R., HIBMA, M., JENKINS, D., LAMBERT, P., COLEMAN, N. & DOORBAR, J. 2003. Organization of human papillomavirus productive cycle during neoplastic progression provides a basis for selection of diagnostic markers. *J Virol,* 77**,** 10186-201.

MILLIGAN, S. G., VEERAPRADITSIN, T., AHAMET, B., MOLE, S. & GRAHAM, S. V. 2007. Analysis of novel human papillomavirus type 16 late mRNAs in differentiated W12 cervical epithelial cells. *Virology,* 360**,** 172-81.

MINCHEVA, A., GISSMANN, L. & ZUR HAUSEN, H. 1987. Chromosomal integration sites of human papillomavirus DNA in three cervical cancer cell lines mapped by in situ hybridization. *Med Microbiol Immunol,* 176**,** 245-56.

MIZUHARA, E., NAKATANI, T., MINAKI, Y., SAKAMOTO, Y., ONO, Y. & TAKAI, Y. 2005. MAGI1 recruits Dll1 to cadherin-based adherens junctions and stabilizes it on the cell surface. *J Biol Chem,* 280**,** 26499-507.

MORAL, M. & PARAMIO, J. M. 2008. Akt pathway as a target for therapeutic intervention in HNSCC. *Histol Histopathol,* 23**,** 1269-78.

MORGAN, T. H. 1917. The theory of the gene. *The American Naturalist,* 51**,** 513-544.

MORRIS, P. J., DENT, C. L., RING, C. J. & LATCHMAN, D. S. 1993. The octamer binding site in the HPV16 regulatory region produces opposite effects on gene expression in cervical and non-cervical cells. *Nucleic Acids Res,* 21**,** 1019-23.

MOSCHOS, S. A., FRICK, M., TAYLOR, B., TURNPENNY, P., GRAVES, H., SPINK, K. G., BRADY, K., LAMB, D., COLLINS, D., ROCKEL, T. D., WEBER, M., LAZARI, O., PEREZ-TOSAR, L., FANCY, S. A., LAPTHORN, C., GREEN, M. X., EVANS, S., SELBY, M., JONES, G., JONES, L., KEARNEY, S., MECHICHE, H., GIKUNJU, D., SUBRAMANIAN, R., UHLMANN, E., JURK, M., VOLLMER, J., CIARAMELLA, G. & YEADON, M. 2011. Uptake, efficacy, and systemic distribution of naked, inhaled short interfering RNA (siRNA) and locked nucleic acid (LNA) antisense. *Mol Ther,* 19**,** 2163-8.

MOSICKI, B., STOLLER, M., WRIGHT, T., KINNEY, W., PETRY, U. & TATTI, S. CIN 2: To treat or not to treat a lesion that may or may not exist. 28th International Papillomavirus Conference and Clinical and Public Health Workshops, December 5th 2012 San Juan, Puerto Rico.

MOUNTS, P., SHAH, K. V. & KASHIMA, H. 1982. Viral etiology of juvenile- and adult-onset squamous papilloma of the larynx. *Proc Natl Acad Sci U S A,* 79**,** 5425-9.

MULLIGAN, P., YANG, F., DI STEFANO, L., JI, J. Y., OUYANG, J., NISHIKAWA, J. L., TOIBER, D., KULKARNI, M., WANG, Q., NAJAFI-SHOUSHTARI, S. H., MOSTOSLAVSKY, R., GYGI, S. P., GILL, G., DYSON, N. J. & NAAR, A. M. 2011. A SIRT1-LSD1 corepressor complex regulates Notch target gene expression and development. *Mol Cell,* 42**,** 689-99.

MUMM, J. S. & KOPAN, R. 2000. Notch signaling: from the outside in. *Dev Biol,* 228**,** 151-65.

MUNGER, K., WERNESS, B. A., DYSON, N., PHELPS, W. C., HARLOW, E. & HOWLEY, P. M. 1989. Complex formation of human papillomavirus E7 proteins with the retinoblastoma tumor suppressor gene product. *EMBO J,* 8**,** 4099-105.

NAGASAKA, K., NAKAGAWA, S., YANO, T., TAKIZAWA, S., MATSUMOTO, Y., TSURUGA, T., NAKAGAWA, K., MINAGUCHI, T., ODA, K., HIRAIKE-WADA, O., OOISHI, H., YASUGI, T. & TAKETANI, Y. 2006. Human homolog of Drosophila tumor suppressor Scribble negatively regulates cell-cycle progression from G1 to S phase by localizing at the basolateral membrane in epithelial cells. *Cancer Sci,* 97**,** 1217-25.

NAIR, P., SOMASUNDARAM, K. & KRISHNA, S. 2003. Activated Notch1 inhibits p53-induced apoptosis and sustains transformation by human papillomavirus type 16 E6 and E7 oncogenes through a PI3K-PKB/Akt-dependent pathway. *J Virol,* 77**,** 7106-12.

NAKAGAWA, S. & HUIBREGTSE, J. M. 2000. Human scribble (Vartul) is targeted for ubiquitin-mediated degradation by the high-risk papillomavirus E6 proteins and the E6AP ubiquitin-protein ligase. *Mol Cell Biol,* 20**,** 8244-53.

NAKAHARA, T., PEH, W. L., DOORBAR, J., LEE, D. & LAMBERT, P. F. 2005. Human papillomavirus type 16 E1circumflexE4 contributes to multiple facets of the papillomavirus life cycle. *J Virol,* 79**,** 13150-65.

NALDINI, L., BLOMER, U., GALLAY, P., ORY, D., MULLIGAN, R., GAGE, F. H., VERMA, I. M. & TRONO, D. 1996. In vivo gene delivery and stable transduction of nondividing cells by a lentiviral vector. *Science,* 272**,** 263-7.

NARAYAN, N., SUBBAIAH, V. K. & BANKS, L. 2009. The high-risk HPV E6 oncoprotein preferentially targets phosphorylated nuclear forms of hDlg. *Virology,* 387**,** 1-4.

NAVARRO, C., NOLA, S., AUDEBERT, S., SANTONI, M. J., ARSANTO, J. P., GINESTIER, C., MARCHETTO, S., JACQUEMIER, J., ISNARDON, D., LE BIVIC, A., BIRNBAUM, D. & BORG, J. P. 2005. Junctional recruitment of mammalian Scribble relies on E-cadherin engagement. *Oncogene,* 24**,** 4330-9.

NAVARRO, P., GOMEZ, M., PIZARRO, A., GAMALLO, C., QUINTANILLA, M. & CANO, A. 1991. A role for the E-cadherin cell-cell adhesion molecule during tumor progression of mouse epidermal carcinogenesis. *J Cell Biol,* 115**,** 517-33.

NEES, M., GEOGHEGAN, J. M., HYMAN, T., FRANK, S., MILLER, L. & WOODWORTH, C. D. 2001. Papillomavirus type 16 oncogenes downregulate expression of interferon-responsive genes and upregulate proliferation-associated and NF-kappaB-responsive genes in cervical keratinocytes. *J Virol,* 75**,** 4283-96.

NGUYEN, C. L. & MUNGER, K. 2008. Direct association of the HPV16 E7 oncoprotein with cyclin A/CDK2 and cyclin E/CDK2 complexes. *Virology,* 380**,** 21-5.

NGUYEN, M. L., NGUYEN, M. M., LEE, D., GRIEP, A. E. & LAMBERT, P. F. 2003. The PDZ ligand domain of the human papillomavirus type 16 E6 protein is required for E6's induction of epithelial hyperplasia in vivo. *J Virol,* 77**,** 6957-64.

NI, C. Y., MURPHY, M. P., GOLDE, T. E. & CARPENTER, G. 2001. gamma - Secretase cleavage and nuclear localization of ErbB-4 receptor tyrosine kinase. *Science,* 294**,** 2179-81.

NICOLAIDES, L. 2011. *Interactions of the Human Papillomavirus E6 protein and their role in the persistence of viral episomes* Doctoral thesis, University College London, London, United Kingdom.

NICOLAIDES, L., DAVY, C., RAJ, K., KRANJEC, C., BANKS, L. & DOORBAR, J. 2011. Stabilization of HPV16 E6 protein by PDZ proteins, and potential implications for genome maintenance. *Virology,* 414**,** 137-45.

NICOLAS, M., WOLFER, A., RAJ, K., KUMMER, J. A., MILL, P., VAN NOORT, M., HUI, C. C., CLEVERS, H., DOTTO, G. P. & RADTKE, F. 2003. Notch1 functions as a tumor suppressor in mouse skin. *Nat Genet,* 33**,** 416-21.

NIU, X. Y., PENG, Z. L., DUAN, W. Q., WANG, H. & WANG, P. 2006. Inhibition of HPV 16 E6 oncogene expression by RNA interference in vitro and in vivo. *Int J Gynecol Cancer,* 16**,** 743-51.

O'SHAUGHNESSY, R. F., AKGUL, B., STOREY, A., PFISTER, H., HARWOOD, C. A. & BYRNE, C. 2007a. Cutaneous human papillomaviruses down-regulate AKT1, whereas AKT2 up-regulation and activation associates with tumors. *Cancer Res,* 67**,** 8207-15.

O'SHAUGHNESSY, R. F., WELTI, J. C., COOKE, J. C., AVILION, A. A., MONKS, B., BIRNBAUM, M. J. & BYRNE, C. 2007b. AKT-dependent HspB1 (Hsp27) activity in epidermal differentiation. *J Biol Chem,* 282**,** 17297-305.

OBENAUER, J. C., DENSON, J., MEHTA, P. K., SU, X., MUKATIRA, S., FINKELSTEIN, D. B., XU, X., WANG, J., MA, J., FAN, Y., RAKESTRAW, K. M., WEBSTER, R. G., HOFFMANN, E., KRAUSS, S., ZHENG, J., ZHANG, Z. & NAEVE, C. W. 2006. Large-scale sequence analysis of avian influenza isolates. *Science,* 311**,** 1576-80.

OSWALD, F., TAUBER, B., DOBNER, T., BOURTEELE, S., KOSTEZKA, U., ADLER, G., LIPTAY, S. & SCHMID, R. M. 2001. p300 acts as a transcriptional coactivator for mammalian Notch-1. *Mol Cell Biol,* 21**,** 7761-74.

OZBUN, M. A. & MEYERS, C. 1997. Characterization of late gene transcripts expressed during vegetative replication of human papillomavirus type 31b. *J Virol,* 71**,** 5161-72.

PAAVONEN, J., NAUD, P., SALMERON, J., WHEELER, C. M., CHOW, S. N., APTER, D., KITCHENER, H., CASTELLSAGUE, X., TEIXEIRA, J. C., SKINNER, S. R., HEDRICK, J., JAISAMRARN, U., LIMSON, G., GARLAND, S., SZAREWSKI, A., ROMANOWSKI, B., AOKI, F. Y., SCHWARZ, T. F., POPPE, W. A., BOSCH, F. X., JENKINS, D., HARDT, K., ZAHAF, T., DESCAMPS, D., STRUYF, F., LEHTINEN, M. & DUBIN, G. 2009. Efficacy of human papillomavirus (HPV)-16/18 AS04-adjuvanted vaccine against cervical infection and precancer caused by oncogenic HPV types (PATRICIA): final analysis of a double-blind, randomised study in young women. *Lancet,* 374**,** 301-14.

PADDISON, P. J. & HANNON, G. J. 2002. RNA interference: the new somatic cell genetics? *Cancer Cell,* 2**,** 17-23.

PARDOSSI-PIQUARD, R., YANG, S. P., KANEMOTO, S., GU, Y., CHEN, F., BOHM, C., SEVALLE, J., LI, T., WONG, P. C., CHECLER, F., SCHMITT-ULMS, G., ST GEORGE-HYSLOP, P. & FRASER, P. E. 2009. APH1 polar transmembrane residues regulate the assembly and activity of presenilin complexes. *J Biol Chem,* 284**,** 16298-307.

PARK, J. S., KIM, E. J., KWON, H. J., HWANG, E. S., NAMKOONG, S. E. & UM, S. J. 2000. Inactivation of interferon regulatory factor-1 tumor suppressor protein by HPV E7 oncoprotein. Implication for the E7-mediated immune evasion mechanism in cervical carcinogenesis. *J Biol Chem,* 275**,** 6764-9.

PECORARO, G., MORGAN, D. & DEFENDI, V. 1989. Differential effects of human papillomavirus type 6, 16, and 18 DNAs on immortalization and transformation of human cervical epithelial cells. *Proc Natl Acad Sci U S A,* 86**,** 563-7.

PEH, W. L. & DOORBAR, J. 2005. Detection of papillomavirus proteins and DNA in paraffin-embedded tissue sections. *Methods Mol Med,* 119**,** 49-59.

PEH, W. L., MIDDLETON, K., CHRISTENSEN, N., NICHOLLS, P., EGAWA, K., SOTLAR, K., BRANDSMA, J., PERCIVAL, A., LEWIS, J., LIU, W. J. & DOORBAR, J. 2002. Life cycle heterogeneity in animal models of human papillomavirus-associated disease. *J Virol,* 76**,** 10401-16.

PENG, X. D., XU, P. Z., CHEN, M. L., HAHN-WINDGASSEN, A., SKEEN, J., JACOBS, J., SUNDARARAJAN, D., CHEN, W. S., CRAWFORD, S. E., COLEMAN, K. G. & HAY, N. 2003. Dwarfism, impaired skin development, skeletal muscle atrophy, delayed bone development, and impeded adipogenesis in mice lacking Akt1 and Akt2. *Genes Dev,* 17**,** 1352-65.

PETCHERSKI, A. G. & KIMBLE, J. 2000. Mastermind is a putative activator for Notch. *Curr Biol,* 10**,** R471-3.

PFISTER, H. 1992. Human papillomaviruses and skin cancer. *Semin Cancer Biol,* 3**,** 263-71.

PFISTER, H. 2003. Chapter 8: Human papillomavirus and skin cancer. *J Natl Cancer Inst Monogr***,** 52-6.

PHALON, C., RAO, D. D. & NEMUNAITIS, J. 2010. Potential use of RNA interference in cancer therapy. *Expert Rev Mol Med,* 12**,** e26.

PHELPS, W. C. & HOWLEY, P. M. 1987. Transcriptional trans-activation by the human papillomavirus type 16 E2 gene product. *J Virol,* 61**,** 1630-8.

PICCINI, A., STOREY, A., ROMANOS, M. & BANKS, L. 1997. Regulation of human papillomavirus type 16 DNA replication by E2, glucocorticoid hormone and epidermal growth factor. *J Gen Virol,* 78 (Pt 8)**,** 1963-70.

PIM, D., MASSIMI, P., DILWORTH, S. M. & BANKS, L. 2005. Activation of the protein kinase B pathway by the HPV-16 E7 oncoprotein occurs through a mechanism involving interaction with PP2A. *Oncogene,* 24**,** 7830-8.

PIM, D., THOMAS, M., JAVIER, R., GARDIOL, D. & BANKS, L. 2000. HPV E6 targeted degradation of the discs large protein: evidence for the involvement of a novel ubiquitin ligase. *Oncogene,* 19**,** 719-25.

PROKOP, S., SHIROTANI, K., EDBAUER, D., HAASS, C. & STEINER, H. 2004. Requirement of PEN-2 for stabilization of the presenilin N-/C-terminal fragment heterodimer within the gamma-secretase complex. *J Biol Chem,* 279**,** 23255-61.

PUTRAL, L. N., BYWATER, M. J., GU, W., SAUNDERS, N. A., GABRIELLI, B. G., LEGGATT, G. R. & MCMILLAN, N. A. 2005. RNA interference against human papillomavirus oncogenes in cervical cancer cells results in increased sensitivity to cisplatin. *Mol Pharmacol,* 68**,** 1311-9.

PYEON, D., PEARCE, S. M., LANK, S. M., AHLQUIST, P. & LAMBERT, P. F. 2009. Establishment of human papillomavirus infection requires cell cycle progression. *PLoS Pathog,* 5**,** e1000318.

QI, Z., XU, X., ZHANG, B., LI, Y., LIU, J., CHEN, S., CHEN, G. & HUO, X. 2010. Effect of simultaneous silencing of HPV-18 E6 and E7 on inducing apoptosis in HeLa cells. *Biochem Cell Biol,* 88**,** 697-704.

QIN, Y., CAPALDO, C., GUMBINER, B. M. & MACARA, I. G. 2005. The mammalian Scribble polarity protein regulates epithelial cell adhesion and migration through E-cadherin. *J Cell Biol,* 171**,** 1061-71.

RAMPIAS, T., SASAKI, C., BURTNESS, B. A. & PSYRRI, A. 2008. Gene expression differences associated with silencing of E6 and E7 viral oncogenes in HPV16+ oropharyngeal cancer cell lines. *Journal of Clinical Oncology,* 26**,** 6009.

RANGARAJAN, A., SYAL, R., SELVARAJAH, S., CHAKRABARTI, O., SARIN, A. & KRISHNA, S. 2001a. Activated Notch1 signaling cooperates with papillomavirus oncogenes in transformation and generates resistance to apoptosis on matrix withdrawal through PKB/Akt. *Virology,* 286**,** 23-30.

RANGARAJAN, A., TALORA, C., OKUYAMA, R., NICOLAS, M., MAMMUCARI, C., OH, H., ASTER, J. C., KRISHNA, S., METZGER, D., CHAMBON, P., MIELE, L., AGUET, M., RADTKE, F. & DOTTO, G. P. 2001b. Notch signaling is a direct determinant of keratinocyte growth arrest and entry into differentiation. *EMBO J,* 20**,** 3427-36.

RESTIVO, G., NGUYEN, B. C., DZIUNYCZ, P., RISTORCELLI, E., RYAN, R. J., OZUYSAL, O. Y., DI PIAZZA, M., RADTKE, F., DIXON, M. J., HOFBAUER, G. F., LEFORT, K. & DOTTO, G. P. 2011. IRF6 is a mediator of Notch pro-differentiation and tumour suppressive function in keratinocytes. *EMBO J,* 30**,** 4571-85.

REYA, T., MORRISON, S. J., CLARKE, M. F. & WEISSMAN, I. L. 2001. Stem cells, cancer, and cancer stem cells. *Nature,* 414**,** 105-11.

RICHARDS, R. M., LOWY, D. R., SCHILLER, J. T. & DAY, P. M. 2006. Cleavage of the papillomavirus minor capsid protein, L2, at a furin consensus site is necessary for infection. *Proc Natl Acad Sci U S A,* 103**,** 1522-7.

RICHART, R. M. 1973. Cervical intraepithelial neoplasia. *Pathol Annu,* 8**,** 301-28.

RISTRIANI, T., MASSON, M., NOMINE, Y., LAURENT, C., LEFEVRE, J. F., WEISS, E. & TRAVE, G. 2000. HPV oncoprotein E6 is a structure-dependent DNA-binding protein that recognizes four-way junctions. *J Mol Biol,* 296**,** 1189-203.

ROBBINS, M., JUDGE, A. & MACLACHLAN, I. 2009. siRNA and innate immunity. *Oligonucleotides,* 19**,** 89-102.

ROBERTS, J. N., BUCK, C. B., THOMPSON, C. D., KINES, R., BERNARDO, M., CHOYKE, P. L., LOWY, D. R. & SCHILLER, J. T. 2007. Genital transmission of HPV in a mouse model is potentiated by nonoxynol-9 and inhibited by carrageenan. *Nat Med,* 13**,** 857-61.

ROGAEV, E. I., SHERRINGTON, R., ROGAEVA, E. A., LEVESQUE, G., IKEDA, M., LIANG, Y., CHI, H., LIN, C., HOLMAN, K., TSUDA, T. & ET AL. 1995. Familial Alzheimer's disease in kindreds with missense mutations in a gene on chromosome 1 related to the Alzheimer's disease type 3 gene. *Nature,* 376**,** 775-8.

ROMANCZUK, H., THIERRY, F. & HOWLEY, P. M. 1990. Mutational analysis of cis elements involved in E2 modulation of human papillomavirus type 16 P97 and type 18 P105 promoters. *J Virol,* 64**,** 2849-59.

RONCO, L. V., KARPOVA, A. Y., VIDAL, M. & HOWLEY, P. M. 1998. Human papillomavirus 16 E6 oncoprotein binds to interferon regulatory factor-3 and inhibits its transcriptional activity. *Genes Dev,* 12**,** 2061-72.

ROSENBERGER, S., DE-CASTRO ARCE, J., LANGBEIN, L., STEENBERGEN, R. D. & ROSL, F. 2010. Alternative splicing of human papillomavirus type-16 E6/E6* early mRNA is coupled to EGF signaling via Erk1/2 activation. *Proc Natl Acad Sci U S A,* 107**,** 7006-11.

RUESCH, M. N., STUBENRAUCH, F. & LAIMINS, L. A. 1998. Activation of papillomavirus late gene transcription and genome amplification upon differentiation in semisolid medium is coincident with expression of involucrin and transglutaminase but not keratin-10. *J Virol,* 72**,** 5016-24.

SARNOW, P., HO, Y. S., WILLIAMS, J. & LEVINE, A. J. 1982. Adenovirus E1b-58kd tumor antigen and SV40 large tumor antigen are physically associated with the same 54 kd cellular protein in transformed cells. *Cell,* 28**,** 387-94.

SCHAPER, I. D., MARCUZZI, G. P., WEISSENBORN, S. J., KASPER, H. U., DRIES, V., SMYTH, N., FUCHS, P. & PFISTER, H. 2005. Development of skin tumors in mice transgenic for early genes of human papillomavirus type 8. *Cancer Res,* 65**,** 1394-400.

SCHEFFNER, M., HUIBREGTSE, J. M., VIERSTRA, R. D. & HOWLEY, P. M. 1993. The HPV-16 E6 and E6-AP complex functions as a ubiquitin-protein ligase in the ubiquitination of p53. *Cell,* 75**,** 495-505.

SCHEFFNER, M., WERNESS, B. A., HUIBREGTSE, J. M., LEVINE, A. J. & HOWLEY, P. M. 1990. The E6 oncoprotein encoded by human papillomavirus types 16 and 18 promotes the degradation of p53. *Cell,* 63**,** 1129-36.

SCHIFFMAN, M., CASTLE, P. E., JERONIMO, J., RODRIGUEZ, A. C. & WACHOLDER, S. 2007. Human papillomavirus and cervical cancer. *Lancet,* 370**,** 890-907.

SCHIFFMAN, M., HERRERO, R., DESALLE, R., HILDESHEIM, A., WACHOLDER, S., RODRIGUEZ, A. C., BRATTI, M. C., SHERMAN, M. E., MORALES, J., GUILLEN, D., ALFARO, M., HUTCHINSON, M., WRIGHT, T. C., SOLOMON, D., CHEN, Z., SCHUSSLER, J., CASTLE, P. E. & BURK, R. D. 2005. The carcinogenicity of human papillomavirus types reflects viral evolution. *Virology,* 337**,** 76-84.

SCHIFFMAN, M. & KJAER, S. K. 2003. Chapter 2: Natural history of anogenital human papillomavirus infection and neoplasia. *J Natl Cancer Inst Monogr***,** 14-9.

SCHILLER, J. T., DAY, P. M. & KINES, R. C. 2010. Current understanding of the mechanism of HPV infection. *Gynecol Oncol,* 118**,** S12-7.

SCHLEGEL, R., PHELPS, W. C., ZHANG, Y. L. & BARBOSA, M. 1988. Quantitative keratinocyte assay detects two biological activities of human papillomavirus DNA and identifies viral types associated with cervical carcinoma. *EMBO J,* 7**,** 3181-7.

SCHLEGELMILCH, K., MOHSENI, M., KIRAK, O., PRUSZAK, J., RODRIGUEZ, J. R., ZHOU, D., KREGER, B. T., VASIOUKHIN, V., AVRUCH, J., BRUMMELKAMP, T. R. & CAMARGO, F. D. 2011. Yap1 acts downstream of alpha-catenin to control epidermal proliferation. *Cell,* 144**,** 782-95.

SCHMIDT, M. T., OLEJNIK, A. K. & GOZDZICKA-JOZEFIAK, A. 2005. The HPV16 E2 transcriptional regulator mode of action depends on the physical state of the viral genome. *Acta Biochim Pol,* 52**,** 823-32.

SCHMITT, A., ROCHAT, A., ZELTNER, R., BORENSTEIN, L., BARRANDON, Y., WETTSTEIN, F. O. & IFTNER, T. 1996. The primary target cells of the high-risk cottontail rabbit papillomavirus colocalize with hair follicle stem cells. *J Virol,* 70**,** 1912-22.

SCHNEIDER-GADICKE, A., KAUL, S., SCHWARZ, E., GAUSEPOHL, H., FRANK, R. & BASTERT, G. 1988. Identification of the human papillomavirus type 18 E6 and E6 proteins in nuclear protein fractions from human cervical carcinoma cells grown in the nude mouse or in vitro. *Cancer Res,* 48**,** 2969-74.

SCHNEIDER-GADICKE, A. & SCHWARZ, E. 1986. Different human cervical carcinoma cell lines show similar transcription patterns of human papillomavirus type 18 early genes. *EMBO J,* 5**,** 2285-92.

SEGRELLES, C., RUIZ, S., PEREZ, P., MURGA, C., SANTOS, M., BUDUNOVA, I. V., MARTINEZ, J., LARCHER, F., SLAGA, T. J., GUTKIND, J. S., JORCANO, J. L. & PARAMIO, J. M. 2002. Functional roles of Akt signaling in mouse skin tumorigenesis. *Oncogene,* 21**,** 53-64.

SEKARIC, P., CHERRY, J. J. & ANDROPHY, E. J. 2008. Binding of human papillomavirus type 16 E6 to E6AP is not required for activation of hTERT. *J Virol,* 82**,** 71-6.

SELKOE, D. J. 2001. Alzheimer's disease: genes, proteins, and therapy. *Physiol Rev,* 81**,** 741-66.

SHAI, A., BRAKE, T., SOMOZA, C. & LAMBERT, P. F. 2007. The human papillomavirus E6 oncogene dysregulates the cell cycle and contributes to cervical carcinogenesis through two independent activities. *Cancer Res,* 67**,** 1626-35.

SHERR, C. J. 1994. The ins and outs of RB: coupling gene expression to the cell cycle clock. *Trends Cell Biol,* 4**,** 15-8.

SHERRINGTON, R., ROGAEV, E. I., LIANG, Y., ROGAEVA, E. A., LEVESQUE, G., IKEDA, M., CHI, H., LIN, C., LI, G., HOLMAN, K., TSUDA, T., MAR, L., FONCIN, J. F., BRUNI, A. C., MONTESI, M. P., SORBI, S., RAINERO, I., PINESSI, L., NEE, L., CHUMAKOV, I., POLLEN, D., BROOKES, A., SANSEAU, P., POLINSKY, R. J., WASCO, W., DA SILVA, H. A., HAINES, J. L., PERKICAK-VANCE, M. A., TANZI, R. E., ROSES, A. D., FRASER, P. E., ROMMENS, J. M. & ST GEORGE-HYSLOP, P. H. 1995. Cloning of a gene bearing missense mutations in early-onset familial Alzheimer's disease. *Nature,* 375**,** 754-60.

SHIRAKATA, Y. 2010. Regulation of epidermal keratinocytes by growth factors. *J Dermatol Sci,* 59**,** 73-80.

SHIROTANI, K., EDBAUER, D., KOSTKA, M., STEINER, H. & HAASS, C. 2004. Immature nicastrin stabilizes APH-1 independent of PEN-2 and presenilin: identification of nicastrin mutants that selectively interact with APH-1. *J Neurochem,* 89**,** 1520-7.

SHOPE, R. E. & HURST, E. W. 1933. INFECTIOUS PAPILLOMATOSIS OF RABBITS : WITH A NOTE ON THE HISTOPATHOLOGY. *J Exp Med,* 58**,** 607-24.

SILINS, I., WANG, Z., AVALL-LUNDQVIST, E., FRANKENDAL, B., VIKMANIS, U., SAPP, M., SCHILLER, J. T. & DILLNER, J. 1999. Serological evidence for protection by human papillomavirus (HPV) type 6 infection against HPV type 16 cervical carcinogenesis. *J Gen Virol,* 80 (Pt 11)**,** 2931-6.

SILVIS, M. R., KREGER, B. T., LIEN, W. H., KLEZOVITCH, O., RUDAKOVA, G. M., CAMARGO, F. D., LANTZ, D. M., SEYKORA, J. T. & VASIOUKHIN, V. 2011. alpha-catenin is a tumor suppressor that controls cell accumulation by

regulating the localization and activity of the transcriptional coactivator Yap1. *Sci Signal,* 4**,** ra33.

SIMA, N., WANG, W., KONG, D., DENG, D., XU, Q., ZHOU, J., XU, G., MENG, L., LU, Y., WANG, S. & MA, D. 2008. RNA interference against HPV16 E7 oncogene leads to viral E6 and E7 suppression in cervical cancer cells and apoptosis via upregulation of Rb and p53. *Apoptosis,* 13**,** 273-81.

SINGHANIA, R., KHAIRUDDIN, N., CLARKE, D. & MCMILLAN, N. A. 2012. RNA interference for the treatment of papillomavirus disease. *Open Virol J,* 6**,** 204-15.

SMOLARKIEWICZ, M., SKRZYPCZAK, T. & WOJTASZEK, P. 2013. The very many faces of presenilins and the gamma-secretase complex. *Protoplasma*.

SMOTKIN, D., PROKOPH, H. & WETTSTEIN, F. O. 1989. Oncogenic and nononcogenic human genital papillomaviruses generate the E7 mRNA by different mechanisms. *J Virol,* 63**,** 1441-7.

SMOTKIN, D. & WETTSTEIN, F. O. 1986. Transcription of human papillomavirus type 16 early genes in a cervical cancer and a cancer-derived cell line and identification of the E7 protein. *Proc Natl Acad Sci U S A,* 83**,** 4680-4.

SOLOMON, D. 1989. The 1988 Bethesda System for reporting cervical/vaginal cytologic diagnoses. Developed and approved at the National Cancer Institute Workshop, Bethesda, Maryland, U.S.A., December 12-13, 1988. *Acta Cytol,* 33**,** 567-74.

SONG, S., PITOT, H. C. & LAMBERT, P. F. 1999. The human papillomavirus type 16 E6 gene alone is sufficient to induce carcinomas in transgenic animals. *J Virol,* 73**,** 5887-93.

SOTO, U., DAS, B. C., LENGERT, M., FINZER, P., ZUR HAUSEN, H. & ROSL, F. 1999. Conversion of HPV 18 positive non-tumorigenic HeLa-fibroblast hybrids to invasive growth involves loss of TNF-alpha mediated repression of viral transcription and modification of the AP-1 transcription complex. *Oncogene,* 18**,** 3187-98.

SOTO, U., DENK, C., FINZER, P., HUTTER, K. J., ZUR HAUSEN, H. & ROSL, F. 2000. Genetic complementation to non-tumorigenicity in cervical-carcinoma cells correlates with alterations in AP-1 composition. *Int J Cancer,* 86**,** 811-7.

SOUCEK, T., PUSCH, O., HENGSTSCHLAGER-OTTNAD, E., ADAMS, P. D. & HENGSTSCHLAGER, M. 1997. Deregulated expression of E2F-1 induces cyclin A- and E-associated kinase activities independently from cell cycle position. *Oncogene,* 14**,** 2251-7.

SPALHOLZ, B. A., YANG, Y. C. & HOWLEY, P. M. 1985. Transactivation of a bovine papilloma virus transcriptional regulatory element by the E2 gene product. *Cell,* 42**,** 183-91.

SPINK, K. M. & LAIMINS, L. A. 2005. Induction of the human papillomavirus type 31 late promoter requires differentiation but not DNA amplification. *J Virol,* 79**,** 4918-26.

SRIVENUGOPAL, K. S. & ALI-OSMAN, F. 2002. The DNA repair protein, O(6)-methylguanine-DNA methyltransferase is a proteolytic target for the E6 human papillomavirus oncoprotein. *Oncogene,* 21**,** 5940-5.

ST CROIX, B., SHEEHAN, C., RAK, J. W., FLORENES, V. A., SLINGERLAND, J. M. & KERBEL, R. S. 1998. E-Cadherin-dependent growth suppression is mediated by the cyclin-dependent kinase inhibitor p27(KIP1). *J Cell Biol,* 142**,** 557-71.

STAMBOLIC, V., SUZUKI, A., DE LA POMPA, J. L., BROTHERS, G. M., MIRTSOS, C., SASAKI, T., RULAND, J., PENNINGER, J. M., SIDEROVSKI, D. P. & MAK, T. W. 1998. Negative regulation of PKB/Akt-dependent cell survival by the tumor suppressor PTEN. *Cell,* 95**,** 29-39.

STANLEY, M. A. 2009. Immune responses to human papilloma viruses. *Indian J Med Res,* 130**,** 266-76.

STANLEY, M. A. 2012. Genital human papillomavirus infections: current and prospective therapies. *J Gen Virol,* 93**,** 681-91.

STANLEY, M. A., BROWNE, H. M., APPLEBY, M. & MINSON, A. C. 1989. Properties of a non-tumorigenic human cervical keratinocyte cell line. *Int J Cancer,* 43**,** 672-6.

STEGER, G. & CORBACH, S. 1997. Dose-dependent regulation of the early promoter of human papillomavirus type 18 by the viral E2 protein. *J Virol,* 71**,** 50-8.

STEINER, H., WINKLER, E., EDBAUER, D., PROKOP, S., BASSET, G., YAMASAKI, A., KOSTKA, M. & HAASS, C. 2002. PEN-2 is an integral component of the gamma-secretase complex required for coordinated expression of presenilin and nicastrin. *J Biol Chem,* 277**,** 39062-5.

STORRS, C. H. & SILVERSTEIN, S. J. 2007. PATJ, a tight junction-associated PDZ protein, is a novel degradation target of high-risk human papillomavirus E6 and the alternatively spliced isoform 18 E6. *J Virol,* 81**,** 4080-90.

STROOPER, B. D. & ANNAERT, W. 2001. Presenilins and the intramembrane proteolysis of proteins: facts and fiction. *Nat Cell Biol,* 3**,** E221-5.

STRUHL, G. & ADACHI, A. 2000. Requirements for presenilin-dependent cleavage of notch and other transmembrane proteins. *Mol Cell,* 6**,** 625-36.

SUN, L., ZHANG, G., LEI, T., HUANG, C., SONG, T. & SI, L. 2008. Two different HPV-11E6 fusion proteins trap p53 in the cytoplasm and induce apoptosis. *Cancer Biol Ther,* 7**,** 1909-15.

TAKIZAWA, S., NAGASAKA, K., NAKAGAWA, S., YANO, T., NAKAGAWA, K., YASUGI, T., TAKEUCHI, T., KANDA, T., HUIBREGTSE, J. M.,

AKIYAMA, T. & TAKETANI, Y. 2006. Human scribble, a novel tumor suppressor identified as a target of high-risk HPV E6 for ubiquitin-mediated degradation, interacts with adenomatous polyposis coli. *Genes Cells,* 11**,** 453-64.

TALORA, C., CIALFI, S., SEGATTO, O., MORRONE, S., KIM CHOI, J., FRATI, L., PAOLO DOTTO, G., GULINO, A. & SCREPANTI, I. 2005. Constitutively active Notch1 induces growth arrest of HPV-positive cervical cancer cells via separate signaling pathways. *Exp Cell Res,* 305**,** 343-54.

TALORA, C., SGROI, D. C., CRUM, C. P. & DOTTO, G. P. 2002. Specific down-modulation of Notch1 signaling in cervical cancer cells is required for sustained HPV-E6/E7 expression and late steps of malignant transformation. *Genes Dev,* 16**,** 2252-63.

TAN, M. J., WHITE, E. A., SOWA, M. E., HARPER, J. W., ASTER, J. C. & HOWLEY, P. M. 2012. Cutaneous beta-human papillomavirus E6 proteins bind Mastermind-like coactivators and repress Notch signaling. *Proc Natl Acad Sci U S A,* 109**,** E1473-80.

TANG, S., TAO, M., MCCOY, J. P., JR. & ZHENG, Z. M. 2006. The E7 oncoprotein is translated from spliced E6*I transcripts in high-risk human papillomavirus type 16- or type 18-positive cervical cancer cell lines via translation reinitiation. *J Virol,* 80**,** 4249-63.

THIERRY, F. 2009. Transcriptional regulation of the papillomavirus oncogenes by cellular and viral transcription factors in cervical carcinoma. *Virology,* 384**,** 375-9.

THIERRY, F., SPYROU, G., YANIV, M. & HOWLEY, P. 1992. Two AP1 sites binding JunB are essential for human papillomavirus type 18 transcription in keratinocytes. *J Virol,* 66**,** 3740-8.

THINAKARAN, G., BORCHELT, D. R., LEE, M. K., SLUNT, H. H., SPITZER, L., KIM, G., RATOVITSKY, T., DAVENPORT, F., NORDSTEDT, C., SEEGER, M., HARDY, J., LEVEY, A. I., GANDY, S. E., JENKINS, N. A., COPELAND, N. G., PRICE, D. L. & SISODIA, S. S. 1996. Endoproteolysis of presenilin 1 and accumulation of processed derivatives in vivo. *Neuron,* 17**,** 181-90.

THOMAS, G. B. & VAN MEYEL, D. J. 2007. The glycosyltransferase Fringe promotes Delta-Notch signaling between neurons and glia, and is required for subtype-specific glial gene expression. *Development,* 134**,** 591-600.

THOMAS, J. T., HUBERT, W. G., RUESCH, M. N. & LAIMINS, L. A. 1999. Human papillomavirus type 31 oncoproteins E6 and E7 are required for the maintenance of episomes during the viral life cycle in normal human keratinocytes. *Proc Natl Acad Sci U S A,* 96**,** 8449-54.

THOMAS, M. & BANKS, L. 1998. Inhibition of Bak-induced apoptosis by HPV-18 E6. *Oncogene,* 17**,** 2943-54.

THOMAS, M. & BANKS, L. 1999. Human papillomavirus (HPV) E6 interactions with Bak are conserved amongst E6 proteins from high and low risk HPV types. *J Gen Virol,* 80 (Pt 6)**,** 1513-7.

THOMAS, M., GLAUNSINGER, B., PIM, D., JAVIER, R. & BANKS, L. 2001. HPV E6 and MAGUK protein interactions: determination of the molecular basis for specific protein recognition and degradation. *Oncogene,* 20**,** 5431-9.

THOMAS, M., LAURA, R., HEPNER, K., GUCCIONE, E., SAWYERS, C., LASKY, L. & BANKS, L. 2002. Oncogenic human papillomavirus E6 proteins target the MAGI-2 and MAGI-3 proteins for degradation. *Oncogene,* 21**,** 5088-96.

THOMAS, M., MASSIMI, P., NAVARRO, C., BORG, J. P. & BANKS, L. 2005. The hScrib/Dlg apico-basal control complex is differentially targeted by HPV-16 and HPV-18 E6 proteins. *Oncogene,* 24**,** 6222-30.

THRASH, B. R., MENGES, C. W., PIERCE, R. H. & MCCANCE, D. J. 2006. AKT1 provides an essential survival signal required for differentiation and stratification of primary human keratinocytes. *J Biol Chem,* 281**,** 12155-62.

TODARO, G. J. & GREEN, H. 1963. Quantitative studies of the growth of mouse embryo cells in culture and their development into established lines. *J Cell Biol,* 17**,** 299-313.

TOMAIC, V., PIM, D. & BANKS, L. 2009. The stability of the human papillomavirus E6 oncoprotein is E6AP dependent. *Virology,* 393**,** 7-10.

TOMMASINO, M., ADAMCZEWSKI, J. P., CARLOTTI, F., BARTH, C. F., MANETTI, R., CONTORNI, M., CAVALIERI, F., HUNT, T. & CRAWFORD, L. 1993. HPV16 E7 protein associates with the protein kinase p33CDK2 and cyclin A. *Oncogene,* 8**,** 195-202.

UREN, A., FALLEN, S., YUAN, H., USUBUTUN, A., KUCUKALI, T., SCHLEGEL, R. & TORETSKY, J. A. 2005. Activation of the canonical Wnt pathway during genital keratinocyte transformation: a model for cervical cancer progression. *Cancer Res,* 65**,** 6199-206.

VAN TETERING, G., BOVENSCHEN, N., MEELDIJK, J., VAN DIEST, P. J. & VOOIJS, M. 2011. Cleavage of Notch1 by granzyme B disables its transcriptional activity. *Biochem J,* 437**,** 313-22.

VARNUM-FINNEY, B., XU, L., BRASHEM-STEIN, C., NOURIGAT, C., FLOWERS, D., BAKKOUR, S., PEAR, W. S. & BERNSTEIN, I. D. 2000. Pluripotent, cytokine-dependent, hematopoietic stem cells are immortalized by constitutive Notch1 signaling. *Nat Med,* 6**,** 1278-81.

VEERARAGHAVALU, K., SUBBAIAH, V. K., SRIVASTAVA, S., CHAKRABARTI, O., SYAL, R. & KRISHNA, S. 2005. Complementation of human papillomavirus type 16 E6 and E7 by Jagged1-specific Notch1-phosphatidylinositol 3-kinase signaling involves pleiotropic oncogenic functions independent of CBF1;Su(H);Lag-1 activation. *J Virol,* 79**,** 7889-98.

VELDMAN, T., HORIKAWA, I., BARRETT, J. C. & SCHLEGEL, R. 2001. Transcriptional activation of the telomerase hTERT gene by human papillomavirus type 16 E6 oncoprotein. *J Virol,* 75**,** 4467-72.

VESSEY, C. J., WILDING, J., FOLARIN, N., HIRANO, S., TAKEICHI, M., SOUTTER, P., STAMP, G. W. & PIGNATELLI, M. 1995. Altered expression and function of E-cadherin in cervical intraepithelial neoplasia and invasive squamous cell carcinoma. *J Pathol,* 176**,** 151-9.

VOGELSTEIN, B., LANE, D. & LEVINE, A. J. 2000. Surfing the p53 network. *Nature,* 408**,** 307-10.

VON KNEBEL DOEBERITZ, M., BAUKNECHT, T., BARTSCH, D. & ZUR HAUSEN, H. 1991. Influence of chromosomal integration on glucocorticoid-regulated transcription of growth-stimulating papillomavirus genes E6 and E7 in cervical carcinoma cells. *Proc Natl Acad Sci U S A,* 88**,** 1411-5.

VON KNEBEL DOEBERITZ, M., OLTERSDORF, T., SCHWARZ, E. & GISSMANN, L. 1988. Correlation of modified human papilloma virus early gene expression with altered growth properties in C4-1 cervical carcinoma cells. *Cancer Res,* 48**,** 3780-6.

VON KNEBEL DOEBERITZ, M., RITTMULLER, C., AENGENEYNDT, F., JANSEN-DURR, P. & SPITKOVSKY, D. 1994. Reversible repression of papillomavirus oncogene expression in cervical carcinoma cells: consequences for the phenotype and E6-p53 and E7-pRB interactions. *J Virol,* 68**,** 2811-21.

WAI, L. K. 2004. Telomeres, telomerase, and tumorigenesis--a review. *MedGenMed,* 6**,** 19.

WALBOOMERS, J. M., JACOBS, M. V., MANOS, M. M., BOSCH, F. X., KUMMER, J. A., SHAH, K. V., SNIJDERS, P. J., PETO, J., MEIJER, C. J. & MUNOZ, N. 1999. Human papillomavirus is a necessary cause of invasive cervical cancer worldwide. *J Pathol,* 189**,** 12-9.

WANG, L., QIN, H., CHEN, B., XIN, X., LI, J. & HAN, H. 2007. Overexpressed active Notch1 induces cell growth arrest of HeLa cervical carcinoma cells. *Int J Gynecol Cancer,* 17**,** 1283-92.

WANG, Q., KENNEDY, A., DAS, P., MCINTOSH, P. B., HOWELL, S. A., ISAACSON, E. R., HINZ, S. A., DAVY, C. & DOORBAR, J. 2009. Phosphorylation of the human papillomavirus type 16 E1--E4 protein at T57 by ERK triggers a structural change that enhances keratin binding and protein stability. *J Virol,* 83**,** 3668-83.

WATT, F. M. 2001. Stem cell fate and patterning in mammalian epidermis. *Curr Opin Genet Dev,* 11**,** 410-7.

WATT, F. M., ESTRACH, S. & AMBLER, C. A. 2008. Epidermal Notch signalling: differentiation, cancer and adhesion. *Curr Opin Cell Biol,* 20**,** 171-9.

WECHSLER-REYA, R. J. & SCOTT, M. P. 1999. Control of neuronal precursor proliferation in the cerebellum by Sonic Hedgehog. *Neuron,* 22**,** 103-14.

WEIJZEN, S., RIZZO, P., BRAID, M., VAISHNAV, R., JONKHEER, S. M., ZLOBIN, A., OSBORNE, B. A., GOTTIPATI, S., ASTER, J. C., HAHN, W. C., RUDOLF, M., SIZIOPIKOU, K., KAST, W. M. & MIELE, L. 2002. Activation of Notch-1 signaling maintains the neoplastic phenotype in human Ras-transformed cells. *Nat Med,* 8**,** 979-86.

WEIJZEN, S., ZLOBIN, A., BRAID, M., MIELE, L. & KAST, W. M. 2003. HPV16 E6 and E7 oncoproteins regulate Notch-1 expression and cooperate to induce transformation. *J Cell Physiol,* 194**,** 356-62.

WEISSMAN, I. L. 2000. Stem cells: units of development, units of regeneration, and units in evolution. *Cell,* 100**,** 157-68.

WELTERS, M. J., DE JONG, A., VAN DEN EEDEN, S. J., VAN DER HULST, J. M., KWAPPENBERG, K. M., HASSANE, S., FRANKEN, K. L., DRIJFHOUT, J. W., FLEUREN, G. J., KENTER, G., MELIEF, C. J., OFFRINGA, R. & VAN DER BURG, S. H. 2003. Frequent display of human papillomavirus type 16 E6-specific memory t-Helper cells in the healthy population as witness of previous viral encounter. *Cancer Res,* 63**,** 636-41.

WERNESS, B. A., LEVINE, A. J. & HOWLEY, P. M. 1990. Association of human papillomavirus types 16 and 18 E6 proteins with p53. *Science,* 248**,** 76-9.

WHYTE, P., BUCHKOVICH, K. J., HOROWITZ, J. M., FRIEND, S. H., RAYBUCK, M., WEINBERG, R. A. & HARLOW, E. 1988. Association between an oncogene and an anti-oncogene: the adenovirus E1A proteins bind to the retinoblastoma gene product. *Nature,* 334**,** 124-9.

WILDING, J., VOUSDEN, K. H., SOUTTER, W. P., MCCREA, P. D., DEL BUONO, R. & PIGNATELLI, M. 1996. E-cadherin transfection down-regulates the epidermal growth factor receptor and reverses the invasive phenotype of human papilloma virus-transfected keratinocytes. *Cancer Res,* 56**,** 5285-92.

WILSON, R. & LAIMINS, L. A. 2005. Differentiation of HPV-containing cells using organotypic "raft" culture or methylcellulose. *Methods Mol Med,* 119**,** 157-69.

WINTERS, Z. E., LEEK, R. D., BRADBURN, M. J., NORBURY, C. J. & HARRIS, A. L. 2003. Cytoplasmic p21WAF1/CIP1 expression is correlated with HER-2/ neu in breast cancer and is an independent predictor of prognosis. *Breast Cancer Res,* 5**,** R242-9.

WOLFE, M. S. 2001. gamma-Secretase inhibitors as molecular probes of presenilin function. *J Mol Neurosci,* 17**,** 199-204.

WONG, P. P., PICKARD, A. & MCCANCE, D. J. 2010. p300 alters keratinocyte cell growth and differentiation through regulation of p21(Waf1/CIP1). *PLoS One,* 5**,** e8369.

WOO, R. A. & POON, R. Y. 2003. Cyclin-dependent kinases and S phase control in mammalian cells. *Cell Cycle,* 2**,** 316-24.

WOODMAN, C. B., COLLINS, S. I. & YOUNG, L. S. 2007. The natural history of cervical HPV infection: unresolved issues. *Nat Rev Cancer,* 7**,** 11-22.

WOODS, D. F. & BRYANT, P. J. 1989. Molecular cloning of the lethal(1)discs large-1 oncogene of Drosophila. *Dev Biol,* 134**,** 222-35.

WOODWORTH, C. D., DONIGER, J. & DIPAOLO, J. A. 1989. Immortalization of human foreskin keratinocytes by various human papillomavirus DNAs corresponds to their association with cervical carcinoma. *J Virol,* 63**,** 159-64.

WU, L., ASTER, J. C., BLACKLOW, S. C., LAKE, R., ARTAVANIS-TSAKONAS, S. & GRIFFIN, J. D. 2000a. MAML1, a human homologue of Drosophila mastermind, is a transcriptional co-activator for NOTCH receptors. *Nat Genet,* 26**,** 484-9.

WU, N., ROLLIN, J., MASSE, I., LAMARTINE, J. & GIDROL, X. 2012. p63 regulates human keratinocyte proliferation via MYC-regulated gene network and differentiation commitment through cell adhesion-related gene network. *J Biol Chem,* 287**,** 5627-38.

WU, X., HEPNER, K., CASTELINO-PRABHU, S., DO, D., KAYE, M. B., YUAN, X. J., WOOD, J., ROSS, C., SAWYERS, C. L. & WHANG, Y. E. 2000b. Evidence for regulation of the PTEN tumor suppressor by a membrane-localized multi-PDZ domain containing scaffold protein MAGI-2. *Proc Natl Acad Sci U S A,* 97**,** 4233-8.

YAMAMOTO, M., YOSHIDA, M., ONO, K., FUJITA, T., OHTANI-FUJITA, N., SAKAI, T. & NIKAIDO, T. 1994. Effect of tumor suppressors on cell cycle-regulatory genes: RB suppresses p34cdc2 expression and normal p53 suppresses cyclin A expression. *Exp Cell Res,* 210**,** 94-101.

YANG, L. T., NICHOLS, J. T., YAO, C., MANILAY, J. O., ROBEY, E. A. & WEINMASTER, G. 2005. Fringe glycosyltransferases differentially modulate Notch1 proteolysis induced by Delta1 and Jagged1. *Mol Biol Cell,* 16**,** 927-42.

YOSHINOUCHI, M., YAMADA, T., KIZAKI, M., FEN, J., KOSEKI, T., IKEDA, Y., NISHIHARA, T. & YAMATO, K. 2003. In vitro and in vivo growth suppression of human papillomavirus 16-positive cervical cancer cells by E6 siRNA. *Mol Ther,* 8**,** 762-8.

YOU, J., CROYLE, J. L., NISHIMURA, A., OZATO, K. & HOWLEY, P. M. 2004. Interaction of the bovine papillomavirus E2 protein with Brd4 tethers the viral DNA to host mitotic chromosomes. *Cell,* 117**,** 349-60.

YUAN, H., ITO, S., SENGA, T., HYODO, T., KIYONO, T., KIKKAWA, F. & HAMAGUCHI, M. 2009. Human papillomavirus type 16 oncoprotein E7 suppresses cadherin-mediated cell adhesion via ERK and AP-1 signaling. *Int J Oncol,* 35**,** 309-14.

YUGAWA, T., HANDA, K., NARISAWA-SAITO, M., OHNO, S., FUJITA, M. & KIYONO, T. 2007. Regulation of Notch1 gene expression by p53 in epithelial cells. *Mol Cell Biol,* 27**,** 3732-42.

ZAGOURAS, P., STIFANI, S., BLAUMUELLER, C. M., CARCANGIU, M. L. & ARTAVANIS-TSAKONAS, S. 1995. Alterations in Notch signaling in neoplastic lesions of the human cervix. *Proc Natl Acad Sci U S A,* 92**,** 6414-8.

ZERFASS, K., SCHULZE, A., SPITKOVSKY, D., FRIEDMAN, V., HENGLEIN, B. & JANSEN-DURR, P. 1995. Sequential activation of cyclin E and cyclin A gene expression by human papillomavirus type 16 E7 through sequences necessary for transformation. *J Virol,* 69**,** 6389-99.

ZERFASS-THOME, K., ZWERSCHKE, W., MANNHARDT, B., TINDLE, R., BOTZ, J. W. & JANSEN-DURR, P. 1996. Inactivation of the cdk inhibitor p27KIP1 by the human papillomavirus type 16 E7 oncoprotein. *Oncogene,* 13**,** 2323-30.

ZHANG, B., CHEN, W. & ROMAN, A. 2006. The E7 proteins of low- and high-risk human papillomaviruses share the ability to target the pRB family member p130 for degradation. *Proc Natl Acad Sci U S A,* 103**,** 437-42.

ZHANG, Y. W., LUO, W. J., WANG, H., LIN, P., VETRIVEL, K. S., LIAO, F., LI, F., WONG, P. C., FARQUHAR, M. G., THINAKARAN, G. & XU, H. 2005. Nicastrin is critical for stability and trafficking but not association of other presenilin/gamma-secretase components. *J Biol Chem,* 280**,** 17020-6.

ZHAO, B., TUMANENG, K. & GUAN, K. L. 2011. The Hippo pathway in organ size control, tissue regeneration and stem cell self-renewal. *Nat Cell Biol,* 13**,** 877-83.

ZHAO, K. N., HENGST, K., LIU, W. J., LIU, Y. H., LIU, X. S., MCMILLAN, N. A. & FRAZER, I. H. 2000. BPV1 E2 protein enhances packaging of full-length plasmid DNA in BPV1 pseudovirions. *Virology,* 272**,** 382-93.

ZHENG, Z. M. & BAKER, C. C. 2006. Papillomavirus genome structure, expression, and post-transcriptional regulation. *Front Biosci,* 11**,** 2286-302.

ZHENG, Z. M., TAO, M., YAMANEGI, K., BODAGHI, S. & XIAO, W. 2004. Splicing of a cap-proximal human Papillomavirus 16 E6E7 intron promotes E7 expression, but can be restrained by distance of the intron from its RNA 5' cap. *J Mol Biol,* 337**,** 1091-108.

ZHOU, B. P., LIAO, Y., XIA, W., SPOHN, B., LEE, M. H. & HUNG, M. C. 2001. Cytoplasmic localization of p21Cip1/WAF1 by Akt-induced phosphorylation in HER-2/neu-overexpressing cells. *Nat Cell Biol,* 3**,** 245-52.

ZHOU, J., PENG, C., LI, B., WANG, F., ZHOU, C., HONG, D., YE, F., CHENG, X., LU, W. & XIE, X. 2012. Transcriptional gene silencing of HPV16 E6/E7 induces growth inhibition via apoptosis in vitro and in vivo. *Gynecol Oncol,* 124**,** 296-302.

ZHOU, J., SUN, X. Y., STENZEL, D. J. & FRAZER, I. H. 1991. Expression of vaccinia recombinant HPV 16 L1 and L2 ORF proteins in epithelial cells is sufficient for assembly of HPV virion-like particles. *Virology,* 185**,** 251-7.

ZHOU, S., ZHOU, H., WALIAN, P. J. & JAP, B. K. 2005. CD147 is a regulatory subunit of the gamma-secretase complex in Alzheimer's disease amyloid beta-peptide production. *Proc Natl Acad Sci U S A,* 102**,** 7499-504.

ZHOU, S., ZHOU, H., WALIAN, P. J. & JAP, B. K. 2006. The discovery and role of CD147 as a subunit of gamma-secretase complex. *Drug News Perspect,* 19**,** 133-8.

ZUR HAUSEN, H. 2002. Papillomaviruses and cancer: from basic studies to clinical application. *Nat Rev Cancer,* 2**,** 342-50.

ZUR HAUSEN, H. 2009. Papillomaviruses in the causation of human cancers - a brief historical account. *Virology,* 384**,** 260-5.